

**SYNTHETIC STUDIES ON APOPTOLIDIN CONGENERS IN SUPPORT OF
TARGET IDENTIFICATION OF A CELL SELECTIVE CYTOTOXIC AGENT**

By

JINGQI WANG

Dissertation

Submitted to the Faculty of the
Graduate School of Vanderbilt University
in partial fulfillment of the requirements

for the degree of

DOCTOR OF PHILOSOPHY

in

Chemistry

December, 2009

Nashville, Tennessee

Approved:

Professor Gary A. Sulikowski

Professor Eva Harth

Professor Daniel C. Liebler

Professor Brian O. Bachmann

ACKNOWLEDGMENTS

First and foremost, I would like to thank my wonderful research advisor, Dr. Gary A. Sulikowski, for his guidance and help during my graduate study. Dr. Sulikowski's broad knowledge in organic chemistry and strong enthusiasm for science encouraged me making progress on my research project and finally making accomplishment. Appreciation also goes to my current and previous Ph.D. committee members: Dr. Eva Harth, Dr. Carmelo J. Rizzo, Dr. Brian O. Bachmann and Dr. Daniel C. Liebler for their time and effort. Special gratefulness goes to Dr. Brian O. Bachmann for his directions on bioglycosylation studies. I am also indebted to Dr. Lawrence J. Marnett for his guidances on biological studies.

I would like to thank Dr. Qingsong Liu, who gave me thoughtful help in my early stages of this project. I would also like to thank Dr. Victor P. Ghidu for his contribution to the total synthesis of apoptolidinone A and D. I appreciate the help from Dr. Aaron T. Jacobs for his wonderful work on biological studies of apoptolidin A and its analogues; Dr. Ioanna Ntai for her feeding studies on apoptolidinone A and D; Dr. Yu Du and Ms. Vanessa Phelan, for their help on mycelia fermentation and LC-MS experiments; Dr. Donald Stec and Dr. Markus Voehler, for their assistance on NMR experiments. I am grateful to Dr. Michelle M. Sulikowski, Dr. Donald Stec and Dr. Bruce Melancon for providing helpful advice on this thesis. I have been very fortunate to work in Sulikowski Group and I am grateful for the time with all past and present lab members. I would also like

to thank the National Institutes of Health for financial support.

Finally, my earnest appreciation goes to my family. My husband's endless love and understanding always gave me the strongest support during my research. I must thank my Mom, Dad, sisters and brother for your love and proud. Without the support and understanding from all of you, I couldn't accomplish herein.

TABLE OF CONTENTS

	Page
ACKNOWLEDGEMENTS.....	ii
TABLE OF CONTENTS	iv
LIST OF FIGURES.....	vii
LIST OF TABLES.....	xii
LIST OF SCHEMES	xiii
CHAPTER	
I ISOLATION, HYPOTHETICAL BIOSYNTHESIS AND BIOLOGICAL ACTIVITY OF APOPTOLIDINS.....	1
1.1 Introduction.....	1
1.2 Isolation of apoptolidins and hypothetical biosynthesis	2
1.3 Discovery of isoapoptolidin A, B, D.....	6
1.4 Biological activities of apoptolidins and isoapoptolidin A.....	7
II PREVIOUS SYNTHETIC STUDIES TOWARDS APOPTOLIDIN A AND APOPTOLIDINONE A	10
2.1 Introduction.....	10
2.2 Nicolaou's synthesis of apoptolidin A	11
2.3 Koert's synthesis of apoptolidin A.....	16
2.4 Crimmins' synthesis of apoptolidin A.....	22
2.5 Sulikowski's synthesis of apoptolidinone A.....	27
III PREVIOUS STUDIES ON THE MECHANISM OF ACTION OF APOPTOLIDIN A AND APPLICATION OF A PROBE DERIVED FROM APOPTOLIDIN A TO TARGET IDENTIFICATION	36
3.1 Introduction.....	36
3.2 Apoptosis and autophagic cell death.....	37
3.3 Study on the action mechanism of apoptolidin A.....	39
3.4 SAR studies and target revaluation.....	43
3.5 Application of probes derived from apoptolidin A to target identification	44
3.6 Dissertation statement.....	47

IV	CHEMICAL SYNTHESSES OF 6-NORMETHYL APOPTOLIDINONE A (APOPTOLIDINONE D), 2-NORMETHYL APOPTOLIDINONE D AND 12-OXY-APOPTOLIDINONE D	48
4.1	Introduction.....	48
4.2	Total synthesis of 6-normethyl apoptolidinone A.....	49
4.2.1	Preparation of vinyl boronate 4.8	50
4.2.2	Investigation into the Mukaiyama aldol reaction	53
4.2.3	Alternative route for C(22)-C(23) bond connection	57
4.2.4	Assembly of 6-normethyl apoptolidinone A.....	60
4.3	Total synthesis of 2,6-dinormethyl apoptolidinone A	61
4.3.1	Preparation of carboxylic acid 4.37	61
4.3.2	Assembly of 2,6-dinormethyl apoptolidinone A.....	62
4.4	Total synthesis of 12-oxymethyl apoptolidinone D	63
4.4.1	Preparation of bromide 4.48	65
4.4.2	Assembly of 12-oxymethyl apoptolidinone D.....	67
4.5	Experimental section	69
V	METHODS OF PRECURSOR DIRECTED BIOSYNTHESES AND APPLICATION TO APOPTOLIDIN CONGENERS.....	112
5.1	Introduction.....	112
5.2	Bioglycosylation of synthetic apoptolidinones.....	117
5.2.1	Titration of cerulenin	117
5.2.2	Bioglycosylation of apoptolidinone A	119
5.2.3	Bioglycosylation of 6-normethylapoptolidinone A (a.k.a. apoptolidinone D)	120
5.2.4	Bioglycosylation of 12-oxymethylapoptolidinone D.....	121
5.3	Discussion	122
5.4	Experimental section	123
VI	BIOLOGICAL EFFECTS OF APOPTOLIDIN A AND CONGENERS AGAINST HUMAN LUNG CANCER H292 CELLS AND PROGRESS TOWARDS THE SYNTHESIS OF APOPTOLIDIN PROBES FOR TARGET IDENTIFICATION.....	133
6.1	Introduction.....	133
6.2	Biological effects of apoptolidin A and isoapoptolidin A.....	136
6.3	SAR studies of sugar units of apoptolidin A.....	141
6.4	Apoptolidin probe design and future directions.....	146
6.5	Summary	152
6.6	Experimental section	154
	APPENDIX	163

REFERENCES	229
VITA	241

LIST OF FIGURES

FIGURE		Page
1.1	Structure of apoptolidin A 1.1	2
1.2	Structures of apoptolidin B 1.2 , C 1.3 and D 1.4	4
1.3	Hypothetical biosynthesis of apoptolidins.....	6
1.4	Structures of isoapoptolidin A 1.5 , B 1.6 and D 1.7	7
2.1	Structures of apoptolidin A 2.1 and apoptolidinone A 2.2	11
3.1	Structures of apoptolidin A 3.1 , truncated apoptolidin A 3.2 , Ossamycin 3.3 , cytovaricin aglycone 3.4 and oligomycin 3.5	41
3.2	Biological activities of apoptolidin A 3.1 and C-9 sugar congener 3.6	43
3.3	Wender's PAL probes of apoptolidin A.....	46
4.1	Structures of apoptolidinone A and unnatural apoptolidinones.....	49
4.2	GC chromatograph of silyl enol ethers 4.9 and 4.29	72
4.3	HPLC chromatograph for purification of aldol 4.30	76
4.4	HPLC chromatograph for purification of ester 4.63	104
5.1	Structure of Cerulenin 5.4	118
5.2	Structure of apoptolidin A disaccharide 5.20	120
5.3	Structures of apoptolidin disaccharide 5.20 and 5.21 and LC/MS detection.....	121
5.4	HPLC chromatograph for apoptolidin A and isoapoptolidin A purification	128
5.5	HPLC chromatograph for apoptolidin D disaccharide purification.....	130
6.1	Structures of apoptolidin A 6.1 , isoapoptolidin A 6.2 ,	

	apoptolidinone A 6.3 , apoptolidinone D 6.4 , and apoptolidin D disaccharide 6.5	135
6.2	Cytotoxicity of apoptolidins to H292 cells (cell density: 500/well).....	138
6.3	Glucose starvation effect on apoptolidin A cytotoxicity.....	139
6.4	Cytotoxicity of apoptolidins to H292 cells (cell density: 5000/well).....	140
6.5	Cytotoxicity of apoptolidin sugar congeners.....	141
6.6	Cytotoxicity of apoptolidinones to H292 cells.....	143
6.7	Cytotoxicity of apoptolidin D C-27 disaccharide to H292 cells.....	144
6.8	Structures of Ammocidin A-D and apoptolidin A.....	145
6.9	Cytotoxicity of apoptolidin derivative 6.18 in H292 cells.....	151
6.10	Structures of apoptolidin probes 6.19 and 6.20	152
A1a	The 500 MHz ¹ H NMR spectrum of 4.9 in C ₆ D ₆	164
A1b	The 125 MHz ¹³ C NMR spectrum of 4.9 in CDCl ₃	165
A1c	The 600 MHz NOESY NMR spectrum of 4.9 in C ₆ D ₆	166
A2a	The 500 MHz NOESY NMR spectrum of 4.29 in CDCl ₃	167
A3a	The 600 MHz NOESY NMR spectrum of 4.32 in CD ₃ OD	168
A4a	The 400 MHz ¹ H NMR spectrum of 4.37 in CDCl ₃	169
A4b	The 100 MHz ¹³ C NMR spectrum of 4.37 in CDCl ₃	170
A5a	The 600 MHz ¹ H NMR spectrum of 4.43 in C ₆ D ₆	171
A5b	The 150 MHz ¹³ C NMR Spectrum of 4.43 in C ₆ D ₆	172
A6a	The 600 MHz ¹ H NMR spectrum of 4.44 in C ₆ D ₆	173

A6b	The 150 MHz ^{13}C NMR spectrum of 4.44 in C_6D_6	174
A7a	The 600 MHz ^1H NMR spectrum of 4.45 in C_6D_6	175
A7b	The 150 MHz ^{13}C NMR spectrum of 4.45 in C_6D_6	176
A8a	The 600 MHz ^1H NMR spectrum of 4.46 in C_6D_6	177
A8b	The 150 MHz ^{13}C NMR spectrum of 4.46 in C_6D_6	178
A9a	The 600 MHz ^1H NMR spectrum of 4.36 in C_6D_6	179
A9b	The 150 MHz ^{13}C NMR spectrum of 4.36 in C_6D_6	180
A10a	The 600 MHz ^1H NMR spectrum of 4.3 in CD_3OD	181
A10b	The 150 MHz ^{13}C NMR spectrum of 4.3 in CD_3OD	182
A11a	The 300 MHz ^1H NMR spectrum of 4.53 in C_6D_6	183
A11b	The 75 MHz ^{13}C NMR spectrum of 4.53 in C_6D_6	184
A12a	The 300 MHz ^1H NMR spectrum of 4.54 in C_6D_6	185
A12b	The 75 MHz ^{13}C NMR spectrum of 4.54 in C_6D_6	186
A13a	The 400 MHz ^1H NMR spectrum of 4.54b in C_6D_6	187
A13b	The 75 MHz ^{13}C NMR spectrum of 4.54b in C_6D_6	188
A14a	The 400 MHz ^1H NMR spectrum of 4.55 in C_6D_6	189
A14b	The 75 MHz ^{13}C NMR Spectrum of 4.55 in C_6D_6	190
A15a	The 300 MHz ^1H NMR spectrum of 4.56 in C_6D_6	191
A15b	The 75 MHz ^{13}C NMR spectrum of 4.56 in C_6D_6	192
A16a	The 300 MHz ^1H NMR spectrum of 4.57 in C_6D_6	193
A16b	The 75 MHz ^{13}C NMR spectrum of 4.57 in C_6D_6	194
A17a	The 300 MHz ^1H NMR spectrum of 4.48 in C_6D_6	195
A17b	The 75 MHz ^{13}C NMR spectrum of 4.48 in C_6D_6	196

A18a	The 300 MHz ^1H NMR spectrum of 4.58 in C_6D_6	197
A18b	The 125 MHz ^{13}C NMR spectrum of 4.58 in CDCl_3	198
A19a	The 400 MHz ^1H NMR spectrum of 4.59 in C_6D_6	199
A19b	The 125 MHz ^{13}C NMR spectrum of 4.59 in C_6D_6	200
A20a	The 400 MHz ^1H NMR spectrum of 4.60 in C_6D_6	201
A20b	The 125 MHz ^{13}C NMR spectrum of 4.60 in C_6D_6	202
A21a	The 400 MHz ^1H NMR spectrum of 4.61 in CDCl_3	203
A21b	The 75 MHz ^{13}C NMR spectrum of 4.61 in C_6D_6	204
A22a	The 500 MHz ^1H NMR spectrum of 4.62 in C_6D_6	205
A22b	The 125 MHz ^{13}C NMR spectrum of 4.62 in C_6D_6	206
A23a	The 300 MHz ^1H NMR spectrum of 4.63 in C_6D_6	207
A23b	The 125 MHz ^{13}C NMR spectrum of 4.63 in C_6D_6	208
A24a	The 500 MHz ^1H NMR spectrum of 4.64 in C_6D_6	209
A24b	The 100 MHz ^{13}C NMR spectrum of 4.64 in C_6D_6	210
A25a	The 400 MHz ^1H NMR spectrum of 4.65 in C_6D_6	211
A25b	The 75 MHz ^{13}C NMR spectrum of 4.65 in C_6D_6	212
A26a	The 400 MHz ^1H NMR spectrum of 4.66 in C_6D_6	213
A26b	The 75 MHz ^{13}C NMR Spectrum of 4.66 in C_6D_6	214
A27a	The 600 MHz ^1H NMR spectrum of 4.47 in C_6D_6	215
A27b	The 75 MHz ^{13}C NMR spectrum of 4.47 in C_6D_6	216
A28a	The 600 MHz ^1H NMR spectrum of 4.4 in CD_3OD	217
A28b	The 150 MHz ^{13}C NMR spectrum of 4.4 in CD_3OD	218
A29a	The 500 MHz ^1H NMR spectrum of 6.16 in CD_3OD	219

A29b	The 500 MHz COSY NMR spectrum of 6.16 in CD ₃ OD	220
A29c	The 500 MHz HSQC NMR spectrum of 6.16 in CD ₃ OD	221
A30a	The 400 MHz ¹ H NMR spectrum of 6.17 in CD ₃ OD.....	222
A30b	The 125 MHz ¹³ C NMR spectrum of 6.17 in CD ₃ OD	223
A31a	The 600 MHz ¹ H NMR spectrum of 6.18 in CD ₃ OD.....	224
A31b	The 125 MHz ¹ H NMR spectrum of 6.18 in CD ₃ OD.....	225
A31c	The 600 MHz COSY NMR spectrum of 6.18 in CD ₃ OD	226
A31d	The 600 MHz HSQC NMR spectrum of 6.18 in CD ₃ OD	227
A31e	The 600 MHz HMBC NMR spectrum of 6.18 in CD ₃ OD	228

LIST OF TABLES

TABLE		Page
1.1	Cytotoxicity of apoptolidin A 1.1 against transformed and normal cells.....	8
1.2	Cytotoxicity of apoptolidin A-D and isoapoptolidin A.....	9
3.1	<i>In vitro</i> and <i>In vivo</i> biological activities of apoptolidin A and isoapoptolidin A.....	44
5.1	¹ H (600 MHz) and ¹³ C (150 MHz) NMR spectral data of apoptolidin D disaccharide 5.21 and apoptolidin D in CD ₃ OD	132
6.1	Antiproliferative activities of ammocidins.....	146
6.2	NMR spectroscopic data for apoptolidin A congeners in CD ₃ OD	160

LIST OF SCHEMES

SCHEME		Page
1.1	Isomerization between apoptolidins and isoapoptolidins.....	7
2.1	Strategic analysis in Nicolaou's synthesis of apoptolidin A 2.1	12
2.2	Nicolaou's synthetic strategy for vinyl stannane 2.4	13
2.3	Nicolaou's synthetic strategy for vinyl iodide 2.3	14
2.4	Nicolaou's synthetic strategy for two sugar units.....	15
2.5	Nicolaou's assembly of apoptolidin A 2.1	16
2.6	Strategic analysis in Koert's synthesis of apoptolidin A 2.1 ...	17
2.7	Koert's synthetic strategy for building blocks 2.36 and 2.37 ..	18
2.8	Koert's synthetic strategy for vinyl iodide 2.40 and pyran 2.42	19
2.9	Koert's syntheses of apoptolidinone A 2.1	20
2.10	Koert's synthetic strategy for two sugar units.....	21
2.11	Koert's assembly of apoptolidin A 2.1	22
2.12	Strategic analysis in Crimmins's synthesis of apoptolidin A 2.1	23
2.13	Crimmins's synthetic strategy for building blocks 2.61 and 2.62	24
2.14	Crimmins's synthesis of apoptolidinone A 2.2	25
2.15	Crimmins's synthetic strategy for two sugar units	26
2.16	Crimmins's assembly of apoptolidin A 2.1	27
2.17	Strategic analysis in Sulikowski's synthesis of apoptolidinone A 2.2	29
2.18	Sulikowski's synthetic strategy for aldehyde 2.90	30

2.19	Sulikowski's synthetic strategy for bromide 2.41	30
2.20	Sulikowski's synthetic strategy for carboxylic acid 2.89	31
2.21	Sulikowski's synthetic strategy for aldehyde 2.86	32
2.22	Sulikowski's synthetic strategy for boronate 2.87	33
2.23	Sulikowski's assembly of apoptolidinone A 2.2	35
4.1	Synthetic strategy for 6-normethyl apoptolidinone A 4.2	50
4.2	Synthesis of vinyl iodide 4.21	51
4.3	Synthesis of aldehyde 4.24 and vinyl boronate 4.8	52
4.4	Synthesis of silyl enol ether 4.9 and 4.29	53
4.5	Open transition state models for Mukaiyama reactions	55
4.6	1,3-induction models for Mukaiyama additions	55
4.7	Prediction for stereoselectivity in Mukaiyama aldol reaction .	56
4.8	Diastereoselectivity in Mukaiyama aldol reaction	57
4.9	Synthesis of silyl enol ether 4.29	58
4.10	Formation of C-22/C-23 conjunction with Mukaiyama aldol reaction	59
4.11	Final assembly of 6-normethyl apoptolidinone A 4.2 (apoptolidinone D)	60
4.12	Retrosynthetic analysis for 2,6-dinormethyl apoptolidinone A 4.3	61
4.13	Synthesis of carboxylic acid 4.37	62
4.14	Assembly of 2,6-dinormethyl apoptolidinone A 4.3	63
4.15	Retrosynthetic analysis for oxy-apoptolidinone D 4.4	65
4.16	Synthesis of bromide 4.48	66
4.17	Assembly of oxy-apoptolidinone D 4.4	67

5.1	Omura's hybrid synthesis of protylonolide derivatives.....	115
5.2	Hypothetical biosynthesis of apoptolidin A-D	116
5.3	Precursor directed bioglycosylation of apoptolidinones.....	117
5.4	Flow chart for apoptolidin fermentation	125
6.1	Initial apoptolidin probe design.....	148
6.2	Synthesis of apoptolidin derivatives 6.16 , 6.17 and 6.18	149

CHAPTER I

ISOLATION, HYPOTHETICAL BIOSYNTHESIS AND BIOLOGICAL ACTIVITY OF APOPTOLIDINS

1.1 Introduction

As reported by the American Cancer Society, 7.6 million people died of various cancers in 2007 (<http://www.cancer.org>), cancer is one of the leading causes of mortality worldwide. Clinically, cancer is defined as malignant neoplasm, a group of cells with uncontrolled growth properties and malignant behavior. The mechanism of cancer development is extremely complex, and is still not fully understood at the molecular or genetic level. However, it is widely accepted that genetic changes will disturb the balance between proliferation and apoptosis, activation of oncogenes leads to cell proliferation and resistance against programmed cell death, which initiates the development of cancers. During the progression of cancers, somatic alterations in oncogenes, tumor suppressor genes, and microRNA genes are observed.¹

Cancer chemotherapy is the use of cytotoxic drugs to kill cancer cells and currently one of the most effective methods to treat cancer. In a general sense, traditional chemotherapy acts by killing all quickly proliferating cells, either healthy or malignant. The major concern with conventional chemotherapy is insufficient selectivity, which causes severe side effects during the treatment. Today, cancer is viewed as a chronic disease. The goal of anticancer drug

development is to find specific apoptosis inducing agents targeting only cancer cells with minimal effect on normal cells.

Cells transformed with certain type of oncogenes can model key aspects of cancer. This provides a powerful screening system for the discovery of small molecules as specific anticancer drugs. Natural products continue to be one of the major sources for drug discovery.² Screening natural products using cellular models is an effective strategy for discovery of a new generation anticancer agents for the treatment of specific types cancers.

1.2 Isolation of Apoptolidin A-D and Hypothetical Biosynthesis

In a screening program, initiated by Seto and coworkers in Japan, targeted to identify specific apoptosis inducing agents in E1A-transformed cells, an antinomycete secondary metabolite, apoptolidin A **1.1** (Figure 1.1), was isolated from the fermentation broth of *Nocardopsis. Sp.* in 1997.³

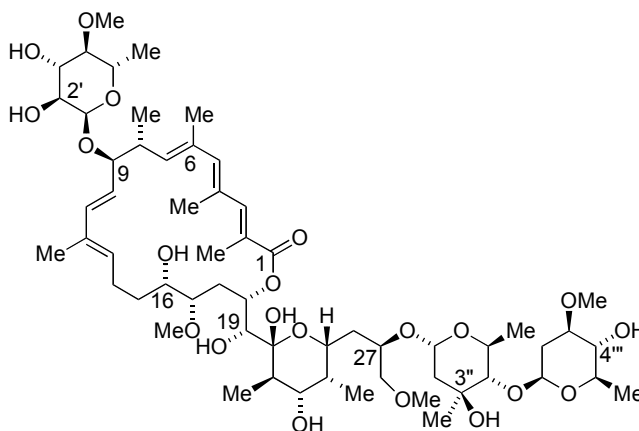


Figure 1.1 Structure of Apoptolidin A (**1.1**)

Apoptolidin A **1.1** was isolated from the fermentation medium of producing microorganism *Nocardioopsis. Sp.* in the amount of 110 mg/L as reported by Seto's group. The molecular formula of apoptolidin A **1.1** was determined to be $C_{58}H_{96}O_{21}$ using high resolution FAB-MS.³ The two-dimensional structure and the stereochemistry were later elucidated by extensive NMR analysis and chemical degradation studies by the same group in 1998.⁴ Apoptolidin A **1.1** belongs to a family of macrocyclic polyketide type natural products. The structure of apoptolidin A **1.1** consists of a macrocyclic aglycone and two α -linked sugar units located at C-9 and C-27. A novel sugar, 6-deoxy-4-O-methyl-L-glucose is connected to the aglycone at C-9. A disaccharide located at C-27 consists of a D-oleandrose and a L-olivomycose interconnected through a β -glycoside linkage. The aglycone structure is composed of a highly unsaturated 20-membered macrolactone and a hemiketal pyranose populated with four stereogenic centers. The *E* geometry of all four tri-substituted olefins in the aglycone was assigned by COSY, HMQC, HMBC and ROESY analysis. The stereochemistry of the sugar units were used as an internal reference for the assignment of the absolute stereochemistry of apoptolidin A **1.1** by observed NOE correlations.

Three minor congeners, apoptolidin B **1.2**, apoptolidin C **1.3** and apoptolidin D **1.4** were later identified from the culture broth of the same microorganism by Wender's group at Stanford University in 2005⁵ and 2006, respectively (Figure 1.2).⁶

Apoptolidin B **1.2** and apoptolidin C **1.3** were isolated from the culture medium in the amount of 2-5 mg/L.⁵ The molecular formulas for apoptolidin B **1.2**

and apoptolidin C **1.3** were determined to be $C_{58}H_{96}O_{20}$ and $C_{58}H_{96}O_{19}$ respectively by high-resolution mass spectroscopy. Structure analysis reveals apoptolidin B **1.2** lacks one hydroxyl group at C-16 position, and apoptolidin C **1.3** lacks two hydroxyl groups at the C-16 and C-20 positions. The remaining stereocenters of apoptolidin B **1.2** and C **1.3** were identical to apoptolidin A **1.1**, established by extensive two-dimensional NMR data analysis (COSY, TOCSY, HMBC, HMQC, ROESY).

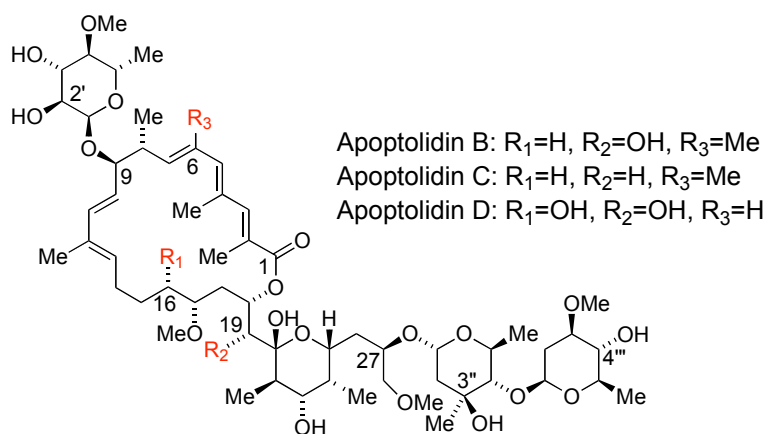


Figure 1.2 Structure of apoptolidin B (**1.2**), C (**1.3**), D (**1.4**)

Apoptolidin D **1.4** is the most recent metabolite discovered in the apoptolidin family. The isolated yield of apoptolidin D **1.4** is 7 mg per liter of fermentation medium.⁶ Its molecular formula was determined to be $C_{57}H_{94}O_{21}$ by high-resolution mass spectrometric analysis. Extensive NMR analysis revealed that apoptolidin D **1.4** lacks a C-6 methyl group in comparison to apoptolidin A **1.1**. The absolute stereochemistry of apoptolidin D **1.4** is identical to apoptolidin A **1.1**. Once again, the four tri-substituted olefins present *E*-geometry. Apoptolidin

D **1.4** is the only apoptolidin that has a different carbon skeleton relative to apoptolidin A **1.1**.

The biosynthetic pathway leading to apoptolidin A **1.1** has not been elucidated. Hypothetically, either glycolate or its methoxy derivative may serve as a starter unit, which could be determined by examination of the PKS gene cluster of apoptolidin producer *Nocardioopsis. Sp.*⁷ The carbon chain is presumably extended with malonyl or methylmalonyl extender units, following reduction by ketoreductase and dehydratase in PKS and finally macrolactonization release the macrolide core from the PKS. Glycosylation is required to attach the sugar units, methylation of C-17 hydroxyl group, oxidation of C-16 and C-19 completes the unique structure of apoptolidin A **1.1**. According to the above proposed biosynthetic pathway of apoptolidin A **1.1**, apoptolidin B **1.2** and apoptolidin C **1.3** are shunt metabolites, result of incomplete oxygenation. Apoptolidin D **1.4** is the biosynthetic product derived from incorporation of the malonyl extender unit in place of the methylmalonyl unit used for apoptolidin A **1.1** biosynthesis (Figure 1.3).

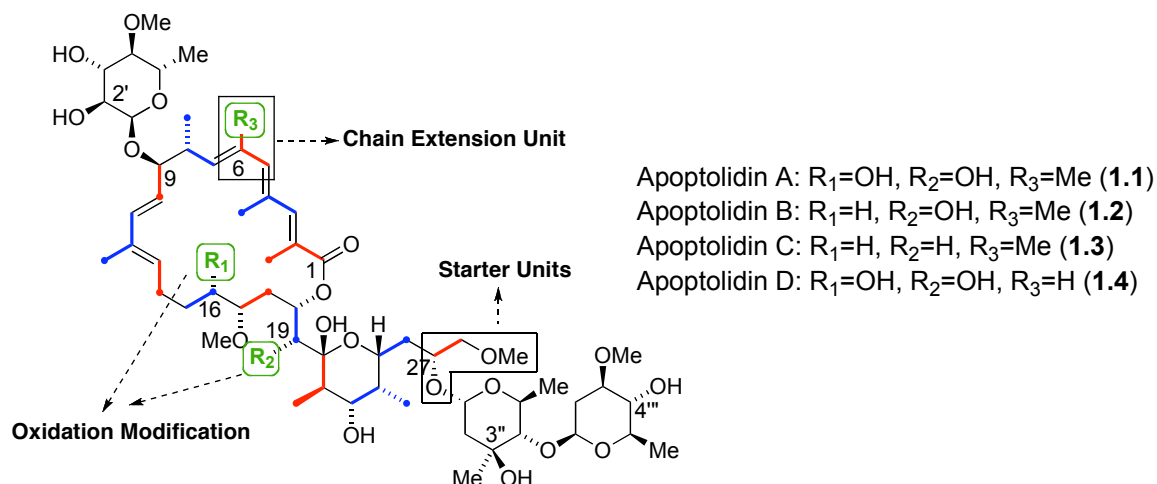


Figure 1.3 Hypothetical Biosynthesis of Apoptolidins

1.3 Discovery of Isoapoptolidin A, B, D

In 2002, Wender and Sulikowski groups independently discovered an isomer of apoptolidin A **1.1** as the fermentation product of *Nocardioopsis. Sp.* Careful analysis of COSY and HMBC correlations revealed that this compound is the result of an acyl migration from the C-19 to C-20 hydroxyl group as shown in Figure 1.4. This 21-membered macrolide was named as isoapoptolidin A **1.5**.^{8,9} The facile inter-conversion between apoptolidin A **1.1** and isoapoptolidin A **1.5** produces an approximate 1:1 mixture in aqueous solution at ambient temperature. The isomerization of apoptolidin A **1.1** to isoapoptolidin A **1.5** could be catalyzed by triethylamine in methanol solution. Since apoptolidin B **1.2** and apoptolidin D **1.4** both feature a C-20 hydroxyl group, they can also establish equilibrium with their ring expansion isomers, isoapoptolidin B **1.6** and isoapoptolidin D **1.7** respectively.⁵

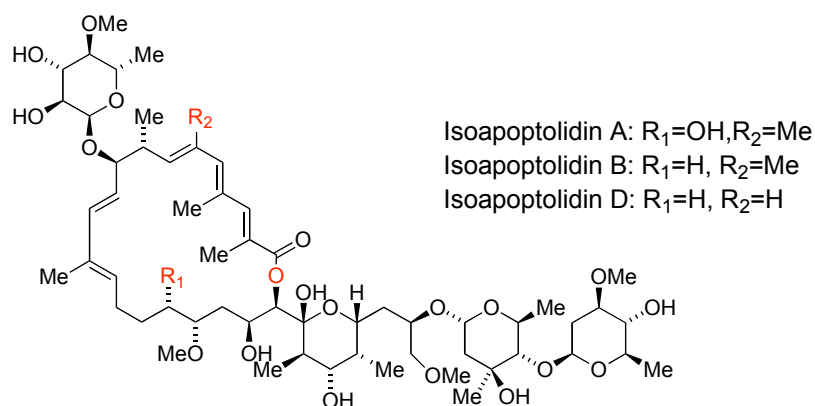
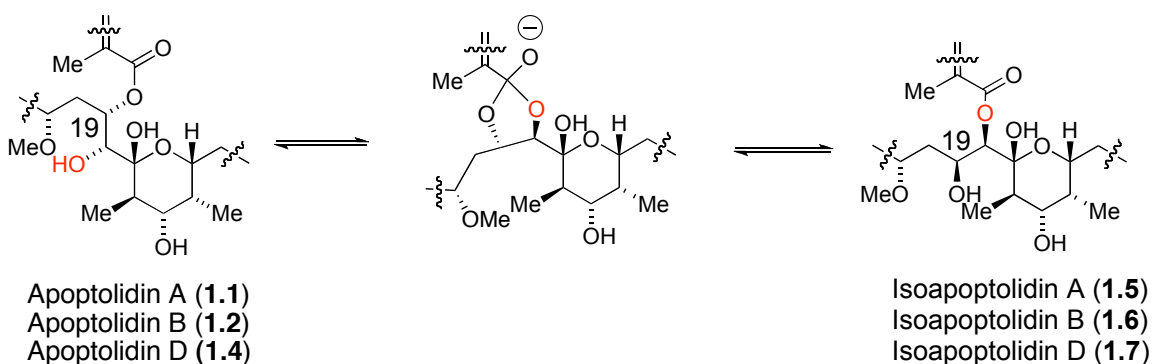


Figure 1.4. Structures of isoptolidin A (1.5), B (1.6), D (1.7)

The mechanism of ring expansion isomerization reaction can be rationalized as an intramolecular rearrangement through tetrahedral intermediates as shown in Scheme 1.1, a similar pathway was proposed for isomerization between bafilomycin and isobafilomycin.¹⁰



Scheme 1.1 Isomerization between apoptolidins and isoptolidins

1.4 Biological Activities of Apoptolidin A-D and Isoptolidin A

Seto's group used rat glia cells transformed with the adenovirus type 12 oncogenes including E1A as an activity based screen leading to the identification

of apoptolidin A **1.1** from the extracts of *Nocardiosis Sp.* The preliminary biological screening showed that apoptolidin A **1.1** induce programmed cell death only in E1A transformed glia cells with minimal effects on normal glia cells and other oncogenes transformed cells, such as 3Y-1 rat fibroblasts transformed with *H-ras*, *v-src*, and SV40 large T antigen. Seto's group also observed that the apoptosis induced by apoptolidin A **1.1** was not suppressed by E1B gene products. The cytotoxicity of apoptolidin A **1.1** was observed over a 3-day cell-assay as summarized in Table 1.1.³

Table 1.1 Cytotoxicity of apoptolidin A (**1.1**) against transformed and normal cells

Cell line	Oncogene	IC ₅₀ (ng/ml)
RG-E1A-7	E1A	11
RG-E1A19K-2	E1A, E1B19K	10
RG-E1A54K-9	E1A, E1B54K	13
RG-E1-4	E1A, E1B19K, E1B54K	10
Ad12-3Y1	E1A, E1B19K, E1B54K	17
Glia		> 100,000
3Y1		> 100,000
HR-3Y1	<i>H-ras</i>	> 100,000
SR-3Y1	<i>v-src</i>	> 100,000
SV-3Y1	SV 40 large T antigen	> 100,000

Apoptolidin A **1.1** was discovered to be a highly selective and potent apoptosis inducing agent based on cell assays, which makes apoptolidin A **1.1** a very valuable candidate as an anticancer lead agent. The biological activity of apoptolidin A **1.1** was further evaluated against NCI-60 different human cancer cell lines, the results of this screening revealed that many cancer cell lines are

sensitive to apoptolidin A **1.1**, and determined to be one of the most selective anticancer agents among more than 37,000 agents examined.^{11,12,13,14}

The cytotoxicity effects against H292 lung cancer cells showed that apoptolidin A **1.1**, B **1.2**, C **1.3** and D **1.4** can inhibit the cell growth in nanomolar range, among which, apoptolidin B **1.2** exhibited a slightly higher potency. Isoapoptolidin A **1.5** showed similar potency as apoptolidin A **1.1** in Ad12-3Y1 transformed glia cells assay.^{5,6,15}

Table 1.2 Cytotoxicity of apoptolidin A-D and isoapoptolidin A

Compounds	GI₅₀(μM) (H292)	EC₅₀(μM) (H292)	GI₅₀(μM) (Ad12-3Y1)
Apoptolidin A (1.1)	0.032 \pm 0.003	0.050(0.025~0.100)	0.0065
Apoptolidin B (1.2)	0.007 \pm 0.004		
Apoptolidin C (1.3)	0.024 \pm 0.005		
Apoptolidin D (1.4)		0.110(0.060~0.21)	
Isoapoptolidin A (1.5)			0.009

CHAPTER II

PREVIOUS SYNTHETIC STUDIES TOWARDS APOPTOLIDIN A AND APOPTOLIDINONE A

2.1 Introduction

Apoptolidin A **2.1**, which can induce apoptosis in cancer cells with minimal effects on normal cells, is of potentially high significance in the treatment of cancers. Apoptolidin A **2.1** features a complex molecular architecture including 25 stereocenters, a conjugated polyene system, and 3 carbohydrate units. These synthetically challenging attributes have attracted considerable interests from the synthetic community. Construction of this complex natural product in a convergent fashion poses an obvious challenge for synthetic chemists. Specifically, the acid and base labile nature of apoptolidin A **1.1** has to be carefully considered in planning the later stages of a total synthesis. To date, three total syntheses of apoptolidin A **2.1**^{16,17,18,19,20,21,22} and three total syntheses of apoptolidinone A **2.2** (the aglycone of apoptolidin A **2.1** as shown in Figure 2.1) have been accomplished, including our group's efforts directed towards the syntheses of apoptolidinone A **2.2**.^{23,24,25} Several fragment syntheses have also been reported.^{26,27,28,29,30,31,32,33,34,35,36,37,38,39}

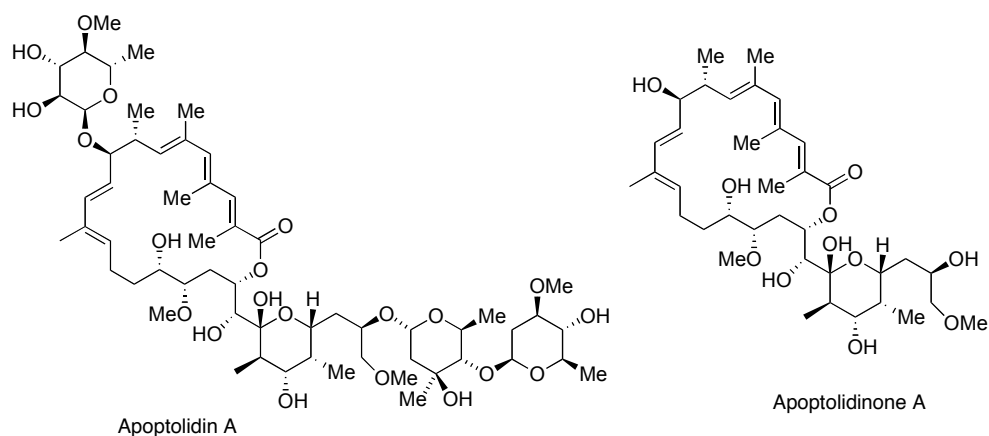
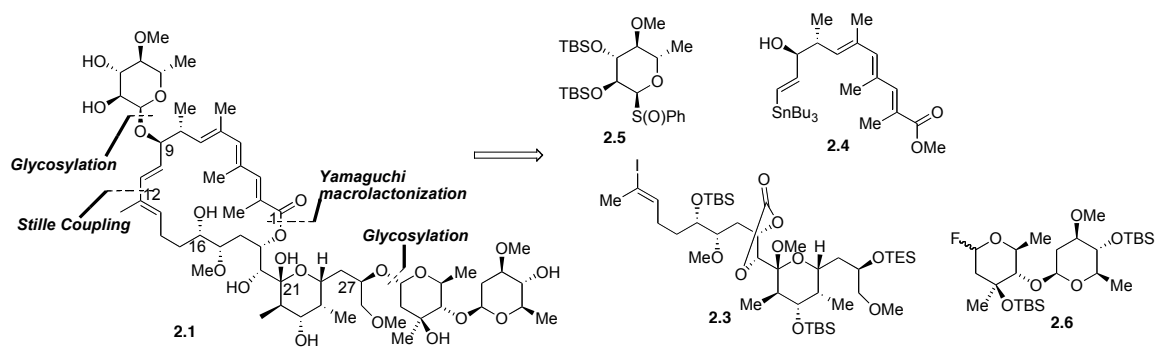


Figure 2.1 Structure of apoptolidin A (**2.1**) and apoptolidinone A (**2.2**)

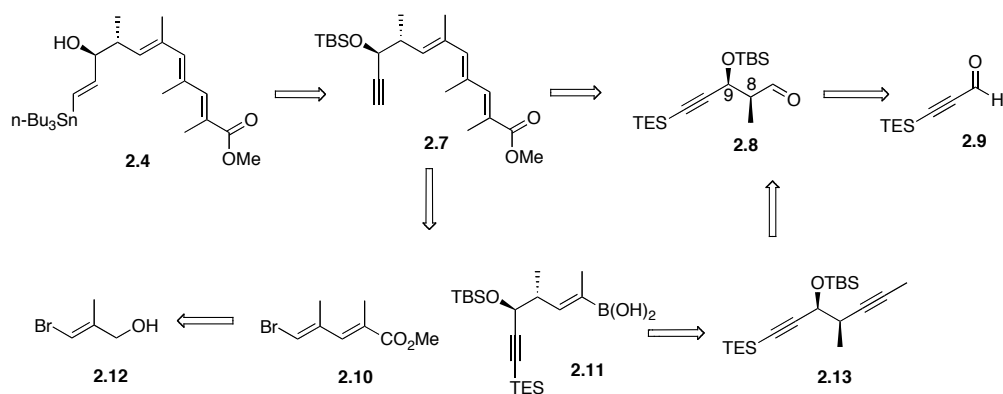
2.2 Nicolaou's Synthesis of Apoptolidin A

In 2001, Nicolaou's group reported the first total synthesis of apoptolidin A **2.1**.^{16,17} As shown in Scheme 2.1, their synthetic strategy leading to apoptolidin A **2.1** relied on the installation of sugar units at the later stage of the total synthesis. A Stille coupling reaction was used to install the C-11/C-12 bond, and Yamaguchi macrolactonization was utilized to form the 20 membered ring system. Retrosynthetic analysis indicates vinyl iodide **2.3**, vinyl stannane **2.4**, and 2 sugar units **2.5** and **2.6** as the key building blocks. In 2003, a second generation synthesis of apoptolidin A **2.1** was published, in which, more convergent synthetic routes for the construction of two of the major building blocks vinyl iodide **2.3** and vinyl stannane **2.4** was reported.^{18,19}



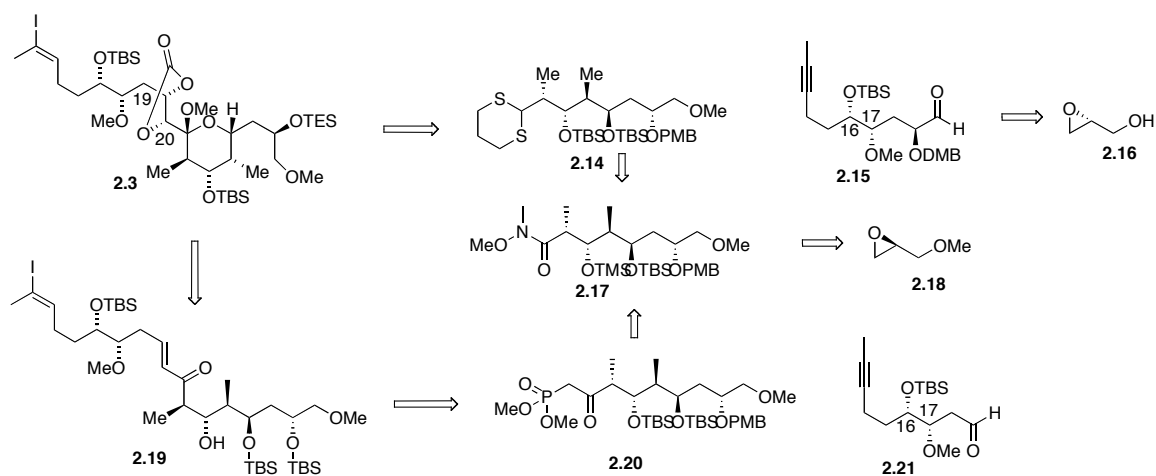
Scheme 2.1 Strategic analysis in Nicolaou's syntheses of apoptolidin A (**2.1**)

The *E*-geometry in vinyl stannane **2.4** was realized by a palladium(0) catalyzed regioselective hydrostannylation from alkyne **2.7**, which was originally prepared by a linear, iterative *E*-selective Wittig or Horner-Wadsworth-Emmons olefination-reduction-oxidation sequence on aldehyde **2.8**. In the revised synthetic route, a Suzuki coupling strategy between vinyl bromide **2.10** and vinyl boronic acid **2.11** was employed. Vinyl bromide **2.10** was prepared from known vinyl bromide **2.12** by oxidation followed by *E*-selective Wittig olefination. Suzuki coupling partner, vinyl boronic acid **2.11** was prepared by chemoselective hydroboration with catecholborane on diyne **2.13** following an aqueous hydrolysis. Homologation with aldehyde **2.8** using the Ohira-Bestmann reagent followed by methylation of the terminal acetylene gave diyne **2.13**. The stereochemistry at C-8 and C-9 in aldehyde **2.8** was set by Brown's asymmetric crotylation with known propargylic aldehyde **2.9**.



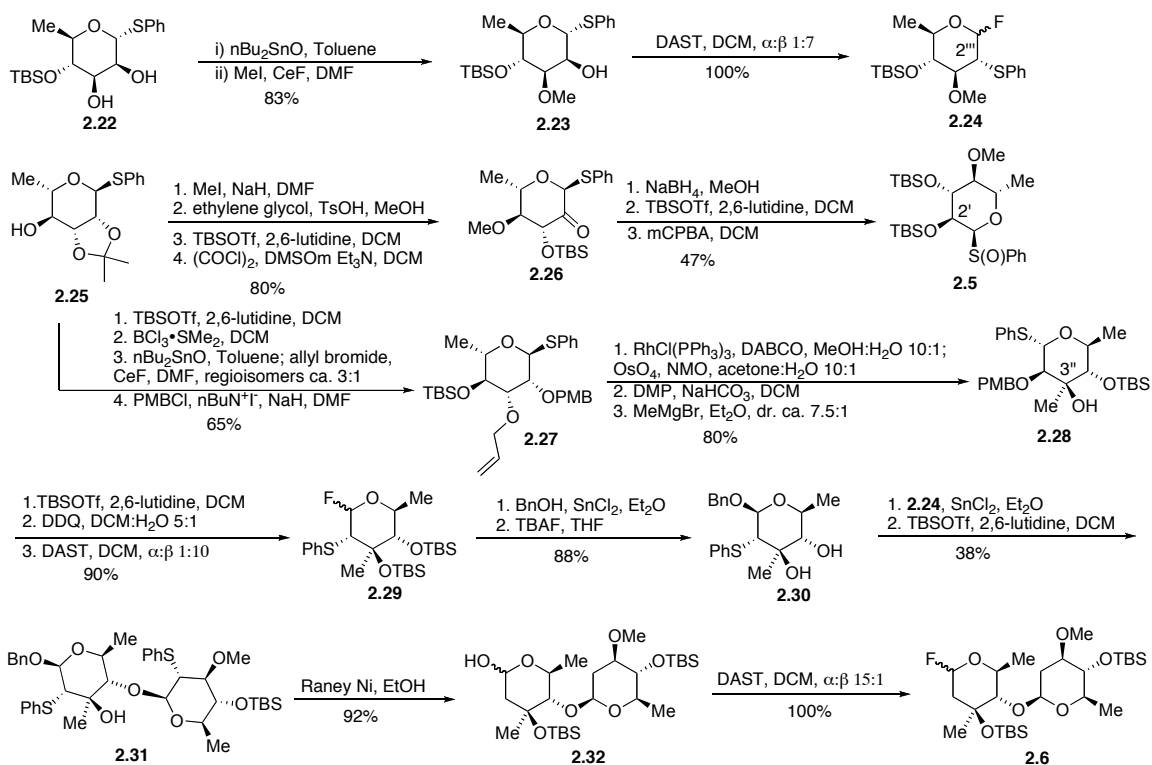
Scheme 2.2 Nicolaou's synthetic strategy for vinyl stannane (**2.4**)

The initial attempt to set the stereochemistry at C-19 and C-20 in the synthesis of vinyl iodide **2.3** depended on a chelation-controlled dithiane coupling reaction between dithiane **2.14** and aldehyde **2.15**. However, the poor stereoselectivity prompted the evolution of a better strategy based on a late stage Sharpless asymmetric dihydroxylation of enone **2.19**. Horner-Wadsworth-Emmons olefination between phosphonate **2.20** and aldehyde **2.21** constructed the *E*-geometry in enone **2.19**. The stereochemistry at C-16 in aldehyde **2.15** and **2.21** were derived from commercially available pro-chiral starting material **2.16**, the other stereocenter at C-17 in aldehyde **2.15** and **2.21** were established by Brown's asymmetric allylation reaction. Both dithiane **2.14** and phosphonate **2.20** were obtained from Weinreb amide **2.17**, in which, the asymmetry was achieved by using pro-chiral epoxide **2.18**, Brown's asymmetric crotylation, and Evan's asymmetric aldol reaction.



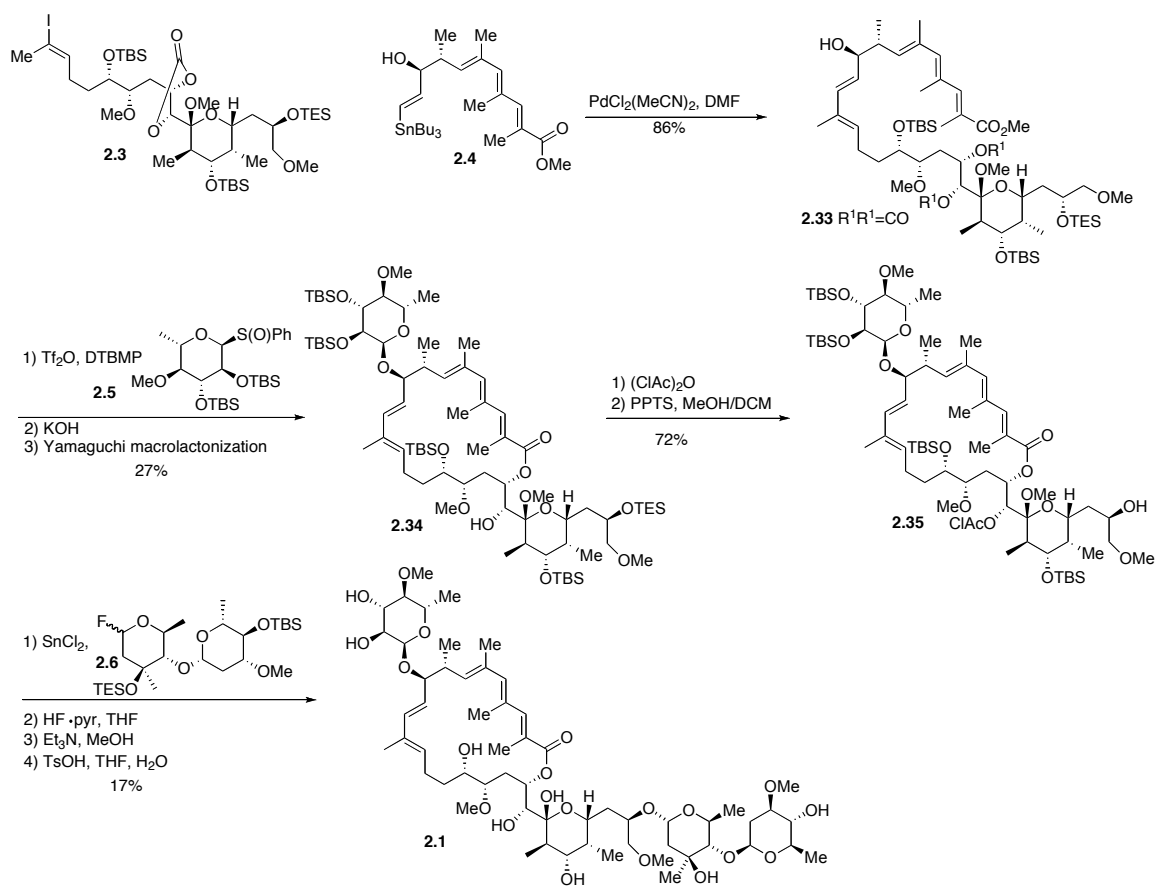
Scheme 2.3 Nicolaou's synthetic strategy for vinyl iodide (**2.3**)

Two of the glycosyl building blocks **2.5** and **2.30** were synthesized starting from thioglycoside **2.25**, which was prepared from L-rhamnose following known procedures. Glycosyl sulfoxide **2.5** was obtained after a series of protecting group manipulations and stereocenter inversion at C-2' position by an oxidation-reduction sequence. Phenylthioglycoside **2.30** was prepared from **2.25** over 12 steps. The C-3'' quaternary methyl group in phenylthioglycoside **2.30** was introduced by chelation-controlled addition of methyl Grignard reagent. Phenylthioglycoside **2.24** was synthesized from phenylthioglycoside **2.22** in two steps. Glycosylation between phenylthioglycosides **2.30** and **2.24** in presence of stannum (II) chloride, removal of thiophenyl groups and benzyl protecting group provided a lactol intermediate **2.32**, which was converted to glycosyl fluoride **2.6** by treatment with DAST. Formation of the β -linkage in glycosyl fluoride **2.31** was directed by the C-2'' phenylthio group in the glycosyl donor **2.24**.



Scheme 2.4 Nicolaou's synthetic strategy for two sugar moieties

In the construction of apoptolidin A **2.1**, the key coupling of fragment **2.3** and **2.4** employed Stille reaction conditions to afford **2.33** in 86% yield. The C-9 sugar moiety **2.5** was installed following the Kahne protocol. The ring-size selective macrolactone closing was realized under Yamaguchi conditions after hydrolysis of the corresponding methyl ester. The C-27 disaccharide moiety was installed by stannum (II) mediated activation of glycosyl fluoride **2.6** to afford the desired alpha stereochemistry. Finally, stepwise global deprotection gave the target molecule apoptolidin A **2.1**.

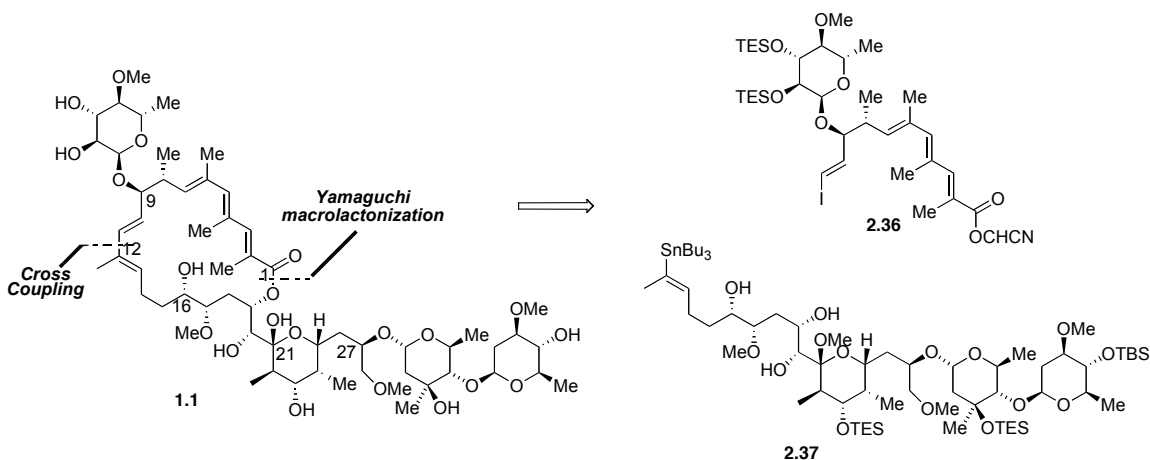


Scheme 2.5 Nicolaou's Final Assembly of Apoptolidin A (**2.1**)

2.3 Koert's Synthesis of Apoptolidinone A and Apoptolidin A

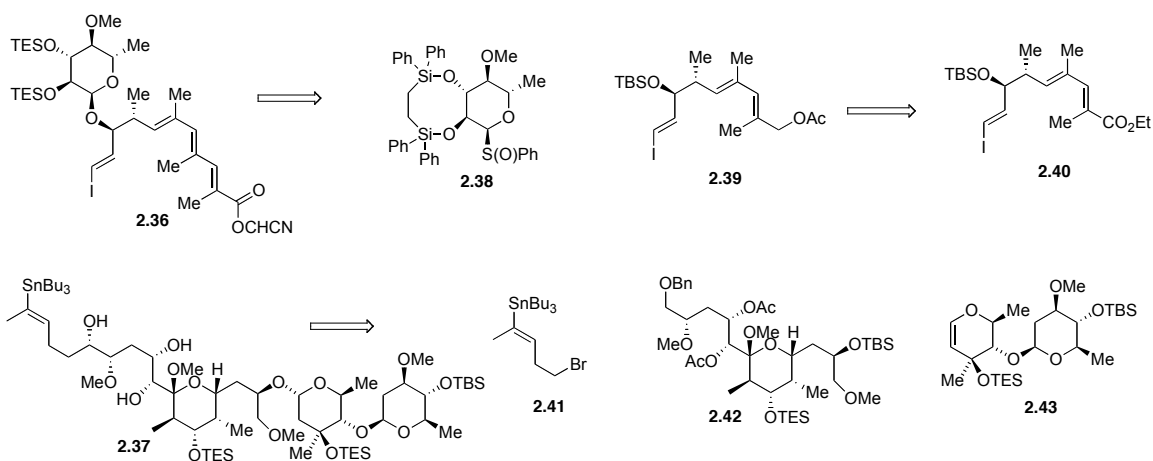
In 2004, Ulrich Koert accomplished a total synthesis of apoptolidin A **2.1**,²⁰ following their reported first total synthesis of apoptolidinone A **2.2** in 2001.²³ The synthetic strategy adopted by Koert's group was very similar to Nicolaou's approach. However, in contrast to Nicolaou's approach, the sugar moieties were introduced at an earlier stage of the syntheses, which increased the overall synthetic efficiency. A copper mediated cross-coupling reaction was selected to couple the two fully glycosylated northern building blocks **2.36** and southern building block **2.37** and form C-11/C-12 bond connection. Yamaguchi

macrolactonization was chosen to close the macrolide ring in a regio-selective fashion.



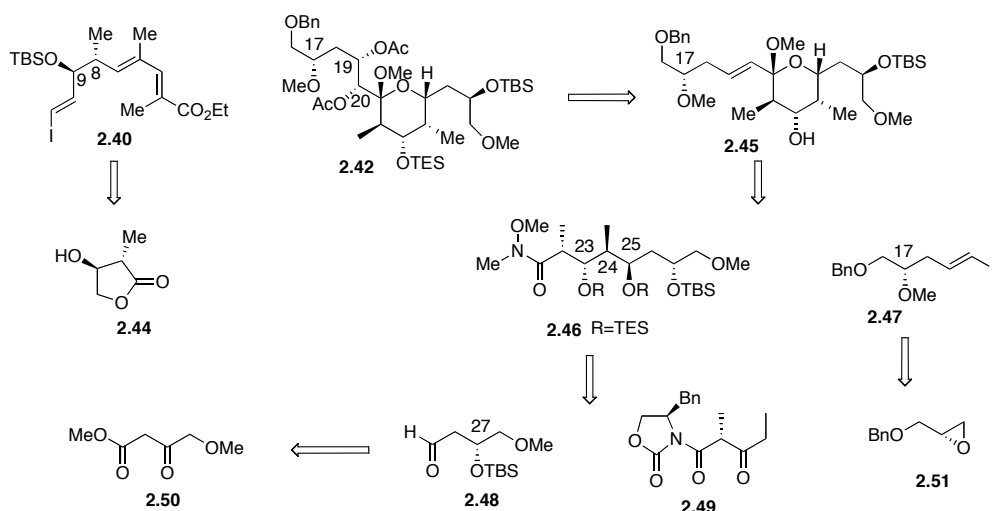
Scheme 2.6 Strategic analysis in Koert's syntheses of apoptolidin A (**2.1**)

The trienoate system in the northern building block **2.36** was prepared by iterative *E*-selective olefination. Vinyl iodide **2.39** was the glycosyl acceptor, and glycosylsulfoxide **2.38** was the glycosyl donor, coupling of these two partners, under Kahne's glycosylation condition, gave the highest α -stereoselectivity. Vinyl iodide **2.39** was prepared from vinyl iodide **2.40**. The stereocenters at C-8 and C-9 in vinyl iodide **2.40** were derived from commercially available starting compound β -hydroxylactone **2.44**. The southern building block **2.28** was prepared by an α -selective glycosylation of desilylated **2.42** with *N*-iodosuccinimide activated disaccharide precursor **2.43**, and a subsequent chelation-controlled Grignard addition of bromide **2.41**.



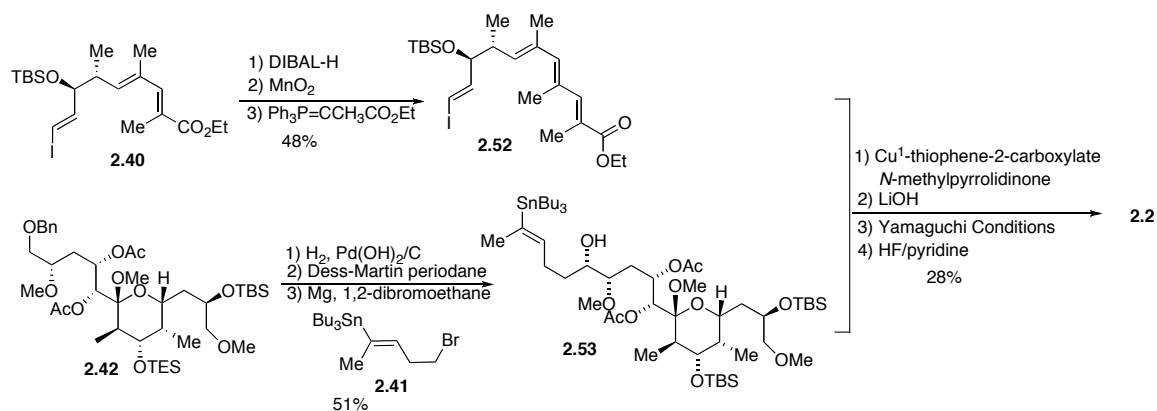
Scheme 2.7 Koert's synthetic strategy for major building blocks **2.36** and **2.37**

The stereochemistry at C-19 and C-20 in pyran **2.42** were set by substrate-controlled dihydroxylation on olefin **2.45**, which was formed by addition of a vinyl lithium reagent derived from vinyl iodide **2.47** to Weinreb amide **2.46**, followed by a spontaneous ketal formation after protodesilylation. The C-17 stereocenter was derived from chiral epoxide **2.51**, a similar chiral epoxide used by Nicolaou's group to introduce chirality at other centers in the apoptolidin backbone structure. Noyori's asymmetric hydrogenation of β -keto ester **2.50** was employed to set the stereocenter at C-27. Evan's dienolate addition and anti-selective reduction were adopted to introduce the stereocenters at C-23, C-24 and C-25 in Weinreb amide **2.46**.



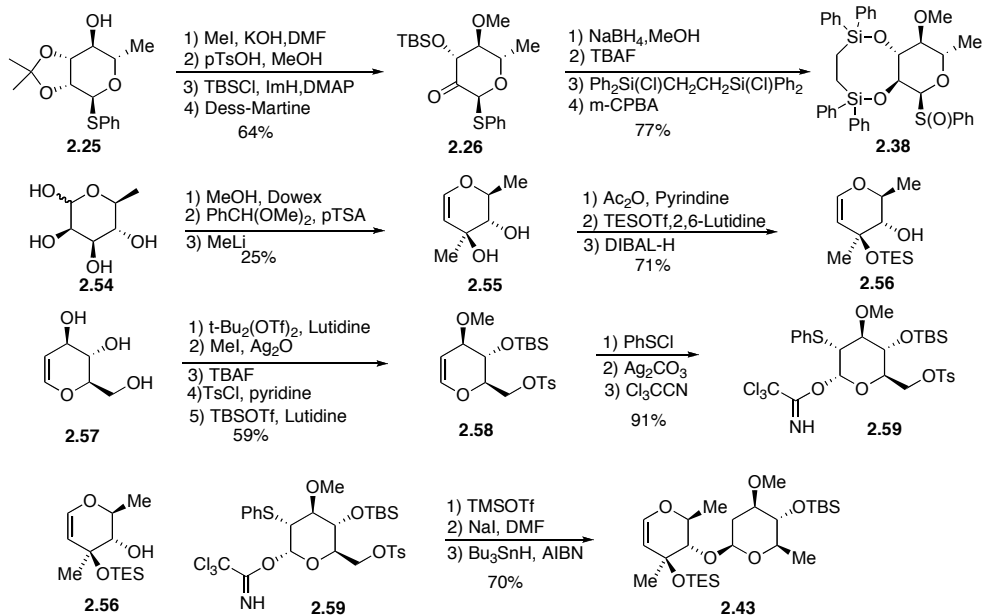
Scheme 2.8 Koert's synthetic strategy for vinyl iodide **2.40** and pyran **2.42**

The Koert's group reported a total synthesis of apoptolidinone A **2.2** in 2001. In which, vinyl iodide **2.40** was converted to vinyl iodide **2.52** following a reduction-oxidation-olefination sequence. Pyran **2.42** was transformed into vinyl stannane **2.53** by reductive debenzoylation, Dess-Martin oxidation and chelation-controlled addition of a Grignard reagent derived from bromide **2.41**. The northern **2.52** and southern halves **2.53** were coupled together under copper promoted cross-coupling conditions, the following hydrolysis of the corresponding ethyl ester under basic condition, macrocyclization under Yamaguchi's condition, and global deprotection completed the total synthesis of apoptolidinone A **2.2**.



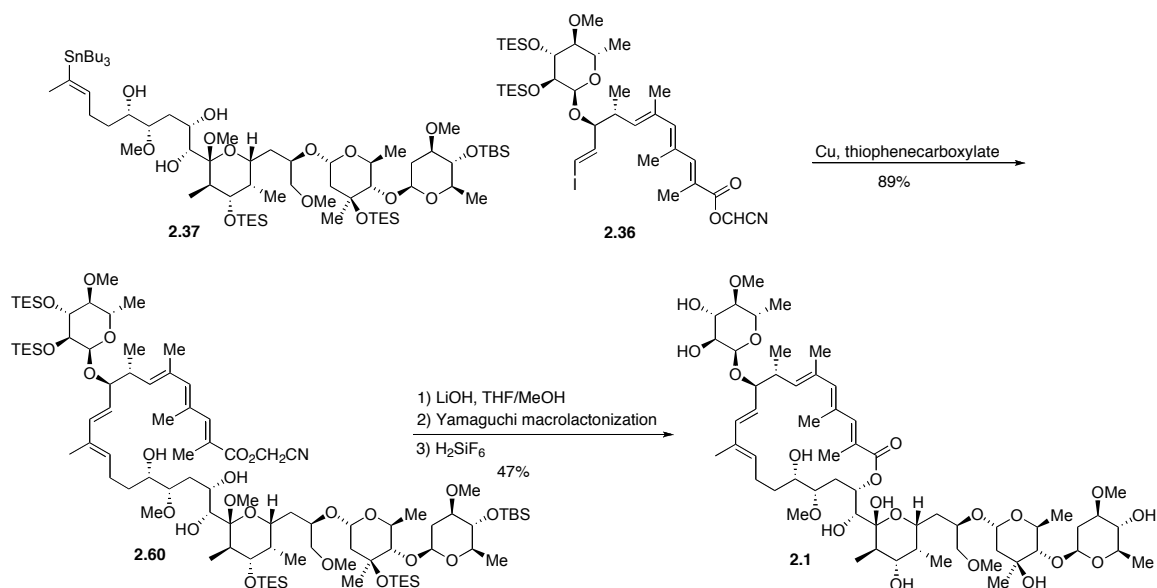
Scheme 2.9 Koert's synthesis of apoptolidinone A (**2.1**)

Two carbohydrate units **2.38** and **2.43** were required in the synthesis of apoptolidin A **2.1**. The glycosyl sulfoxide **2.38** was prepared from acetonide-protected L-rhamnose thioglycoside **2.25**, which was the same starting material used in Nicolaou's preparation of C-9 sugar residue. Methylation of the secondary alcohol, removal of the acetonide protecting group, selective protection 4-hydroxyl as a TBS ether and Dess-Martin oxidation provided ketone **2.26**. Reduction of the ketone in **2.26** with NaBH₄ and desilylation generated an intermediate diol, which was protected employing a new protecting group, 1,1,4,4-tetra-phenyl-1,4-disilabutyl (SIBA). Then *m*-CPBA was used to convert the corresponding phenylthiol to glycosylsulfoxide **2.38**.



Scheme 2.10 Koert's synthetic strategies for two sugar building blocks

The C-27 disaccharide precursor **2.43** was prepared starting from L-rhamnose **2.54** and D-glucal **2.57**. Treatment of benzylidene protected methyl acetal with excess MeLi afforded diol **2.55** via a cyclohexenone intermediate. Selective acylation of the secondary alcohol, TES protection of the tertiary alcohol followed by cleavage of the acetate protecting group furnished olivomycal building block **2.56**. The precursor of the glycosyl donor **2.59** was prepared from D-glucal **2.57**. A 5-step protecting group manipulation provided a tosylate **2.58**, which was converted to trichloroacetimidate **2.59** via a three-step reaction sequence. β -Selective glycosylation of **2.56** with **2.59** in presence of TMSOTf produced a disaccharide, which was reduced to give C-27 disaccharide building fragment **2.43**.



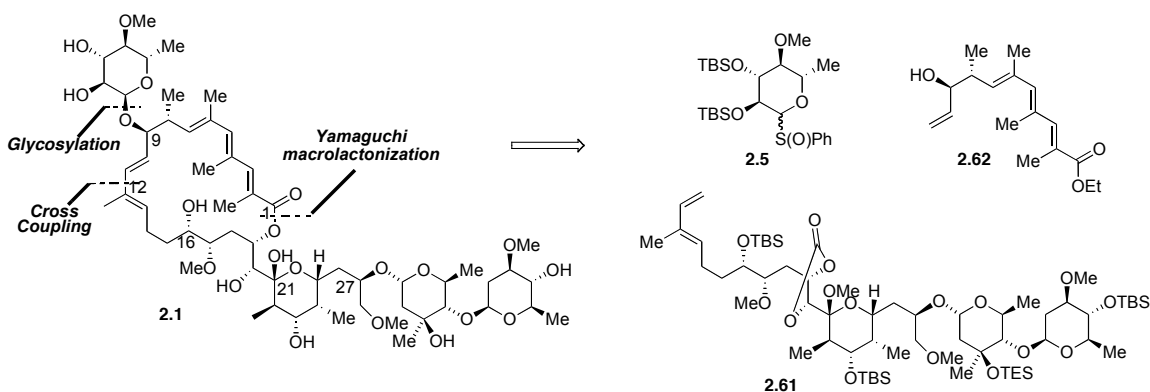
Scheme 2.11 Koert's assembly of apoptolidin A (**2.1**)

Copper (I) mediated cross-coupling conditions optimized by Koert's group in the total synthesis of apoptolidinone A **2.2**, worked well in the coupling reaction between fully glycosylated northern half **2.36** and southern half **2.37**. Cyanomethyl ester **2.60** was then subjected to hydrolysis and Yamaguchi macrolactonization to produce the 20-membered macrolide. Global deprotection with H₂SiF₆ accomplished the total synthesis of apoptolidin A **2.1**.

2.4 Crimmins's Syntheses of Apoptolidinone A and Apoptolidin A

In early 2009, Crimmins's group claimed a total synthesis of apoptolidin A **2.1** following their previously published total synthesis of apoptolidinone A **2.2** and individual sugar units.^{22,25,32} Both Nicolaou and Koert divided the carbon backbone of apoptolidin A **2.1** into northern and southern halves at C-11/C-12 bond and C-1/O-19 bond. Crimmins disconnected the macrolide skeleton at C-

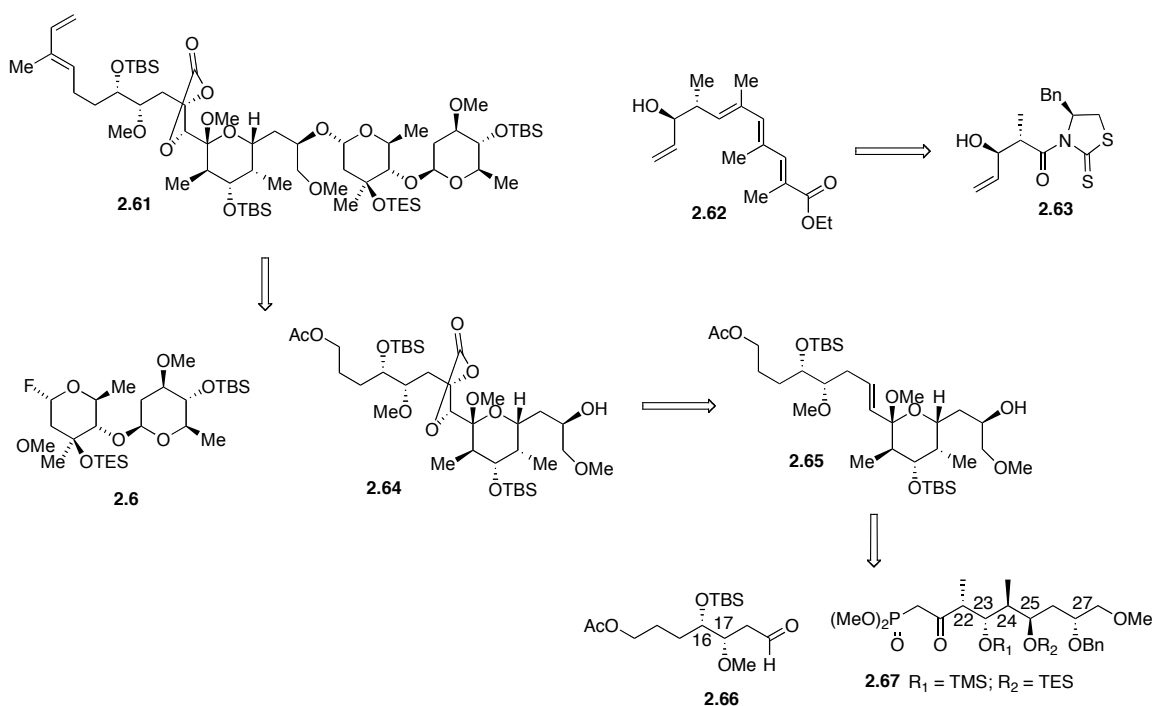
10/C-11 and C-1/O-19 bonds, which was formed via a regio- and stereoselective cross metathesis reaction and a regio-selective Yamaguchi macrolactonization. As previous attempts to couple fully glycosylated northern half with fully glycosylated southern partner resulted unsuccessful, glycosylation of the C-9 oxygen was performed after the cross metathesis, This completed syntheses established 12 of the 24 stereocenters of apoptolidin A **2.1** via diastereoselective aldol reactions with Crimmins's thiazolidinethione chiral auxiliaries.



Scheme 2.12 Strategic analysis in Crimmins's synthesis of apoptolidin A (**2.1**)

The diene unit in the southern part **2.61** was incorporated by two sequential Wittig olefinations, and the C-27 dissaccharide **2.6** was attached directly to ketal **2.64** or at a later stage after installation of diene unit. The C-20 and C-21 stereogenic centers in ketal **2.64** were introduced by Sharpless asymmetric dihydroxylation on olefin **2.65**, which was generated from Horner-Wadsworth-Emmons olefination between aldehyde **2.66** and ketophosphonate **2.67** under Sinisterra and Paterson modified conditions. This strategy was initially developed by Nicolaou's group in the total synthesis of apoptolidin A **2.1**. Both C-

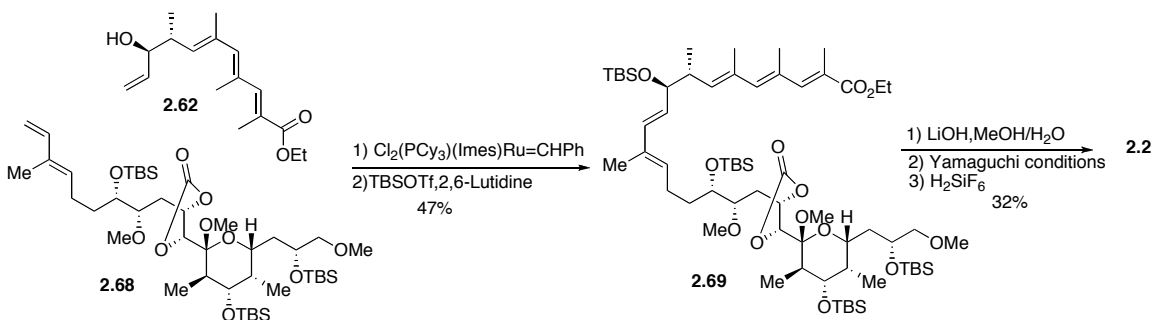
17 stereocenter in **2.66** and C-27 stereocenter in **2.67** were set by glycolate alkylations with Evan's chiral auxiliaries. Chelation controlled nucleophilic addition was used to establish the stereocenter at C-16 in **2.66**. All stereocenters at C-22, C-23, C-24, C-25 in **2.67** were constructed by iterative chlorotitanium enolate aldol reactions. To prepare the northern half building block **2.62**, the known *syn*-aldol adduct **2.63** was chosen as the starting point, the following three iterations of reduction-oxidation-Wittig olefination sequence provided trienoate **2.62**.



Scheme 2.13 Crimmins's synthetic strategy for building blocks **2.61** and **2.62**

In Crimmins's total synthesis of apoptolidinone **2.2**, cross metathesis between trienoate **2.62** and ketal **2.68** in the presence of Grubbs' ruthenium carbene catalyst, and the following TBS protection of secondary alcohol

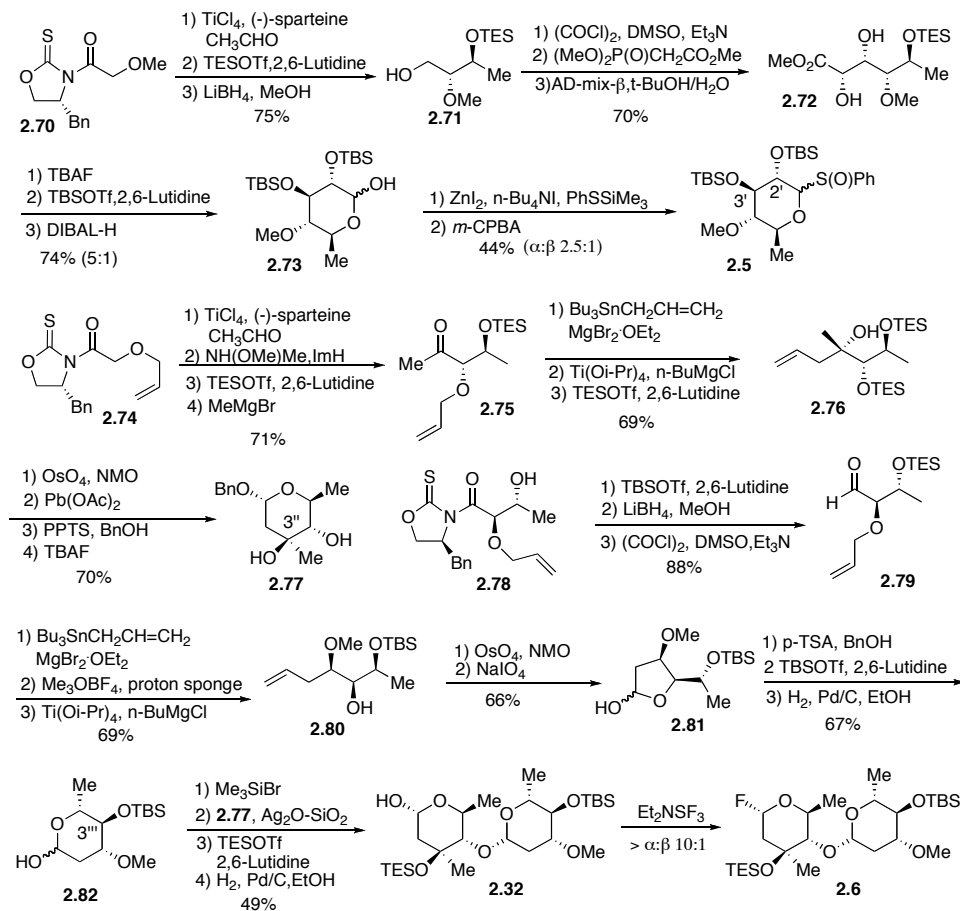
intermediate provided *E*-polyene intermediate **2.69**. Hydrolysis of the ethyl ester and C-19/C-20 carbonate, regio-selective Yamaguchi macrolactonization yielded a lactone intermediate. Finally, treatment with H_2SiF_6 removed the methyl ketal in addition to all the silyl protecting groups, which completed the total synthesis of apoptolidinone A **2.2**.



Scheme 2.14 Crimmins's synthesis of apoptolidinone A (**2.2**)

To prepare the carbohydrate fragments of apoptolidin A **2.1**, both Nicolaou and Koert groups chose natural carbohydrates as starting materials and used chemical methods to modify and transform the known carbohydrates into the desired glycosyl donors. As Crimmins' group employed the same stereoselective glycosylation strategy used by Nicolaou's group, the same glycosyl donors **2.5** and **2.6** were required. In contrast, Crimmins' group developed *de novo* synthetic routes to prepare the three monosaccharides. An asymmetric anti glycolate aldol addition with oxazolidinethione chiral auxiliaries was utilized to establish the C-4 and C-5 stereocenters in each of the monosaccharides. In the synthesis of C-9 glycosyl donor **2.5**, a Sharpless asymmetric dihydroxylation was executed to set the C-2' and C-3' stereocenters. In the synthesis of the C-27 disaccharide **2.6**,

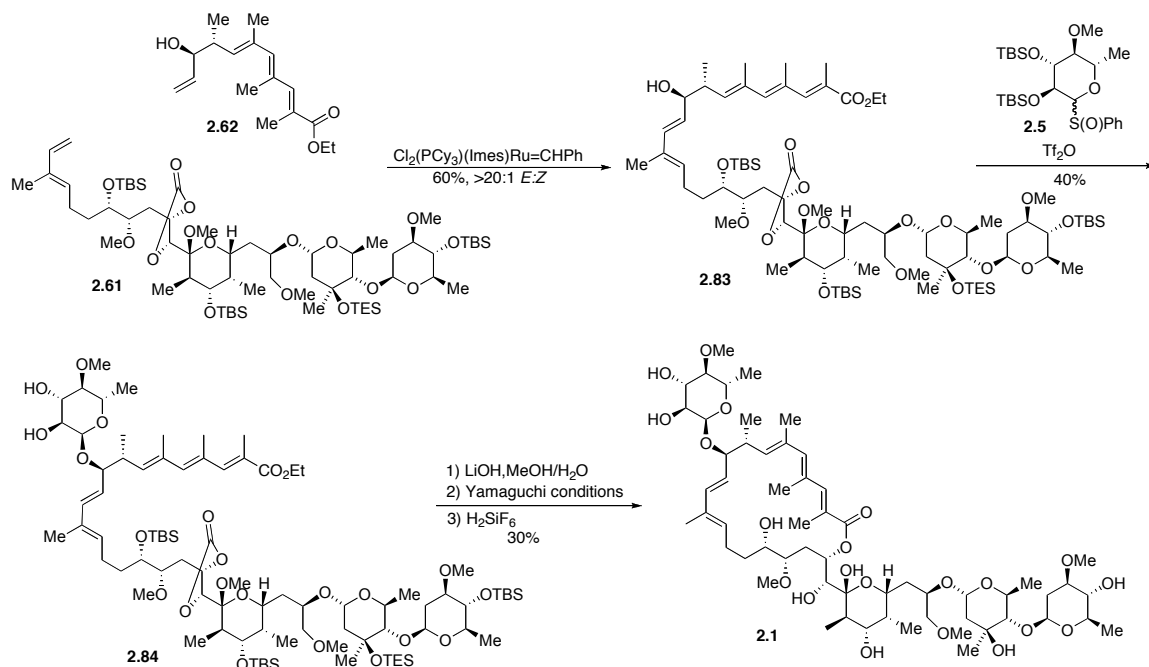
both of the carbinol centers C-3'' and C-3''' were established by a chelation-controlled allylation, and the β -glycoside linkage in C-27 disaccharide precursor **2.6** was formed by the coupling of *in situ* generated glycosyl donor **2.77** with glycosyl receptor **2.82** using Binkley's conditions.



Scheme 2.15 Crimmins's synthetic strategy for two sugar units

In the final construction of apoptolidin A **2.1**, exposure of trienoate **2.62** and fully glycosylated ketal **2.61** to the Grubbs heterocyclic carbene catalyst yielded *E*-isomer **2.83** as the major cross metathesis product. Glycosylation with sulfoxide **2.5** resulted glycoside **2.84** in decent yield and high stereoselectivity.

Finally, regio-selective Yamaguchi macrolactonization following hydrolysis of the ethyl ester and C-19/C-20 carbonate, and global deprotection with H_2SiF_6 released the synthetic target apoptolidin A **2.1**.



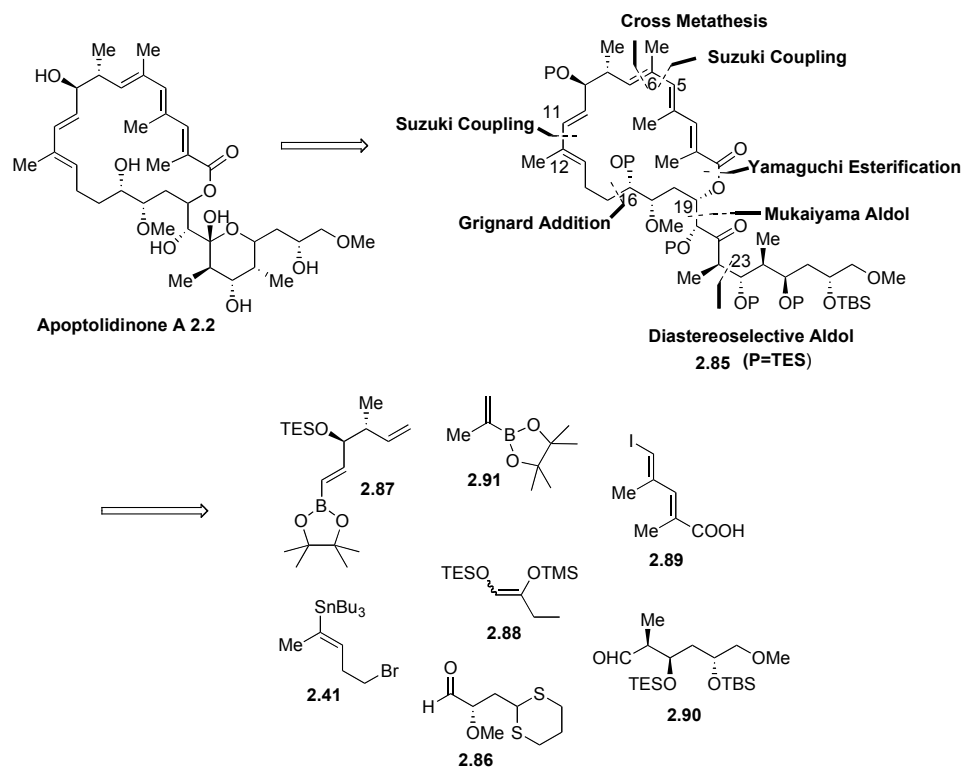
Scheme 2.16 Crimmins's assembly of apoptolidin A (**2.1**)

2.5 Sulikowski's Synthesis of Apoptolidinone A

Our group accomplished the total synthesis of apoptolidinone A **2.1** in 2004.⁴⁰ The synthetic strategy used by our group was different from other groups' approaches in the following aspects: firstly, all other groups' syntheses toward either apoptolidin A **2.1** or apoptolidinone A **2.2** relied on a linear approach to assemble the seco acid and which was subjected to a Yamaguchi macrolactonization to provide the macrocycle in apoptolidin A **2.1**. Whereas, in our approach to apoptolidinone A **2.2**, a Suzuki-Miyaura cross-coupling reaction

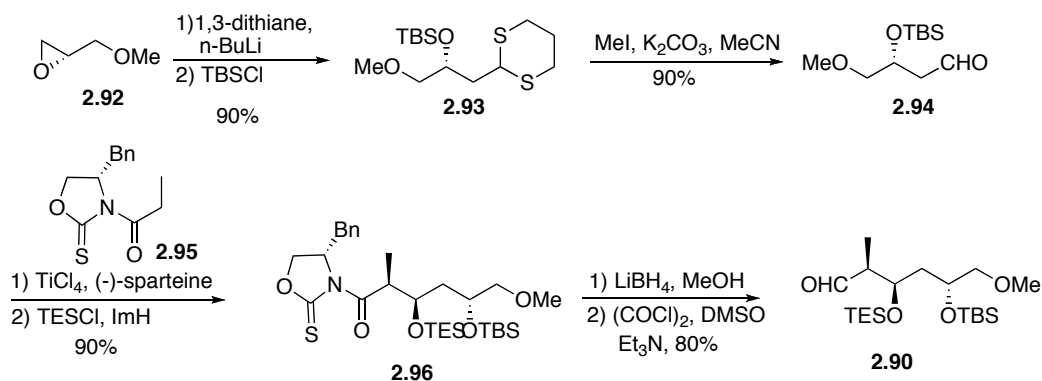
was employed to form C-5/C-6 bond connection and close the macrocycle at late stage. We also explored closure of the macrocycle at C-5/C-6 juncture by using ring-closing metathesis and Horner-Wadsworth-Emmons reactions, but all attempts resulted in failure. It was later reported in Roush's apoptolidin fragment synthesis that C-5/C-6 bond formation via intermolecular Horner-Wadsworth-Emmons olefination was unsuccessful for an unknown reason.⁴¹ To our knowledge, utilizing a cross-coupling reaction to close macrocycle has been rarely reported in the synthesis of the macrolide in polyketide natural products. It was only reported by Toshima's group that they successfully constructed the apoptolidin macrolactone ring via an intramolecular Stille coupling reaction to form C-12/C-13 bond.⁴² Secondly, other groups have employed a Sharpless asymmetric dihydroxylation strategy to establish the stereocenters at C-19 and C-20 without exclusion.^{16,17,18,19,20,21,22,23} Alternatively, our group employed a Mukaiyama aldol condensation reaction to build the *syn* relationship between C-19 and C-20.

In our synthetic strategy, apoptolidinone A **2.2** was generated from macrolactone **2.85** by *in situ* formation of the pyran ring after removal of the protecting groups. In a more convergent fashion, we divided macrolide **2.85** into 7 small building fragments **2.41**, **2.86**, **2.87**, **2.88**, **2.89**, **2.90** and **2.91** by a combination of one chelation-controlled Grignard addition, two diastereoselective aldol reactions, one Grubbs cross-metathesis reaction, one intermolecular and one intramolecular Suzuki-Miyaura coupling reaction.



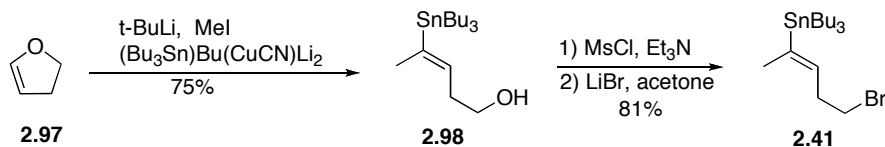
Scheme 2.17 Strategic analysis in Sulikowski's synthesis of apoptolidinone A **2.2**

The synthesis began with the preparation of 7 small building fragments **2.41**, **2.86**, **2.87**, **2.88**, **2.89**, **2.90** and **2.91**. Fragment **2.90** was synthesized from (*R*)-glycidyl methyl ether **2.92**. Epoxide opening with the lithium anion of 1,3-dithiane, TBS protection of the resulting secondary alcohol, and hydrolysis of dithiol acetal with MeI provided aldehyde **2.94**. The following Crimmins *syn* aldol reaction with chlorotitanium enolate derived from **2.95** established the C-24 and C-25 stereocenters and TES protection of the newly formed alcohol gave aldol adduct **2.96**. Reductive removal of oxazolidinethione chiral auxiliary followed by oxidation of the corresponding alcohol under Swern conditions completed the synthesis of aldehyde **2.90**.



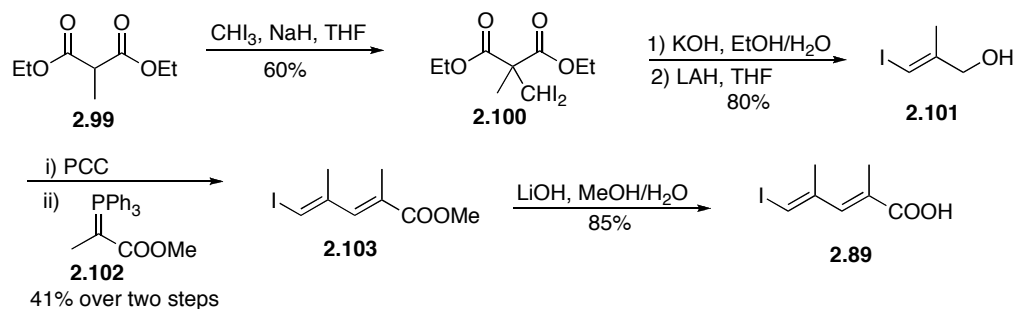
Scheme 2.18 Sulikowski's synthetic strategy for aldehyde **2.90**

The preparation of bromide **2.41** started from dihyrofuran **2.97** following Kocienski's procedure as described in Koert's total synthesis of apoptolidinone A **2.2**.²⁰ Alcohol **2.98** was then transformed into bromide **2.39** via a standard two-step Finkelstein reaction sequence.



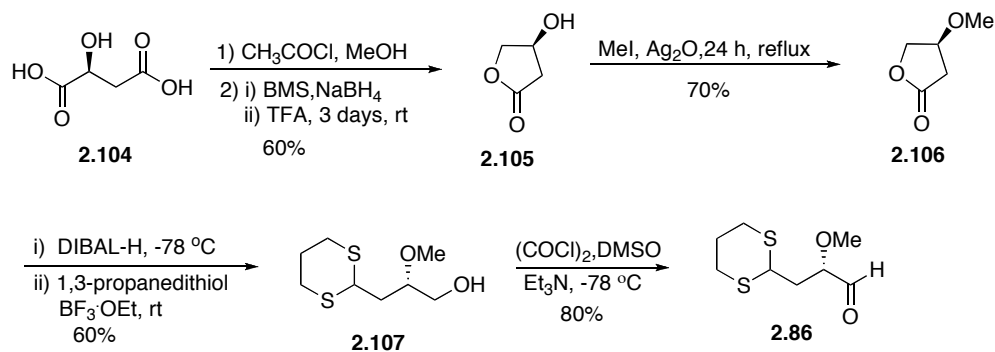
Scheme 2.19 Sulikowski's synthetic strategy for bromide **2.41**

The synthesis of carboxylic acid **2.89** began with 2-methyl diethyl malonate **2.99**, which was converted to allylic alcohol **2.101** via basic hydrolysis, decarboxylation and lithium aluminum hydride reduction. PCC oxidized and *E*-selective Wittig olefination afforded the *trans*-dienoate **2.103**. The methyl ester in **2.103** was then hydrolyzed to provide desired carboxylic acid **2.89**.



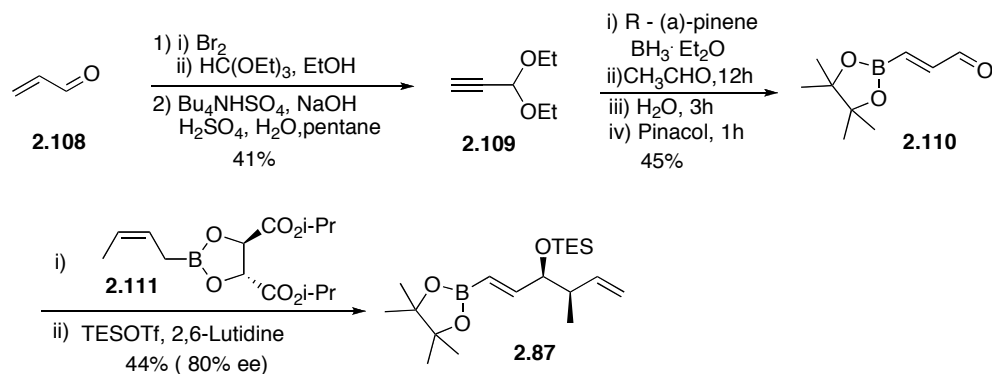
Scheme 2.20 Sulikowski's synthetic strategies for carboxylic acid **2.89**

Our final route to aldehyde **2.86** began with β -hydroxy lactone **2.105**, which was originally prepared from (S)-malic acid **2.104** by 3-step reaction sequence including Fisher esterification, NaBH_4 effected regioselective reduction and *in situ* acid mediated cyclization. Since β -hydroxy lactone **2.105** became a commercially available material at a relatively cheap price, it was used as starting compound for the synthesis of aldehyde **2.86**. Methylation of β -hydroxy lactone **2.105** followed by reduction with DIBAL-H and *in situ* condensation with 1,3-propanedithiol provided dithiane **2.107**. At last, Swern oxidation of the primary alcohol afforded aldehyde **2.86**. So the only stereocenter in aldehyde **2.86**, corresponding to the C-17 carbon in apoptolidin A **2.1** was derived from chiral starting material **2.105**.



Scheme 2.21 Sulikowski's synthetic strategy for aldehyde **2.86**

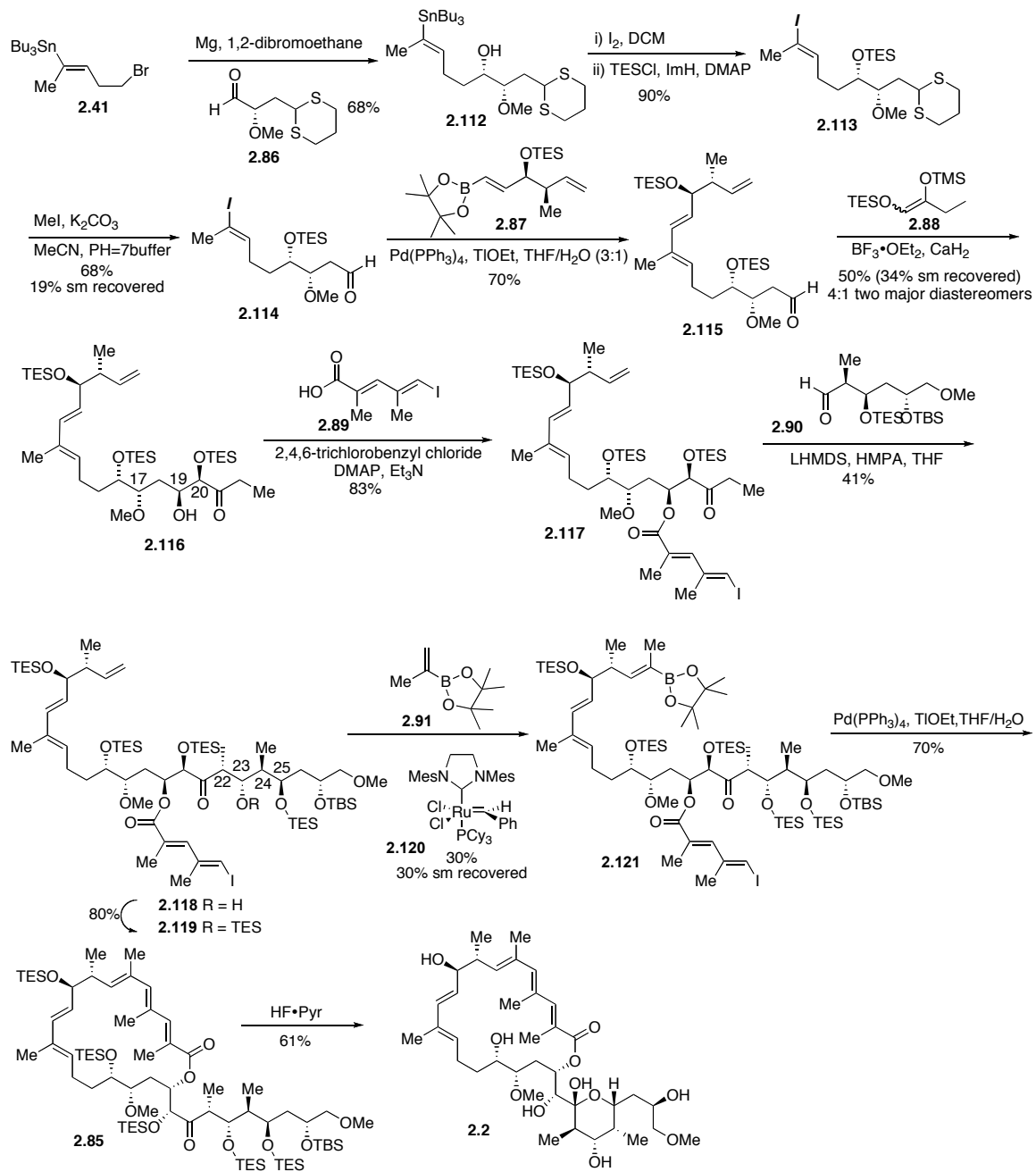
There are two stereocenters in fragment **2.87**, and we planned to establish these centers by using an asymmetric crotylation reaction. The aldehyde **2.110** was prepared from acrolein **2.108**, which was subjected to bromination, aldehyde protection and elimination sequence to afford acetylene **2.109**. Then a Hall's procedure was utilized to convert diethyl acetal **2.109** to 3-boronoacrolein **2.110**. Addition of the Z-crotylboronate reagent **2.111** to aldehyde **2.110** followed by *in situ* TES protection of the newly generated secondary alcohol gave syn homoallylic ether **2.87** with modest enantioselectivity (80% ee) and fair yield (40-43%).



Scheme 2.22 Sulikowski's synthetic strategy for boronate **2.87**

The assembly of these small synthetic fragments began with the construction of C(6)-C(19) large fragment. Grignard reagent generated from bromide **2.41** was added to a solution of aldehyde **2.86** in Et₂O. The addition proceeded through a chelation-controlled process as described in Koert's synthesis of apoptolidin, and gave syn-addition product **2.112** as a single isomer. Sequential iodine-tin exchange and *in situ* silylation of the secondary alcohol delivered vinyl iodide **2.113** in 90% yield over 2 steps. Effective hydrolysis of dithiane **2.113** using the Fetizon-Jurion procedure gave aldehyde **2.114** in 64-74% yield. Suzuki coupling between vinyl iodide **2.114** and vinyl boronate **2.87** under Roush modified coupling conditions (Pd(PPh₃)₄, TIOEt, THF_(aq)) accomplished the synthesis of C(6)-C(19) fragment **2.115** in 71% yield consistently. Mukaiyama aldol condensation between advanced intermediate **2.115** and enol silane **2.88** afforded ketone **2.116** as the major diastereomer, the ratio of the two major isomers was 4:1. The relative stereochemistry of C(17)-C(20) was assigned based on the observed coupling constant between H(19) and H(20) ($J_{19,20}=3.5$ Hz) and the 1,3-asymmetric induction model proposed by

Evans and coworkers for β -methoxyaldehydes. Yamaguchi esterification of Mukaiyama aldol product **2.116** with carboxylic acid **2.89** provided ester **2.117**. A matched double diastereoselective aldol reaction between aldehyde **2.90** and lithium enolate generated from ketone **2.117** under kinetic deprotonation condition, afforded syn aldol adduct **2.118** as a single stereoisomer in 41% yield (57% yield based on recovered starting material). The C-23 hydroxyl group was protected as TES ether **2.119**, which was then subjected to cross metathesis with propenyl boronate **2.91** in the presence of Grubbs secondary generation catalyst **2.120** and furnished vinyl pinacol boronate **2.121** in 30% yield (*E:Z*=10:1). The geometric byproduct could be detected by HPLC, however, it couldn't be completely isolated from other byproducts. Using the same Grubbs catalyst, we switched the solvent from CH₂Cl₂ to toluene, which allowed us to alleviate the reaction temperature to 50 °C. Under these optimized conditions, the amount of the geometric isomer was significantly reduced. Subjection of vinyl pinacol boronate **2.121** to Roush modified Suzuki coupling condition afforded the macrolide **2.85**. Finally, exhaustive global desilylation with HF·Pyridine and *in situ* pyran cyclization achieved apoptolidinone A **2.2** in 61% yield.



Scheme 2.23 Sulikowski's assembly of apoptolidinone A **2.2**

CHAPTER III

PREVIOUS STUDIES ON THE MECHANISM OF ACTION OF APOPTOLIDIN A AND APPLICATION OF A PROBE DERIVED FROM APOPTOLIDIN A TO TARGET IDENTIFICATION

3.1 Introduction

Cancer, which is characterized as uncontrolled cell growth, is an example of a disorder in which genetic disruption of the normal mechanism of cell proliferation/death leads to cell accumulation. Some types of cancers exhibit an over-proliferation of cells while others display decreased elimination of cells. Apoptosis and autophagy are two major types of programmed cell death, which are mediated by genes or their protein products involved in various signaling pathways required to execute cell killings (i.e. elimination of cells). Programmed cell death is different from necrotic cell death, which is the result of acute tissue injury, infection, cancer, infarction, poisons and inflammation. These different forms of cell death can be differentiated by distinctive cell morphological changes.

Historically, cancer chemotherapy has primarily utilized anticancer drugs that inhibit the cell division of fast growing cancer cells at different stages of the cellular cycle, which results in disruption of vital metabolic functions. It is now generally accepted that programmed cell death plays an important role in the expressed cytotoxicity of anticancer drugs. Information about the correlations between dysregulation of programmed cell death and the development and

progression of cancers, and understanding of the molecular mechanisms of the cell death and molecular switches between different cell death pathways have unraveled the mechanisms of drug action and paved the way for more novel cell-selective therapeutic approaches which may increase the effectiveness of cancer treatment.^{43,44,45,}

3.2 Apoptosis and Autophagic Cell Death

The concept of apoptosis was first postulated in 1972 to describe programmed cell death. Apoptotic cells are morphologically characterized by chromatin condensation, nuclear fragmentation, plasma membrane blebbing, cell shrinkage and finally formation of apoptotic bodies.⁴⁶ The morphological changes associated with apoptosis are directly or indirectly caused by a proteolytic cascade activation of caspases, which are a group of intracellular cysteine-aspartic-acid-proteases.⁴⁷

The mechanism of apoptosis is extremely complex and sophisticated. To date, two different apoptosis mechanisms have been well defined: the intrinsic or mitochondrial pathway and the extrinsic or death receptor pathway. However, these two pathways are linked and some effectors in one pathway can also influence the other. In the death receptor pathway, death factors (TNF- α or Fas) bind to death receptors (TNF-R-1) on the cell surface, which recruit multiple pro-caspase-8, leading to the activation of caspase-8. Regarding the mitochondrial pathway, internal signals (such as oxidative stress, DNA damage, p53 activation and hypoxia) cause the release of pro-apoptotic factors leading to the release of

cytochrome c from mitochondria inter-membrane space, which then activate caspase-9 by binding to Apaf-1 and pro-caspase-9. The release of cytochrome c is controlled by Bcl-2 family proteins, which include pro-apoptotic members (such as Bax, Bak, Bad) and anti-apoptotic members (such as Bcl-2, Bcl-x, bcl-w). Bcl-2 family proteins can regulate mitochondria membrane permeability by an unknown mechanism.^{47,48,49}

Autophagic cell death was initially described by Schweichel and Merker in 1973.⁵⁰ However, it was neglected for the following three decades by the majority of the scientific community because of the dominant concept of apoptosis versus necrosis. Recently, increasing evidence indicates that autophagic cell death plays an important role in tumor development. There are many literature reviews on the topic of autophagic cell death and its role in anticancer therapy.^{44,45,48,51} The distinctive morphological change of autophagic cell death is the formation of double membrane autophagic vacuoles in the cytoplasm. An autophagic vacuole or autophagosome is derived from part of the endoplasmic reticulum or from the cytoplasmic lipid pool. The autophagosome fuses with lysosome to form autolysosome in which the cytoplasmic contents are degraded by lysosomal hydrolytic proteases. The degraded materials are then released into cytosol for recycling.⁵⁰

Many signaling pathways have been implicated in the mechanism of autophagic cell death. However, the mechanism details are not well understood. Anticancer treatment and low nutrient conditions are thought to be the initial signals needed to induce autophagic cell death in cancer.^{44,45,48,51}

Apoptosis and autophagic cell death are not completely separate.⁴⁸ It's been observed that inhibition of apoptosis can trigger autophagic cell death, and inhibition of autophagic cell death can induce, delay or antagonize apoptosis. However, the molecular mechanisms underlying the interaction between apoptosis and autophagic cell death are not known till now.

3.3 Stanford Group Studies on The Action Mechanism of Apoptolidin A

In the preliminary biological tests, Seto's group observed condensed chromatin and fragmented nuclei by staining with Hoechst Dye. 33258 when E1A transformed rat glia cells (RG-E1A-7) were treated with 1 $\mu\text{g}/\text{mL}$ of apoptolidin A **3.1** for 24 hours. This observation led Seto's group to conclude that the cell death induced by apoptolidin A **3.1** is resulted from apoptosis. This led Khosla and co-workers at Stanford University to compare the structure of apoptolidin A **3.1** with other cytotoxic macrocyclic polyketides with known action mechanism of action, and conducted a series of experiments utilizing molecular and cell-based pharmacological assays to propose a mechanism of action of apoptolidin A **3.1** leading to apoptosis.^{52,53,54}

Since the molecular mechanisms of apoptosis are well understood, the Khosla group first examined knockouts of key apoptosis related proteins, such as p53, BCL-2 and caspases, on apoptolidin induced cell death using sensitive cell lines including mouse B cell lymphoma cells and human colon cancer cells HCT116. These experiments showed that the cell death induced by apoptolidin A **3.1** was independent of p53 status, inhibited by BCL-2 and dependent on the

action of caspase-9. These results suggested that the biological responses of apoptolidin A **3.1** were associated with a target within the mitochondria pathway. Next, the Stanford group identified structurely related natural products of known mechanism of action that demonstrated a high correlation in the cytotoxic profile with apoptolidin when evaluated against the NCI 60-cell line panel. To this end, the Khosla group searched chemical database for polyketides with similar structure features to the apoptolidin A **3.1**. This structural search led to the identification of ossamycin **3.3**, cytovaricin aglycone **3.4**, and oligomycin A **3.5**. Interestingly, this group of polyketides are all inhibitors of mitochondrial F_0F_1 -ATPase, and all display a similar pattern of cytotoxicity against NCI-60 human cancer cell line panel. These results prompted the Khosla group to evaluate the ability of apoptolidin A **3.1** to inhibit mitochondrial F_0F_1 -ATPase, which led to the conclusion that apoptolidin A **3.1** was an inhibitor mitochondrial F_0F_1 -ATPase ($K_i = 5 \mu\text{M}$).^{52,53}

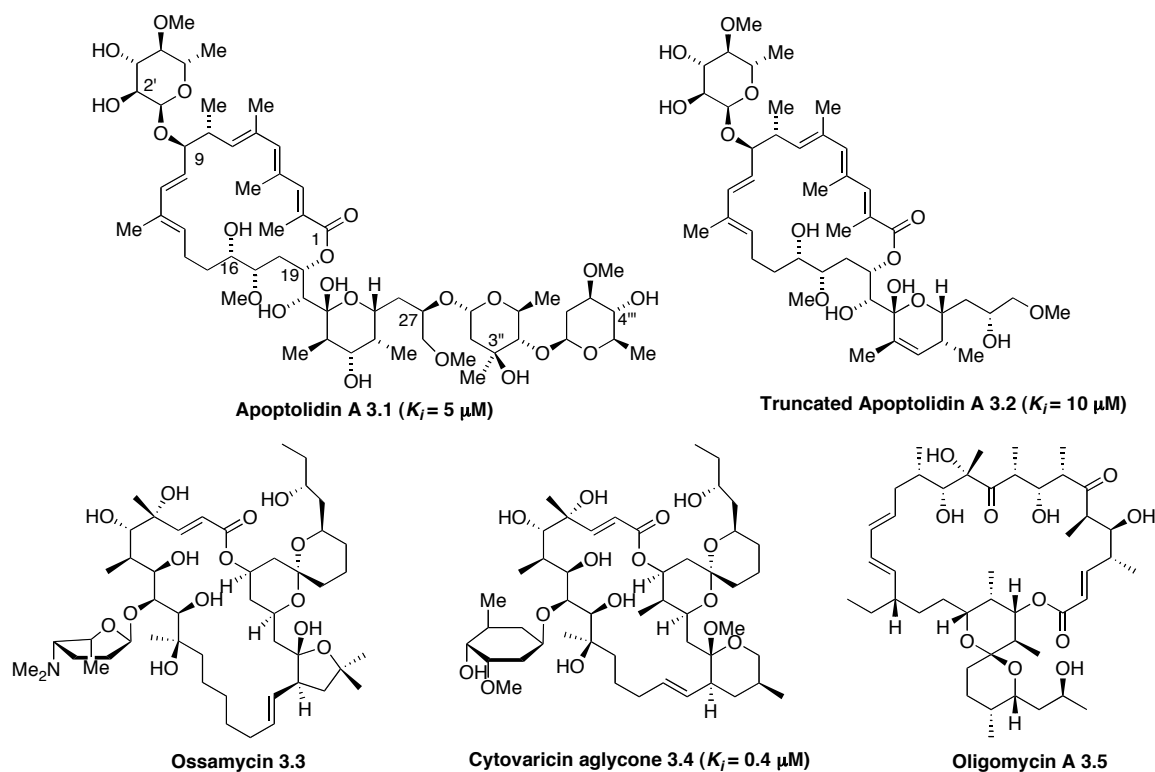


Figure 3.1 Structures of apoptolidin A (**3.1**), truncated apoptolidin A (**3.2**), Ossamycin (**3.3**), cytovaricin aglycone (**3.4**) and oligomycin (**3.5**)

Examination of the pattern of cytotoxicity of macrolides shown in Figure **3.1** against the NCI-60 human cancer cell line panel shows leukemia cell lines including HL-50, K-562, MOLT-4, RPMI-8226, CCRF-CEM and SR are particularly sensitive to those structurally similar macrolides. In contrast, a small group of cell lines including HCT-116, HT-29, IGR-OV-1, M14, SN12C, 780-0 and SF-539 do not respond to the same group of macrolides. The common characteristic of the latter group of cells is that they have low ATP demand, and all exhibit a high level of anaerobic carbon metabolism by the Embden-Meyerhof pathway even in the presence of oxygen, a phenomenon known as the Warburg

effect, while the leukemial cells have high ATP demand from mitochondria and do not exhibit Warburg effect.^{55,56,52,53}

Oxmate is an inhibitor of lactate dehydrogenase and 2-deoxyglucose is an inhibitor of Embden-Meyerhof pathway. Theoretically, these inhibitors can modulate the carbon flux from Embden-Meyerhof pathway to mitochondria, and increase the cell demand for ATP biosynthesized aerobically from mitochondria. Further experiments revealed that apoptolidin A **3.1** non-sensitive cells that exhibit the Warburg effect indeed became sensitive to apoptolidin A **3.1** when incubated with either oxmate or 2-deoxyglucose. These results provided additional evidence on the close correlations between the mitochondria pathway and apoptolidin A **3.1** induced cell death.⁵²

In Khosla's structure comparison study, the truncated apoptolidin A **3.2** was obtained by acidic methanolysis of apoptolidin A **3.1**. The biological activity of this degradation product **3.2** and apoptolidin A **3.1** were compared in a yeast ATPase assay and cell assays. The truncated apoptolidin **3.2** retained substantial activity against yeast mitochondrial ATPase ($K_i = 10 \mu\text{M}$) comparing to apoptolidin A **3.1** ($K_i = 5 \mu\text{M}$); whereas, the apoptolidin derivative **3.2**, without C-27 disaccharide, only retained 1% cellular toxicity relative to apoptolidin A **3.1** using apoptolidin sensitive cell lines (a human breast tumor cell line MCF-7 and a murine B cell lymphoma cell line LYas). To explain the significant drop in cellular cytotoxicity of **3.2** Khosla proposed that the missing sugar units of **3.2** are important in facilitating the transportation of the apoptolidin structure to its cellular targets F_0F_1 -ATPase.⁵⁴

3.4 SAR Studies and Target Revaluation

Several other groups have investigated the cytotoxicity of apoptolidin A **3.1** and its derivatives against different sensitive human cancer cell lines.^{15,19,21,57} Both Nicolaou's and Koert's groups observed that apoptolidin A derivative **3.6** without a C-27 disaccharide lost significant biological activity.^{19,21} These observations are consistent with Khosla's hypothesis that the aglycone structure contributes to the biological activity and carbohydrates facilitate cellular transport or are directly involved in binding to the cellular target.

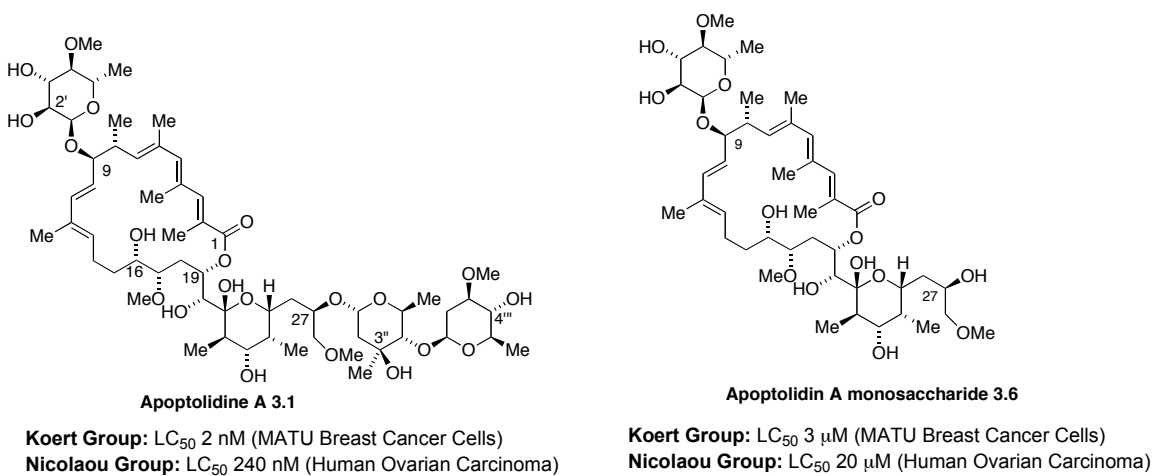


Figure 3.2 Biological activities of apoptolidin A (**3.1**) and C-9 sugar congener (**3.6**)

Wender's group devised a systematic method for the preparation of hydroxyl protected derivatives of apoptolidin A by semi-synthesis, and conducted extensive studies on the structure and biological activity relationship using both a cell-free mitochondria F₀F₁-ATPase assay and apoptolidin sensitive Ad12-3Y1 cells.^{15,57} The observed biological activity in these two assays did not correlate.

First, isoapoptolidin A **3.7** ($IC_{50} = 17 \mu\text{M}$) was 24-fold less active than apoptolidin A **3.1** ($IC_{50} = 0.7 \mu\text{M}$) in the enzyme assay. Whereas, apoptolidin A **3.1** ($GI_{50} = 0.0065 \mu\text{M}$) and isoapoptolidin A **3.7** ($GI_{50} = 0.009 \mu\text{M}$) are equally potent in the cell assay, which is consistent with the facile isomerization between these two compounds under the assay conditions. Second, apoptolidin A **3.1** ($GI_{50} = 6.5 \text{ nM}$) induces cell death at sub-micromolar concentration. However, its potency decreased by 2 orders of magnitude in the cell free enzyme assay ($IC_{50} = 0.7 \mu\text{M}$). Third, apoptolidin derivatives displayed different potencies in the cell free mitochondria F_0F_1 -ATPase assay and antiproliferative cell assay. Based on these observations Wender suggested a different cellular target exists or apoptolidin's mechanism of action is significantly more complex.¹⁵

Table 3.1 *In vitro* and *In vivo* biological activities of apoptolidin A **3.1** and isoapoptolidin A **3.7**

Compounds	$IC_{50}(\mu\text{M})(F_0F_1\text{-ATPase})$	$GI_{50}(\mu\text{M}) (\text{Ad12-3Y1})$
Apoptolidin A (3.1)	0.7 ± 0.25	0.0065
Isoapoptolidin A (3.7)	17 ± 0.25	0.009

3.5 Application of Probes Derived from Apoptolidin A to Target Identification

As the *in vivo* cell cytotoxicity of apoptolidin A **3.1** and various analogues does not always correlate with *in vitro* mitochondria F_0F_1 -ATPase inhibition, Wender's group turned their attention to the construction of photo-affinity probes

of apoptolidin A for the identification of alternate protein targets.⁵⁸ Photoaffinity techniques were developed for the identification of protein targets by photochemical labeling of interacting sites by the interacting ligand (small molecule).^{59,60} A photoaffinity probe is composed of three general elements: a binding group that promotes interactions with the active sites of specific classes of proteins, a reactive group (photoaffinity label) that covalently labels these active sites via photoreactions, and a reporter group (e.g., radioactive fluorophore or biotin) for the visualization and affinity purification of probe-labeled proteins. As natural products are protective weapons produced by organisms for extrogenous threats or stress, they can cause various biological responses. Therefore, natural product photoaffinity probes have been used as chemical-biological tools to elucidate the cellular mechanisms of such products.^{59,61,62,63,64,65,66}

According to Jankowski's dissertation (Stanford University, 2004), four different photo-affinity label (PAL) conjugates of apoptolidin A using three different photo-reactive functionalities were synthesized and evaluated.⁵⁸ Specifically, ATFB-based apoptolidin PAL **3.8**, one benzophenone-based PAL **3.10**, and two diazirine-based probes **3.9** and **3.11** were prepared by chemical synthesis. They expected that these PAL apoptolidins would form covalent bonds with specific protein target through C-H insertion upon irradiation; the targeted protein is then purified by affinity chromatography and identified using mass spectrometry analysis. Unfortunately, none of these four photo-affinity systems leads to the identification of protein targets of apoptolidin A **3.1**. Since further biological activity screening revealed these four PAL apoptolidins maintained

moderate toxicity of apoptolidin A, the failure of applying PAL labeled apoptolidin to identify a cellular target was rationalized by Wender's group being the following reasons: First, apoptolidin A **3.1** will undergo photo-isomerization to form two new unstable apoptolidins when exposed to light of 300 nm wavelength, the structures of the two apoptolidin A photoisomers were not completely assigned.^{67,58} Therefore it is highly possible that PAL attached apoptolidin derivatives decompose and/or rearrange before binding to the cellular target; PAL may cross interact with cell lysates and lead to non-specific labeling; PAL on sugar units may affect the affinity to target. In conclusion, PAL is not a suitable choice for construction of apoptolidin probe for identification of apoptolidin's target protein.

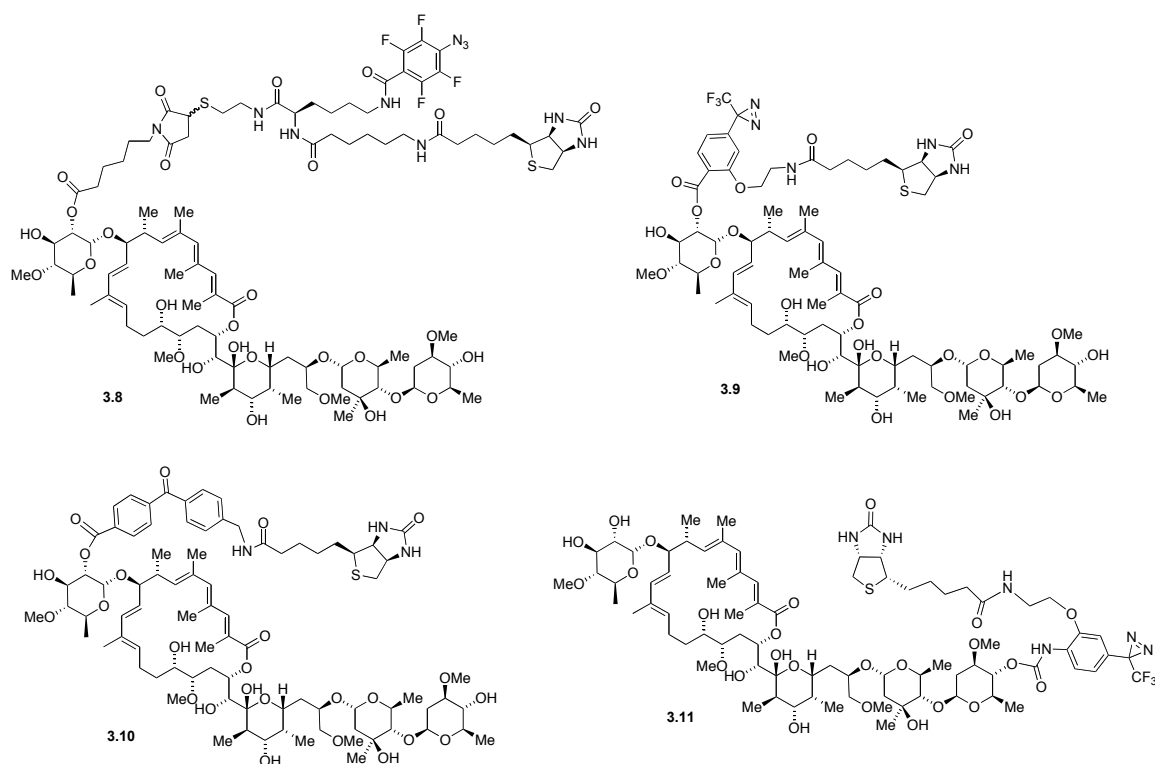


Figure 3.3 Wender's PAL probes of apoptolidin A

3.6 Dissertation Statement

Since the discovery of apoptolidin A by Seto's group in 1997, organic chemists have devoted significant efforts in the investigation of convergent strategies towards total synthesis of apoptolidin A and its analogues. In the parallel research, chemists in collaboration with biologists have made extensive contribution in the exploration of the action mechanism of apoptolidin A in various ways. Although mitochondrial F_0F_1 -ATPase was proposed by Khosla's group to be a promising cellular target of apoptolidin A, results from Wender's SAR studies suggested the existence of a more relevant target to apoptolidin cytotoxicity. This dissertation describes recent efforts by Sulikowski's group in construction of an apoptolidin probe towards the cellular target identification of apoptolidin A.

CHAPTER IV

CHEMICAL SYNTHESSES OF 6-NORMETHYL APOPTOLIDINONE A (APOPTOLIDINONE D), 2-NORMETHYL APOPTOLIDINONE D AND 12-OXY-APOPTOLIDINONE D

4.1 Introduction

Our group accomplished a total synthesis of apoptolidinone A **4.1** in 2004.⁴⁰ However, our interest in apoptolidin A **4.1** was not limited to the chemical synthesis of the aglycone of this compound, but to its use as a biological probe for target identification studies. In order to investigate apoptolidin A **4.1** as a biological probe, unnatural apoptolidinones including 6-normethyl apoptolidinone A **4.2**, 2,6-dinormethyl apoptolidinone A **4.3**, and 12-oxy-apoptolidinone D **4.4** were selected for chemical synthesis. Comparison of **4.2-4.4** to the parent aglycone **4.1** reveals apoptolidinone **4.2** lacks one methyl group on C-6 position, **4.3** lacks two methyl groups (C-2 and C-6) and **4.4** lacks a methyl group at C-6 position and features an extra hydroxyl group at C-12 methyl terminal that we projected as a point of attachment to either a fluorescent or affinity tag reagent.

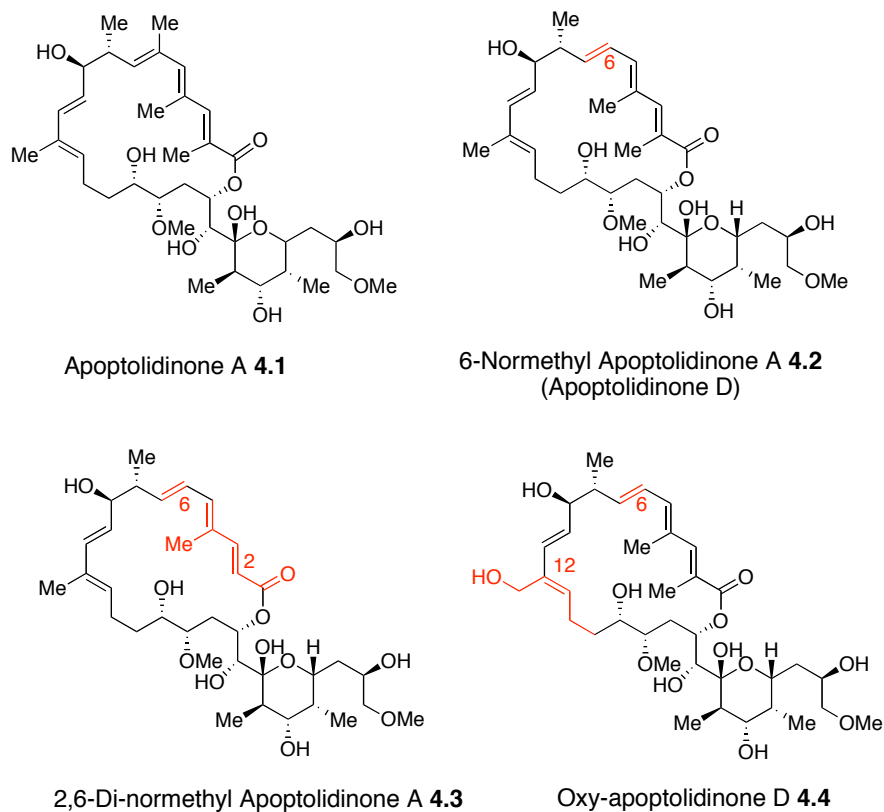
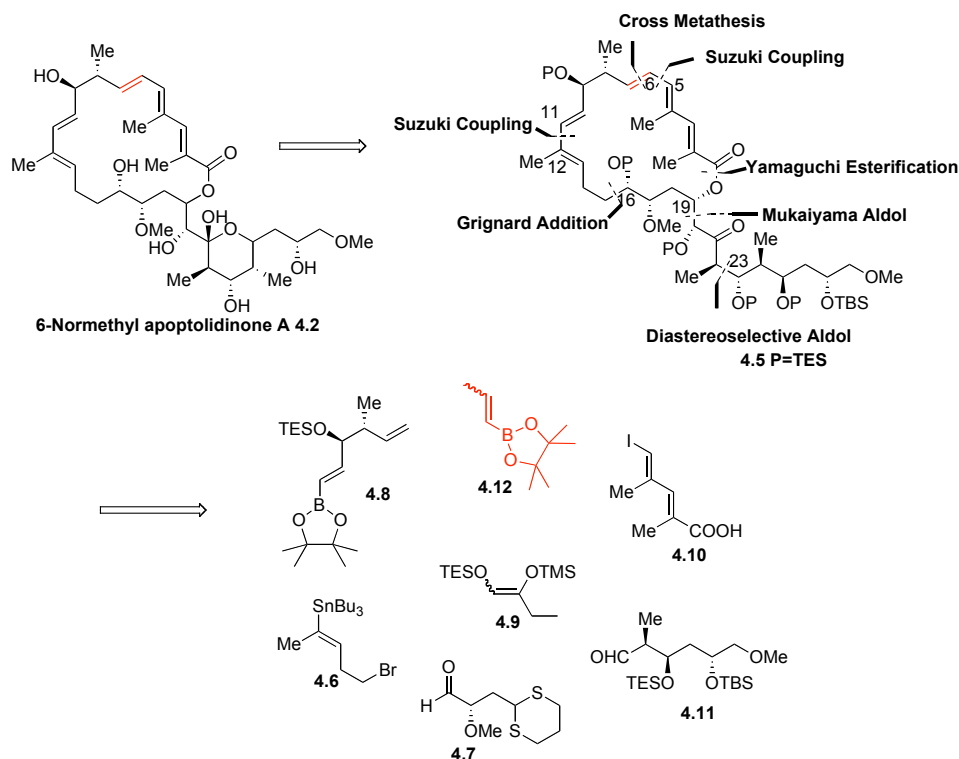


Figure 4.1 Structures of apoptolidinone A and unnatural apoptolidinones

4.2 Total Synthesis of 6-Normethyl Apoptolidinone A

The successful synthetic strategy leading to apoptolidinone A **4.1** featured two Suzuki cross-coupling reactions, two aldol reactions, one chelation controlled Grignard addition, a Yamaguchi esterification and a cross-metathesis reaction. Since 6-normethyl apoptolidinone A **4.2** lacks only one methyl group on C-6 carbon, the synthesis of **4.2** required only a change in the cross-metathesis partner from isopropenyl boronate to 1-propenyl boronate **4.12**, which can be easily prepared from 1-propenyl magnesium bromide. In the course of assembling the 6-normethyl apoptolidinone A **4.2**, we modified the synthesis of vinyl boronate **4.8** and carefully examined the stereoselectivity of the key

Mukaiyama aldol reaction, and explored an alternative route for introduction of the C(22)-C(23) bond connection by reversing the original sequence of two aldol reactions. Fragments **4.6-4.11** were prepared following the procedures developed by our earlier total synthesis of apoptolidinone A **4.1**.²⁴ The work included in this section has been published in the *Journal of Organic Chemistry*.⁶⁸

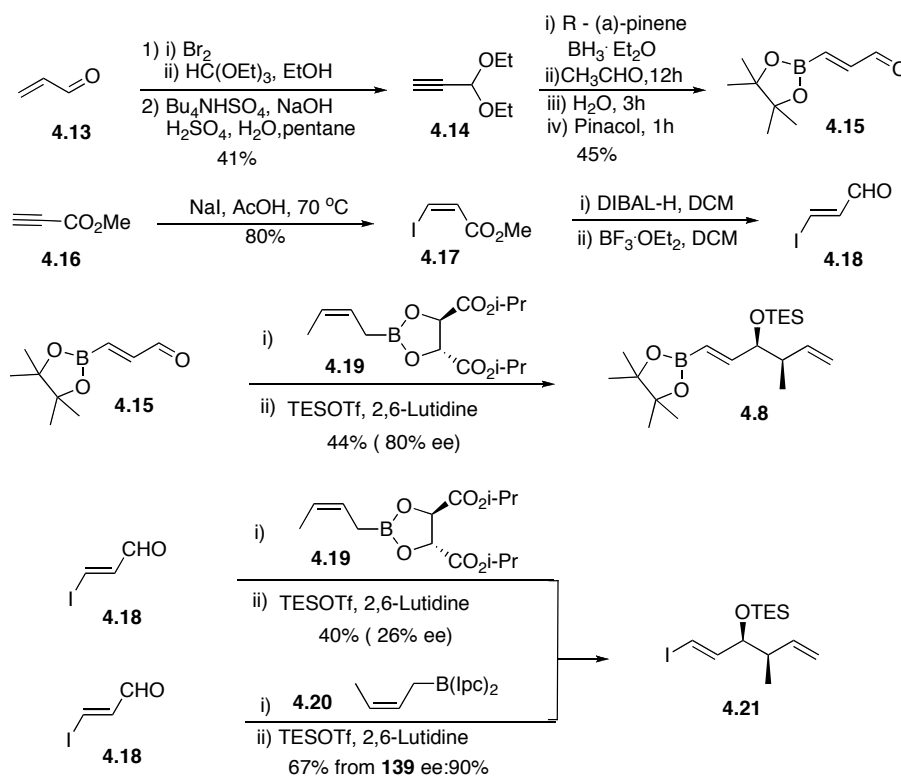


Scheme 4.1 Synthetic strategy for 6-normethyl apoptolidinone A **4.2**

4.2.1 Preparation of Vinyl Boronate **4.8**

In our previous synthesis of vinyl boronate **4.8**, a Roush crotylation employing (*Z*)-crotyl boronate **4.19** and aldehyde **4.15** provided **4.8** in 44% yield and 80% ee.^{69,70} In order to improve the enantioselectivity of the crotylation

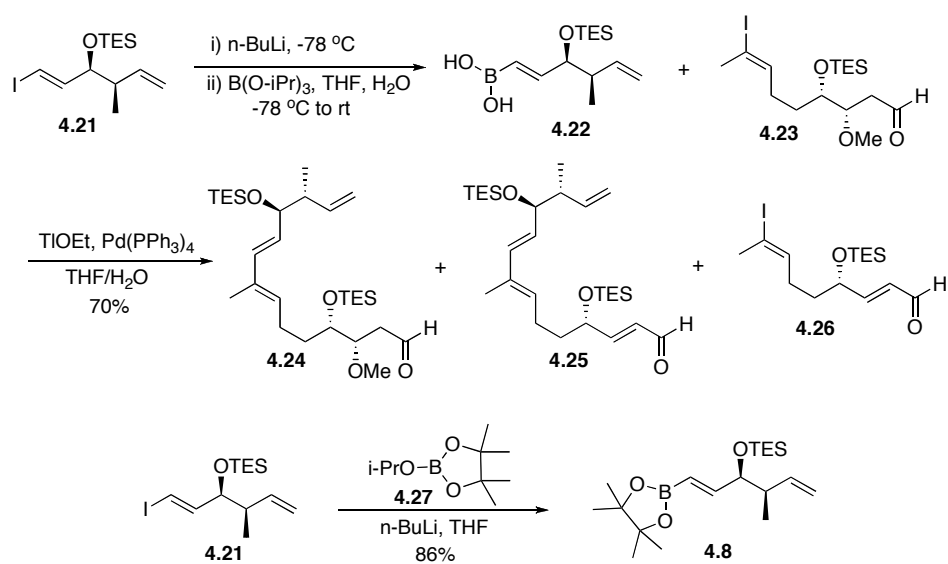
process, a previous group member Dr. Qingsong Liu, compared Roush's **4.19** and Brown's **4.20** crotylating agent addition to 3-iodoacrolein **4.18**.⁷¹ The crotylation substrate **4.18** was easily accessed from methyl propiolate **4.16** following a known procedure.^{72,73} The enantiomeric excess for **4.19** was only 26% ee. On the other hand, the addition of Brown's reagent **4.20** to **4.18** provided the desired *syn* crotylation product **4.21** in superior yield (67%) and higher enantiomeric excess (90% ee).^{73,74,75}



Scheme 4.2 Synthesis of vinyl iodide **4.21**

Towards the assembly of aldehyde **4.24**, vinyl iodide **4.21** was converted to vinyl boronic acid **4.22**, which was employed *in situ* in a Suzuki-Miyaura cross-

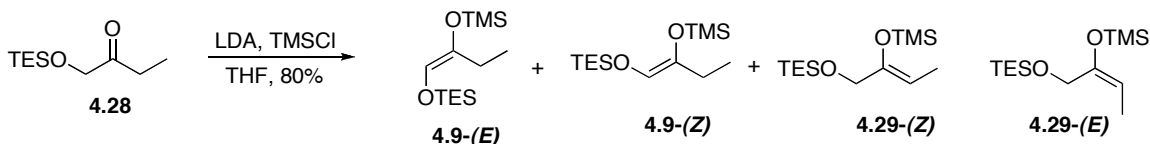
coupling (SMCC) with vinyl iodide **4.23** (Scheme **4.3**). However, the SMCC reaction was proven to be irreproducible and led to several side-reactions. Careful analysis of the crude ^1H NMR spectra of SMCC reaction indicated that three products resulted the desired diene **4.24** and two by-products **4.25** and **4.26** resulting from base-induced β -elimination of a methoxy group. For this reason the vinyl borate coupling partner was purified prior to the key coupling. To this end, vinyl iodide **4.21** was converted to **4.8** by lithium-iodine exchange followed by trapping with isopropyl pinacol borate **4.27** in THF. Following the purification of vinyl borate **4.8** by flash chromatography, the intermolecular Suzuki coupling reaction now consistently occurs in 70% yield in presence of $\text{Pd}(\text{PPh}_3)_4$ and TIOEt in a 3:1 mixture of THF and H_2O . With a reliable method of obtaining vinyl boronate **4.8** in quantity, multi-grams quantities of aldehyde **4.24** can be prepared under the desired SMCC conditions.



Scheme 4.3 Synthesis of aldehyde **4.24** and vinyl boronate **4.8**

4.2.2 Studies into the Mukaiyama Aldol Reaction

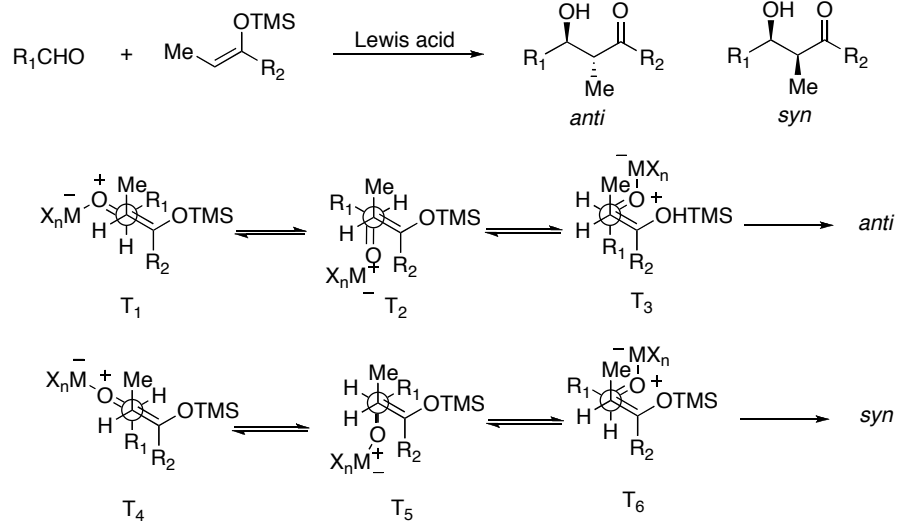
After solving the problem of large-scale preparation of aldehyde **4.24**, we focused our attention on the diastereoselectivity of the key Mukaiyama aldol reaction. Mukaiyama aldol partner, silyl enol ether **4.9** was prepared from TES protected 1-hydroxy-2-butanone **4.28**, which is easily accessible either from 1,2-butane diol in a 2-step reaction sequence or one-step from commercially available 1-hydroxy-2-butanone.⁷⁶ Kinetic deprotonation of ketone **4.28** with LDA followed by TMSCl quench provided a mixture of isomeric silyl enol ethers *E*-**4.9**, *E*-**4.29**, *Z*-**4.9** and *Z*-**4.29** (73:12:14.7:0.3).⁷⁷ The ratio of these isomers was determined by GC analysis, the double bond geometry of isomers **4.9** and **4.29** were assigned by NOESY analysis.



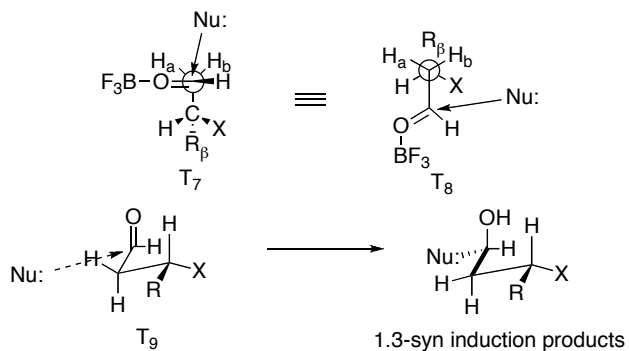
Scheme 4.4 Synthesis of silyl enol ether **4.9** and **4.29**

Danishefsky and coworkers demonstrated that reactions between achiral siloxydienes and chiral aldehydes generated *syn* aldol products irrespective of the geometry of silyl enolsilanes.⁷⁸ To explain the stereochemical outcome of Lewis acid mediated Mukaiyama reactions between silyl enol ethers and aldehydes, Heathcock and coworkers hypothesized the involvement of open transition-state structures as shown in Scheme 4.5 (synclinal and/or

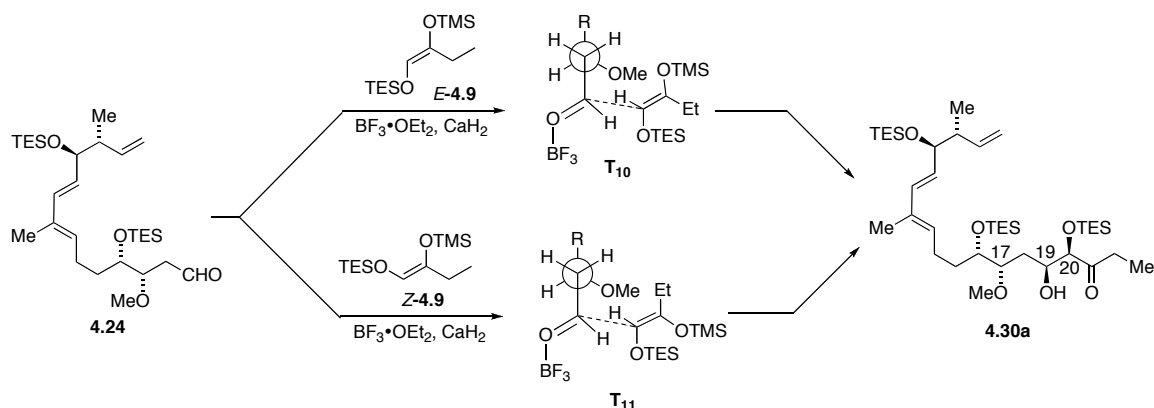
antiperiplanar transition structures) and excluded the involvement of closed transition state structures, which were widely used for prediction of stereoselectivity in lithium enolate aldol condensations.^{79,80,81,82} In addition, Evans and coworkers proposed an extended Felkin-Anh model for 1,3-asymmetric induction in Mukaiyama aldol additions to β -alkoxy aldehydes via systematic investigation into the stereoselectivity of Mukaiyama aldol reaction as shown in Scheme 4.6.^{83,84} Based on these literature precedents and proposed model systems, we predicted that Mukaiyama aldol reaction of aldehyde **4.24** with silyl enol ethers *E*-**4.9** would proceed via an antiperiplanar transition state **T₁₀** to minimize electrostatic repulsion between TMSO oxygen and aldehyde carbonyl oxygen as well as steric interactions between TESO and R' substituents on the aldehyde and provide the desired *anti*, *syn* aldol adduct **4.30a** as the major isomer. Mukaiyama reaction of the same aldehyde **4.24** with *Z*-**4.9** was predicted to proceed via an antiperiplanar transition state **T₁₁** for the same reasons and also provide **4.30a** as the major adduct (Scheme **4.7**). Therefore, the stereoselectivity in Mukaiyama aldol reaction between aldehyde **4.24** and silyl enol ether **4.9** was anticipated to be independent of the double geometry of silyl enol ether **4.9**.



Scheme 4.5 Open transition state models for Mukaiyama reactions



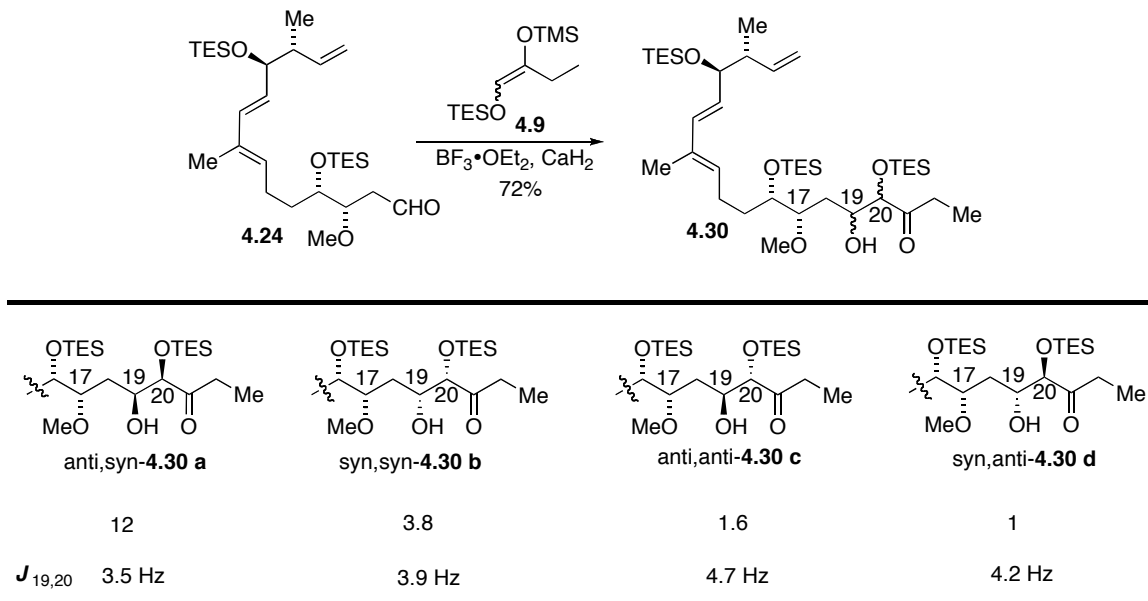
Scheme 4.6 1,3-induction models for Mukaiyama additions



Scheme 4.7 Prediction for stereoselectivity in Mukaiyama aldol reaction

In the event, Mukaiyama aldol reaction between a mixture of silyl enol ethers **4.9** (cf. Scheme 4.4) and aldehyde **4.24** provided a mixture of aldol products consisting of two major diastereomers (4:1) determined by ^1H NMR analysis of the crude product mixture. The major isomer was determined to be the desired *anti,syn* isomer based on the small coupling constant between H-19 and H-20 (3.5 Hz) and model analysis.⁸⁵ The minor isomers were removed in the late stage synthesis, and their structures were not assigned. Since a mixture of silyl enol ethers (Scheme 4.4) were used in the Mukaiyama aldol reaction, it was not known whether the isomers generated from Mukaiyama aldol reaction were diastereomers or regioisomers. To answer this question, in the synthesis of 6-normethyl apoptolidinone A **4.2**, the reaction mixture from Mukaiyama aldol condensation was further purified by Varian preparative HPLC after normal flash chromatography. No products corresponding to the reactions between aldehyde **4.24** and silyl enol ethers **E-4.29** and **Z-4.29** were separated. To our pleasure, four diastereomers resulting from the reaction between **4.24** and silyl enol ethers **E-4.9** and **Z-4.9** were separated. The ratio of isomers was determined to be

12:3.8:1.6:1 (Scheme 4.8). As predicted the major isomer was *anti,syn*-**4.30a**. The assignment of relative stereochemistry between C-19 and C-20 was based on the observed coupling constants between H-19 and H-20 in all four aldol adducts, the relative configuration across C-17 and C-19 was assigned based on the 1,3-asymmetric induction model proposed by Evans and coworkers as shown in Scheme 4.8 and confirmed by the total synthesis of apoptolidinones. These results proved the effectiveness of using the Heathcock open transition state models and the Evans 1,3-induction models for prediction of reaction diastereoselection in synthetic design.

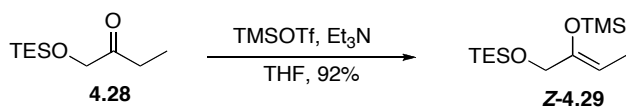


Scheme 4.8 Diastereoselectivity in Mukaiyama aldol reaction

4.2.3 Alternative Route for C(22)-C(23) Bond Connection

In the previous synthesis of apoptolidinone A **4.1**, the C-22 and C-23 stereogenic centers were established by using a double diastereoselective

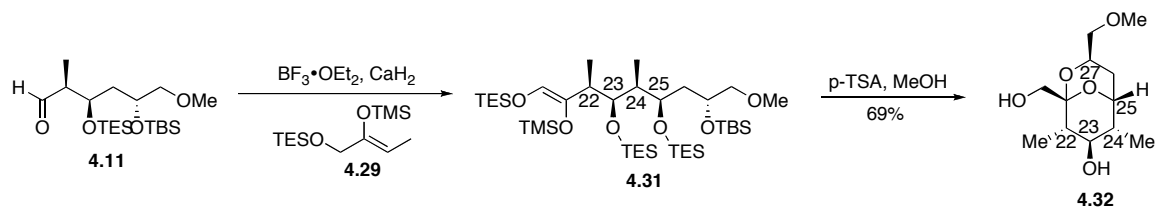
lithium enolate aldol reaction.²⁴ Even though this reaction gave high diastereoselectivity, the yield of this step was modest (48%). Therefore, an alternative aldol strategy was investigated for the construction of C-22 and C-23 bond formation in the progress towards the total synthesis of 6-normethyl apoptolidinone A **4.2**. Thus, the corresponding Mukaiyama aldol addition partner silyl ketene acetal **4.29** was obtained from same starting material ketone **4.28**. Thermodynamic silylation of ketone **4.28** with Et₃N followed by TMSOTf quench gave silyl ketene acetal **Z-4.29** as a single isomer.



Scheme 4.9 Synthesis of silyl enol ether **4.29**

Previous studies by Evans' group revealed that Mukaiyama aldol reactions with β -oxygen substituted aldehydes proceeded with high 1,3-*anti* diastereoselection due to electrostatic interactions between the carbonyl and polar β -oxygen substituent.^{85,86} It was also pointed out that addition of enolsilanes to α -alkyl substituted aldehydes proceeded with excellent 1,2-*syn* diastereoselection through the Felkin-Anh transition state model. Therefore, Mukaiyama aldol reactions with *anti*- α,β -disubstituted aldehydes could proceed with high diastereoselectivity, since α and β stereoinduction factors mutually reinforce this selectivity. However, when *syn*- α,β -disubstituted aldehydes were chosen as Mukaiyama aldol partner, such as aldehyde **4.11**, the stereochemical

outcome was difficult to predict, since the 1,2-induction and 1,3 induction factors were nonreinforcing.⁸⁷ Based on the above literature precedents, the stereoselection in Mukaiyama addition of silyl enol ether *E*-**4.29** to aldehyde **4.11** could not be predicted with confidence.

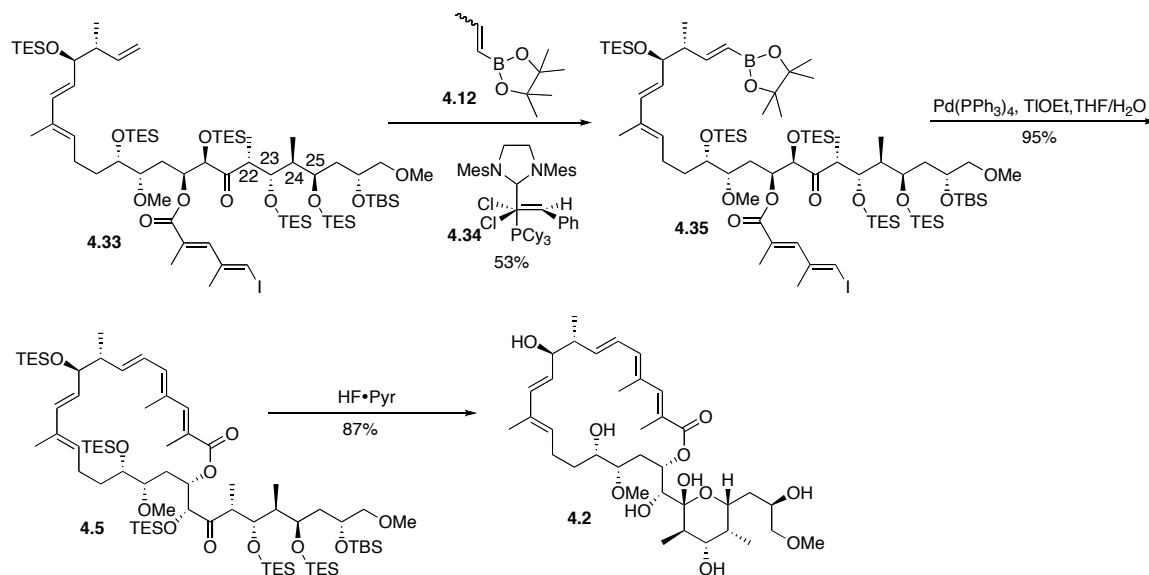


Scheme 4.10 Formation of C-22/C-23 conjunction with Mukaiyama aldol reaction

To our surprise, the reaction of silyl enol ether *E*-**4.29** and aldehyde **90** under Mukaiyama condition generated a single diastereomer **4.31**. None of the products corresponding to Mukaiyama aldol pathway was detected. This experimental result suggested that alcohol **4.31** could be generated through a Prins or heteroene reaction pathway.⁸⁸ When Alcohol **4.31** was subjected to an acidic desilylation condition, a bicyclic product **4.32** was obtained. From the NOESY spectrum of **4.32**, strong NOE correlations between H-23 and H-27, and between H-23 and 22-Me, 24-Me were observed. Through a combination of NOE correlations and large coupling constants ($J_{22-23} = 9.9$ Hz, $J_{23-24} = 9.9$ Hz), the relative stereochemistry of **4.32** was assigned as shown in Scheme 4.8. Unfortunately, the coupling of aldehyde **4.11** and silyl enol ether *E*-**4.29** did not led to the desired stereochemistry required for completion of the total synthesis of apoptolidinones. Therefore, efforts returned back to the original lithium enolate

aldol strategy utilized in the total synthesis of apoptolidinone A **4.1** for the construction of C-22/C-23 bond of 6-normethyl apoptolidinone A **4.2**.

4.2.4 Assembly of 6-Normethyl Apoptolidinone A

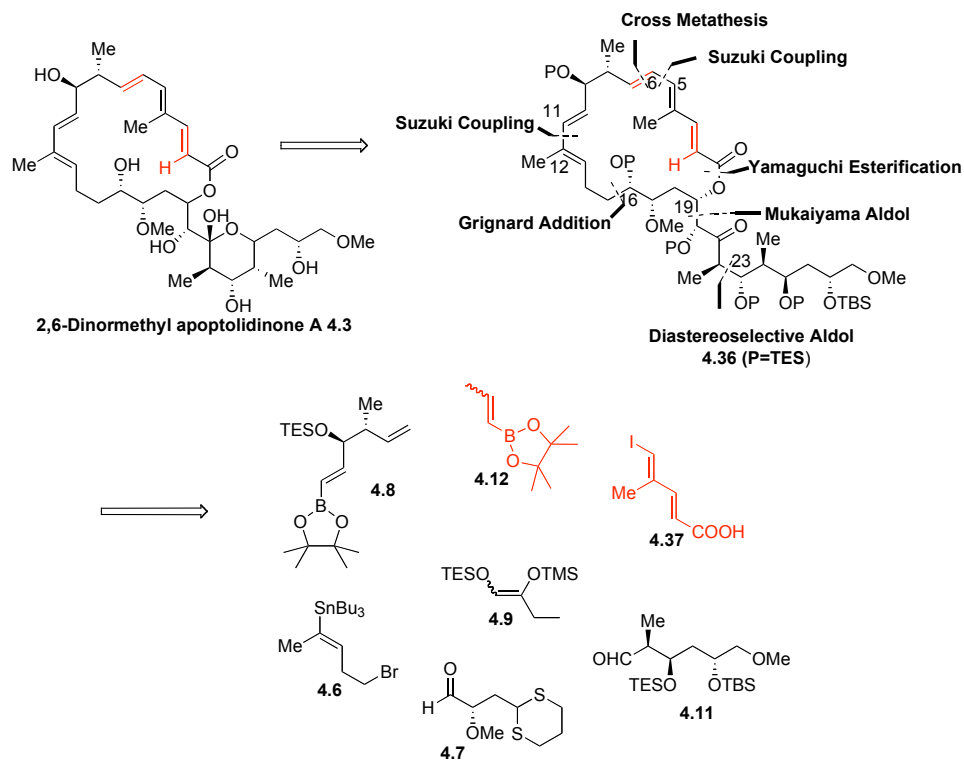


Scheme 4.11 Final assembly of 6-normethyl apoptolidinone A **4.2** (apoptolidinone D)

To assemble 6-normethyl apoptolidinone A **4.2**, the cross-metathesis of 1-propenyl boronate **4.12** with the common advanced synthetic intermediate **4.33** in presence of the Grubbs 2nd generation catalyst **4.34** provided vinyl boronate **4.35** as a single geometric isomer in a superior yield (53%) relative iso-propenyl borate (22%). Macrocyclization under Suzuki cross-coupling conditions and exhaustive desilylation completed the total synthesis of 6-normethyl apoptolidinone A **4.2**. 6-normethyl apoptolidinone A **4.2** adopted the name of apoptolidinone D after it was reported by Wender's group who isolated

apoptolidin D as a minor metabolite from the fermentation medium of *Nocardioopsis* sp.⁶

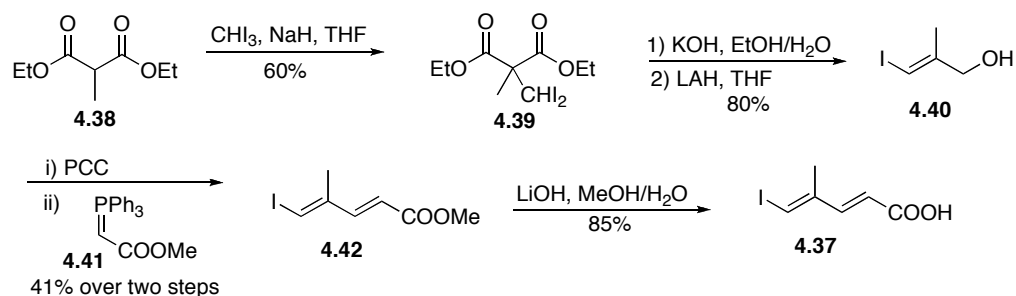
4.3 Total Synthesis of 2,6-Dinormethyl Apoptolidinone A



Scheme 4.12 Retrosynthetic analysis for 2,6-dinormethyl apoptolidinone A **4.3**

Structurally, 2,6-dinormethyl apoptolidinone A **4.3** lacks two methyl groups at both C-2 and C-6 positions. The total synthesis of this unnatural apoptolidin aglycone **4.3** requires changing both the Yamaguchi esterification and cross-metathesis partners while utilizing the same synthetic strategy used in the total synthesis of apoptolidinone A **4.1**.

4.3.1 Preparation of Carboxylic Acid **4.37**



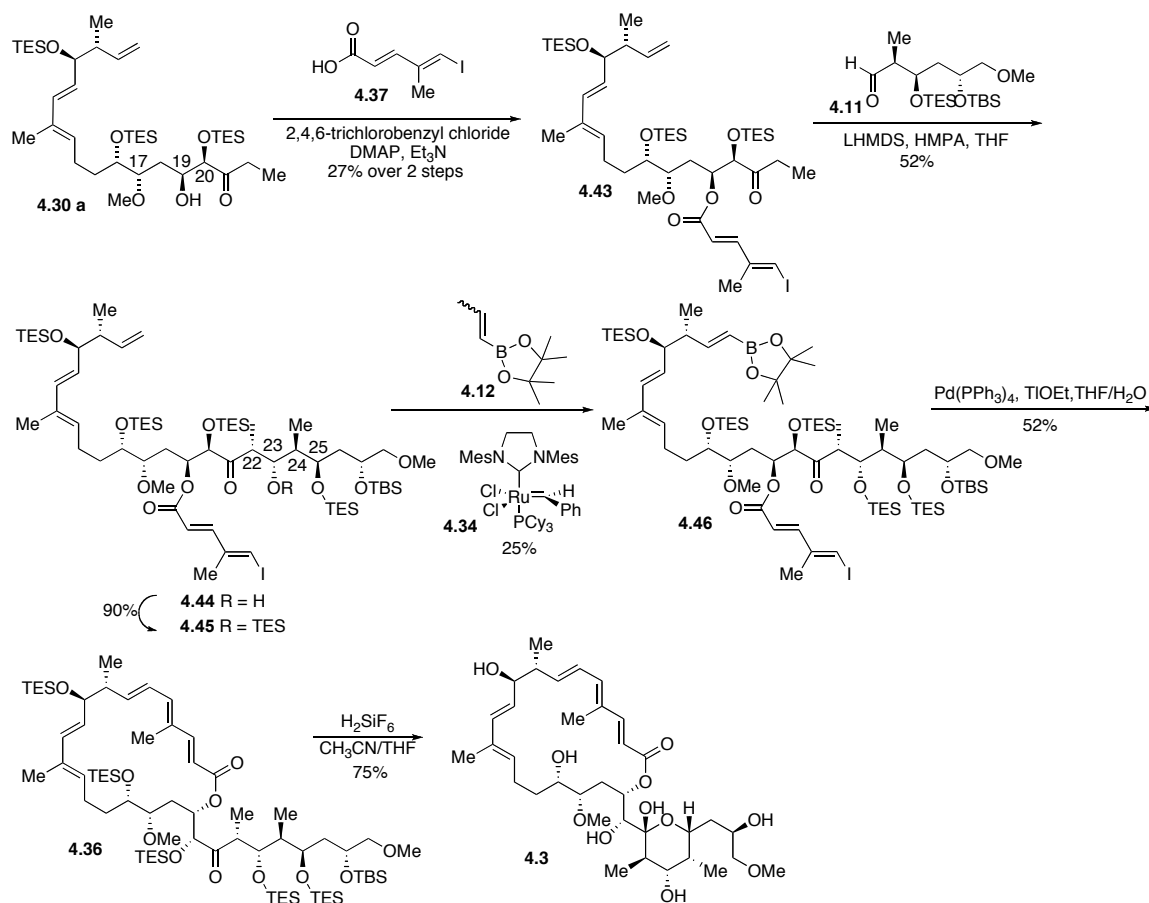
Scheme 4.13 Synthesis of carboxylic acid **4.37**

The synthesis of carboxylic acid **4.37** started from 2-methyl diethyl malonate **4.38**, which was converted to allylic alcohol **4.40** via basic hydrolysis, decarboxylation and lithium aluminum hydride reduction.⁸⁹ After PCC oxidation, the corresponding aldehyde then reacted with commercially available phosphine ylide **4.41** yielded the Wittig olefination product *E*-dienoate **4.42**. The methyl ester in **4.42** was then hydrolyzed to produce the desired carboxylic acid **4.37**.

4.3.2 Assembly of 2,6-Dinormethyl Apoptolidinone A **4.3**

In the synthesis of 2,6-dinormethyl apoptolidinone A **4.3**, the major diastereomer **4.30a** resulting from the key Mukaiyama aldol reaction was coupled with carboxylic acid **4.37** under typical Yamaguchi esterification conditions provided the ester **4.43**, which was subsequently treated with LHMDs in presence of HMPA to generate the desired *Z*-enolate, and further reacted with aldehyde **4.11** to afford aldol product **4.44** as a single diastereomer. The resulting alcohol was protected as a TES ether **4.45**, which was subjected to a cross-metathesis reaction with 1-propenyl boronate **4.12** catalyzed by Grubbs secondary generation catalyst **4.34** to give an intra-molecular Suzuki coupling

precursor **4.46**. The following macrocyclization afforded macrolactone **4.36**. In the final desilylation step, a less acidic reagent, H_2SiF_6 , was used to complete the total synthesis of 2,6-dinormethyl apoptolidinone A **4.3**.



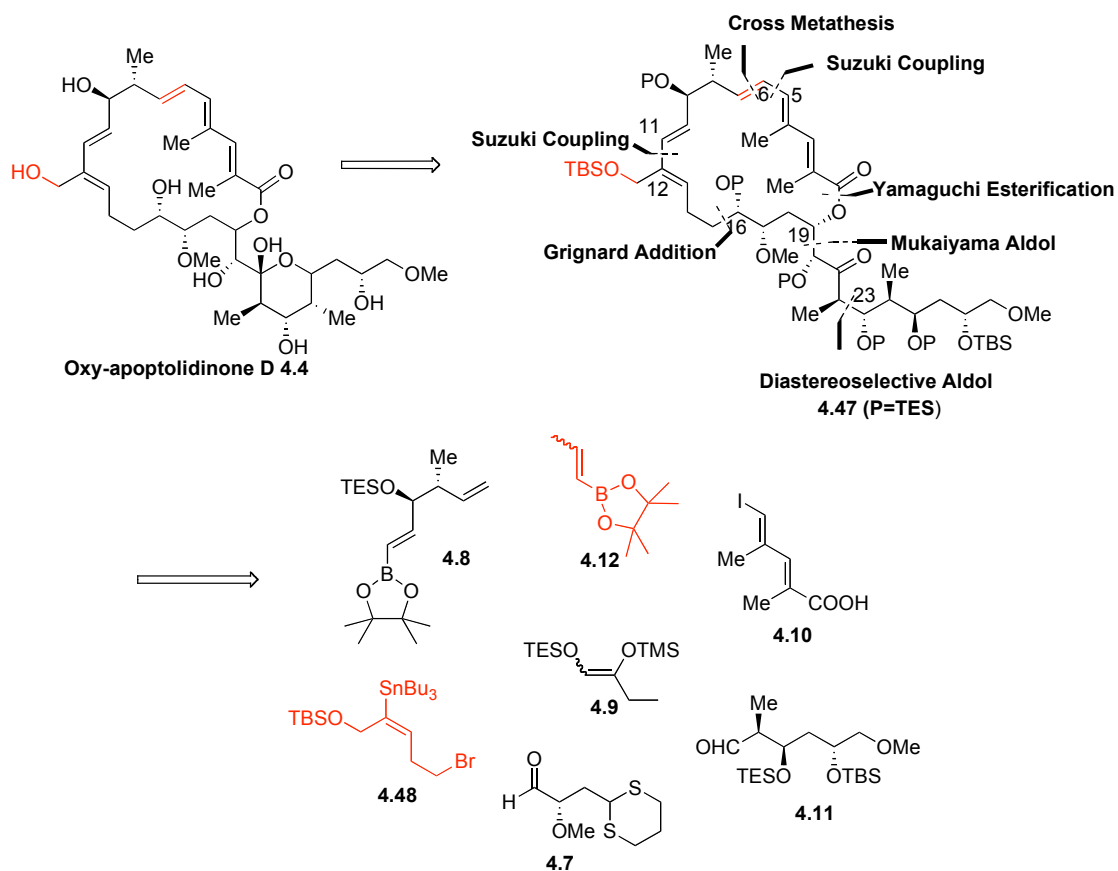
Scheme 4.14 Assembly of 2,6-dinormethyl apoptolidinone A **4.3**

4.4 Total Synthesis of 12-Oxymethyl-Apoptolidinone D

In comparing apoptolidinone D **4.2** to oxy-apoptolidinone D **4.4**, the latter incorporates one extra hydroxyl group at C-12 methyl group. Our attention was to incorporate a C-12 hydroxyl group as a point of attachment for probe development in connection with target identification. Detailed discussion of

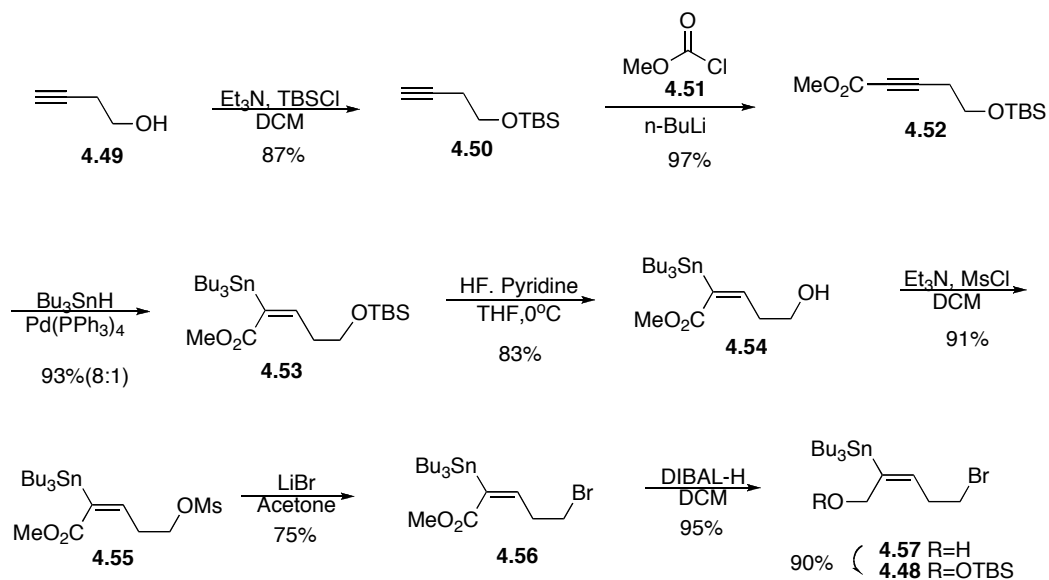
apoptolidin labeling for the purpose of biological target identification is described in Chapter VI of this thesis.

The total synthesis of oxy-apoptolidinone D **4.4** was based on the same synthetic strategy developed by our group for the total synthesis of apoptolidinone A **4.1**. Disconnections with Suzuki couplings, Yamaguchi esterification, Mukaiyama aldol reaction, lithium enolate aldol reaction, and chelation-controlled Grignard addition revealed bromide **4.48**, aldehyde **4.7**, silyl keten acetal **4.9**, aldehyde **4.10**, carboxylic acid **4.11**, vinyl borate **4.8** and **4.12** were the building blocks for oxy-apoptolidinone D **4.4**. According to this strategy, the synthesis of oxy-apoptolidinone D **4.4** shared six common building blocks that were used in the synthesis of apoptolidinone D **4.2**. A new synthetic plan was required for the preparation of bromide **4.48**.



Scheme 4.15 Retrosynthetic analysis for oxy-apoptolidinone D 4.4

4.4.1 Preparation of Bromide 4.48

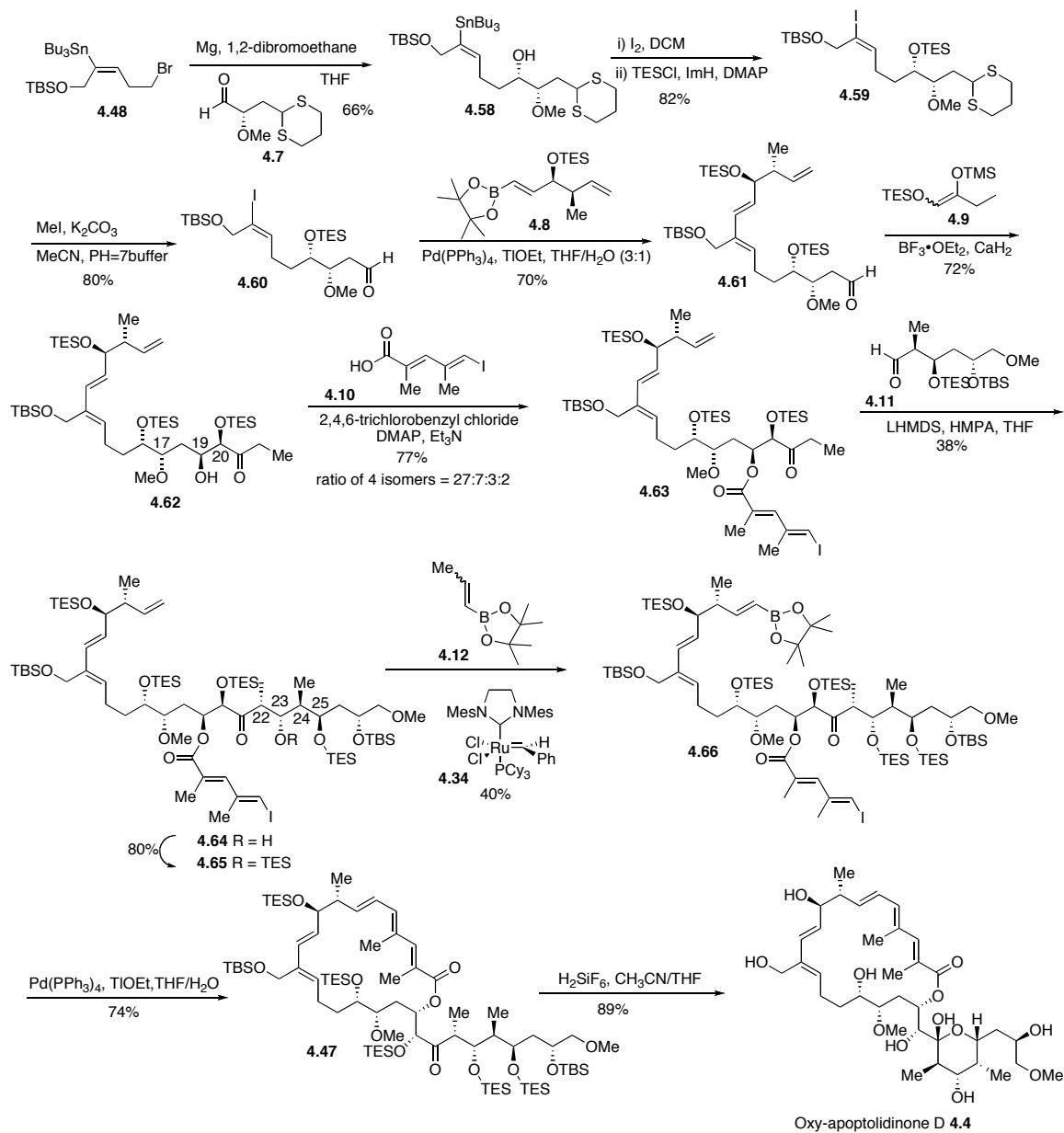


Scheme 4.16 Synthesis of bromide **4.48**

In the total synthesis of apoptolidinone A **4.1**, apoptolidinone D **4.2** and 2,6-dinormetyl apoptolidinone **4.3**, the common building block *E*-vinyl tin compound **4.6** was prepared from 1,2-dihydrofuran utilizing Koceinski's methodology.⁹⁰ To prepare vinyl tin **4.48** for the synthesis of oxy-apoptolidinone D **4.4**, a regio- and stereo-selective hydrostannylation was used to establish the *E*-geometry in vinyl tin **4.48**. Starting from 3-butyn-1-ol **4.49**, TBS protection followed by acetylation of the terminal alkyne **4.50** with chloromethyl formate **4.51** generated the methyl ester **4.52**. The key palladium catalyzed hydrostannylation reaction yielded **4.53** in 93% yield with 8:1 regioselectivity.^{91,92} The minor regioisomer generated from this step was removed following the desilylation step. Removal of the TBS protective group under acidic conditions resulted in primary alcohol **4.54**, which was converted into bromide **4.56** under typical Finkelstein reaction conditions via intermediate mesylate **4.55**. Finally, DIBAL-H

reduction of the methyl ester **4.56** followed by TBS protection of the corresponding alcohol **4.57** finished the assembly of fragment **4.48**.

4.4.2 Assembly of 12-Oxymethyl Apoptolidinone D



Scheme 4.17 Assembly of oxy-apoptolidinone D **4.4**

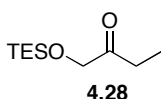
The synthesis of oxy-apoptolidinone D **4.4** starting from bromide **4.48** is shown in Scheme 4.17. In contrast to the earlier bromide **4.6**, the generation of the corresponding Grignard reagent from **4.48** requires higher reaction temperature. Therefore, tetrahydrofuran was selected in place of diethyl ether due to its higher boiling point. The chelation controlled Grignard addition to aldehyde **4.7** set the stereocenters at C16 and C17 in *syn* fashion and generated alcohol **4.58**. Then iodine-tin exchange followed by TES protection of the newly formed secondary alcohol provided vinyl iodide **4.59**. Hydrolysis of the dithiane with MeI and K₂CO₃ afforded aldehyde **4.60**, which was coupled with vinyl borate **4.8** to provide aldehyde **4.61**. The key Mukaiyama aldol reaction with silyl enol ether **4.9** gave a mixture of four diastereomers **4.62**. To which, carboxylic acid **4.10** was attached under Yamaguchi conditions and provided the ester **4.63**. At this stage, four diastereomers resulted from Mukaiyama aldol reaction that could be separated and purified by preparative HPLC. The ratio among these four isomers was determined to be 27:7:3:2, which correlated well with the results obtained in the total synthesis of apoptolidinone D **4.2** (*vide supra*). The major isomer, featuring the desired chirality at C-19 and C-20, was then subjected to a double diastereoselective aldol reaction with **4.11** setting up the pyran ring precursor **4.64**. Silylation of the secondary alcohol in **4.64** resulted in the intermediate **4.65** and made the cross metathesis precursor ready for further reactions. Grubbs cross metathesis with 1-propenyl pinacol borate **4.12** provided vinyl boronate **4.66**, and set the stage for macrolactonization. An intramolecular

Suzuki coupling reaction closed the 20-membered lactone under Roush modified condition and generated intermediate **4.47**. Global deprotection with fluorosilic acid released all the hydroxyl groups and simultaneously closed the pyran ring, which finished the total synthesis of oxy-apoptolidinone D **4.4**.

4.5 Experimental Section

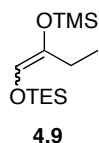
General Procedures: Unless indicated, all commercial reagents were used as received without further purification. All reactions were carried out under a nitrogen or argon atmosphere using dry glassware that had been flame-dried under a stream of nitrogen, unless otherwise noted. All solvents were purified prior to use. Tetrahydrofuran and diethyl ether were distilled from sodium/benzophenone; dichloromethane and benzene were distilled from calcium hydride. Chloroform was washed twice with water, dried over potassium carbonate, refluxed, and distilled from phosphorus pentoxide. All solvents were determined to contain less than 50 ppm water by Karl Fisher coulometric moisture analysis. Triethylamine was distilled from calcium hydride and stored over sodium hydroxide. Reactions were monitored by thin-layer chromatography (TLC) using 0.25-mm E. Merck precoated silica gel plates. Visualization was accomplished with UV light and aqueous ceric ammonium molybdate solution, anisaldehyde stain or KMnO_4 followed by charring on a hotplate. Flash chromatography was performed with the indicated solvents using silica gel 60 (particle size 230-400 mesh) with the indicated solvent. An automated chromatography system was also employed. Chromatography methods were

created based on R_f values. Yields refer to chromatographically and spectroscopically pure compounds unless otherwise stated. Melting points are uncorrected unless otherwise noted. ^1H and ^{13}C NMR spectra were recorded on Bruker 300, 400, 500 and 600 MHz spectrometers at ambient temperature. ^1H and ^{13}C NMR data are reported as δ values relative to chloroform, benzene or methanol. Enantiomeric excess was determined by chiral GC analysis by Varian 3900 with chiral column (BETA DEX 120, 30 M x 0.25 mm, 0.25 μm film, column : # 17411-02B). High-resolution mass spectra were conducted either at Texas A&M University Mass Spectrometry Service Center by Dr. Shane Tichy on an API QSTAR Pulsar Instrument or at the Department of Chemistry and Biochemistry, University of Notre Dame on a JEOL AX505HA or JEOL JMS-GCmate mass spectrometer. Infrared (IR) spectra were recorded as thin films or solutions in the indicated solvent.



Silyl Ether 4.28: To a solution of 1-hydroxybutan-2-one (0.021 g, 2.384 mmol) in dichloromethane (24 mL) cooled to 0 °C was added imidazole (0.032 g, 4.767 mmol, 2 equiv) followed by TESCI (0.60 mL, 3.575 mmol, 1.5 equiv). The mixture was stirred overnight at room temperature and quenched with H_2O (10 mL). The aqueous layer was extracted with dichloromethane (3 X 20 mL) and the combined organic layers were washed with brine (20 mL), dried (MgSO_4), filtered and concentrated *in vacuo*. The residue was purified by flash chromatography

(Hexanes/EtOAc, 40:1 to 10:1) to afford 0.338 g (70%) of TES ether **4.28** as a colorless oil: IR (neat) 2955, 2878, 1720 cm^{-1} ; ^1H NMR (500 MHz, CDCl_3): 4.18 (s, 2H), 2.54 (q, $J = 7.0$ Hz, 2H), 1.07 (t, $J = 7.0$ Hz, 3H), 0.97 (t, $J = 8.0$ Hz, 9H), 0.64 (q, $J = 8.0$ Hz, 6H); ^{13}C NMR (100 MHz, CDCl_3): 211.7, 68.7, 31.5, 7.2, 6.6, 4.3; HRMS (ESI) m/z 209.1571 [(M+Li) $^+$ calculated for $\text{C}_{10}\text{H}_{22}\text{LiO}_2\text{Si}$: 209.1549].



Silyl Enol Ethers 4.9: To a solution of diisopropylamine (4.0 mL, 29.2 mmol) in THF (100 mL) was added n-BuLi (2.5 M in hexanes, 11.7 mL, 29.2 mmol) at 0 °C. After 15 min at 0 °C, the mixture was cooled to -78 °C and a solution of silyl ether **4.28** (4.9 g, 24.3 mmol) in THF (20 mL) was added dropwise. The resulted solution was stirred for 30 min at -78 °C. TMSCl (3.7 mL, 29.2 mmol) was added dropwise and the resulted solution was stirred for 2 h at -78 °C. The reaction was quenched with NaHCO_3 (20 mL) and extracted with Et_2O (3 X 100 mL). The combined organic layer were dried (Na_2SO_4), filtered and concentrated *in vacuo*. The residue was purified by distillation under reduced pressure (85-90 °C, 1 mm Hg) to afford 5.3 g (80%) isolated as a light yellow and mixture of silyl enol ethers (Z)-**4.9**/(E)-**4.9**/(Z)-**4.29**/(E)-**4.29** (ca. 14.7:73:0.3:12 as determined by GC analysis: Varian 3900 with normal column from J & W Scientific, Cat. No.: 1231012, 15 M X 0.32 mm, 0.25 micron, starting from 50 °C, hold for 10 min, then 1 °C/min to 100 °C, hold for 50 min, totally 60 min, major isomer showed up

at 22.11 min, 3 minor isomers showed at 20.88 min, 24.53 min, and 27.05 min respectively). The double bond geometry of (*E*)-**4.9** and (*Z*)-**4.29** was assigned by NOESY NMR analysis: IR (neat) 1266, 1162 cm⁻¹; ¹H NMR (300 MHz, C₆D₆): 6.32 (s, 1H), 2.42 (q, *J* = 7.5 Hz, 2H), 1.17 (t, *J* = 7.5 Hz, 3H), 0.99 (t, *J* = 8.0 Hz, 9H), 0.60 (q, *J* = 8.0 Hz, 6H), 0.17 (s, 9H); ¹³C NMR (125 MHz, CDCl₃): 143.4, 125.3, 21.9, 11.0, 6.5, 4.4, 4.3, 0.3; HRMS (ESI) *m/z* 281.1946 [(*M*+*Li*)⁺ calculated for C₁₃H₃₀LiO₂Si₂: 281.1944].

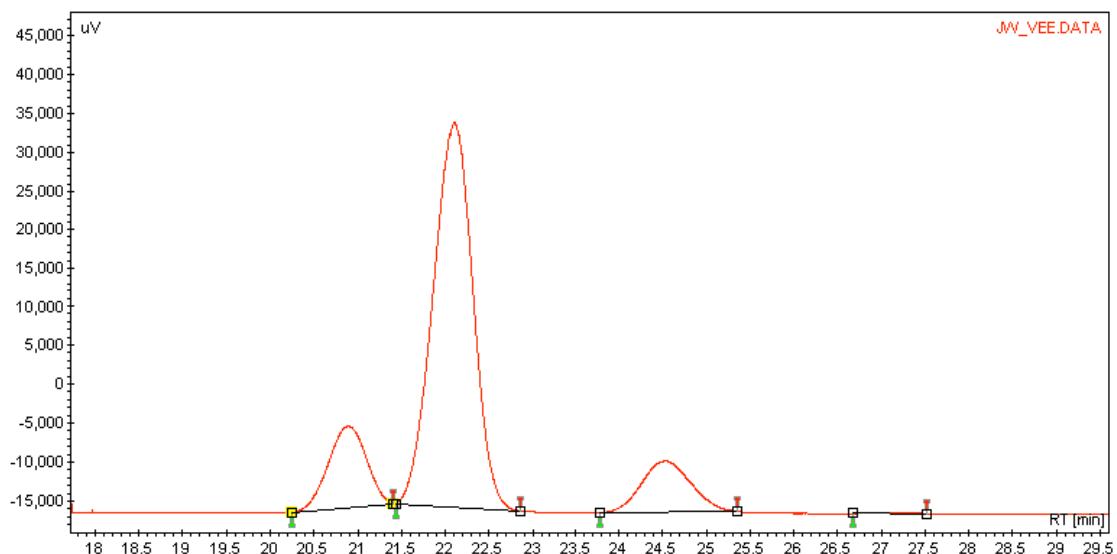
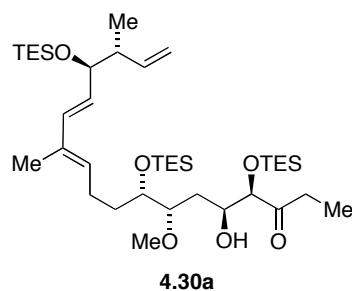


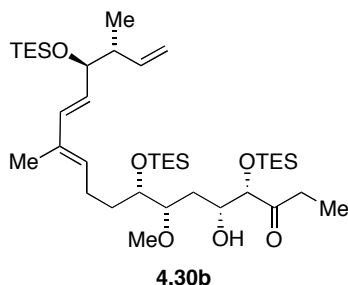
Figure 4.2 GC chromatograph of silyl enol ethers **4.9** and **4.29**



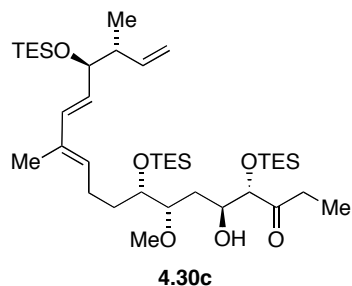
Aldol 4.30: To a solution of aldehyde **4.24** (0.40 g, 0.76 mmol) and silyl enol ethers (7:1, **4.9/4.29**; 0.83 g, 3.03 mmol, 4 equiv) in dichloromethane (32 mL) at 0 °C was added CaH₂ (64 mg, 1.52 mmol, 2 equiv). After 15 min, the reaction was cooled to -94 °C and BF₃·OEt₂ (105 μL, 1.52 mmol, 2 equiv) was added. The reaction mixture was stirred for 45 min at -94 °C and quenched with saturated NaHCO₃ (25 mL), and the aqueous layer was extracted with dichloromethane (30-50 mL). The combined organic layers were dried (MgSO₄), filtered, and concentrated *in Vacuo*. The residue was purified by flash chromatography (hexanes/EtOAc, 20:1-15:1) to afford 0.39 g (72%) of alcohol **4.30a-d** as a 12:3.8:1.6:1 mixture of diastereoisomers (by Varian HPLC, 21.4 mm X 25 cm column, 49 min gradient, 0-10% ethyl acetate in hexanes). For synthetic purposes the mixture can be advanced to the next step without further purification, as the resulting mixture of Yamaguchi esterification products can be easily separated to afford the desired ester product.

Data for 4.30a: t_R 34.25 min; $[\alpha]_D^{25}$ -9.1 (c 2.1, CHCl₃); IR (neat) 2953, 2873, 1724, 1462, 1244, 1091, 1018 cm⁻¹; ¹H NMR (500 MHz C₆D₆) δ 6.25 (d, J = 16.0 Hz, 1H), 6.05-5.98 (m, 1H), 5.63 (dd, J = 16.0, 7.5 Hz, 1H), 5.55 (t, J = 7.0 Hz, 1H), 5.08-5.03 (m, 2H), 4.24-4.18 (m, 1H), 4.07 (t, J = 7.5 Hz, 1H), 4.04 (d, J = 4.0 Hz, 1H), 3.99-3.95 (m, 1H), 3.66 (ddd, J = 10.0, 4.0, 2.0 Hz, 1H), 3.30 (s, 3H), 2.61 (d, J = 9.0 Hz, 1H), 2.53-2.38 (m, 4H), 2.25-2.16 (m, 1H), 1.95-1.89 (m, 1H), 1.88-1.82 (m, 1H), 1.76 (s, 3H), 1.66-1.60 (m, 1H), 1.60-1.52 (m, 1H), 1.11 (d, J = 6.5 Hz, 3H), 1.05-0.99 (m, 21H), 0.91 (t, J = 8.0 Hz, 9H), 0.68-0.62 (m, 12 H),

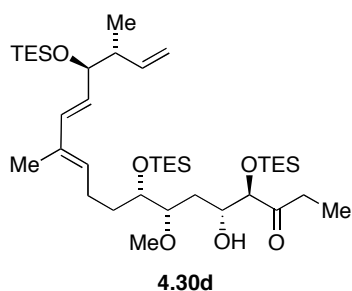
0.52 (q, $J = 8.0$ Hz, 6H); ^{13}C NMR (125 MHz, C_6D_6) δ 213.3, 141.3, 135.7, 133.7, 132.5, 128.6, 114.2, 81.7, 80.8, 78.1, 71.6, 70.6, 58.2, 45.2, 33.5, 32.2, 31.7, 25.3, 15.0, 12.6, 7.3, 7.1, 7.1, 6.9, 5.4, 5.4, 5.0; HRMS (MALDI) m/z 749.5078 [(M + Na) $^+$ calcd for $\text{C}_{39}\text{H}_{78}\text{O}_6\text{Si}_3\text{Na}$, 749.5004].



Data for 4.30b: t_{R} 31.75 min; $[\alpha]_{\text{D}}^{25}$ -2.6 (c 0.16, CHCl_3); IR (neat) 2955, 2877, 1716, 1459, 1239, 1083, 1006, 677 cm^{-1} ; ^1H NMR (500 MHz C_6D_6) δ 6.27 (dd, $J = 15.5, 4.5$ Hz, 1H), 6.07-5.98 (m, 1H), 5.65 (dd, $J = 15.5, 7$ Hz, 1H), 5.56-5.50 (m, 1H), 5.10-5.04 (m, 2H), 4.25-4.19 (m, 1H), 4.17 (d, $J = 4$ Hz, 1H), 4.09 (t, $J = 6.2$ Hz, 1H), 3.93-3.88 (m, 1H), 3.44-3.39 (m, 1H), 3.30 (d, $J = 4.5$ Hz, 1H), 3.09 (s, 3H), 2.73-2.58 (m, 2H), 2.45-2.32 (m, 2H), 2.24-2.14 (m, 1H), 2.04 (d, $J = 15$ Hz, 1H), 1.83-1.73 (m, 2H), 1.76 (s, 3H), 1.59-1.52 (m, 1H), 1.15-1.09 (m, 6H), 1.07-0.94 (m, 27H), 0.69-0.56 (m, 18H); ^{13}C NMR (125 MHz, C_6D_6) δ 211.9, 141.4, 135.7, 133.8, 132.4, 128.8, 114.3, 84.5, 81.9, 78.1, 73.8, 71.6, 57.1, 45.2, 32.9, 31.9, 31.8, 25.2, 15.1, 12.7, 7.4, 7.2, 7.0, 5.5, 5.4, 5.2; HRMS (MALDI) m/z 749.5020 [(M + Na) $^+$ calcd for $\text{C}_{39}\text{H}_{78}\text{O}_6\text{Si}_3\text{Na}$, 749.5004].



Data for 4.30c: t_R 32.80 min; $[\alpha]_D^{25}$ -9.3 (c 0.08, CHCl_3); IR (neat) 2955, 2878, 2361, 1714, 1459, 1238, 1096, 1008, 741 cm^{-1} ; ^1H NMR (500 MHz C_6D_6) δ 6.26 (d, J = 19.5 Hz, 1H), 6.08-5.97 (m, 1H), 5.65 (dd, J = 19.5, 9.2 Hz, 1H), 5.58-5.52 (m, 1H), 5.10-5.04 (m, 2H), 4.25-4.20 (m, 1H), 4.14 (d, J = 5.8 Hz, 1H), 4.09 (t, J = 7.9 Hz, 1H), 4.00-3.95 (m, 1H), 3.60-3.57 (m, 1H), 3.27 (s, 3H), 3.01 (d, J = 5 Hz, 1H), 2.62-2.47 (m, 2H), 2.45-2.32 (m, 2H), 2.27-2.15 (m, 1H), 2.00-1.92 (m, 1H), 1.77 (s, 3H), 1.65-1.55 (m, 1H), 1.13 (d, J = 8.6 Hz, 3H), 1.08-1.00 (m, 18H), 0.95 (t, J = 10.0 Hz, 9H), 0.66 (q, J = 9.8 Hz, 12H), 0.58 (q, J = 9.9 Hz, 6H); ^{13}C NMR (150 MHz, C_6D_6) δ 141.4, 135.8, 133.8, 132.5, 128.7, 114.2, 84.5, 82.4, 81.9, 78.1, 73.9, 72.4, 71.6, 71.1, 58.0, 57.1, 45.3, 32.9, 32.5, 32.0, 31.9, 25.2, 15.1, 12.7, 7.4, 7.2, 7.0, 6.9, 5.6, 5.5, 5.4, 5.2, 5.1; HRMS (MALDI) m/z 749.5038 $[(M+Na)^+$ calcd for $\text{C}_{39}\text{H}_{78}\text{O}_6\text{Si}_3\text{Na}$, 749.5004].



Data for 4.30d: t_R 36.80 min; $[\alpha]_D^{25}$ -50.0 (c 0.01, CHCl_3); IR (neat) 2955, 2878, 1713, 1459, 1239, 1105, 1007, 741 cm^{-1} ; ^1H NMR (500 MHz C_6D_6) δ 6.30 (d, J = 19.6 Hz, 1H), 6.08-5.98 (m, 1H), 5.67 (dd, J = 19.5, 9.1 Hz, 1H), 5.56-5.50 (m, 1H), 5.11-5.04 (m, 2H), 4.30-4.17 (m, 1H), 4.11 (t, J = 7.9 Hz, 1H), 4.07 (d, J = 5.2 Hz, 1H), 3.94-3.89 (m, 1H), 3.48 (d, J = 12.6 Hz, 1H), 3.29 (s, 3H), 2.55-2.32 (m, 4H), 2.22-2.12 (m, 1H), 1.91-1.85 (m, 1H), 1.78 (s, 3H), 1.71-1.59 (m, 2H), 1.51-1.42 (m, 1H), 1.13 (d, J = 8.5 Hz, 3H), 1.10-1.00 (m, 18H), 0.94 (t, J = 9.9 Hz, 9H), 0.75-0.62 (m, 12H), 0.56 (q, J = 9.9 Hz, 6H); ^{13}C NMR (150 MHz, C_6D_6) δ 141.4, 135.7, 133.8, 132.2, 128.9, 114.3, 82.1, 81.5, 78.1, 72.9, 70.7, 57.9, 45.3, 34.2, 34.0, 32.1, 25.3, 15.1, 12.7, 7.3, 7.2, 7.1, 7.0, 5.6, 5.5, 5.0; HRMS (MALDI) m/z 749.5030 $[(M + \text{Na})^+]$ calcd for $\text{C}_{39}\text{H}_{78}\text{O}_6\text{Si}_3\text{Na}$, 749.5004].

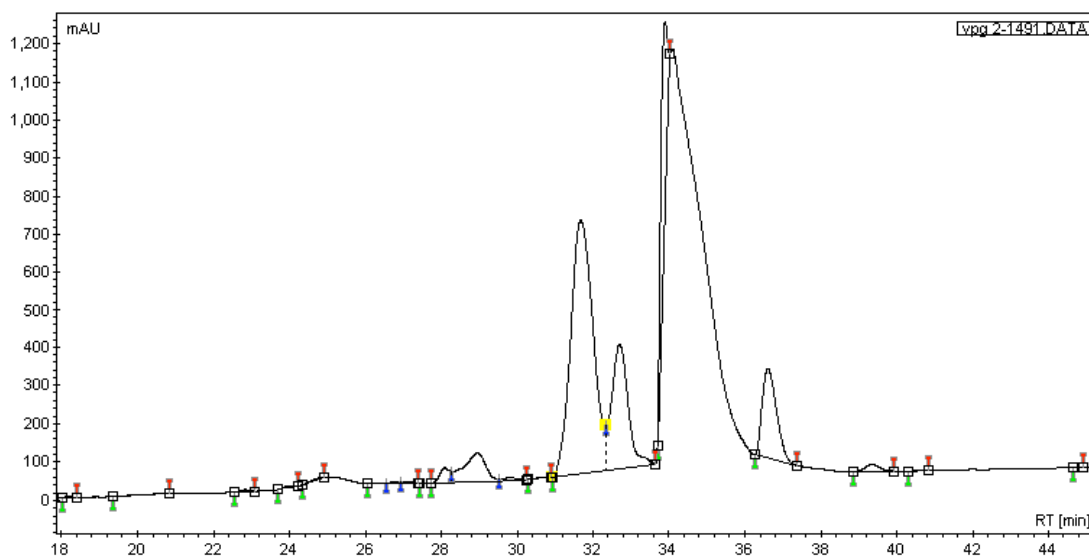
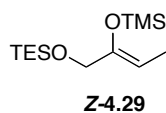
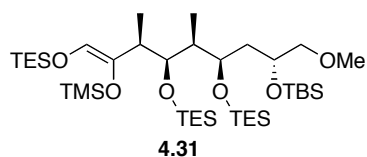


Figure 4.3 HPLC chromatograph for purification of aldol **4.30**

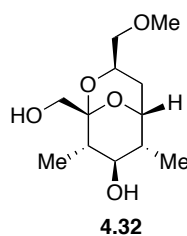


Silyl Enol Ether (Z)-4.29: To a solution of silyl ether **4.28** (0.54 g, 2.67 mmol) in THF (10 mL) at 0 °C, triethyl amine (0.6 mL, 1.6 equiv) was added dropwise followed by TMSOTf (0.72 mL, 1.5 equiv). Stirred at 0 °C for 30 min then quenched with water (10 mL). The mixture was extracted with Et₂O (3 x 50 mL). The combined organic phase was dried over MgSO₄ and the solvent was removed in vacuo to afford 0.67 g (92%) of (Z)-**4.29** as a yellow oil: IR (neat) 1251, 1064 cm⁻¹; ¹H NMR (300 MHz, C₆D₆): δ 4.90 (q, *J* = 6.7 Hz, 1H), 4.01 (s, 2H), 1.62 (d, *J* = 6.9 Hz, 3H), 0.99 (t, *J* = 7.9 Hz, 9H), 0.60 (q, *J* = 7.8 Hz, 6H), 0.23 (s, 9H); ¹³C NMR (75 MHz, CDCl₃): δ 103.1, 65.1, 10.7, 7.0, 6.8, 4.8, 0.8; HRMS (ESI) *m/z* 281.1948 [(M+Li)⁺ calculated for C₁₃H₃₀LiO₂Si₂: 281.1944].



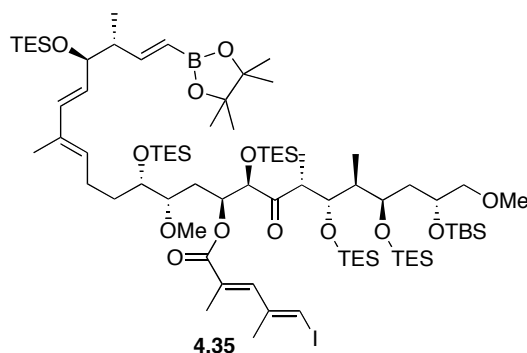
Silyl Enol Ether 4.31: To a solution of aldehyde **4.11** (0.15 g, 0.37 mmol) in dichloromethane (5 mL) at 0 °C K₂CO₃ (77 mg, 0.56 mmol, 1.5 equiv) was added. The reaction mixture was cooled to -78 °C at which time BF₃•OEt₂ (9 μL, 0.074 mmol, 0.2 equiv) was added dropwise followed by (Z)-**4.29** silyl enol ether (0.2 g, 0.74 mmol, 2 equiv). The resultant solution was stirred for 3 h at -78 °C, quenched with saturated NaHCO₃ aqueous solution (5 mL). The aqueous layer

was extracted with dichloromethane (3 x 5 mL) and the combined organic layers were dried over MgSO₄, filtered and concentrated *in vacuo*. The residue was purified by flash chromatography (Hexanes/Ethyl Acetate, 25/1) to afford 0.17 g (68%) of silyl enol ether **4.31** as a slightly yellow oil: $[\alpha]_D^{25}$ -45.5 (c 0.69, CHCl₃); IR (neat) 2956, 2878, 1682, 1460, 1248, 1154, 1003, 837, 744 cm⁻¹; ¹H NMR (500 MHz, C₆D₆): δ 5.72 (s, 1H), 4.24 (td, *J* = 6.8, 2.5 Hz, 1H), 4.08 (d, *J* = 8.5 Hz, 1H), 4.02-3.98 (m, 1H), 3.37-3.31 (m, 2H), 3.17 (s, 3H), 3.08 (d, *J* = 1.5 Hz, 1H), 2.26 (q, *J* = 7 Hz, 1H), 2.05-1.95 (m, 3H), 1.44 (d, *J* = 6.5 Hz, 3H), 1.21 (d, *J* = 6.5 Hz, 3H), 1.05-1.02 (m, 18H), 0.98 (t, *J* = 8 Hz, 9H), 0.70 (q, *J* = 8 Hz, 6H), 0.61 (q, *J* = 8 Hz, 6H), 0.33 (s, 9H), 0.22 (s, 3H), 0.20 (s, 3H); ¹³C NMR (100 MHz, C₆D₆): δ 139.4, 120.8, 77.5, 77.1, 75.6, 69.8, 58.8, 41.2, 40.6, 38.9, 26.2, 18.4, 16.0, 7.2, 6.8, 6.6, 5.8, 4.7, 1.1, -3.9, -4.4; HRMS (ESI) *m/z* 701.4455 [(M+Na)⁺ calculated for C₃₃H₇₄NaO₆Si₄: 701.4460].



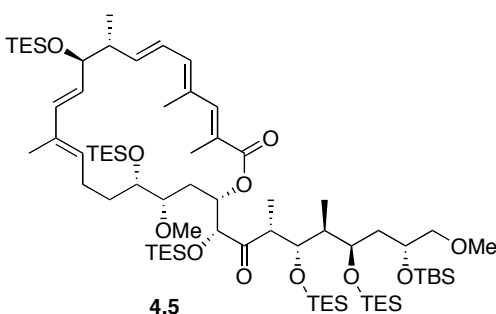
Pyran 4.32: A solution of silyl enol ether **4.31** (4 mg, 5.9 μ mol) and *p*-TsOH (1 mg, 5.2 μ mol) in 1 mL MeOH was stirred overnight at room temperature. The solvent was removed *in vacuo* and the residue was purified by flash chromatography (CH₂Cl₂/MeOH, 25/1) to afford 1 mg (69%) of pyran **4.32** as a colorless oil: ¹H NMR (600 MHz, CD₃OD): δ 4.02 (t, *J* = 5.4 Hz, 1H), 3.95 (ddt, *J*

= 12, 5.4, 4.2 Hz, 1H), 3.59 (t, $J = 9.9$ Hz, 1H), 3.41 (d, $J = 12$ Hz, 1H), 3.36 (d, $J = 11.4$ Hz, 1H), 3.35 (s, 3H), 3.33 – 3.31 (m, 1H), 1.99 dqd, $J = 10.2, 7.2, 5.4$ Hz, 1H), 1.96 (dq, $J = 9.6, 6.6$ Hz, 1H), 1.71 (ddd, $J = 13.8, 12.6, 6$ Hz, 1H), 1.64 (ddd, $J = 13.8, 3.6, 0.6$ Hz, 1H), 1.05 (d, $J = 6.6$ Hz, 3H), 1.02 (d, $J = 7.2$ Hz, 3H); HRMS (ESI) m/z 253.1625 $[(M+Li)^+]$ calculated for $C_{12}H_{22}LiO_5$: 253.1627].



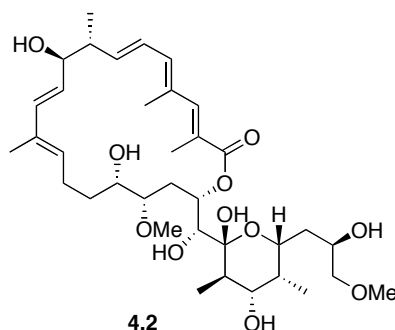
Vinyl Boronate 4.35: To a solution of alkene **4.33** (28.9 mg, 19.5 μ mol) in toluene (0.2 mL) was added 1-propenyl pinacol boronic ester **4.12** (33 mg, 195 μ mol, 10 equiv) followed by Grubbs second-generation catalyst **4.34** (1.7 mg, 1.95 μ mol, 0.1 equiv). The resulting solution was stirred at 80 °C for 6 h, then 0.2 mL toluene were added and the mixture stirred at 40 °C for 24 h. The reaction mixture was then cooled to room temperature and diluted with dichloromethane (5 mL). The resultant solution was filtered through a short silica gel plug. The solvent was removed *in vacuo* and the residue was purified by HPLC (Hexanes/EtOAc, 0-5% gradient over 50 min) to afford 16.6 mg (53%) vinyl boronate **4.35** as a colorless oil: IR (neat) 2954, 2365, 1708, 1638, 1459, 1362, 1242, 1112, 1007 cm^{-1} ; 1H NMR (500 MHz, C_6D_6): δ 7.27 (s, 1H), 7.12 (d, $J = 7$ Hz, 1H), 6.27 (s, 1H), 6.26 (d, $J = 15.5$ Hz, 1H), 5.98 (d, $J = 11$ Hz, 1H), 5.85 (d,

$J = 18$ Hz, 1H), 5.64 (dd, $J = 15.5, 7$ Hz, 1H), 5.52 (t, $J = 6.8$ Hz, 1H), 4.88 (d, $J = 3$ Hz, 1H), 4.32 (dd, $J = 8.5, 5.5$ Hz, 1H), 4.22 (d, $J = 8$ Hz, 1H), 4.18 (t, $J = 5.8$ Hz, 1H), 4.00-3.92 (m, 2H), 3.48 (q, $J = 7$ Hz, 1H), 3.43-3.40 (m, 2H), 3.38 (s, 3H), 3.30 (dd, $J = 11, 4$ Hz, 1H), 3.21 (s, 3H), 2.49-2.36 (m, 3H), 2.26-2.15 (m, 1H), 2.14-2.07 (m, 1H), 2.05-1.92 (m, 2H), 1.90 (s, 3H), 1.89-1.82 (m, 1H), 1.78 (s, 3H), 1.75-1.73 (m, 1H), 1.72 (s, 3H), 1.64-1.53 (m, 1H), 1.37 (d, $J = 7$ Hz, 3H), 1.20-1.00 (m, 72H), 0.99-0.89 (m, 6H), 0.88-0.82 (m, 6H), 0.79-0.73 (m, 6H), 0.68-0.59 (m, 12H), 0.22 (s, 3H), 0.20 (s, 3H); ^{13}C NMR (150 MHz, C_6D_6): δ 209.5, 167.8, 157.2, 143.9, 139.5, 135.6, 133.9, 132.3, 128.8, 86.5, 82.9, 80.7, 79.9, 77.6, 77.1, 74.7, 72.5, 70.9, 70.4, 70.1, 58.9, 58.3, 47.2, 47.0, 43.9, 40.7, 31.5, 31.2, 25.4, 24.9, 24.8, 24.3, 14.4, 14.2, 12.7, 12.1, 10.2, 7.6, 7.5, 7.3, 7.2, 6.7, 5.9, 5.8, -3.9, -4.4; HRMS (MALDI) m/z 1627.9080 [(M+Na) $^+$ calcd for $\text{C}_{78}\text{H}_{154}\text{BINaO}_{13}\text{Si}_6$: 1627.9040].



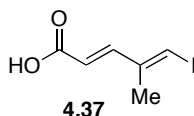
Macrolactone 4.5: To a solution of vinyl boronate **4.35** (16.6 mg, 10.3 μmol) in THF/ H_2O (12 mL, 3:1, degassed) was added $\text{Pd}(\text{Ph}_3\text{P})_4$ (2.4 mg, 2.06 μmol , 0.2 equiv). The resulting yellow solution was stirred for 5 min before $\text{Ti}(\text{OEt})_4$ (1.1 μL , 15.45 μmol , 1.5 equiv) was added. The solution was stirred for 15 min (color

turns from yellow to grey). The reaction was quenched with saturated NaHCO₃ (5 mL) and the aqueous layer was extracted with dichloromethane (3 x 10 mL). The combined organic layers were dried (MgSO₄), filtered and concentrated *in vacuo*. The residue was diluted with hexanes and filtrated through a small silica gel plug (washed with Hexanes until no more product eluted) to afford 13.3 mg (95%) of macrolactone **3.5** as a colorless oil: IR (neat) 2954, 2876, 1723, 1699, 1458, 1239, 1110, 1007, 740 cm⁻¹; ¹H NMR (500 MHz, C₆D₆): δ 7.53 (s, 1H), 6.27 (d, *J* = 11 Hz, 1H), 6.05 (dd, *J* = 14.5, 11 Hz, 1H), 5.92 (d, *J* = 16 Hz, 1H), 5.75 (d, *J* = 8 Hz, 1H), 5.53 (t, *J* = 7.3 Hz, 1H), 5.40-5.30 (m, 2H), 5.00 (d, *J* = 4 Hz, 1H), 4.33 (dd, *J* = 8.5, 4.5 Hz, 1H), 4.27 (d, *J* = 8 Hz, 1H), 3.98-3.92 (m, 1H), 3.82 (t, *J* = 8.5 Hz, 1H), 3.65 (t, *J* = 6.5 Hz, 1H), 3.57-3.51 (m, 1H), 3.54 (s, 3H), 3.43-3.39 (m, 2H), 3.20 (s, 3H), 3.03 (t, *J* = 7.8 Hz, 1H), 2.54-2.46 (m, 1H), 2.41-2.34 (m, 1H), 2.16-1.93 (m, 6H), 2.09 (s, 3H), 1.84-1.78 (m, 1H), 1.72 (s, 3H), 1.70-1.64 (m, 1H), 1.61 (s, 3H), 1.46 (d, *J* = 7 Hz, 3H), 1.44-1.36 (m, 1H), 1.27 (d, *J* = 6.5 Hz, 3H), 1.22-1.03 (m, 56H), 1.02-0.86 (m, 12H), 0.79-0.65 (m, 18H), 0.22 (s, 3H), 0.19 (s, 3H); ¹³C NMR (150 MHz, C₆D₆): 209.9, 168.2, 144.9, 144.5, 140.9, 136.2, 133.6, 132.6, 131.9, 131.0, 126.1, 123.9, 82.2, 80.6, 78.3, 77.2, 76.2, 74.1, 73.1, 70.5, 70.1, 61.0, 58.8, 47.3, 46.7, 43.7, 40.9, 35.6, 34.9, 26.1, 24.8, 18.6, 15.4, 14.1, 12.2, 11.3, 10.4, 7.6, 7.5, 7.4, 7.3, 7.2, 6.7, 6.0, 5.9, 5.6, 5.5, -3.9, -4.4; HRMS (MALDI) *m/z* 1373.9100 [(M+Na)⁺ calcd for C₇₂H₁₄₂NaO₁₁Si₆: 1373.9065].

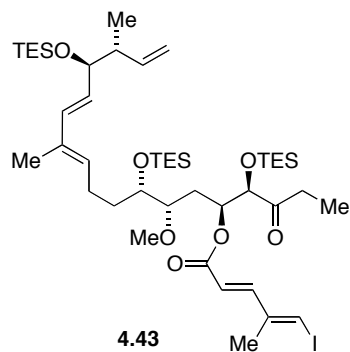


Apoptolidinone D 4.2. To solution of 19.9 mg (14.7 μ Mol) macrolactone **4.5** in 4 mL of THF at -10 °C was added HF•Py (0.2 mL) dropwise. After 1 h the temperature was raised to 0 °C and after an additional 12 h to 10 °C. After 36 h the reaction mixture was diluted with Et₂O, washed with water, and concentrated in vacuo leaving ca. 4 mL of Et₂O. (It was noticed that drying over MgSO₄ significantly decreased the amount of product in the solution.) The residue was purified by flash chromatography (CH₂Cl₂/MeOH, 15:1) to afford 8.5 mg (87%) of apoptolidinone D **4.2** as a off-white solid: $[\alpha]_D^{25} +67.5$; IR (neat) 3382, 2927, 2362, 1666, 1390, 1255, 1100, 1024, 965, 754 cm⁻¹; ¹H NMR (600 MHz, CD₃OD) δ 7.39 (s, 1H), 6.27-6.22 (m, 2H), 5.99 (d, $J = 15.6$ Hz, 1H), 5.57 (t, $J = 8.1$ Hz, 1H), 5.48-5.44 (m, 1H), 5.32-5.28 (m, 2H), 4.08 (dt, $J = 8.4, 2.4$ Hz, 1H), 3.78-3.73 (m, 2H), 3.55-3.50 (m, 1H), 3.53 (d, $J = 1.2$ Hz, 1H), 3.42-3.35 (m, 2H), 3.37 (s, 3H), 3.26 (s, 3H), 3.18-3.12 (m, 2H), 2.66 (dd, $J = 9.6, 5.4$ Hz, 1H), 2.49-2.42 (m, 1H), 2.30-2.23 (m, 1H), 2.17-1.95 (m, 5H), 2.13 (s, 3H), 2.08 (s, 3H), 1.79-1.72 (m, 2H), 1.72-1.53 (m, 3H), 1.64 (s, 3H), 1.43-1.22 (m, 4H), 1.18 (d, $J = 6.6$ Hz, 3H), 1.02 (d, $J = 6.6$ Hz, 3H), 0.87 (d, $J = 6.6$ Hz, 3H); ¹³C NMR (150 MHz, CD₃OD) δ 172.6, 147.5, 146.0, 143.0, 137.4, 135.0, 133.5, 132.2, 130.9, 126.6, 124.2, 101.3, 84.0, 80.0, 78.5, 75.4, 74.9, 73.8, 72.5, 69.2, 68.1, 61.4, 59.4, 46.7,

40.9, 38.5, 38.3, 36.3, 36.1, 24.8, 18.6, 15.6, 13.9, 12.2, 12.1, 5.3; HRMS (MALDI) m/z 689.3881 [(M + Na)⁺ calcd for C₃₆H₅₈NaO₁₁, 689.3877].

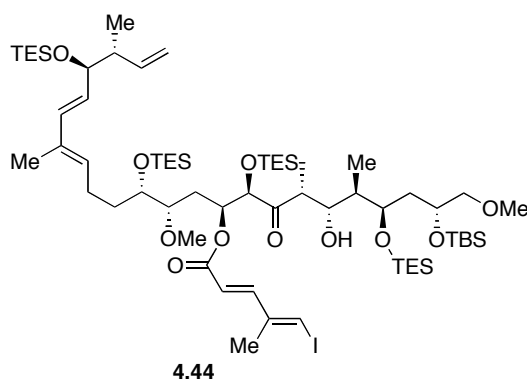


Carboxylic Acid 4.37: To a solution of ester **4.42** (2.0 g, 7.9 mmol) in MeOH/H₂O (7.5 mL/2.5 mL) was added lithium hydroxide hydrate (1.7 g, 39.7 mmol). The clear solution was stirred at ambient temperature for 6.5 h. Solvent was removed in *vacuo* and the residue was diluted with CH₂Cl₂ (20 mL) and water (10 mL). The biphasic mixture was then acidified with concentrated aqueous HCl to pH=3. The aqueous layer was separated and extracted with CH₂Cl₂ (3 x 50 mL). The combined organic layers were dried over Na₂SO₄ and concentrated in *vacuo*. Flash chromatography of the residue (petroleum ether:ether: 4:1) gave 1.7 g (90%) of **4.37** as a yellow solid: IR (neat) 3049, 2917, 1671, 1420, 1290, 976 cm⁻¹; ¹H NMR (400 MHz, CDCl₃): δ 7.43 (d, *J* = 15.6 Hz, 1H), 7.03 (s, 1H), 5.97 (d, *J* = 15.6 Hz, 1H), 2.03 (s, 3H); ¹³C NMR (100 MHz, CDCl₃): δ 172.3, 146.6, 144.0, 117.4, 95.1, 19.6.



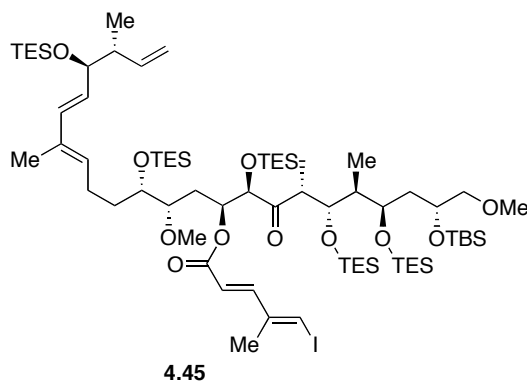
Ester 4.43: To a solution of aldol **4.30a** (0.78 g, 1.08 mmol) and acid **4.37** (0.32 g, 1.35 mmol) in toluene and THF (1:1 36 mL) was added DMAP (1.98 g, 16.21 mmol) at 0 °C. After DMAP dissolved completely the mixture was cooled to -78 °C, and Et₃N (1.66 mL, 11.89 mmol) was added followed by 2,4,6-trichlorobenzoyl chloride (1.70 mL, 10.81 mmol). The resulting slurry was slowly warmed to room temperature over 2.5 h. The reaction was stirred overnight at room temperature, quenched with saturated NaHCO₃ (10 mL) and the aqueous layer was extracted with Et₂O (3 x 25 mL). The combined organic layers were dried (Na₂SO₄), filtered and concentrated *in vacuo*. The residue was purified by flash chromatography (Hexanes/EtOAc, 50:1) to afford 0.35 g (35%) of desired ester diastereomer **4.43** as a colorless oil: $[\alpha]_D^{20} -13.7$ (c 1.0, CHCl₃); IR (neat) 2954, 2877, 2362, 2342, 1718, 1622, 1458, 1284, 1107, 1007, 726 cm⁻¹; ¹HMR (600 MHz, C₆D₆): δ 7.35 (d, *J* = 15.6 Hz, 1H), 6.27 (d, *J* = 13.8 Hz, 1H), 6.26 (s, 1H), 6.06-6.01 (m, 1H), 5.93 (d, *J* = 16.2 Hz, 1H), 5.90 (ddd, *J* = 10.8, 4.2, 1.8 Hz, 1H), 5.65 (dd, *J* = 15.6, 7.2 Hz, 1H), 5.56 (t, *J* = 6.6 Hz, 1H), 5.09-5.06 (m, 2H), 4.30 (d, *J* = 4.2 Hz, 1H), 4.09 (dd, *J* = 6.6, 6.6 Hz, 1H), 3.99-3.97 (m, 1H), 3.38 (s, 3H), 3.37-3.34 (m, 1H), 2.70-2.63 (m, 1H), 2.44-2.35 (m, 3H), 2.33 -2.28

(m, 1H), 2.24-2.19 (m, 1H), 1.89-1.82 (m, 1H), 1.78 (s, 3H), 1.59-1.57 (m, 1H), 1.57 (s, 3H), 1.14 (d, $J = 4.2$ Hz, 3H), 1.05-0.97 (m, 27H), 0.91 (t, $J = 7.2$ Hz, 3H), 0.67-0.59 (m, 18H); ^{13}C NMR (150 MHz, C_6D_6): δ 209.2, 166.4, 145.0, 144.0, 141.4, 135.8, 133.9, 132.4, 128.8, 118.3, 114.3, 94.1, 80.8, 80.5, 78.2, 72.0, 71.0, 58.3, 45.2, 32.0, 31.5, 31.0, 25.4, 19.2, 15.1, 12.8, 7.6, 7.2, 7.2, 7.0, 5.5, 5.5, 5.1; HRMS (ESI) m/z 969.4393, $[(\text{M}+\text{Na})^+]$ calculated for $\text{C}_{45}\text{H}_{83}\text{I}\text{NaO}_7\text{Si}_3$: 969.4383].



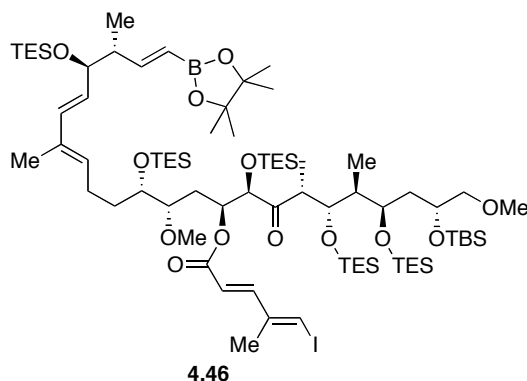
Aldol 4.44: To a solution of LHMDS (0.14 mL, 0.13 mmol, 1M in THF) in THF (2 mL) at -78 °C was added a solution of ketone **4.43** (0.064 g, 0.068 mmol) and HMPA (0.034 mL, 0.20 mmol) in THF (2 mL). The reaction mixture was stirred at -78 °C for 2 h before a solution of aldehyde **4.11** (0.081 g, 0.20 mmol) in THF (1 mL) was added dropwise. The solution was stirred at -78 °C for 3 h, quenched with saturated NH_4Cl (5 mL) and warmed to room temperature. The aqueous layer was extracted with Et_2O (3 x 10 mL) and the combined organic layers were dried (Na_2SO_4), filtered and concentrated *in vacuo*. The residue was purified by HPLC: 21.4 mm x 25 cm column, 49 min gradient, 0–5% ethyl acetate in hexanes to afford 0.016 g (18%) of aldol **4.44** as a colorless oil:

$[\alpha]_D^{20}$ -22.37 (c 0.8, CHCl_3); IR (neat) 3474, 2955, 2877, 1716, 1622, 1459, 1283, 1109, 1005, 742 cm^{-1} ; ^1H NMR (600 MHz, C_6D_6): δ 7.37 (d, $J = 15.6$ Hz, 1H), 6.31 (s, 1H), 6.27 (d, $J = 15.6$ Hz, 1H), 6.10-6.07 (m, 1H), 6.06-6.00 (m, 1H), 5.96 (d, $J = 15.6$ Hz, 1H), 5.65 (dd, $J = 15.6, 7.2$ Hz, 1H), 5.54 (t, $J = 7.2$ Hz, 1H), 5.09-5.06 (m, 2H), 4.92 (d, $J = 3.6$ Hz, 1H), 4.44 (d, $J = 9.6$ Hz, 1H), 4.36-4.33 (m, 1H), 4.12-4.08 (m, 2H), 4.04 (s, 1H), 4.02-3.97 (m, 1H), 3.43 (s, 3H), 3.39-3.35 (m, 1H), 3.32-3.28 (m, 1H), 3.27 (d, $J = 4.8$ Hz, 1H), 3.09 (s, 3H), 2.45-2.35 (m, 3H), 2.26-2.18 (m, 1H), 2.09-2.05 (m, 1H), 1.99-1.83 (m, 4H), 1.78 (s, 3H), 1.61 (s, 3H), 1.61-1.56 (m, 1H), 1.34 (d, $J = 6.6$ Hz, 3H), 1.13 (d, $J = 6.6$ Hz, 3H), 1.10-1.00 (m, 45H), 0.94 (d, $J = 7.2$ Hz, 3H), 0.80-0.74 (m, 6H), 0.70-0.62 (m, 18H), 0.23 (s, 3H), 0.20 (s, 3H); ^{13}C NMR (150 MHz, C_6D_6): δ 209.9, 166.6, 145.1, 144.1, 141.4, 135.8, 133.8, 132.5, 128.7, 118.5, 114.3, 94.2, 81.0, 79.4, 78.2, 73.5, 72.9, 72.3, 71.1, 70.1, 58.4, 58.3, 45.4, 45.2, 41.0, 39.0, 31.6, 31.4, 26.2, 25.4, 19.2, 18.6, 15.1, 12.8, 12.2, 7.7, 7.6, 7.3, 7.3, 7.2, 7.2, 7.1, 5.7, 5.5, 5.4, -3.3, -4.5; HRMS (ESI) m/z 1373.7184, $[(M+\text{Na})^+]$ calculated for $\text{C}_{65}\text{H}_{127}\text{INaO}_{11}\text{Si}_5$: 1373.7162].



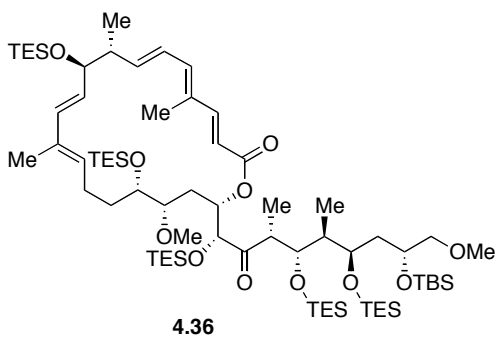
Silyl Ether 4.45: To a solution of alcohol **4.44** (0.08 g, 0.05 mmol) in dichloromethane (11 mL) at -78 °C was added 2,6-lutidine (0.05 mL, 0.46 mmol) followed by TESOTf (0.08 mL, 0.35 mmol). The mixture was stirred for 30 min at -78 °C, then 30 min at 0 °C and quenched with H₂O (10 mL). The aqueous layer was extracted with dichloromethane (3 x 10 mL) and the combined organic layers were dried (Na₂SO₄), filtered and concentrated *in vacuo*. The residue was purified by flash chromatography (Hexanes:EtOAc = 50:1) to afford 0.12 g quantitative yield of TES ether **4.45** as a colorless oil: $[\alpha]_D^{20}$ -51.67 (c 1.2, CHCl₃); IR (neat) 2954, 2877, 1717, 1622, 1459, 1283, 1109, 1006, 740 cm⁻¹; ¹HMR (600 MHz, C₆D₆): δ 7.35 (d, *J* = 15.6 Hz, 1H), 6.30 (s, 1H), 6.20 (d, *J* = 15.6 Hz, 1H), 6.07-5.99 (m, 2H), 5.94 (d, *J* = 15.6 Hz, 1H), 5.65 (dd, *J* = 15.6, 7.2 Hz, 1H), 5.56 (t, *J* = 7.2 Hz, 1H), 5.10-5.06 (m, 2H), 4.93 (d, *J* = 3.0 Hz, 1H), 4.33 (ddd, *J* = 8.4, 5.4, 1.2 Hz, 1H), 4.23 (dd, *J* = 8.4, 1.2 Hz, 1H), 4.09 (t, *J* = 7.2 Hz, 1H), 4.01-3.98 (m, 1H), 3.95-3.93 (m, 1H), 3.56 (dq, *J* = 6.6, 1.2 Hz, 1H), 3.41 (s, 3H), 3.30 (ddd, *J* = 10.8, 4.2, 0 Hz, 1H), 3.21 (s, 3H), 2.48-2.39 (m, 3H), 2.26-2.19 (m, 1H), 2.14-2.09 (m, 1H), 2.05-2.00 (m, 1H), 1.95-1.85 (m, 2H), 1.78 (s, 3H), 1.78-1.74 (m, 1H), 1.62-1.57 (m, 1H), 1.60 (s, 3H), 1.41 (d, *J* = 7.2 Hz, 1H), 1.19-1.15 (m, 18H), 1.13 (d, *J* = 6.6 Hz, 3H), 1.10-1.01 (m, 39H), 0.99-0.90 (m, 6H), 0.86 (q, *J* = 7.8 Hz, 6H), 0.76 (q, *J* = 7.8 Hz, 6H), 0.70-0.62 (m, 12H), 0.21 (s, 3H), 0.19 (s, 3H); ¹³C NMR (150 MHz, C₆D₆): δ 208.9 166.2, 144.9, 143.8, 141.2, 135.5, 133.6, 132.2, 128.7, 118.0, 114.0, 94.1, 80.4, 77.9, 76.8, 74.7, 71.8, 70.6, 70.2, 69.8, 58.7, 58.0, 47.0, 45.0, 43.7, 40.4, 31.2, 25.9, 25.2, 18.9, 18.1, 14.9, 12.6, 11.9, 10.0, 7.3, 7.3, 7.1, 7.0, 6.9, 6.5, 5.7, 5.3, -4.2, -4.6; HRMS

(ESI) m/z 1487.8015 [(M+Na)⁺ calculated for C₇₁H₁₄₁INaO₁₁Si₆: 1487.8026].



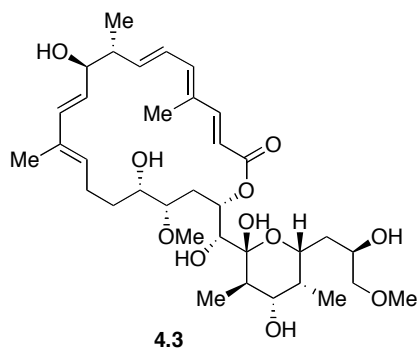
Vinyl Boronate 4.46: To a solution of alkene **4.45** (120.0 mg, 57.7 μmol) in dichloromethane (11.0 mL) was added 1-propenyl pinacol boronic ester **4.12** (89 mg, 576 μmol) followed by Grubbs second-generation catalyst **4.34** (5 mg, 5.77 μmol) at room temperature. The resulting solution was stirred at 50 °C for 46 h, cooled to room temperature and diluted with dichloromethane (10 mL). The resultant solution was filtered through a short silica gel plug. The solvent was removed *in vacuo* and the residue was purified by HPLC (Hexanes/EtOAc, 0-5% gradient over 50 min) to afford 25 mg (25%) vinyl boronate **4.46** as a colorless oil: $[\alpha]_{\text{D}}^{20}$ 42.76 (c 1.3, CHCl₃); IR (neat) 2955, 2877, 1718, 1623, 1459, 1243, 1109, 1007, 741 cm^{-1} ; ¹HMR (600 MHz, C₆D₆): δ 7.36 (d, J = 15.6 Hz, 1H), 6.29 (s, 1H), 6.26 (d, J = 15.6 Hz, 1H), 6.07-6.05 (m, 1H), 5.94 (d, J = 15.6 Hz, 1H), 5.85 (d, J = 18.0, Hz, 1H), 5.63 (dd, J = 15.6, 6.6 Hz, 1H), 5.53 (t, J = 6.6 Hz, 1H), 4.34-4.31 (m, 1H), 4.24 (dd, J = 8.4, 1.8 Hz, 1H), 4.18 (dd, J = 6.6, 5.4 Hz, 1H), 4.00-3.97 (m, 1H), 3.96-3.92 (m, 1H), 3.56 (dq, J = 6.6, 1.8 Hz, 1H), 3.41 (s, 3H), 3.41 (d, J = 3.0 Hz, 2H), 3.30 (ddd, J = 11.4, 4.2, 0 Hz, 1H), 3.21 (s, 3H),

2.49-2.39 (m, 3H), 2.24-2.17 (m, 1H), 2.14-2.07 (m, 1H), 2.05-2.00 (m, 1H), 1.95-1.84 (m, 2H), 1.79-1.74 (m, 1H), 1.72 (s, 3H), 1.62-1.57 (m, 1H), 1.60 (s, 3H), 1.41 (d, $J = 7.2$ Hz, 3H), 1.19-1.15 (m, 21H), 1.14-1.07 (m, 24H), 1.06-1.01 (m, 27H), 1.00-0.91 (m, 6H), 0.87 (q, $J = 7.8$ Hz, 6H), 0.76 (q, $J = 6.6$ Hz, 6H), 0.67-0.62 (m, 12H), 0.21 (s, 3H), 0.19 (s, 3H); ^{13}C NMR (150 MHz, C_6D_6): δ 209.0, 166.2, 156.9, 144.9, 143.8, 135.4, 133.7, 132.0, 128.5, 118.0, 94.0, 82.6, 80.4, 77.4, 76.8, 74.7, 71.8, 70.5, 70.1, 69.8, 58.7, 58.0, 47.1, 46.7, 43.7, 40.4, 31.3, 31.2, 25.9, 25.2, 24.7, 24.6, 18.9, 18.1, 14.0, 12.5, 11.9, 9.8, 7.3, 7.3, 7.2, 7.1, 7.0, 7.0, 6.5, 5.7, 5.3, 5.2, -4.2, -4.6; HRMS (ESI) m/z 1613.8924, $[(\text{M}+\text{Na})^+]$ calculated for $\text{C}_{77}\text{H}_{152}\text{BINO}_{13}\text{Si}_6$: 1613.8878].



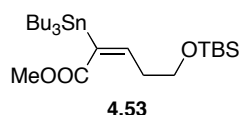
Macrolactone 4.36: To a solution of vinyl boronate **4.46** (26 mg, 15.9 μmol) in THF/ H_2O (8 mL, 3:1, degassed) was added $\text{Pd}(\text{PPh}_3)_4$ (1.8 mg, 1.59 μmol) at room temperature. The resulting yellow solution was stirred for 10 min, then TIOEt (1.3 μL , 18.8 μmol) was added. The reaction mixture was stirred for another 20 min (color turns from yellow to grey) at room temperature. The reaction was quenched with saturated NaHCO_3 (5 mL) and the aqueous layer was extracted with ethyl acetate (3 x 10 mL). The combined organic layers were

dried (Na₂SO₄), filtered and concentrated *in vacuo*. The residue was purified by flash chromatography (Hexanes/EtOAc, 25:1) to afford 11 mg (52%) of lactone **4.36** as a colorless oil: $[\alpha]_D^{20}$ -16 (c 0.45, CHCl₃); IR (neat) 2955, 2877, 2360, 1709, 1459, 1243, 1121, 1077, 1008, 740; ¹HMR (600 MHz, C₆D₆): δ 7.50 (d, *J* = 15.6 Hz, 1H), 6.15 (d, *J* = 10.8 Hz, 1H), 5.91 (dd, *J* = 15.0, 10.8 Hz, 1H), 5.94-5.86 (m, 1H), 5.83 (d, *J* = 15.6 Hz, 1H), 5.79 (d, *J* = 16.2 Hz, 1H), 5.46 (t, *J* = 7.2 Hz, 1H), 5.28-5.21 (m, 2H), 4.97 (d, *J* = 3.6 Hz, 1H), 4.35-4.26 (m, 2H), 3.98-3.93 (m, 1H), 3.75 (dt, *J* = 8.4, 0, 1H), 3.68 (dt, *J* = 7.8, 3.0 Hz, 1H), 3.62-3.58 (m, 1H), 3.60 (s, 3H), 3.41 (d, *J* = 4.8 Hz, 2H), 3.20 (s, 3H), 3.06-3.3.03 (m, 1H), 2.49-2.42 (m, 1H), 2.31-2.26 (m, 1H), 2.18-2.06 (m, 3H), 2.05-2.01 (m, 2H), 1.84-1.78 (m, 1H), 1.72-1.66 (m, 1H), 1.64 (s, 3H), 1.62-1.57 (m, 1H), 1.57 (s, 3H), 1.45 (d, *J* = 7.2 Hz, 3H), 1.42 (s, 3H), 1.25 (d, *J* = 6.6 Hz, 3H), 1.20-1.17 (m, 18H), 1.12-1.02 (m, 30H), 1.02-0.82 (m, 21 H), 0.80-0.65 (m, 18H), 0.22 (s, 3H), 0.19 (s, 3H); ¹³C NMR (150 MHz, C₆D₆): δ 209.8, 165.7, 150.5, 145.7, 140.8, 136.1, 133.7, 131.8, 131.1, 129.0, 126.7, 115.9, 82.0, 80.6, 77.2, 76.2, 72.5, 70.5, 70.1, 68.0, 60.8, 58.8, 46.8, 43.8, 39.2, 35.0, 30.8, 29.3, 26.1, 24.7, 24.1, 18.1, 12.2, 11.8, 10.4, 7.6, 7.5, 7.4, 7.3, 7.1, 6.7, 6.1, 6.0, 5.6, 5.5, -3.9, -4.4; HRMS (ESI) *m/z* 1359.8911 [(M+Na)⁺ calculated for C₇₁H₁₄₀NaO₁₁Si₆: 1359.8903].

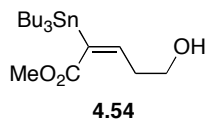


2,6-Dinormethyl Apoptolidinone A 4.3: To solution of 11.0 mg (8.21 μmol) macrolactone **4.36** in 6 mL THF and 6 mL acetonitrile at $-10\text{ }^{\circ}\text{C}$, 0.2 mL H_2SiF_6 (20-25% wt in H_2O) was added dropwise. After stirred for 24 h at $-10\text{ }^{\circ}\text{C}$, the reaction mixture was quenched with saturated NaHCO_3 solution and the aqueous layer was extracted with ethyl acetate (3 x 10 mL). The combined organic layers were dried (Na_2SO_4), filtered and concentrated *in vacuo*. The residue was purified by flash chromatography ($\text{CH}_2\text{Cl}_2/\text{MeOH}$, 20:1) to afford 4.0 mg (75%) of 2,6-Dinormethylapoptolidinone A **4.3** as a white solid: $[\alpha]_{\text{D}}^{20} 57.5$ (c 0.40, CHCl_3); IR (neat) 3399, 2925, 1674, 1601, 1456, 1271, 1097, 1026 cm^{-1} ; ^1H NMR (400 MHz, CD_3OD): δ 7.47 (d, $J = 10.4$ Hz, 1H), 6.32-6.21 (m, 2H), 5.97 (d, $J = 10.4$ Hz, 1H), 5.76 (d, $J = 10.4$ Hz, 1H), 5.57-5.52 (m, 2H), 5.35 (dt, $J = 7.6, 0$ Hz, 1H), 5.28 (dd, $J = 10.4, 6.0$ Hz, 1H), 4.12 (dt, $J = 4.8, 1.6$ Hz, 1H), 3.80-3.74 (m, 2H), 3.68-3.64 (m, 1H), 3.55 (d, $J = 1.2$ Hz, 1H), 3.43 (s, 3H), 3.41-3.37 (m, 1H), 3.25 (s, 3H), 3.17-3.10 (m, 2H), 2.64 (ddd, $J = 5.6, 4.4, 0.0$ Hz, 1H), 2.51-2.45 (m, 1H), 2.30-2.25 (m, 1H), 2.13 (dd, $J = 10.0, 7.6$ Hz, 1H), 2.05 (dd, $J = 7.6, 4.4$ Hz, 1H), 2.08-2.02 (m, 1H), 1.97-1.91 (m, 1H), 1.85 (s, 3H), 1.76-1.73 (m, 1H), 1.65-1.56 (m, 5H), 1.62 (s, 3H), 1.51-1.46 (m, 1H), 1.25-1.21 (m, 1H), 1.20 (d, $J = 4.4$ Hz,

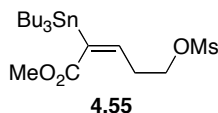
3H), 1.03 (d, $J = 4.4$ Hz, 3H), 0.88 (d, $J = 4.4$ Hz, 3H); ^{13}C NMR (150 MHz, CD_3OD): δ 170.3, 153.6, 147.8, 143.2, 137.5, 134.9, 132.3, 132.2, 130.9, 126.9, 115.8, 101.3, 84.1, 80.1, 78.7, 75.5, 75.1, 73.7, 72.1, 69.1, 68.0, 61.3, 59.4, 54.8, 46.7, 41.0, 38.4, 38.2, 36.3, 35.7, 25.1, 18.3, 12.1, 12.0, 5.3; HRMS (ESI) m/z 675.3723 [(M+Na) $^+$ calculated for $\text{C}_{35}\text{H}_{56}\text{NaO}_{11}$: 675.3715].



Ester 4.53: To a solution of alkyne **4.52** (300 mg, 1.24 mmol) and $\text{Pd}(\text{PPh}_3)_4$ (71 mg, 0.06 mmol) in THF (6 mL) at 0°C was added $(n\text{-Bu})_3\text{SnH}$ (1 mL, 3.71 mmol) dropwise. The resulted solution was continued to stir for 3 h at 0°C and concentrated *in vacuo*. The residue was purified by flash chromatography (Hexanes/ Et_3N , 100:0.01) to afford 614 mg (93%) of ester **4.53** and its regioisomer (>16:1) as a colorless oil: IR (neat) 2926, 1710, 1192, 1092, 834, 776 cm^{-1} ; ^1H NMR (300 MHz, C_6D_6): δ 6.44 (t, $J = 7.0$ Hz, 1H), 3.63 (t, $J = 6.0$ Hz, 2H), 3.43 (s, 3H), 2.85 (dd, $J = 6.0, 12.9$ Hz, 2H), 1.73-1.50 (m, 6H), 1.44-1.32 (m, 6H), 1.07 (t, $J = 7.8$ Hz, 6H), 1.00-0.91 (m, 18H), 0.03 (s, 6H); ^{13}C NMR (75 MHz, C_6D_6): δ 170.7, 151.6, 137.5, 62.6, 50.8, 36.0, 29.4, 27.7, 26.1, 18.4, 13.9, 10.6, -5.2; HRMS (ESI) m/z 541.2718, [(M+Li) $^+$ calculated for $\text{C}_{24}\text{H}_{50}\text{LiO}_3\text{SiSn}$: 541.2711].

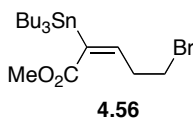


Alcohol 4.54: To a solution of ester **4.53** (300 mg, 0.56 mmol) in THF (12 mL) at 0°C was added HF·Pyridine (4.3 mL), and stirred for 10 min at 0°C. The reaction mixture was quenched with NaHCO₃ (10 mL) and 3 M NaOH aqueous solution was used to adjust the pH to 7. The resulted aqueous layer was extracted with diethyl ether (3 X 15 mL). The combined organic layers were washed with brine (15 mL), dried (Na₂SO₄), filtered and concentrated *in vacuo*. The residue was purified by flash chromatography (Hexanes/EtOAc/Et₃N, 8:1:0.01 to 4:1:0.01) to afford 174 mg (83%) of alcohol **4.54** as a colorless oil: IR (neat) 2923, 1709, 1461, 1194, 1046, 666 cm⁻¹; ¹H NMR (300 MHz, C₆D₆): δ 6.24 (t, *J* = 7.5 Hz, 1H), 3.52 (dd, *J* = 11.7, 6.0 Hz, 2H), 3.40 (s, 3H), 2.66-2.59 (m, 2H), 1.85 (t, *J* = 5.1 Hz, 1H), 1.72-1.45 (m, 6H), 1.41-1.29 (m, 6H), 1.03 (t, *J* = 7.8 Hz, 6H), 0.92 (t, *J* = 7.2 Hz, 9H); ¹³C NMR (75 MHz, C₆D₆): δ 171.5, 150.6, 138.3, 61.5, 51.0, 36.0, 29.3, 27.6, 13.9, 10.5; HRMS (ESI) *m/z* 427.1847, [(M+Li)⁺ calculated for C₁₈H₃₆LiO₃Sn: 427.1846].



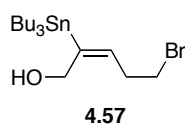
Mesylate 4.55: To a solution of alcohol **4.54** (216 mg, 0.51 mmol) in CH₂Cl₂ (11 mL) at 0°C was added Et₃N (0.11 mL, 0.77 mmol) followed by MsCl

(47 μ L, 0.62 mmol). The reaction mixture was stirred for 5 h at ambient temperature, and quenched with H₂O (10 mL). The aqueous layer was extracted with CH₂Cl₂ (3 X 15 mL). The combined organic layers were washed with brine (15 mL), dried (Na₂SO₄), filtered and concentrated *in vacuo*. The residue was purified by flash chromatography (Hexanes/EtOAc/Et₃N, 8:1:0.01 to 4:1:0.01) to afford 235 mg (91%) of mesylate **4.55** as a colorless oil: IR (neat) 2925, 1704, 1357, 1175, 961, 528 cm⁻¹; ¹H NMR (300 MHz, C₆D₆): δ 6.07 (t, *J* = 6.9 Hz, 1H), 3.92 (t, *J* = 6.3 Hz, 2H), 3.40 (s, 3H), 2.69 (dd, *J* = 13.2, 6.6 Hz, 2H), 2.23 (s, 3H), 1.60-1.50 (m, 6H), 1.40-1.27 (m, 6H), 1.00 (t, *J* = 8.1 Hz, 6H), 0.91 (t, *J* = 7.2 Hz, 9H); ¹³C NMR (75 MHz, C₆D₆): δ 170.5, 147.4, 140.3, 68.4, 51.0, 36.7, 32.0, 29.3, 27.6, 13.9, 10.5; HRMS (ESI) *m/z* 505.1260, [(M+Li)⁺ calculated for C₁₉H₃₈LiO₅SSn: 505.1622].



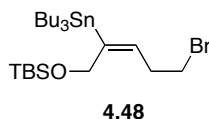
Bromide 4.56: To a solution of mesylate **4.55** (230 mg, 0.46 mmol) in acetone (10 mL) at 0°C was added LiBr (160 mg, 1.85 mmol). The resultant mixture was refluxed at 40°C overnight, cooled down to ambient temperature, diluted with H₂O and Hexane. The aqueous layer was extracted Hexane (3 X 15 mL). The combined organic layers were washed with brine (15 mL), and dried (Na₂SO₄), filtered and concentrated *in vacuo*. The residue was purified by flash chromatography (Hexanes/EtOAc/Et₃N, 8:1:0.01) to afford 200 mg (90%) of

bromide **4.56** as a colorless oil: IR (neat) 2926, 1707, 1462, 1196, 875, 665 cm^{-1} ; ^1H NMR (300 MHz, C_6D_6): δ 6.11 (t, $J = 6.6$ Hz, 1H), 3.38 (s, 3H), 3.02 (t, $J = 6.6$ Hz, 2H), 2.87 (dd, $J = 13.0, 6.3$ Hz, 2H), 1.67-1.50 (m, 6H), 1.42-1.29 (m, 6H), 1.03 (t, $J = 8.1$ Hz, 6H), 0.92 (t, $J = 7.2$ Hz, 9H); ^{13}C NMR (75 MHz, C_6D_6): δ 170.4, 150.1, 139.2, 50.9, 35.0, 32.2, 29.3, 27.6, 13.9, 10.6; HRMS (ESI) m/z 489.1006, $[(\text{M}+\text{Li})^+]$ calculated for $\text{C}_{18}\text{H}_{35}\text{BrLiO}_2\text{Sn}$: 489.1002].

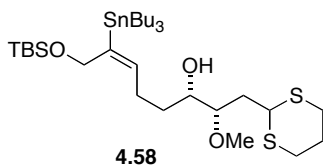


Alcohol 4.57: To a solution of bromide **4.56** (195 mg, 0.40 mmol) in dichloromethane (8 mL) at -78°C was added DIBAL-H (1 M in Hexane) (0.89 mL, 0.89 mmol). The resultant solution was continued to stir at -78°C for 20 min, and quenched with MeOH (2 mL). The resultant mixture was poured into a saturated Rochelle's solution (15 mL), and continued to stir for 1 h. The aqueous layer was extracted with Dichloromethane (3 X 20 mL). The combined organic layers were washed with brine (20 mL), and dried (Na_2SO_4), filtered and concentrated *in vacuo*. The residue was purified by flash chromatography (Hexanes/EtOAc/ Et_3N , 4:1:0.01) to afford 176 mg (97%) of alcohol **4.57** as a colorless oil: IR (neat) 2923, 1462, 1264, 1021, 657; ^1H NMR (300 MHz, C_6D_6): δ 5.43 (t, $J = 6.9$ Hz, 1H), 3.99 (s, 2H), 2.90 (t, $J = 6.9$ Hz, 2H), 2.22 (dd, $J = 13.8, 6.9$ Hz, 2H), 1.71-1.61 (m, 6H), 1.49-1.37 (m, 6H), 1.06 (t, $J = 8.4$ Hz, 6H), 0.97 (t, $J = 7.5$ Hz, 9H);

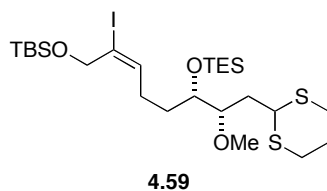
^{13}C NMR (75 MHz, C_6D_6): δ 150.7, 134.3, 63.5, 33.0, 32.2, 29.7, 27.8, 14.0, 10.6;
HRMS (ESI) m/z 489.0577 $[(\text{M}+\text{Cl})^-]$ calculated for $\text{C}_{17}\text{H}_{35}\text{BrClOSn}$: 489.0582].



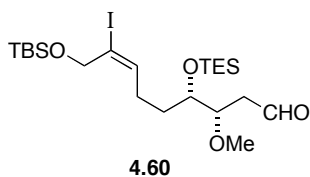
Vinyl Tin 4.48: To a solution of alcohol **4.57** (170 mg, 0.37 mmol) in dimethylformate (7 mL) at 0°C was added imidazole (38 mg, 0.56 mmol) and TBSCl (57 mg, 0.37 mmol). The resultant mixture was continued to stir at ambient temperature overnight, and quenched with H_2O (10 mL). The aqueous layer was extracted with Diethyl ether (3 X 15 mL). The combined organic layers were washed with brine (20 mL), and dried (Na_2SO_4), filtered and concentrated *in vacuo*. The residue was purified by flash chromatography (Hexanes/ Et_3N , 100:0.01) to afford 169 mg (80%) of vinyl tin **4.48** as a colorless oil: IR (neat) 2927, 1463, 1253, 1085, 835, 778; ^1H NMR (300 MHz, C_6D_6): δ 5.48 (t, J = 6.6 Hz, 1H), 4.38 (s, 2H), 2.93 (t, J = 6.9 Hz, 2H), 2.28 (dd, J = 13.2, 6.6 Hz, 2H), 1.79-1.58 (m, 6H), 1.51-1.39 (m, 6H), 1.10 (t, J = 8.4 Hz, 9H), 1.01-0.93 (m, 18H), 0.1 (s, 6H); ^{13}C NMR (75 MHz, C_6D_6): δ 150.5, 134.1, 65.1, 33.0, 32.2, 29.7, 27.9, 26.3, 18.7, 14.0, 10.7, -5.2; HRMS (ESI) m/z 575.1915, $[(\text{M}+\text{Li})^+]$ calculated for $\text{C}_{23}\text{H}_{49}\text{BrLiOSiSn}$: 575.1918].



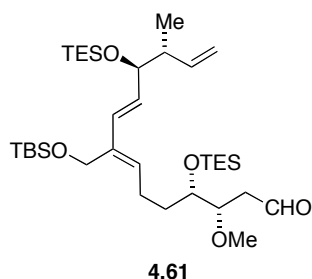
Alcohol 4.58: To a suspension of freshly cut Mg (2.16 g, 90.00 mmol) in THF (50 mL) at room temperature was added 1,2-dibromoethane (0.46 mL, 5.40 mmol) dropwise. A solution of bromide **4.48** (4.1 g, 7.21 mmol) in THF (15 mL) was added to the resulting solution at room temperature over 1 h via syringe pump. The mixture was stirred at room temperature for 1h, and then transferred to a solution of aldehyde **4.7** (0.74 g, 3.60 mmol) in THF (5 mL) at -78 °C via cannula. The reaction mixture was stirred at -78 °C for 4.5 h and quenched with saturated NaHCO₃. The aqueous layer was extracted with Et₂O (3 X 50 mL) and the combined organic layer was dried (Na₂SO₄), filtered and concentrated *in vacuo*. The residue was purified by flash chromatography (Hexane/EtOAc/Et₃N, 20:1:0.01) to afford 1.6 g (64%) of alcohol **4.58** as a colorless oil: $[\alpha]_D^{20}$ -1.8 (c 1.0, CHCl₃); IR (neat) 2927, 2360, 1462, 1252, 1075, 835, 778 cm⁻¹; ¹H NMR (300 MHz, C₆D₆) δ 5.73 (t, *J* = 6.5 Hz, 1H), 4.60 (d, *J* = 6.3 Hz, 2H), 4.19 (t, *J* = 7.2 Hz, 1H), 3.55-3.51 (m, 1H), 3.39 (dd, *J* = 11.4, 6.0 Hz, 1H), 3.22 (s, 3H), 2.40-2.25 (m, 6H), 2.07 (t, *J* = 6.3 Hz, 2H), 1.78-1.67 (m, 6H), 1.54-1.41 (m, 8H), 1.17-1.08 (m, 6H), 1.03-0.97 (m, 18H), 0.14 (s, 6H); ¹³C NMR (125 MHz, C₆D₆) δ 147.7, 137.0, 80.5, 72.5, 64.7, 59.2, 43.8, 36.8, 33.3, 30.5, 30.2, 29.2, 27.4, 26.2, 25.9, 15.2, 13.8, 10.2, -5.3; HRMS (ESI) *m/z* 703.3186, [(M+Li)⁺ calculated for C₃₁H₆₄LiO₃S₂SiSn: 703.3248].



Vinyl iodide 4.59: To a solution of alcohol **4.58** (1.68 g, 2.41 mmol) in DCM (48 mL) at 0 °C was added a solution of I₂ in DCM (632 mg, 2.48 mmol) slowly until the color persisted yellow. After 5 min, Imidazole (493 mg, 7.24 mmol) was added to the solution followed by TESCI (1.21 mL, 7.24 mmol). The reaction mixture was allowed to warm up to room temperature and stirred for 1 h. The reaction was quenched with saturated Na₂S₂O₃ (20 mL) and the aqueous layer was extracted with DCM (3 X 50 mL). The combined organic layer was washed with brine (20 mL), dried (Na₂SO₄), filtered and concentrated *in vacuo*. The residue was purified by flash chromatography (Hexanes/EtOAc, 25:1) to afford 1.5 g (97%) of vinyl iodide **4.59** as a colorless oil: $[\alpha]_D^{20} -3.8$ (c 1.0, CHCl₃); IR (neat) 2953, 2363, 1240, 1098, 1004, 837, 740 cm⁻¹; ¹H NMR (400 MHz, C₆D₆) δ 6.21 (t, *J* = 7.6 Hz, 1H), 4.37 (dd, *J* = 10.8, 4.0 Hz, 1H), 4.21 (s, 2H), 3.82-3.77 (m, 1H), 3.66 (ddd, *J* = 10.0, 4.4, 2.0 Hz, 1H), 3.31 (s, 3H), 2.47-2.31 (m, 4H), 2.26-2.19 (m, 2H), 2.02-1.90 (m, 2H), 1.64-1.51 (m, 2H), 1.44-1.40 (m, 1H), 1.29-1.19 (m, 1H), 1.06-1.01 (m, 18H), 0.65 (q, *J* = 7.6 Hz, 6H), 0.13 (s, 6H) ; ¹³C NMR (125 MHz, C₆D₆) δ 142.5, 103.3, 80.4, 71.3, 65.5, 58.3, 44.9, 35.7, 31.1, 30.6, 30.0, 28.3, 26.2, 26.1, 18.6, 7.3, 5.5, -4.9; HRMS (ESI) *m/e* 653.2027, [(M+Li)⁺ calculated for C₂₅H₅₁ILiO₃S₂Si₂: 653.2023].

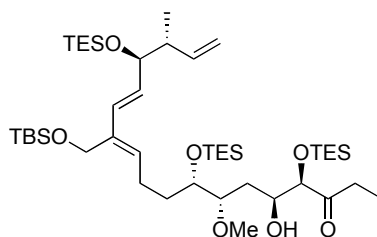


Aldehyde 4.60: To a solution of dithiane **4.59** (1.50 g, 2.34 mmol) in MeCN/pH=7 buffer (90 mL, 4/1) at 0 °C was added K₂CO₃ (0.81 g, 5.85 mmol) and MeI (0.150 ml, 23.4 mmol) in 5 min. The reaction mixture was warmed up to 30 °C and stirred 48 h. The reaction mixture was diluted with EtOAc (50 mL) and the aqueous layer was extracted with EtOAc (3 X 50 mL). The combined organic layers were washed with brine (30 mL), dried (Na₂SO₄), filtered and concentrated *in vacuo*. The residue was purified by flash chromatography (Hexane/EtOAc, 25:1) to afford 1.0 g (77%) of aldehyde **4.60**: [α]_D²⁰ -3.9 (c 1.0, CHCl₃); IR (neat) 2954, 2878, 1728, 1461, 1375, 1097, 836 cm⁻¹; ¹H NMR (400 MHz C₆D₆): δ 9.51 (s, 1H), 6.24 (t, *J* = 7.6 Hz, 1H), 4.21 (s, 2H), 3.73-3.64 (m, 2H), 3.09 (s, 3H), 2.38-2.33 (m, 1H), 2.25-2.14 (m, 2H), 1.97-1.87 (m, 1H), 1.59-1.50 (m, 1H), 1.21-1.10 (m, 1H), 1.00 (s, 9H), 0.95 (t, *J* = 8.0, 9H), 0.90 (t, *J* = 8.0 Hz, 9H), 0.54 (q, *J* = 8.0 Hz, 6H), 0.12 (s, 6H); ¹³C NMR (125 MHz, C₆D₆): δ 199.4, 142.3, 103.4, 78.8, 71.4, 65.5, 57.7, 43.7, 31.3, 28.2, 26.1, 18.5, 7.1, 5.3, -4.9; HRMS (ESI) *m/z* 595.1532, [(M+K)⁺ calculated for C₂₂H₄₅IKO₄Si₂: 595.1538].



Aldehyde 4.61: To a solution of aldehyde **4.60** (1.0 g, 1.8 mmol) and vinyl borate **4.8** (0.83 g, 2.34 mmol) in THF/H₂O (90mL, 3/1, degassed) at room temperature was added Pd(Ph₃P)₄ (208 mg, 0.18 mmol). The mixture was stirred for 10 min, and TIOEt (0.16 mL, 2.25 mmol) was added via syringe. The reaction was kept at room temperature for 20 min, and then quenched with saturated NaHCO₃. The aqueous layer was extracted with EtOAc (3 x 50 mL), and the combined organic layers were washed with brine (50 mL), dried (Na₂SO₄), filtered and concentrated *in vacuo*. The residue was purified by flash chromatography (Hexane/EtOAc, 30:1) to afford 0.91 g (77%) of diene **4.61** as a colorless oil: $[\alpha]_D^{20}$ 0.9 (c 1.0, CHCl₃); IR (neat) 2955, 2876, 1730, 1459, 1253, 1079, 741 cm⁻¹; ¹H NMR (400 MHz CDCl₃): δ 9.83 (s, 1H), 6.01 (d, *J* = 15.6 Hz, 1H), 5.91-5.82 (m, 1H), 5.75 (dd, *J* = 16.0, 7.2 Hz, 1H), 5.51 (t, *J* = 7.2 Hz, 1H), 5.02-4.97 (m, 2H), 4.30 (d, *J* = 6.0 Hz, 2H), 3.99 (t, *J* = 6.0 Hz, 1H), 3.91-3.86 (m, 1H), 3.78-3.74 (m, 1H), 3.38 (s, 3H), 2.69 (ddd, *J* = 16.8, 3.6, 1.2 Hz, 1H), 2.53 (dddd, *J* = 25.2, 16.8, 8.4, 2.4 Hz, 1H), 2.43-2.27 (m, 2H), 2.21-2.11 (m, 1H), 1.71-1.63 (m, 1H), 1.43-1.33 (m, 1H), 1.01-0.90 (m, 30H), 0.65-0.55 (m, 12H), 0.08 (s, 6H); ¹³C NMR (125 MHz, C₆D₆): δ 199.5, 141.4, 137.4, 133.8, 133.0, 130.2, 114.4, 79.0, 78.2, 71.8, 58.5, 57.7, 45.2, 43.8, 32.0, 26.1, 25.4, 24.9, 15.1,

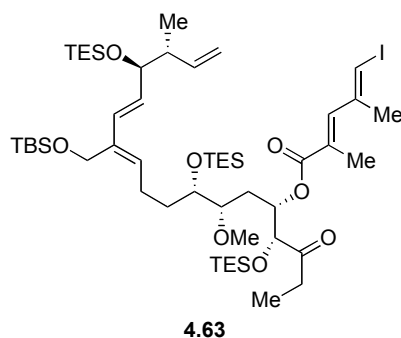
14.2, 7.1, 7.0, -5.1; HRMS (ESI) m/z 661.4693, $[(M+Li)^+]$ calculated for $C_{35}H_{70}LiO_5Si_3$: 661.4691].



4.62

Aldol 4.62: To a solution of diene **4.61** (0.40 g, 0.61 mmol) and a 7:1 mixture of silyl enol ethers *E*-**4.9**/*Z*-**4.9** (0.67 g, 2.44 mmol) in dichloromethane (20.5 mL) was added CaH_2 (190 mg) at 0 °C. After 10 min, the reaction was cooled to -94 °C and a solution of $BF_3 \cdot OEt_2$ in dichloromethane (0.61 mmol, 0.5 M in dichloromethane) was added via syringe. The reaction mixture was stirred for 40 min, quenched with saturated $NaHCO_3$ (20 mL) and the aqueous layer was extracted with EtOAc (3 x 15 mL). The combined organic layers were washed with brine (20 mL), dried (Na_2SO_4), filtered and concentrated *in vacuo*. The residue was purified by flash chromatography (Hexane/EtOAc, 30:1 to 25:1) to afford 0.48 g (91%) of alcohol **4.62** as a 6:2:1:0.3 mixture of 4 diastereoisomers (by HPLC: 21.4 mm x 25 cm column, 49 min gradient, 0–5% ethyl acetate in hexane). For synthetic purposes the mixture can be advanced to the next step without further purification, as the resulting mixture of Yamaguchi esterification adducts can be easily separated to afford the desired ester **4.63**: $[\alpha]_D^{20} -1.3$ (c 1.0, $CHCl_3$); IR (neat) 2955, 2877, 1715, 1461, 1414, 1250, 1098,

1006, 837, 741 cm^{-1} ; ^1H NMR (500 MHz C_6D_6): 6.20 (dd, $J = 16.0, 5.5$ Hz, 1H), 6.13-6.01 (m, 2H), 5.59 (dt, $J = 6.5, 6.5$ Hz, 1H), 5.13-5.08 (m, 2H), 4.45 (s, 2H), 4.24-4.19 (m, 1H), 4.13 (t, $J = 5.5$ Hz, 1H), 4.06 (d, $J = 3.0$ Hz, 1H). 4.00-3.99 (m, 1H), 3.70-3.67 (m, 1H), 3.33 (s, 3H), 2.62 (dd, $J = 9.5, 1.5$ Hz, 1H), 2.59-2.39 (m, 3H), 2.32-2.24 (m, 1H), 1.98-1.91 (m, 1H), 1.90-1.81 (m, 1H), 1.68-1.60 (m, 1H), 1.59-1.51 (m, 1H), 1.17 (d, $J = 6.5$ Hz, 3H), 1.08-1.01 (m, 30H), 0.93 (t, $J = 8.0$ Hz, 9H), 0.71-0.65 (m, 12 H), 0.54 (q, $J = 8.0$ Hz, 6H), 0.16 (s, 6H); ^{13}C NMR (125 MHz, C_6D_6): δ 212.4, 141.5, 137.3, 133.9, 133.1, 130.2, 114.3, 81.8, 80.9, 78.3, 71.8, 70.7, 58.6, 58.3, 45.2, 33.5, 32.3, 32.0, 26.1, 25.6, 18.5, 15.1, 7.4, 7.3, 7.0, 5.5, 5.5, 5.1, -5.0; HRMS (MALDI) m/z 879.5834, $[(\text{M}+\text{Na})^+]$ calculated for $\text{C}_{45}\text{H}_{92}\text{NaO}_7\text{Si}_4$: 879.5818].



Ester 4.63: To a solution of aldol **4.63** (0.43 g, 0.51 mmol) and acid **4.10** (0.18 g, 0.70 mmol) in toluene and THF (1:1 50 mL) was added DMAP (5.4 g, 44.8 mmol) at 0 °C. After DMAP dissolved completely the mixture was cooled to -78 °C, and Et_3N (3.1 mL, 22.4 mmol) was added followed by 2,4,6-trichlorobenzoyl chloride (1.75 mL, 11.2 mmol). The resulting slurry was slowly

warmed to room temperature over 2.5 h. The reaction was stirred overnight at room temperature, quenched with saturated NaHCO₃ (50 mL) and the aqueous layer was extracted with Et₂O (3 x 50 mL). The combined organic layers were dried (Na₂SO₄), filtered and concentrated *in vacuo*. The residue was purified by flash chromatography (Hexanes/EtOAc, 50:1) and further purified by HPLC using a Varian HPLC system equipped with Prostar 210 pumps and a photodiode array (PDA) detector. Preparative normal phase HPLC was conducted using a 0-5% linear gradient (Hexane/EtOAc) over 50 min at a flow rate of 12.0 mL/min with UV detection at 340 nm using a Varian's Dynamax column (60 Å 250 x 21.4 mm, Si 83-121-0, Raiman Instrument Company, Inc., Mack Road, Woburn, MA). The retention time for desired diastereomer is 33.3 min. 0.50 g (36% over two steps) of ester **4.63** was obtained as a colorless oil: $[\alpha]_D^{20} -1.2$ (c 1.0, CHCl₃); IR (neat) 2954, 2876, 1715, 1459, 1240, 1112, 1006, 836, 741 cm⁻¹; ¹HMR (500 MHz, C₆D₆): δ 7.27 (s, 1H), 6.22-6.18 (m, 2H), 6.14-6.01 (m, 2H), 5.84-5.81 (m, 1H), 5.58 (dd, *J* = 14.0, 7.0 Hz, 1H), 5.18-5.09 (m, 2H), 4.45 (s, 2H), 4.29 (d, *J* = 3.5 Hz, 1H), 4.13 (t, *J* = 4.5 Hz, 1H), 3.99-3.96 (m, 1H), 3.35-3.32 (m, 4H), 2.66-2.54 (m, 2H), 2.52-2.44 (m, 1H), 2.42-2.33 (m, 1H), 2.27-2.22 (m, 2H), 1.90 (s, 3H), 1.89-1.84 (t, *J* = 12.5, 2H), 1.75 (s, 3H), 1.58-1.54 (m, 1H), 1.17 (d, *J* = 6.5 Hz, 3H), 1.07-0.96 (m, 39H), 0.70-0.57 (m, 18H), 0.16 (s, 6H); ¹³C NMR (125 MHz, C₆D₆): δ 209.6, 167.6, 143.9, 141.4, 139.4, 137.4, 133.8, 133.1, 130.2, 114.3, 86.2, 80.7, 80.20, 78.3, 72.4, 71.0, 58.6, 58.2, 45.2, 32.1, 31.6, 30.4, 26.1, 25.7, 24.3, 15.0, 14.3, 7.6, 7.5, 7.00, 5.5, 5.0, -5.05; HRMS (MALDI) *m/z* 1113.5378, [(M+Na)⁺ calculated for C₅₂H₉₉INaO₈Si₄: 1113.5359].

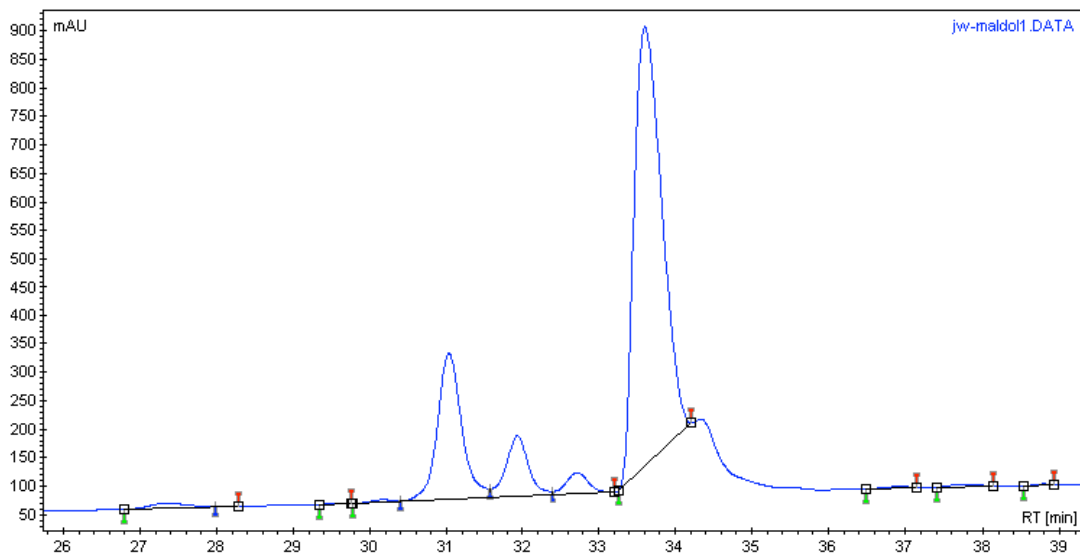
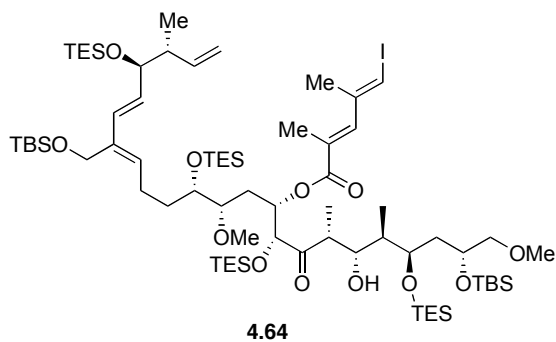
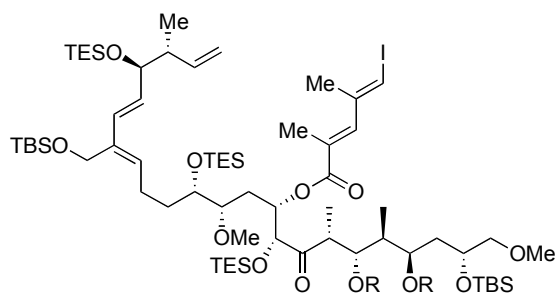


Figure 4.4 HPLC chromatograph for purification of ester **4.63**



Aldol 4.64: To a solution of LHMDS (0.40 mL, 0.37 mmol, 1M in THF) in THF (30 mL) at $-78\text{ }^{\circ}\text{C}$ was added a solution of ketone **4.63** (0.200 g, 0.183 mmol) and HMPA (0.092 mL, 0.55 mmol) in THF (6 mL). The reaction mixture was stirred at $-78\text{ }^{\circ}\text{C}$ for 2 h before a solution of aldehyde **4.11** (0.22 g, 0.55 mmol) in THF (4 mL) was added dropwise. The solution was stirred at $-78\text{ }^{\circ}\text{C}$ for

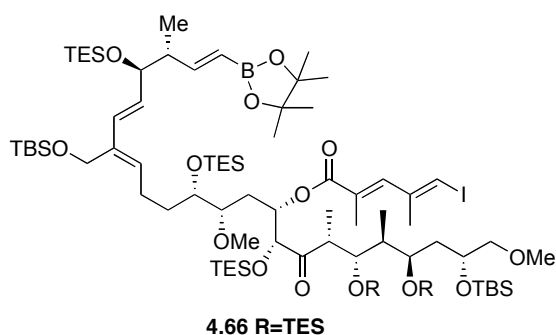
3 h, quenched with saturated NH₄Cl (20 mL) and warmed to room temperature. The aqueous layer was extracted with Et₂O (3 x 20 mL) and the combined organic layers were dried (Na₂SO₄), filtered and concentrated *in vacuo*. The residue was purified by HPLC: 21.4 mm x 25 cm column, 49 min gradient, 0–5% ethyl acetate in hexanes to afford 0.11 g (40%) of aldol **4.64** as colorless oil: $[\alpha]_D^{20} -12.5$ (c 1.0, CHCl₃); IR (neat) 3568, 2955, 2879, 2365, 1702, 1459, 1245, 1109, 1005, 738 cm⁻¹; ¹HMR (500 MHz, C₆D₆): δ 7.28 (s, 1H), 6.26 (s, 1H), 6.20 (d, *J* = 16.0 Hz, 1H), 6.15-6.02 (m, 3H), 5.57 (t, *J* = 7.5 Hz, 1H), 5.14-5.09 (m, 2H), 4.88 (d, *J* = 4.0 Hz, 1H), 4.45 (s, 2H), 4.15 (d, *J* = 10.0 Hz, 1H), 4.37-4.34 (m, 1H), 4.16-4.13 (m, 1H), 4.12-4.08 (m, 1H), 4.04 (s, 1H), 4.00-3.97 (m, 1H), 3.39 (s, 3H), 3.38-3.33 (m, 1H), 3.30 (d, *J* = 5.5 Hz, 2H), 3.27-3.20 (m, 1H), 3.11 (s, 3H), 2.57-2.51 (m, 1H), 2.49-2.44 (m, 1H), 2.39-2.35 (m, 1H), 2.31-2.23 (m, 1H), 2.09-2.04 (m, 1H), 2.01-1.93 (m, 3H), 1.91 (d, *J* = 1.0 Hz, 3H), 1.87-1.81 (m, 1H), 1.78 (d, *J* = 0.5 Hz, 3H), 1.62-1.57 (m, 1H), 1.31 (d, *J* = 6.5 Hz, 3H), 1.18 (d, *J* = 6.5 Hz, 3H), 1.10-1.00 (m, 45H), 0.91 (d, *J* = 7.0 Hz, 3H), 0.81-0.76 (q, *J* = 7.5 Hz, 6H), 0.71-0.62 (m, 18H), 0.38 (s, 9H), 0.24 (s, 3H), 0.21 (s, 3H), 0.17 (s, 3H), 0.17 (s, 3H); ¹³C NMR (150 MHz, C₆D₆): δ 210.3, 167.8, 143.9, 141.4, 139.4, 137.3, 133.9, 130.2, 114.3, 86.3, 81.0, 79.3, 78.3, 78.2, 73.4, 72.8, 72.6, 71.2, 70.1, 58.6, 58.5, 58.2, 45.3, 45.2, 41.0, 39.1, 31.7, 31.1, 26.3, 26.1, 25.6, 24.3, 18.6, 18.5, 15.1, 14.4, 14.3, 14.2, 12.2, 7.6, 7.3, 7.2, 7.2, 7.1, 5.6, 5.5, 5.4, -3.4, -4.4, -5.0, -5.0; HRMS (MALDI) *m/z* 1518.8259, [(M+Na)⁺ calculated for C₇₂H₁₄₃INaO₁₂Si₆: 1517.8138].



4.65 R=TES

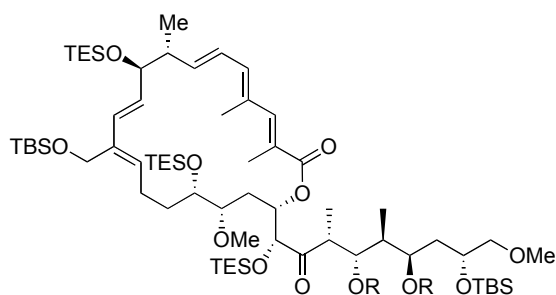
Silyl Ether 4.65: To a solution of alcohol **4.64** (0.08 g, 0.05 mmol) in dichloromethane (11 mL) at $-78\text{ }^{\circ}\text{C}$ was added 2,6-lutidine (0.16 mL, 1.33 mmol) followed by TESOTf (0.24 mL, 1.07 mmol). The mixture was stirred for 30 min at $-78\text{ }^{\circ}\text{C}$, then 30 min at $0\text{ }^{\circ}\text{C}$ and quenched with H_2O (15 mL). The aqueous layer was extracted with dichloromethane (3 x 10 mL) and the combined organic layers were dried (Na_2SO_4), filtered and concentrated *in vacuo*. The residue was purified by flash chromatography (Hexanes/EtOAc 50:1) to afford 0.09 g quantitative yield of TES ether **4.65** as a colorless oil: $[\alpha]_{\text{D}}^{20} -17.2$ (c 1.0, CHCl_3); IR (neat) 2955, 2877, 1460, 1239, 1071, 1004, 738 cm^{-1} ; ^1HMR (400 MHz, C_6D_6): δ 7.28 (s, 1H), 6.28 (s, 1H), 6.20 (d, $J = 15.6$ Hz, 1H), 6.14-5.96 (m, 3H), 5.59 (t, $J = 7.2$ Hz, 1H), 5.14-5.09 (m, 2H), 4.88 (d, $J = 3.2$ Hz, 1H), 4.45 (s, 2H), 4.32 (dd, $J = 8.4, 5.2$ Hz, 1H), 4.21 (d, $J = 8.0$ Hz, 1H), 4.13 (t, $J = 6.0$ Hz, 1H), 4.02-3.97 (m, 1H), 3.97-3.92 (m, 1H), 3.47 (q, $J = 7.2$ Hz, 1H), 3.40 (d, $J = 4.4$ Hz, 2H), 3.38 (s, 3H), 3.30 (dd, $J = 10.8, 4.0$ Hz, 1H), 3.21 (s, 3H), 2.61-2.51 (m, 1H), 2.49-2.37 (m, 2H), 2.33-2.23 (m, 1H), 2.14-1.94 (m, 3H), 1.90 (s, 3H), 1.90-1.83 (m, 1H), 1.79 (s, 3H), 1.79-1.73 (m, 1H), 1.65-1.55 (m, 1H), 1.37 (d, $J = 7.2$ Hz, 3H), 1.19-1.00 (m, 69H), 0.95 (q, $J = 8.0$ Hz, 6H), 0.84 (q, $J = 8.0$ Hz, 6H),

0.76 (q, $J = 8.0$ Hz, 6H), 0.71-0.62 (m, 12H), 0.22 (s, 3H), 0.20 (s, 3H), 0.17 (s, 6H); ^{13}C NMR (75 MHz, C_6D_6): δ 209.5, 167.8, 143.9, 141.4, 139.5, 137.4, 133.8, 133.1, 130.2, 114.3, 86.5, 80.6, 79.8, 78.3, 77.1, 74.7, 72.5, 70.9, 70.4, 70.1, 58.9, 58.6, 58.2, 47.2, 45.2, 43.9, 40.7, 31.6, 31.0, 26.1, 25.7, 24.3, 18.5, 18.4, 15.0, 14.4, 12.0, 10.2, 7.6, 7.5, 7.3, 7.3, 7.2, 6.7, 5.9, 5.9, 5.5, -4.0, -4.4, -5.0, -5.1; HRMS (MALDI) m/z 1632.9115 $[(\text{M}+\text{Na})^+]$ calculated for $\text{C}_{78}\text{H}_{157}\text{I}\text{NaO}_{12}\text{Si}_7$: 1631.9002].



Vinyl Boronate 4.66: To a solution of alkene **4.65** (66.0 mg, 40.9 μmol) in toluene (8.0 mL) was added 1-propenyl pinacol boronic ester **4.12** (32 mg, 205 μmol) followed by Grubbs second-generation catalyst **4.34** (35 mg, 40.9 μmol) at room temperature. The resulting solution was stirred at 50 $^\circ\text{C}$ for 46 h, cooled to room temperature and diluted with dichloromethane (10 mL). The resultant solution was filtered through a short silica gel plug. The solvent was removed *in vacuo* and the residue was purified by HPLC (Hexane/EtOAc, 0-5% gradient over 50 min) to afford 27 mg (38%) vinyl boronate **4.66** as a colorless oil: $[\alpha]_{\text{D}}^{20} -32.4$ (c 1.0, CHCl_3); IR (neat) 2955, 2877, 1712, 1460, 1359, 1242,

1112, 1007, 835, 739 cm^{-1} ; ^1H NMR (400 MHz, C_6D_6): δ 7.28 (s, 1H), 6.29 (s, 1H), 6.19 (d, $J = 15.6$ Hz, 1H), 6.06-5.96 (m, 2H), 5.86 (d, $J = 18.0$ Hz, 1H), 5.55 (t, $J = 7.2$ Hz, 1H), 4.89 (d, $J = 3.2$ Hz, 1H), 4.43 (s, 2H), 4.32 (dd, $J = 8.8, 5.6$ Hz, 1H), 4.23-4.20 (m, 2H), 4.02-3.97 (m, 1H), 3.96-3.92 (m, 1H), 3.47 (dd, $J = 14.0, 6.8$ Hz, 1H), 3.41 (d, $J = 4.8$ Hz, 2H), 3.82 (s, 3H), 3.31 (dd, $J = 10.4, 3.6$ Hz, 1H), 3.21 (s, 3H), 2.60-2.49 (m, 1H), 2.43-2.37 (m, 1H), 2.32-2.22 (m, 1H), 2.15-2.1.94 (m, 3H), 1.90 (s, 3H), 1.90-1.83 (m, 1H), 1.79 (s, 3H), 1.74 (t, $J = 8.4$ Hz, 1H), 1.64-1.57 (m, 1H), 1.37 (d, $J = 7.2$ Hz, 3H), 1.21-0.99 (m, 81 H), 1.01-0.82 (m, 12H), 0.76 (q, $J = 7.6$ Hz, 6H), 0.70-0.62 (m, 12H), 0.22 (s, 3H), 0.20 (s, 9H); ^{13}C NMR (75 MHz, C_6D_6): δ 209.5, 167.8, 157.1, 143.9, 139.5, 137.4, 133.9, 133.0, 130.2, 86.5, 82.8, 80.6, 79.8, 77.8, 77.1, 74.7, 72.5, 70.9, 70.4, 70.1, 58.9, 58.5, 58.2, 47.2, 46.9, 43.9, 40.7, 31.6, 31.0, 26.2, 26.1, 25.7, 25.0, 24.9, 24.3, 18.5, 18.4, 14.4, 14.2, 12.0, 10.2, 7.6, 7.5, 7.3, 7.3, 6.7, 5.9, 5.9, 5.5, 5.5, -4.0, -4.4, -4.9, -4.9; HRMS (MALDI) m/z 1759.0583, $[(\text{M}+\text{Na})^+]$ calculated for $\text{C}_{84}\text{H}_{168}\text{BINA}\text{O}_{14}\text{Si}_7$: 1757.9854].

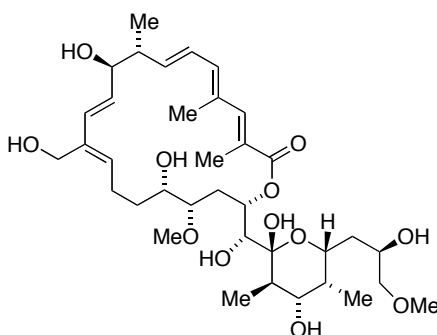


4.47 R=TES

Macrolactone 4.47: To a solution of vinyl boronate **4.66** (27 mg, 15.5 μmol) in THF/ H_2O (4 mL, 3:1, degassed) was added $\text{Pd}(\text{Ph}_3\text{P})_4$ (1.8 mg, 1.56

μmol) at room temperature. The resulting yellow solution was stirred for 10 min before TIOEt (1.4 μL , 19.4 μmol) was added. The solution was stirred for 20 min (color turns from yellow to grey). The reaction was quenched with saturated NaHCO_3 (5 mL) and the aqueous layer was extracted with ethyl acetate (3 x 10 mL). The combined organic layers were dried (Na_2SO_4), filtered and concentrated *in vacuo*. The residue was purified by flash chromatography (Hexane/EtOAc, 25:1) to afford 19 mg (82%) of lactone **4.47** as a colorless oil: $[\alpha]_{\text{D}}^{20} +29.5$ (c 1.0, CHCl_3); IR (neat) 2954, 1701, 1461, 1240, 1109, 1081, 836, 741; ^1H NMR (600 MHz, C_6D_6): δ 7.53 (s, 1H), 6.29 (d, $J = 10.8$ Hz, 1H), 6.10 (dd, $J = 15.0, 6.6$ Hz, 1H), 5.86 (d, $J = 16.2$ Hz, 1H), 5.76-5.70 (m, 2H), 5.51 (dd, $J = 8.4, 6.6$ Hz, 1H), 5.41 (dd, $J = 15.0, 10.2$ Hz, 1H), 4.99 (d, $J = 4.2$ Hz, 1H), 4.30 (dd, $J = 81.6, 12.6$ Hz, 2H), 4.35-4.29 (m, 1H), 4.28 (d, $J = 7.8, 0.6$ Hz, 1H), 3.96-3.92 (m, 1H), 3.84 (t, $J = 9.0$ Hz, 1H), 3.61 (dt, $J = 7.8, 2.4$ Hz, 1H), 3.52 (s, 3H), 3.52-3.49 (m, 1H), 3.42-3.38 (m, 2H), 3.20 (s, 3H), 2.97 (t, $J = 8.4$ Hz, 1H), 2.61-2.53 (m, 1H), 2.42-2.36 (m, 1H), 2.15-2.06 (m, 5H), 2.11 (s, 3H), 2.03-1.99 (m, 2H), 1.84-1.80 (m, 1H), 1.79 (s, 3H), 1.67-1.62 (m, 1H), 1.45 (d, $J = 7.2$ Hz, 3H), 1.27 (d, $J = 6.6$ Hz, 3H), 1.22-1.19 (m, 18H), 1.16(d, $J = 6.0$ Hz, 3H), 1.14-1.08 (m, 27H), 1.04 (s, 9H), 0.98 (s, 9H), 0.97-0.86 (m, 12H), 0.80-0.70 (m, 18H), 0.21 (s, 3H), 0.19 (s, 3H), 0.11 (s, 6H); ^{13}C NMR (75 MHz, C_6D_6): δ 209.9, 168.2, 145.1, 144.7, 141.4, 137.2, 134.1, 133.8, 132.5, 132.0, 125.8, 123.7, 82.4, 81.0, 78.1, 77.2, 76.2, 70.6, 70.1, 61.1, 58.8, 58.0, 47.3, 46.4, 43.7, 40.9, 36.2, 35.0, 26.2, 26.1, 25.0, 18.7, 15.6, 14.0, 11.3, 10.4, 7.6, 7.5, 7.4, 7.4, 7.3, 6.7, 6.0, 5.9, 5.7, 5.6, -3.9, -4.4, -5.1, -5.1; HRMS (ESI) m/z 1489.0229 [(M+Li) $^+$

calcd for C₇₈H₁₅₆O₁₂Si₇Li: 1488.0142].



4.4 12-oxymethyl apoptolidinone D

12-Oxymethyl Apoptolidinone D 4.4: To solution of 10.0 mg (6.74 μmol) macrolactone **4.47** in 3 mL THF at $-10\text{ }^{\circ}\text{C}$, H_2SiF_6 (0.1 mL) was added dropwise. After stirred for 24 h at $-10\text{ }^{\circ}\text{C}$, the reaction mixture was quenched with saturated NaHCO_3 solution and the aqueous layer was extracted with ethyl acetate (3 x 5 mL). The combined organic layers were dried (Na_2SO_4), filtered and concentrated *in vacuo*. The residue was purified by flash chromatography ($\text{CH}_2\text{Cl}_2/\text{MeOH}$, 20:1) to afford 4.1 mg (89%) of 12-oxymethyl apoptolidinone D **4.4** as a white solid: $[\alpha]_{\text{D}}^{20}$ 19.5° (c 0.59, CHCl_3); IR (neat) 3362, 2923, 1665, 1456, 1256, 1098, 1024 cm^{-1} ; ^1H NMR (600 MHz, CD_3OD): δ 7.40 (s, 1H), 6.27-6.25 (m, 2H), 5.94 (d, $J = 15.6$ Hz, 1H), 5.67 (dd, $J = 9.6, 7.2$ Hz, 1H), 5.55 (dd, $J = 16.2, 9.0$ Hz, 1H), 5.50 (dt, $J = 10.2, 2.4$ Hz, 1H), 5.29 (dt, $J = 10.8, 0$ Hz, 1H), 4.18 (dd, $J = 114, 12$ Hz, 2H), 4.11-4.07 (m, 1H), 3.80-3.73 (m, 2H), 3.55-3.53 (m, 1H), 3.55 (d, $J = 1.2$ Hz, 1H), 3.42-3.39 (m, 1H), 3.39 (s, 3H), 3.26 (s, 3H), 3.19-3.12 (m, 2H), 2.66 (dd, $J = 9.0, 6.0$ Hz, 1H), 2.56-2.51 (m, 1H), 2.32-2.27 (m, 1H), 2.19-2.13 (m, 1H), 2.13 (s, 3H), 2.08 (s, 3H), 2.08-1.98 (m, 2H), 1.79-

1.74 (m, 1H), 1.68-1.61 (m, 1H), 1.60-1.55 (m, 1H), 1.51-1.44 (m, 1H), 1.36-1.21 (m, 2H), 1.19 (d, $J = 6.6$ Hz, 3H), 1.02 (d, $J = 6.6$ Hz, 3H), 0.88 (d, $J = 6.6$ Hz, 3H); ^{13}C NMR (150 MHz, CD_3OD) δ 172.7, 147.7, 146.0, 143.2, 138.4, 135.1, 135.0, 133.7, 131.9, 126.8, 124.4, 101.4, 84.2, 80.3, 78.7, 75.5, 74.9, 73.9, 72.7, 69.3, 68.3, 61.4, 59.5, 57.0, 46.6, 41.0, 38.6, 38.4, 36.6, 36.5, 24.9, 18.8, 15.7, 14.0, 12.3, 5.4; HRMS (ESI) m/z 690.4176 $[(\text{M}+\text{Li})^+]$ calculated for $\text{C}_{36}\text{H}_{58}\text{LiO}_{12}$: 690.4088].

CHAPTER V

METHODS OF PRECURSOR DIRECTED BIOSYNTHESSES AND APPLICATION TO APOPTOLIDIN CONGENERS

5.1 Introduction

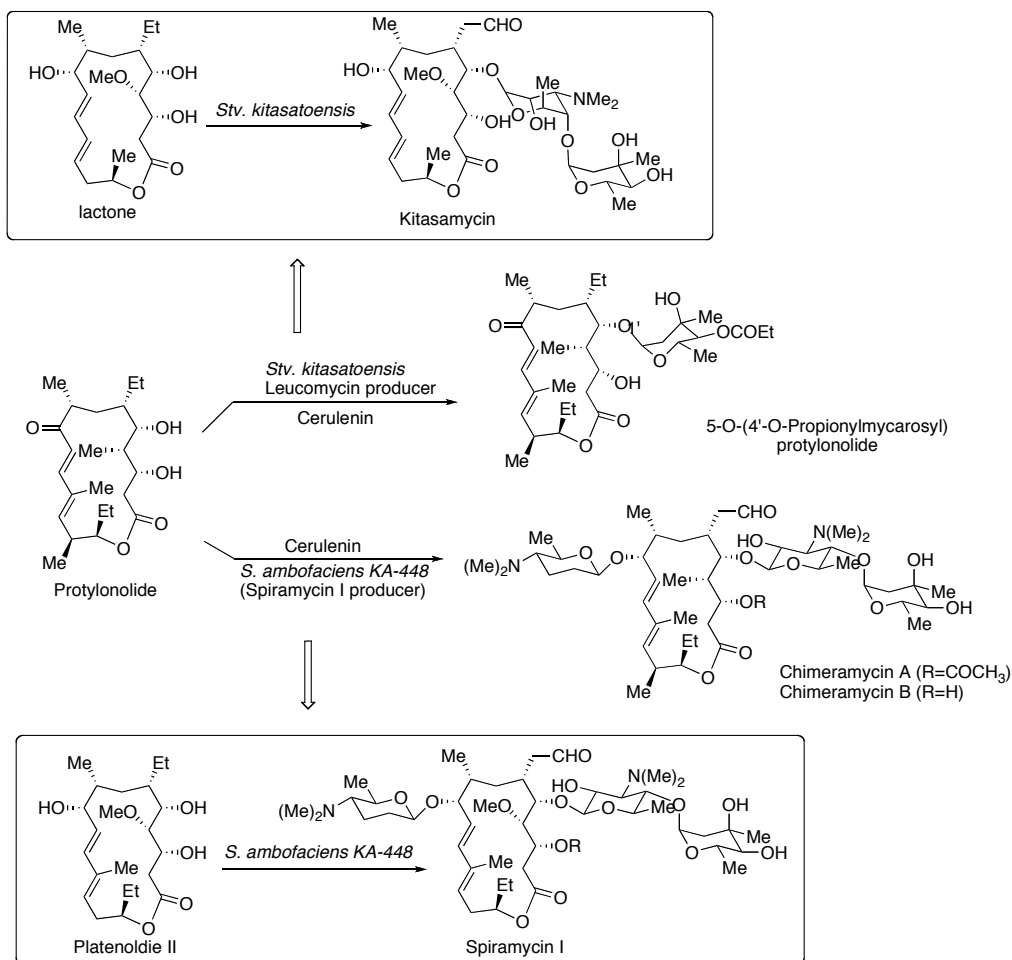
Apoptolidinone A (**5.1**) and apoptolidinone D (**5.2**) prepared by chemical synthesis were evaluated for cytotoxicity against human lung carcinoma cells H292. Exposure of apoptolidinone A (**5.1**) and apoptolidinone D (**5.2**) to H292 cells over a 72 hour period revealed minimum cytotoxic effects ($LC_{50} > 10 \mu\text{M}$) (see Chapter VI for details).⁶⁸ Similarly, Koert's group (Philipps-Universität Marburg, Germany) tested apoptolidinone A (**5.1**) against breast cancer MATU cells ($LC_{50} > 100 \mu\text{M}$).²¹ In contrast, apoptolidin A (**5.3**) showed significant cytotoxicity against H292 cells ($EC_{50} = 25 \text{ nM}$) and MATU cells ($EC_{50} = 2 \text{ nM}$). Apoptolidin A (**5.3**) killed the cancer cells at nanomolar range. These results revealed the significance of the sugar fragments in relation to apoptolidin cell cytotoxicity, a significant observation in relation to the development of an apoptolidin probe for target identification.

From the perspective of total synthesis, the challenge of assembling the complete molecular matrix of apoptolidin A (**5.3**), a complex aglycone conjugated to three deoxy sugar units, remains significant. In particular, the installation of sugar units by chemical synthesis requires the development of complex synthetic schemes often resulting in low overall yields. To prepare apoptolidin deoxy

sugars, both Nicolau's and Koert's groups utilized long reaction sequence by modification of known natural sugar;^{16,17,18,19,20,21} Crimmins' and Roush's groups developed new synthetic route requiring at least 10 steps to prepare apoptolidin deoxy-sugar units starting from commercially available compounds.^{32,35} In addition, the incorporation of sugar units by chemical glycosylation methods poses problems in stereocontrol and yield. The development of alternative methods of glycosylation is an area of significance.

Recent advances in understanding the biosynthetic incorporation of deoxy sugars into polyketide natural products has provided new opportunities to effect the glycosylation of unnatural aglycones leading to new analogues with therapeutic value.^{93,94,95,96,97,98} There are primarily three methods to effect bioglycosylation using the enzymatic machinery of the producing organism, which are *in vitro* enzymatic glycosylation, mutasynthesis, and precursor-directed bioglycosylation. *In vitro* enzymatic glycosylation methods are usually used for validation of the synthetic potential of a glycosyltransferases. This method requires the readily availability of purified glycosyltransferases in soluble and active form, enzymes for the biosynthesis of specific sugar donors and access to aglycone substrates.^{94,95,96,97,98} Mutasynthesis employs engineered microbial with genetic inactivation of polyketide synthase modules to allow the bioconversion of an exogenous aglycone to natural product analogues without competitive interference from the endogenous (natural) aglycone.^{99,100,101} Mutasynthesis presumes the knowledge of the biosynthetic gene cluster and well-developed methods for genetic manipulation of the producing organism,

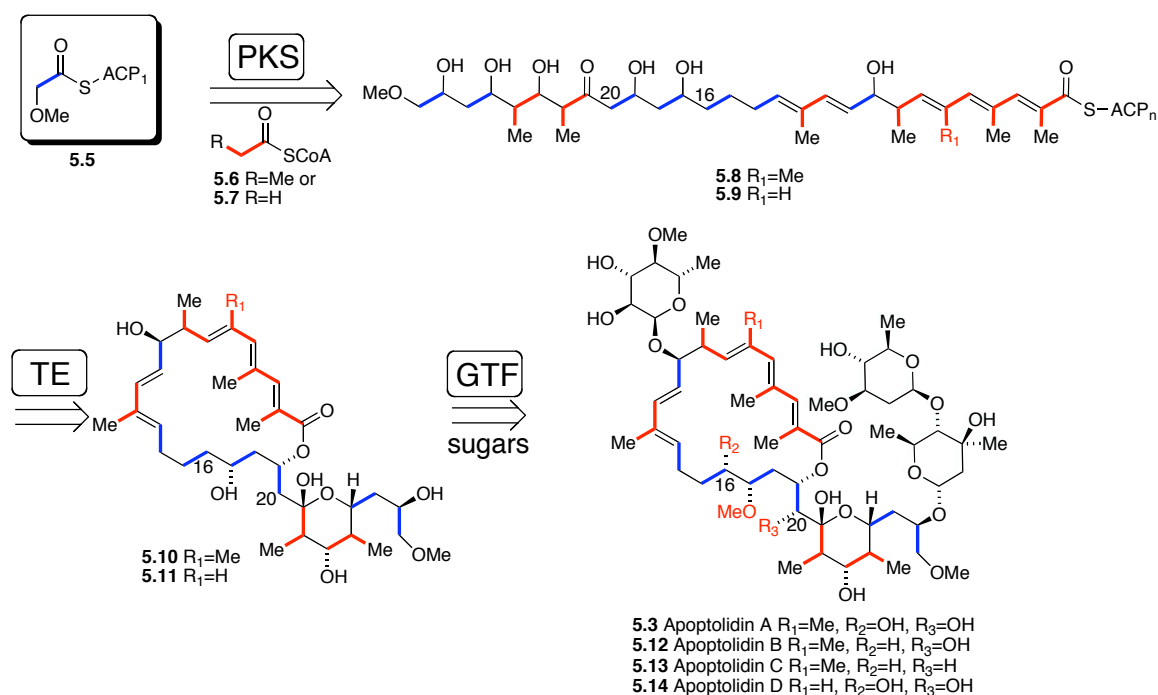
which can be a slow process.^{99,100,101} Precursor-directed biosynthesis is defined as “the derivatization of a secondary metabolite by feeding biosynthetic precursor analogues to the fermentation broth of producing organisms”.¹⁰² One approach to precursor-directed bioglycosylation, which requires no knowledge of the encoding biosynthetic cluster leading to the natural product, is to employ a selective chemical “knockdown” of the polyketide synthase. In this way, polyketide synthase (PKS) inhibitors may facilitate the introduction of a foreign or unnatural aglycone and its subsequent enzymatic glycosylation by the PKS cured system. This strategy has been successfully demonstrated by Omura in the early 1980s in which the ketosynthase inhibitor cerulenin **5.4** was used to disable the biosynthesis of the endogenous aglycones in several polyketide antibiotics producing microorganisms, and allowing for glycosylation of an exogenously introduced aglycone protylonolide to generate various derivatives of protylonolide featuring different sugar units as shown in Scheme **5.1**.^{103,104,105,106}



Scheme 5.1 Omura's hybrid synthesis of protylonolide derivatives

Since the genome of apoptolidin producing organism *Nocardopsis* sp. has not been studied, the hypothetical biogenesis for apoptolidins presented in Scheme 5.2 is proposed based on a classical biosynthetic route for polyketide natural products. The apoptolidin polyketide synthetase (PKS) of *Nocardopsis* sp. affords the biosynthesis of the 20-membered macrolides, apoptolidinones 5.10 and 5.11 from starter unit 5.5. Thioesterase (TE) catalyzed the release of seco acids 5.8 and 5.9 presumably lead to apoptolidinones 5.10 and 5.11 from the

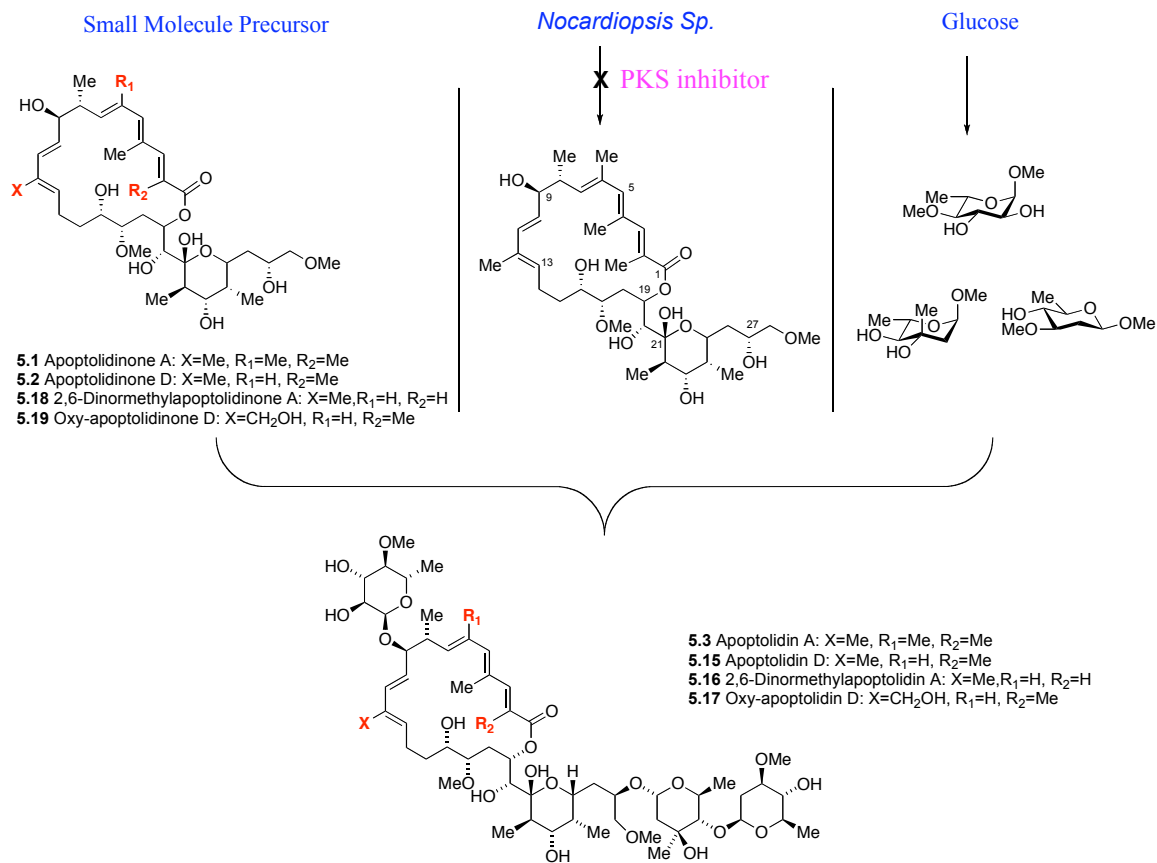
PKS respectively. It is further proposed that apoptolidinones **5.10** and **5.11** undergo further modifications by post-PKS tailoring enzymes including oxygenases and glycosyltransferases. We initially hypothesized that glycosyltransferases catalyzed the C-9 and C-27 glycosylation, either before or following C-16 and C-19 oxidation and O-17 methylation to generate the unique structures of apoptolidins A-D (**5.3**, **5.12-5.14**).



Scheme 5.2 Hypothetical biosynthesis of apoptolidin A-D

Since literature precedent proved that polyketide glycosyltransferases have relaxed substrate specificity,^{103,104,105,106} we proposed to take advantage of the *Nocardopsis* sp. machinery to effect bioglycosylation of unnatural aglycones. We sought to choose the convenient and relatively simple precursor directed

glycosylation of completely synthetic aglycones of apoptolidin **5.1**, **5.2**, **5.18**, **5.19** using chemical knockdown methodology developed by Omura described above, to produce unnatural apoptolidins **5.15-5.17** for biological evaluation and use in the development of molecular probes for cellular target identification.



Scheme 5.3 Precursor directed bioglycosylation of apoptolidinones

5.2 Bioglycosylation of Synthetic Apoptolidinones

The work included in this section has been published in the *Organic Letters*.¹⁰⁷

5.2.1 Titration of Cerulenin

Cerulenin **5.4**, an antifungal antibiotic, was isolated from the culture filtrates of *Caephalosporium caerulens* by Heta and coworkers in 1960.¹⁰⁸ Studies on cerulenin's mechanism of action revealed that it could effectively mimic the transition state of the condensation step catalyzed by beta-ketoacyl-acyl carrier protein synthases.¹⁰⁹ Since beta-ketoacyl-acyl carrier protein synthases are common enzymes to both the biosynthesis of long chain fatty acid and the biosynthesis of polyketide macrolactones, it is been demonstrated that cerulenin **5.4** could inhibit the production of macrolides significantly when administered to the producing microorganisms.¹¹⁰

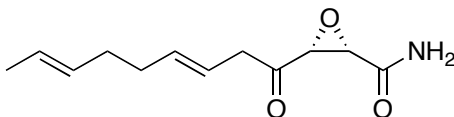


Figure 5.1 Structure of Cerulenin **5.4**

The use of cerulenin **5.4** to inhibit ketosynthase activity can be described as a chemical “knockout”. In order to introduce sugar units onto our synthetic apoptolidinones, we chose to employ precursor-directed biosynthesis using the apoptolidin producer (actinomycete *Nocardioopsis Sp.*) and cerulenin **5.4** as a chemical knockdown to inhibit production of endogenous apoptolidinone (natural aglycone). As cerulenin **5.4** is a fatty acid synthase inhibitor, the optimal concentration of cerulenin **5.4** needs to be identified that would inhibit apoptolidin **5.3** production, as measured by HPLC/MS, without substantially inhibiting cell

growth, as measured by palliated mycelia mass. The optimized conditions required pulsed feeding of 0.2 mM of cerulenin **5.4** per day to a culture of the apoptolidin producer (*Nocardioopsis sp.*). At this concentration of cerulenin **5.4**, apoptolidin **5.3** production was reduced to below 5% relative to a control cultures.

5.2.2 Bioglycosylation of Apoptolidinone A **5.1**

Once conditions to effect the chemical knockdown of ketosynthase were determined, we began to examine the glycosylation of an unnatural apoptolidinone using precursor directed biosynthesis. First, we examined bioglycosylation of apoptolidinone A **5.1** itself to determine if apoptolidin production could be returned. We found that the addition of synthetic apoptolidinone A **5.1** accompanied with pulsed addition of cerulenin **5.4** resulted in only trace amounts of apoptolidin A **5.3** and apoptolidinone A **5.1**. However, a novel apoptolidin was observed by LC-MS that corresponded to apoptolidin A disaccharide **5.20** ($M+NH_4/z = 986.6$) for the first time. Notably, the equivalent mass corresponding to **5.20** was not observed by LC/MS in the control fermentation. Interestingly, this result implied that apoptolidinone A **5.1** could be recognized as the competent substrate for C-27 glycosyltransferases, but not for C-9 glycosyltransferase. One possible explanation is that the C-9 6-deoxy-4-O-methyl-L-glucose sugar is introduced at the seco acid stage and the glycosylation of C-27 disaccharide proceeds after the macrolactonization in apoptolidin biosynthesis.^{111,112}

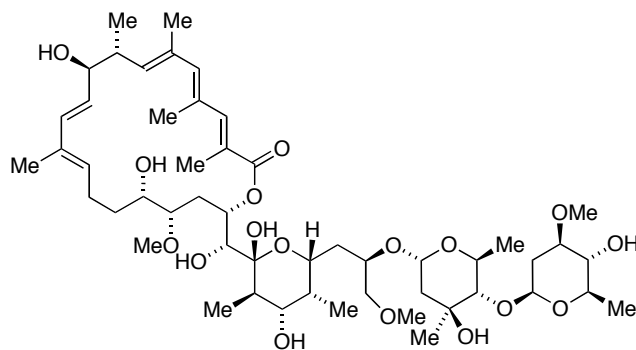


Figure 5.2 Structure of apoptolidin A disaccharide **5.20**

5.2.3 Bioglycosylation of 6-Normethylapoptolidinone A (a.k.a. Apoptolidinone D)

Once we established evidence that apoptolidinone A could be glycosylated by precursor directed biosynthesis, we turned our attention to the bioglycosylation of unnatural apoptolidinones. We examined the glycosylation of 6-normethylapoptolidinone A **5.2** (during the course of our glycosylation studies, Wender's group isolated 6-normethylapoptolidin A as a minor metabolite from *Nocardiosis Sp.* and named it apoptolidin D) by adding **5.2** in combination with cerulenin **5.4** to apoptolidin producer culture. LC/MS analysis of the crude extract of this culture showed that the primary product was disaccharide **5.21** and accompanied by minor amounts of apoptolidin A **5.3** and isoapoptolidin A (see experimental section for HPLC analysis). Apoptolidin D disaccharide **5.21** was coarsely purified by flash chromatography and then carefully purified by preparative HPLC. The structure of **5.21** was assigned by extensive 1D and 2D NMR analysis.

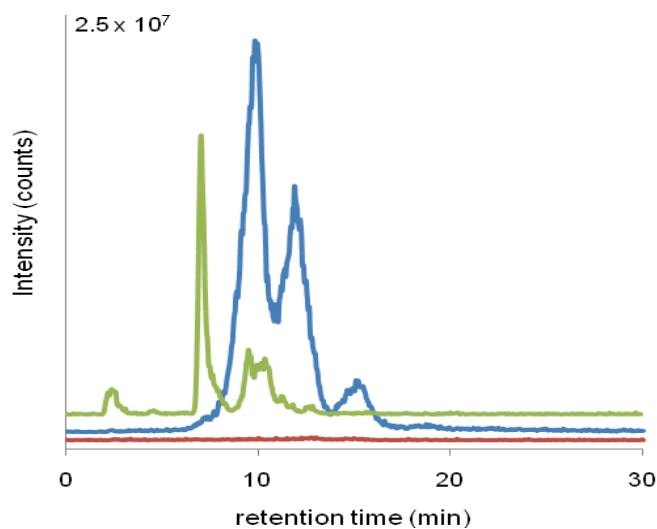
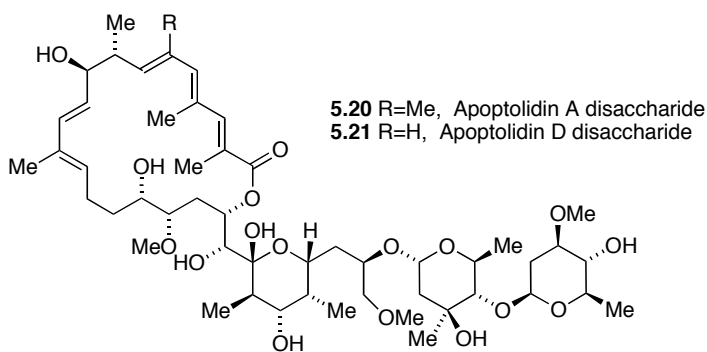


Figure 5.3 Structures of apoptolidin disaccharide **5.20** and **5.21** and HPLC/MS detection of apoptolidins in fermentation extracts of the apoptolidin producer inoculated with 0.2 mM cerulenin **5.4** /day: no aglycone supplementation (red); supplemented with synthetic apoptolidinone A **5.1** (blue ES⁺ M+NH₄/z = 986.6); supplemented with apoptolidinone D **5.2** (green ES⁺ M+NH₄/z = 972.6).

5.2.4 Bioglycosylation of 12-Oxymethyl Apoptolidinone D

Following the same method established in the precursor directed bioglycosylation of apoptolidinone A **5.1** and apoptolidinone D **5.2**, when we fed the synthetic oxy-apoptolidinone D **5.17** as another apoptolidin precursor to the apoptolidin production medium in the presence of cerulenin **5.4** (0.2 mM per day), no new apoptolidin congeners were detected by LC-MS. Analysis of the

crude extract of this culture showed the primary product to be oxy-apoptolidinone D **5.17** accompanied by minor amounts of apoptolidin A **5.3** and isoapoptolidin A. No consumption of oxy-apoptolidinone D **5.17** in the above feeding experiment implied that oxy-apoptolidinone D **5.17** was not a qualified substrate for both C-9 and C-27 glycosyltransferases. One possible explanation is that the extra hydroxyl group at C-12 methyl group may uniquely alter the structure rendering the aglycone an inefficient substrate for the glycosylation transferase. A second explanation is that an undetermined variable of the process may render whole cell glycosylation a difficult method of glycosylation.

5.3 Discussion

In the above biosynthesis of apoptolidin analogues experiments, we have demonstrated the glycosylation of apoptolidinone A **5.1** and apoptolidinone D (6-normethylapoptolidinone A) **5.2** by employing whole cells of the natural apoptolidin producer actinomycete *Nocardioopsis sp.* in the presence of cerulenin **5.4** as a ketosynthase inhibitor. Such chemical knockdowns of polyketide biosynthesis provided rapid methods to access the glycosylation apparatus of a biosynthetic system.

Since the bioglycosylation on apoptolidinones **5.1** and **5.2** generated only C-27 apoptolidin disaccharides **5.20** and **5.21**, and no fully glycosylated apoptolidins were obtained, we proposed that C-9 glycosylation happens at the linear polyketide stage before macrolactonization and C-27 glycosylation proceeds after the macrolactonization step in the biosynthetic pathway leading to

apoptolidins. It is generally accepted that glycosyltransferases-catalyzed bioglycosylation occurs after the cyclic aglycone is released from the PKS in polyketide biosynthesis.¹¹² Liu's group recently reported that linear precursor can be recognized by methymycin macrolide glycosyltransferases.¹¹¹ Since we can not exclude the effects resulting from other chemical and physical conditions in the fermentation process, the best way to verify our proposed pathway for apoptolidin is to study the sequence of the whole genome of apoptolidin producing organism. The apoptolidin biosynthetic gene cluster need be identified and the corresponding genes for dedicated glycosyltransferases need to be verified. This study is currently conducted by Dr. Du in Bachmann's group.

5.4 Experimental Section:

5.4.1 General Experimental Procedures:

Proton nuclear magnetic resonance (¹H NMR) spectra and carbon-13 (¹³C NMR) spectra were recorded on a 600 MHz spectrometer at ambient temperature. ¹H and ¹³C NMR data are reported as δ values relative to residual non-deuterated solvent δ 3.31 ppm from CD₃OD. For ¹³C spectra, chemical shifts are reported relative to the δ 49.00 ppm resonance of CD₃OD. High-resolution mass spectra were obtained at Texas A&M University Mass Spectrometry Service Center by Dr. Shane Tichy on an API QSTAR Pulsar.

5.4.2 Apoptolidin Recovery Fermentation:

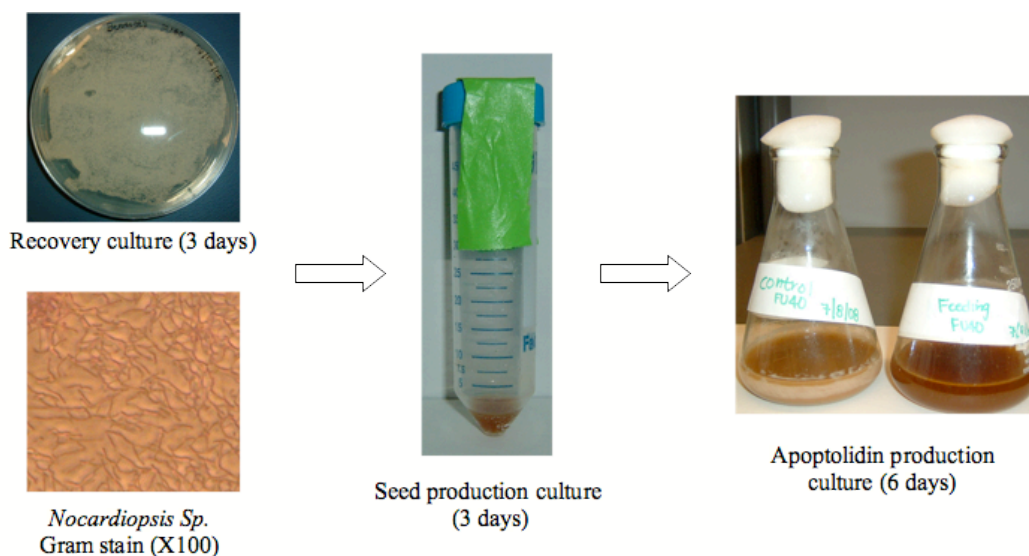
20 microliters of glycerol stock of *Nocardioopsis sp. (FU40)* was plated onto a Petri dish containing Bennett's medium and incubated upside down at 30 °C for 3 days. The composition of Bennett's medium was as follows: yeast extract 1.0 g, beef extract 1.0 g, NZ amine A (casein digest) 2.0 g, glucose 10.0 g, agar 20.0 g per liter of deionized water. The pH of the medium was adjusted to 7.0 with 0.1 M HCl and 0.1 M NaOH. After autoclaving, the solution was cooled to room temperature and poured into sterile Petri dishes (30 mL/dish). Uninoculated agar plates could be stored in a 2~4 °C refrigerator for about 3 months if not used immediately.

5.4.3 Apoptolidin Seed Production Fermentation:

The production protocol suggested by Hayakawa and coworkers was slightly modified.³ The production fermentation was initiated by aseptically inoculating one full loop of mycelia grown on Bennett's agar plate into a sterile 50 mL Falcon tube containing 5 mL of seed medium. The seed cultures were incubated for 4 days in a rotary shaker (300 rpm) at 30 °C. The composition of seed medium was as follows: soluble starch 10.0 g, molasses 10.0 g, peptone 10.0 g, beef extract 10.0 g per liter of deionized water. The pH of the medium was adjusted to 7.2 with 1 M HCl and 1 M NaOH. After autoclaving, the solution was cooled to room temperature and distributed into sterile 50 mL Falcon tubes (5 mL/tube).

5.4.4 Apoptolidin Production Fermentation:

The 5 mL seed culture was transferred into a 250 mL Erlenmeyer flask containing 50 mL of production medium. The flask was incubated for 6 days in a rotary shaker (300 rpm) at 30 °C. The composition of seed medium was as follows: glycerol 20.0 g, molasses 10.0 g, casamino acids 5.0 g, peptone 1.0 g, calcium carbonate (CaCO₃) 4.0 g per liter of deionized water. The pH of the medium was adjusted to 7.2 with 0.1 M HCl and 0.1 M NaOH. The medium solution was distributed into 250 Erlenmeyer flasks (50 mL/flask) and autoclaved.



Scheme 5.4 Flow chart for apoptolidin fermentation

5.4.5 Feeding Experiments:

To determine the appropriate cerulenin concentration, 0.2 mM (4 mg/100 mL production culture) and 0.1 mM (2 mg/100 mL production culture) were dissolved in 1 mL DMSO and administered separately to 100 mL production culture through a sterile syringe filter every 24 hours starting at the time of inoculation for a total of 5 times. To the control culture 1 mL DMSO (no cerulenin)

was added in the same manner daily. For the aglycone feeding studies, aglycones were added at the time of inoculation while cerulenin was pulse fed daily. Specifically, 7 mg apoptolidinone A was dissolved in 1 mL DMSO and added through a sterile syringe filter to a 100 mL production medium at the time of inoculation while 0.2 mM amount of cerulenin (4 mg/100 mL culture) was dissolved in 0.8 mL DMSO and added through a sterile syringe filter every 24 hours for 5 days. To the control culture 1 mL DMSO was added at the time of inoculation and 0.8 mL DMSO in the same manner daily. 15 mg apoptolidinone D were dissolved in 1 mL DMSO and added through a sterile syringe filter to a 200 mL production medium at the time of inoculation while 0.2 mM amount of cerulenin (4 mg/100 mL culture) was dissolved in 1 mL DMSO and added through a sterile syringe filter every 24 hours for 5 days. To the control culture 1 mL DMSO was added at the time of inoculation and 0.8 mL DMSO in the same manner daily.

5.4.6 Apoptolidin A, Isoapoptolidin A and Apoptolidin D Disaccharide Purification:

The production culture was centrifuged at 3750 rpm for 15 min. The supernatant was extracted with ethyl acetate, and the mycelia were stirred with acetone for 1 hour and centrifuged at 3750 rpm for 15 minutes. The acetone supernatant was concentrated and extracted with ethyl acetate. The ethyl acetate extracts were combined, concentrated under reduced pressure at 36 °C after dried over Na₂SO₄. For apoptolidin production purpose, the concentrate was

immediately purified by flash chromatography (CH₂Cl₂:MeOH=15:1). For feeding experiment, a 1 mL CH₃CN/H₂O/NH₄OAc solution of the concentrate was prepared for LC/MS analysis.

5.4.7 LC/MS:

Mass spectrometry was performed using ThermoFinnigan (San Jose, CA) TSQ® Quantum triple quadrupole mass spectrometer equipped with a standard electrospray ionization source outfitted with a 100-µm I.D. deactivated fused Si capillary. Data acquisition and spectral analysis were conducted with Xcalibur™ Software, version 1.3, from ThermoFinnigan (San Jose, CA), on a Dell Optiplex GX240 computer running the Microsoft® Windows 2000 operating system. The source spray head was oriented at an angle of 90° to the ion-transfer tube. Nitrogen was used for both the sheath and auxiliary gas. The sheath and auxiliary gases were set to 33 and 14 (arbitrary units) respectively. Samples were introduced by HPLC. A Surveyor® Autosampler and a Surveyor® MS Pump from ThermoFinnigan (San Jose, CA) were used. The injection volume was 10 µL. Crude apoptolidin extracts were separated using a Jupiter™ minibore 5µm C18 column with an isocratic mobile phase consisting of 65% water, 35% acetonitrile and 10 mM ammonium acetate. The flow rate was 0.2 mL/min. The mass spectrometer was operated in the positive ion mode and the electrospray needle was maintained at 4200V. The ion transfer tube was operated at 35V and 342 °C. The tube lens voltage was set to 85V. Source CID (offset voltage between skimmer and the first ion guide, Q00) was used at 15V. The mass

spectrometer was operated in full scan mode using Quad 1. The mass spectral resolution was set to a peak width of 0.70u (full width at half maximum, FWHM). Full scan spectra were acquired from m/z 600.0 to 1200.0 over 1.0 second. Data were acquired in profile mode. The electron multiplier gain was set to 3×10^5 . Apoptolidin and derivatives formed ammonium adducts and using the Xcalibur™ Software, data was digitally filtered for the m/z of interest ($[M+NH_4]^+$).

5.4.8 HPLC:

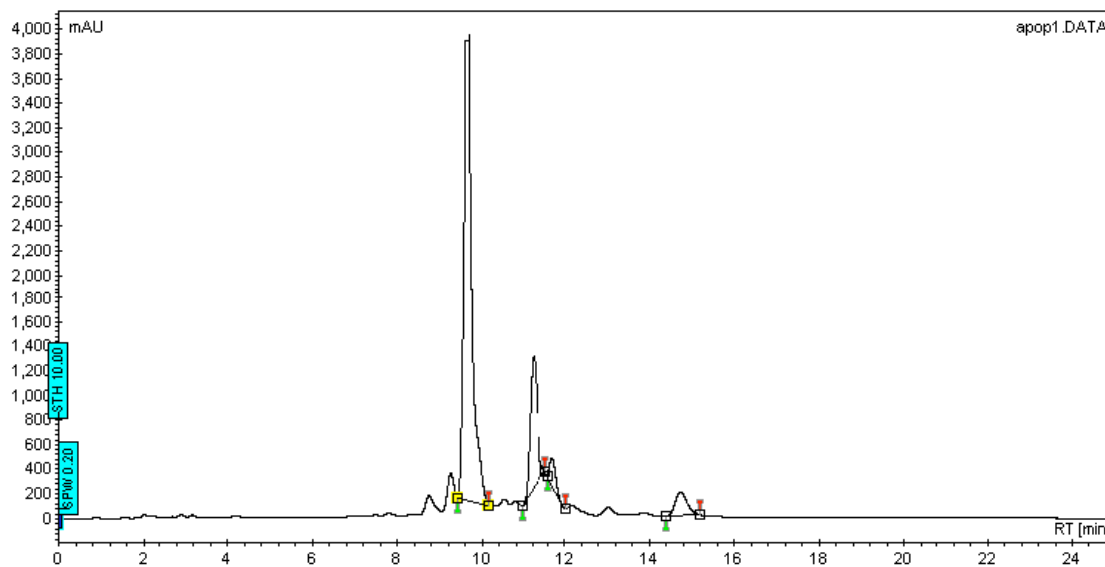


Figure 5.4 HPLC chromatograph for apoptolidin A and isoapoptolidin A purification

The fraction of apoptolidin A and isoapoptolidin A ($R_f=0.23$, $CH_2Cl_2:MeOH=10:1$) from flash chromatography purification was further purified by a Varian HPLC system equipped with Prostar 210 pumps and a photodiode

array (PDA) detector. Preparative reverse phase HPLC was conducted using a 30-80% linear gradient (CH₃CN/H₂O) over 20 min at a flow rate of 21.0 mL/min with UV detection at 220 nm using a Varian's Dynamax column (60 Å 250 x 21.4 mm, C18, Walnut Creek, CA). The retention time for apoptolidin A is 9 min; for isoapoptolidin A is 11.5 min.

In general, 150~200 mg of apoptolidin A and isoapoptolidin A could be isolated from 500 mL fermentation broth as white solids following the above fermentation protocol. Apoptolidin B, C, D were not detected by LC-MS analysis. The ratio of apoptolidin A and isoapoptolidin A varied depending on the pH of the fermentation medium. When CaCO₃ was added into each fermentation flask separately from other ingredients followed by adjustment of pH of medium solution in every single flask, the fermentation will produce majority of apoptolidin A with minor isoapoptolidin A. On the other hand, when CaCO₃ was distributed with other ingredients in the medium solution *after* pH adjustment, isoapoptolidin A was the major isomer. These results were due to the poor solubility of CaCO₃. The varied amount of CaCO₃ in each flasks resulted from distribution process will change the pH value of production medium, which affected the isomerization between apoptolidin A and isoapoptoldin A and give the observed results. Attempts to scale up the fermentation process by increasing the fermentation volume in larger fermentation flask resulted in lower fermentation yield. 4 days seed production time and 6 days production culture period of above stated scale is the optimal condition to give the highest production yield of apoptolidin A and isoapoptolidin A.

Purification of apoptolidin D disaccharide **5.21** was carried out on the same Varian system equipped with Prostar 210 pumps and a photodiode array (PDA) detector. Preparative HPLC was conducted using a Rainin Instrument Company's Dynamax column (300 Å 250 x 10 mm, Woburn, MA) eluted with a mobile phase comprised of 10% methanol in dichloromethane at a flow rate of 3.0 mL/min with UV detection at 254 nm.

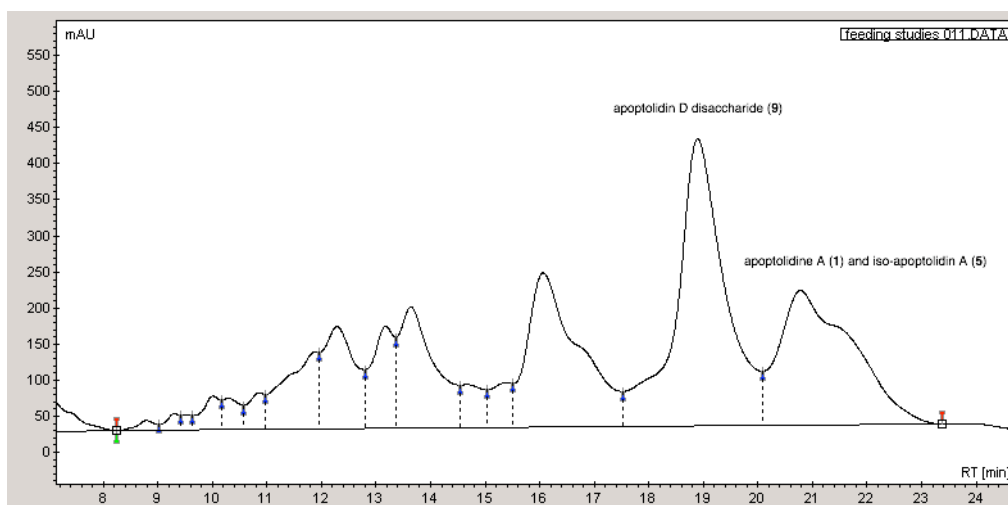


Figure 5.5 HPLC chromatograph for apoptolidin D disaccharide purification

5.4.9 Apotolidin D Disaccharide **5.21** Structure Assignment:

^1H NMR (600 MHz, CD_3OD) δ 7.40 (s, 1H), 6.24-6.23 (m, 2H), 5.98 (d, J = 15.6 Hz, 1H), 5.56 (t, J = 7.8 Hz, 1H), 5.47 (m, 1H), 5.29 (dd, J = 15.6, 8.4 Hz, 1H), 5.27 (d, J = 11.4 Hz, 1H), 4.92 (d, J = 4.2 Hz, 1H), 4.82 (dd, J = 10.2, 1.8 Hz, 1H), 3.94 (dd, J = 5.4, 1.8 Hz, 1H), 3.76 (t, J = 9.0 Hz, 1H), 3.71 (dd, J = 10.8, 4.2 Hz, 1H), 3.65 (dq, J = 9.6, 6.0 Hz, 1H), 3.53 (d, J = 1.8 Hz, 1H), 3.42 (m, 1H), 3.41 (s, 3H), 3.38 (m, 1H), 3.37 (s, 3H), 3.33 (m, 1H), 3.28 (m, 1H), 3.23

(s, 3H), 3.20 (dd, $J = 9.2, 6.2$ Hz), 3.16 (m, 1H), 2.96 (t, $J = 9.3$ Hz, 1H), 2.65 (dd, $J = 9.6, 5.4$ Hz, 1H), 2.46 (m, 1H), 2.43 (m, 1H), 2.26 (m, 1H), 2.14 (m, 1H), 2.13 (s, 3H), 2.07 (s, 3H), 2.05 (m, 1H), 1.97 (m, 1H), 1.91 (m, 1H), 1.79 (m, 1H), 1.71 (m, 1H), 1.67 (m, 1H), 1.64 (s, 3H), 1.58 (ddd, $J = 14.5, 8.5, 2.6$ Hz, 1H), 1.42 (m, 1H), 1.39 (m, 1H), 1.31 (s, 3H), 1.28 (m, 1H), 1.27 (m, 2H), 1.27 (d, $J = 6.6$ Hz, 3H), 1.20 (d, $J = 6.6$ Hz, 3H), 1.18 (d, $J = 6.6$ Hz, 3H), 1.02 (d, $J = 6.6$ Hz, 3H), 0.88 (d, $J = 7.2$ Hz, 3H); ^{13}C NMR (150 MHz, CD_3OD) δ 172.8, 147.7, 146.1, 143.1, 137.4, 135.0, 133.5, 132.2, 130.9, 126.7, 124.0, 101.9, 101.3, 99.6, 85.9, 84.0, 82.0, 80.0, 77.2, 77.0, 76.7, 75.4, 74.9, 73.9, 73.2, 73.0, 72.7, 69.4, 67.4, 61.3, 59.5, 57.3, 46.7, 45.5, 40.8, 38.3, 37.4, 37.2, 36.4, 36.1, 24.8, 22.8, 18.9, 18.6, 18.3, 15.6, 14.0, 12.2, 12.1, 5.2; ; HRMS (TOF MS) m/z 961.5723 [(M+Li)+ calculated for $\text{C}_{50}\text{H}_{82}\text{LiO}_{17}$: 961.5712].

Table 5.1 ^1H (600 MHz) and ^{13}C (150 MHz) NMR spectral data of apoptolidin D disaccharide **5.21** and apoptolidin D in $\text{CD}_3\text{OD}^{\text{a}}$

Apoptolidin D disaccharide			Apoptolidin D		Apoptolidin D disaccharide			Apoptolidin D	
Number	δ_{C}	δ_{H} (J=Hz)	δ_{C}	δ_{H}	Number	δ_{C}	δ_{H} (J=Hz)	δ_{C}	δ_{H}
1	172.8		172.3		2-Me	14.0	2.13	13.9	2.14
2	124.0		123.7		4-Me	15.6	2.07	15.4	2.08
3	147.7	7.40	147.2	7.41	8-Me	18.6	1.20 (6.6)	18.6	1.20
4	133.5		132.9		12-Me	12.2	1.64	12.2	1.65
5	143.1	6.23	142.5	6.26	22-Me	12.1	1.02 (6.6)	12.0	1.03
6	126.7	6.24	127.0	6.30	24-Me	5.2	0.88 (7.2)	5.0	0.90
7	146.1	5.47	144.9	5.48	17-OMe	61.3	3.37	61.1	3.38
8	46.7	2.26	44.5	2.52	28-OMe	59.5	3.23	59.3	3.24
9	80.0	3.76 (9.0)	83.3	3.84	1'			96.0	4.81
10	130.9	5.29 (15.6, 8.4)	127.5	5.21	2'			61.1	3.39
11	137.4	5.98 (15.6)	140.5	6.08	3'			74.7	3.71
12	135.0		134.6		4'			87.2	2.72
13	132.2	5.56 (7.8)	132.7	5.62	5'			67.9	3.74
14	24.8	2.46	24.4	2.48	6'			17.9	1.26
		1.97		1.98	4'-OMe			60.9	3.58
15	36.4	1.42	35.8	1.43	1''	99.6	4.92 (4.2)	99.4	4.93
		1.39		1.33	2''	45.5	1.91	45.2	1.93
16	74.9	3.38	74.1	3.40			1.79		1.80
17	84.0	2.65 (9.6, 5.4)	83.6	2.66	3''	73.0		72.9	
18	38.3	2.14	37.8	2.14	4''	85.9	3.33	85.5	3.33
		1.67		1.66	5''	67.4	3.65 (9.6, 6.0)	67.2	3.66
19	72.7	5.27 (11.4)	72.3	5.28	6''	18.9	1.18 (6.6)	18.6	1.21
20	75.4	3.53	75.1	3.53	3'''-Me	22.8	1.31	22.5	1.32
21	101.3		100.8		1'''	101.9	4.82 (10.2, 1.8)	101.7	4.83
22	36.1	2.05	36.2	2.05	2'''	37.4	2.43	37.0	2.43
23	73.9	3.71 (10.8, 4.2)	74.0	3.72			1.28		1.28
24	40.8	1.71	40.6	1.71	3'''	82.0	3.16	81.7	3.16
25	69.4	3.93 (5.4, 1.8)	69.2	3.95	4'''	77.2	2.96	76.9	2.97
26	37.2	1.58 (14.5, 8.5, 2.6)	37.1	1.59	5'''	73.2	3.20 (9.2, 6.2)	73.0	3.20
		1.27		1.43	6'''	18.3	1.27 (6.6)	17.9	1.27
27	77.0	3.42	76.6	3.42	3'''-OMe	57.3	3.41	57.1	3.42
28	76.7	3.28	76.5	3.28					

^a ^1H NMR for apoptolidin D was referenced from Ref 6

CHAPTER VI

BIOLOGICAL EFFECTS OF APOPTOLIDIN A AND CONGENERS AGAINST HUMAN LUNG CANCER H292 CELLS AND PROGRESS TOWARDS THE SYNTHESIS OF APOPTOLIDIN PROBES FOR TARGET IDENTIFICATION

6.1 Introduction

Natural products are a group of small molecules synthesized by organisms in response to various environmental stress.¹¹³ These small molecules natural products are known to exhibit various degrees of biological activity.¹¹⁴ Previous studies have demonstrated that many of these natural products elicit their biological activity upon binding to various protein targets.¹¹³ A wide range of technologies, including genetic and proteomic methods, have been developed for target identification.^{115,116,117,118,119} The activity of proteins has also been shown to be dependent upon the widespread *in vivo* post-translational regulation of the current physiological states of the cells.^{115,116} Hence, direct identification of protein targets by the studying the binding events between natural products and their targets in the whole proteome is desired. Compared to the genome, the proteome is a much more complex system which consists of a larger set of proteins rather than genes. Classical genetic methods developed through the sequencing of the human genome have encountered multiple problems such as consistency of experimental results and low throughputs. Recently, rapid advances in proteomics techniques, such as 2-D gels, liquid

chromatography, mass spectrometry, have facilitated protein separation and analysis. Profound advances in bioinformatics technology have also facilitated the analysis of large data sets that can be evaluated for the study of whole proteome. The strategies involved in protein profiling and identification of target proteins for natural products rely primarily on biochemical methods including photocrosslinking, radiolabeled ligand binding, and affinity chromatography.¹¹⁷ Since most of these methods are labor intensive and time consuming, application of an integrative technique that incorporates both proteomics and genomics such as a three-hybrid system, which includes protein sequencing followed by subsequent cloning of the cDNAs coding for *in vivo* target proteins, is valuable in providing optimal efficiency in protein profiling.^{117,120,121}

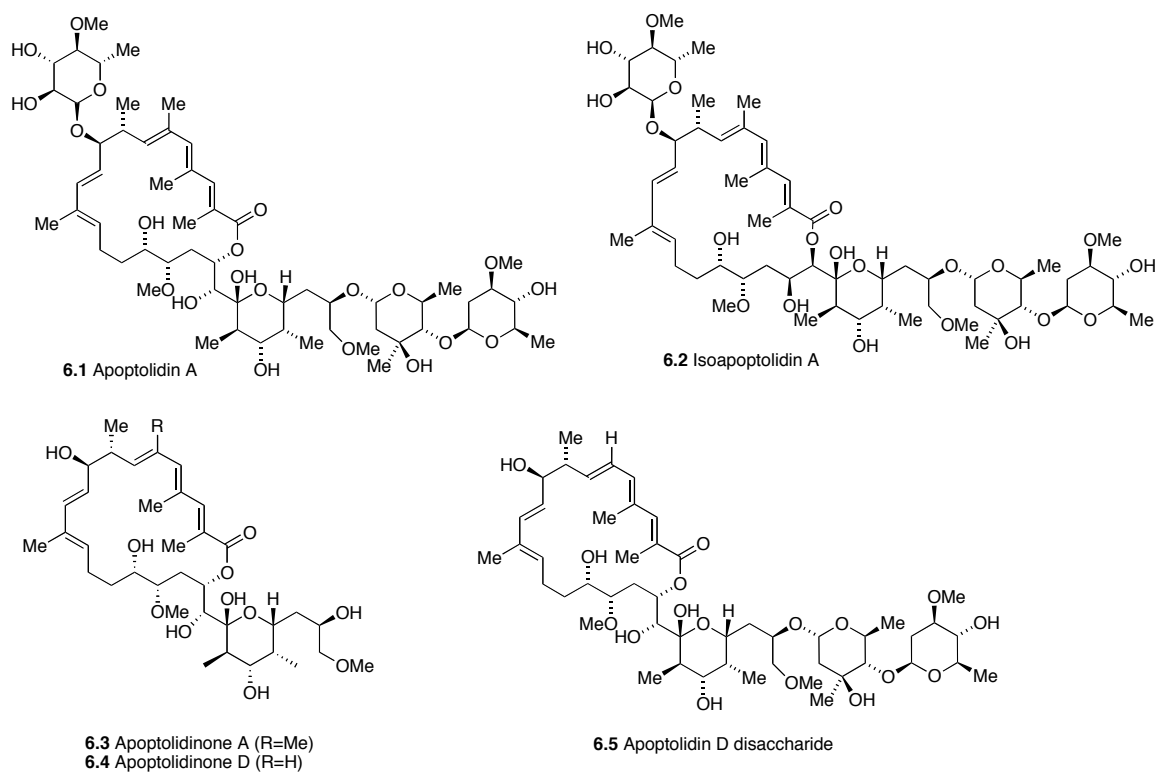


Figure 6.1 Structures of apoptolidin A **6.1**, isoapoptolidin A **6.2**, apoptolidinone A **6.3**, apoptolidinone D **6.4**, and apoptolidin D disaccharide **6.5**

Apoptolidin A **6.1** was identified as a specific apoptosis inducing agent by screening against phenotype transformed glia cells,³ and screening of this lead compound may help to find an effective anticancer agent for the treatment of various types of cancer without significant side effects. To develop apoptolidin into a drug that can be clinically used, one of the key requirements is to understand its action mechanism and identify the cellular target(s). Khosla's action mechanism was developed from pharmaceutical assay analysis and compared to compounds of similar structure with known action targets. Results of these studies suggest that apoptolidin A is an inhibitor of mitochondria F_0F_1 ATPase.^{3,12,13} However, results from Wender's SAR studies using both

mitochondria F_0F_1 ATPase assay and cell assay suggest that there is a more relevant cellular target other than mitochondria F_0F_1 ATPase or a more complex action mechanism for apoptolidin.¹⁵ In order to understand the action mechanism of apoptolidin in more detail, we planned to synthesize an apoptolidin probe to identify the protein target(s) using protein-profiling techniques. We investigated the cytotoxicity of apoptolidin against several cell lines including human lung adenocarcinoma epithelial A549 cells, human lung mucoepidermoid carcinoma H292 cells, and human colon carcinoma HCT116 cells in a collaboration with Dr. Marnett's group. Results of this study suggest that human lung cancer H292 cell line is the most sensitive towards apoptolidin A treatment. Our study also reveals some interesting data with regard to the biological activity associated with apoptolidin A **6.1**. Cytotoxicity results for synthetic apoptolidinone A **6.3**, apoptolidinone D **6.4** and biosynthetic apoptolidin D disaccharide **6.5** against H292 cells emphasized the importance of the biological role of individual sugar units in the structure of apoptolidin A **6.1**. These significant results suggest a new direction for the synthesis of apoptolidin probes with regard to target identification.

6.2 Biological Effects of Apoptolidin A, Isoapoptolidin A on H292 cells

Apoptolidin A **6.1** has been reported to exhibit anti-proliferative effects and cause apoptotic cell death in gene transformed cells and various human cancer lines. In our study, H292 cell line was selected and utilized for the evaluation of the biological effects of apoptolidin A **6.1** and its congeners.

We first examined the effects of apoptolidin A **6.1** on H292 cells with time- and concentration-dependent methods, and then assessed its effects on the cell viability of H292 with Calcein-AM fluorescence assay. In Wender's study, cytostasis effects that lasted over 2-3 days (ca. 72 h) were reported along with GI_{50} values for apoptolidin A **6.1** (32 nM), apoptolidin B (7 nM), apoptolidin C (24 nM), and apoptolidin D (110 nM) when screened against H292 (human lung carcinoma) cells.^{5,6,122} In our study, we observed that treatment of H292 lung carcinoma cells with apoptolidin A **6.1** resulted in growth arrest for the first two days. We also found that extended exposure of H292 cells to apoptolidin A **6.1** resulted in delayed toxicity, which has not been reported by other groups. The effect was drastic, resulting in >95% cell death after 7 days in culture with apoptolidin A **6.1** with concentrations as low as 30 nM (Figure 6.1). In contrast, treatment of lung carcinoma H292 cells with apoptolidin A **6.1** in a concentration as low as 10 nM only resulted in only growth arrest even after maintaining the culture for 7 days.

As apoptolidin A **6.1** can isomerize into its ring expanded isomer isoapoptolidin A **6.2** in aqueous solution (cell assay condition). In order to determine which isomer is the compound with the noted biological effects, we also evaluated the biological activity of isoapoptolidin A **6.2** against H292 cells in comparison with apoptolidin A **6.1**. When H292 cells were treated with isoapoptolidin A **6.2** at 30 nM, all cells succumbed to death in a similar manner as was displayed by apoptolidin A **6.1** after 7 days of co-culture. These results validated the hypothesis that apoptolidin A **6.1** and isoapoptolidin A **6.2** are

equally potent apoptosis inducing agents when added to human lung cancer cells. This finding is in agreement with the results initially reported by Wender's group who used E1A transformed glia cells to examine the cytotoxicity of both apoptolidin A **6.1** and isoapoptolidin A **6.2**.¹⁵

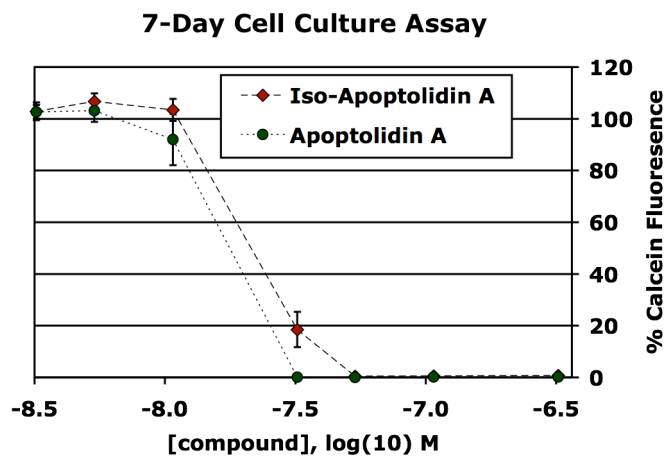
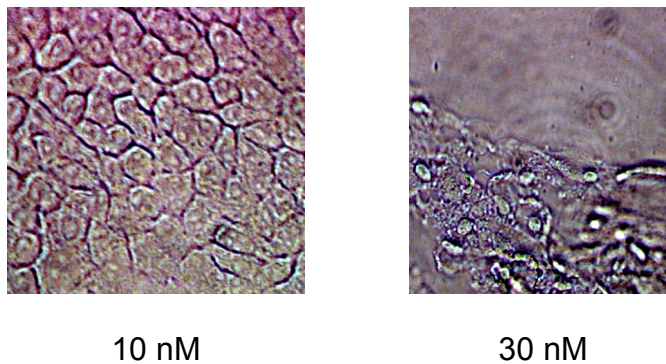


Figure 6.2 Cytotoxicity of apoptolidins to H292 cells (cell density: 500/well)

In general, cancer cells have 200 times higher glycolytic rates than normal cells. Decreased supply of glucose results in a slowdown in metabolism resulting detrimental biological effects. In view of the cell responses caused by decreased glucose supply during the treatment of apoptolidin A **6.1**, H292 cells were

cultured in three different medium MEM, DMEM and RPMI, in which MEM contained 1000 mg/L D-glucose; DMEM contained 4500 mg/L D-glucose; and RPMI contained 2000 mg/L D-glucose. We observed that cells cultured in MEM exhibited higher sensitivity to apoptolidin A **6.1** treatment than cells cultured in higher glucose supply RPMI medium and cells cultured in DMEM medium. These results suggest that glucose deprivation may increase apoptolidin A's **6.1** cytotoxicity against H292 cells, which indicates that insufficient glucose supply may exert an exogeneous force on mitochondria with regard to ATP production, thus triggering cell death by an unknown mechanism.

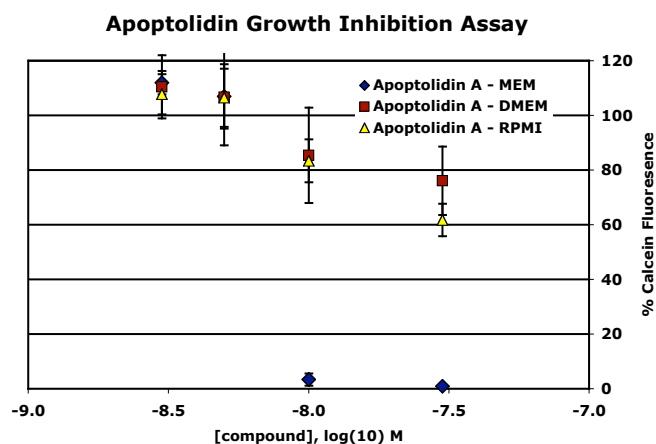


Figure 6.3 Glucose starvation effect on apoptolidin A cytotoxicity

Cell density is another exogeneous parameter that can influence cells function and their interaction with various substances.¹²³ To investigate whether an increase in cell density can affect sensitivity of H292 cells to apoptolidin, we cultured H292 cells in MEM medium with cell densities of 500/well and 5000/well, and examined cell response to apoptolidin A **6.1** and isoapoptolidin A **6.2** at

different concentrations. To our surprise, cell death was both observed within 3 days when being treated with either apoptolidin A **6.1** or isoapoptolidin A **6.2** at 25 nM. These results suggest that cells may be able to survive via an unknown self-protection mechanism (such as autophagy) at low cell density, whereas under crowded conditions, cells may undergo apoptosis under internal stress.

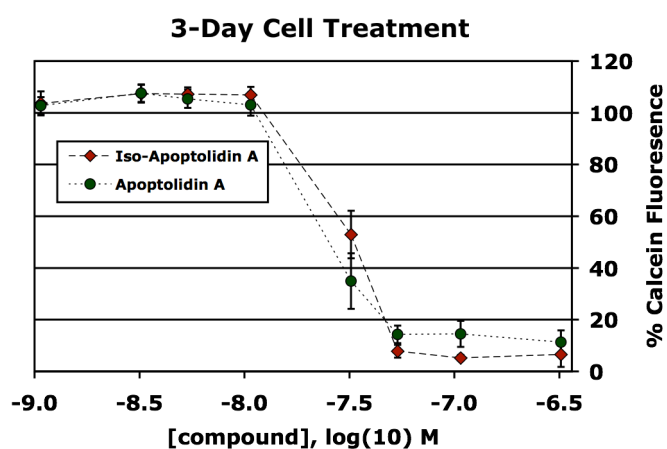


Figure 6.4 Cytotoxicity of apoptolidins to H292 cells (cell density: 5000/well)

In summary, apoptolidin A **6.1** and isoapoptolidin A **6.2** are equally potent cytotoxic agents. Cell death induced by apoptolidin was observed with delayed effect, glucose starvation effect and density effect in H292 cell line. Although cell viability has been evaluated for apoptolidin cytotoxicity, further observation in physiological changes in response to different exogenous environmental changes will provide more useful information for understanding apoptolidin A **6.1** cytotoxicity with regard to types of cell death (apoptosis or autophagy). As cancers are considered to be caused by mutations in the genome of the cells,

and genes or their protein products are usually involved in various signaling pathways to execute cell death, further studies using genetic and proteomic techniques are necessary to provide further information to help determining the molecular mechanisms for apoptolidin A induced cell death, delayed effect, glucose starvation effect and density effect.

6.3 Biological Role of Sugar Units in Apoptolidin A

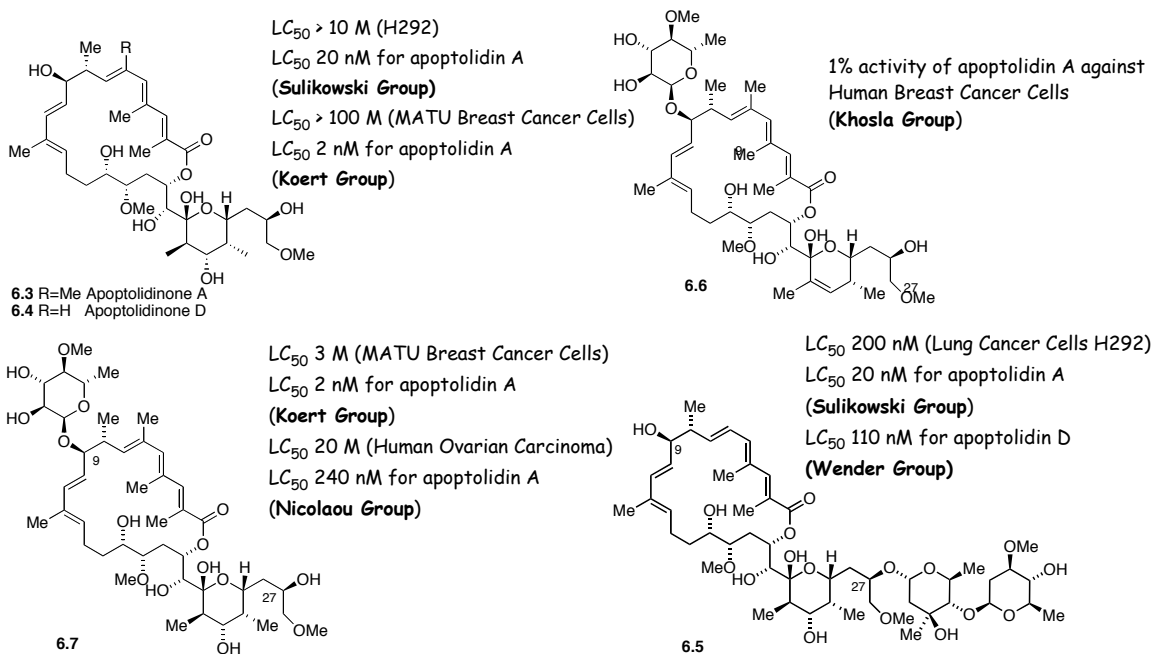


Figure 6.5 Cytotoxicity of apoptolidin sugar congeners

The biological role of sugar units in the structure of natural products is important to several functions including maintaining structural integrity, serving as solubilising auxiliaries, modulating protein functions, providing ligands for specific binding events mediating protein targeting, chemical defensing, as well as storing

and transferring information or energy.^{94,124} Apoptolidin A **6.1** features a C-9 monosaccharide and a C-27 disaccharide, the study on the biological roles of individual sugar units in apoptolidin A **6.1** cytotoxicity requires apoptolidin A glycoconjugates featuring different sugar moieties. Due to its the instability, apoptolidin A **6.1** can only tolerate limited reaction conditions. Even though acidic methanolysis of apoptolidin A **6.1** can provide apoptolidin A C-9 glycoconjugate **6.7**, extended hydrolysis under acidic conditions may cause massive decomposition. Our group has obtained apoptolidinone A **6.3** and apoptolidinone D **6.4** via total synthesis, and apoptolidin D C-27 disaccharide **6.5** via chemical and biological hybrid synthesis. Hence, it is possible to determine the importance of different sugar moieties in apoptolidin cytotoxicity using H292 cell assays.

In our study, H292 cells were exposed to different concentrations of apoptolidinone A **6.3**, apoptolidinone D **6.4** and apoptolidin D disaccharide **6.5** in RPMI culture medium. Toxicity effects of these compounds were evaluated based on the cell viability of H292 cells via Calcein-AM fluorescence assay. We found that the synthetic aglycones apoptolidinone A **6.3** and apoptolidinone D **6.4** were inactive in this cell assay, inhibiting neither cell growth nor viability at the concentrations tested ($EC_{50} > 100 \mu\text{M}$). Apoptolidin D disaccharide **6.5** inhibited cell growth in the submicromolar range ($EC_{50} = 200 \text{ nM}$), showing less than one order loss of activity relative to apoptolidin A (Sulikowski group: $EC_{50} = 30 \text{ nM}$ in H292 cell assay) and similar potency relative to apoptolidin D (Wender group: $EC_{50} = 110 \text{ nM}$ in H292 assay). Notably, the observed significant recovery of cytotoxicity in the incorporation of the C-27 disaccharide **6.5** is

consistent with earlier indications of the biological significance of this sugar residue.^{14,19,21} In the previous studies by both Nicolaou and Koert groups, apoptolidin A C-9 monosugar glycoconjugate **6.7** cytotoxicity (Koert group: LC₅₀=3 μM in MATU Breast Cancer Cells; Nicolaou group: LC₅₀=20 μM in Human Ovarian Carcinoma) decreased by 1000 fold relative to apoptolidin A **6.1** (Koert group: LC₅₀=2 nM in MATU Breast Cancer Cells; Nicolaou group: LC₅₀=240 nM in Human Ovarian Carcinoma).^{19,21} This result indicated that the biological role of C-27 disaccharide is more crucial than C-9 monosaccharide, and the C-27 disaccharide may mediate or interfere with an unknown specific target recognition event in the signaling pathway of apoptolidin-induced apoptosis.

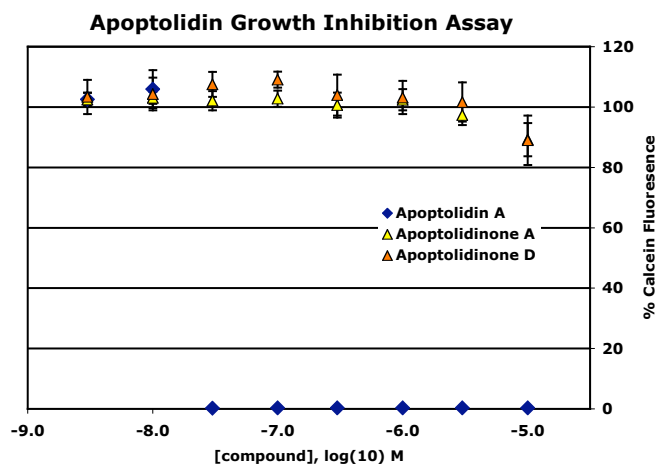


Figure 6.6 Cytotoxicity of apoptolidinones to H292 cells

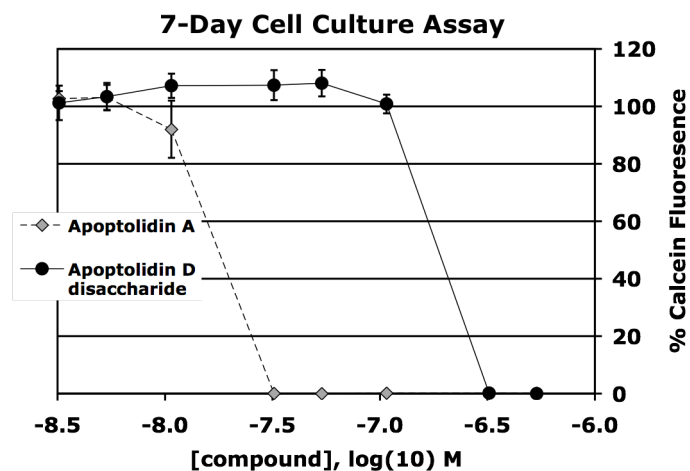


Figure 6.7 Cytotoxicity of apoptolidin D O-27 disaccharide to H292 cells

Similar biological role of sugar moieties in apoptolidin was reflected in another structurally similar 20-membered polyketide natural product, ammocidin A **6.8**.¹²⁵ Ammocidin A **6.8** was isolated from the culture broth of a soil bacteria *Saccharothrix* sp. AJ9571 in 2001 by Hayakawa and co-workers, the same group who discovered apoptolidin A **6.1**.¹²⁶ They reported that ammocidin A **6.8** could induce apoptosis in Ras dependent Ba/F3-V12 transformed hematopoietic cells with an IC_{50} of 66 ng/mL.¹²⁶ Even though the stereochemistry of ammocidin A **6.8** was not completely assigned, ammocidin A **6.8** shared many structural similarities with apoptolidin A **6.1**.¹²⁷ Specifically, both ammocidin A **6.8** and apoptolidin A **6.1** feature a 20 membered macrolactone, a pyran ring, a monosaccharide on C-9 position and a disaccharide. The disaccharide in apoptolidin A **6.1** resides at C-27, while in ammocidin A **6.8**, the disaccharide resides at C-24 on the pyran ring. Recently, the Hayakawa group isolated three minor ammocidin congeners including ammocidin B-D **6.9-6.11** from the culture

broth of ammocidin A-producing strain *Saccharothrix* sp. AJ9571.¹²⁵ Comparing to ammocidin A **6.8**, ammocidin B **6.9** features an extra methyl group at C-3'' position of C-24 disaccharide, ammocidin C **6.10** lacks a hydroxyl group at C-16 position and features a monosaccharide instead of a disaccharide at C-24 position, ammocidin D **6.11** lacks a disaccharide at C-24 position. Evaluation of the biological effects of these ammocidins **6.8-6.11** against A549 human lung carcinoma cells, MCF-7 human breast carcinoma cells and HCT116 human colon carcinoma cells revealed that both ammocidin C **6.10** and ammocidin D **6.11** without O-24 disaccharide lost significant cytotoxicity against all above cancer cell lines (Table 6.1).¹²⁵

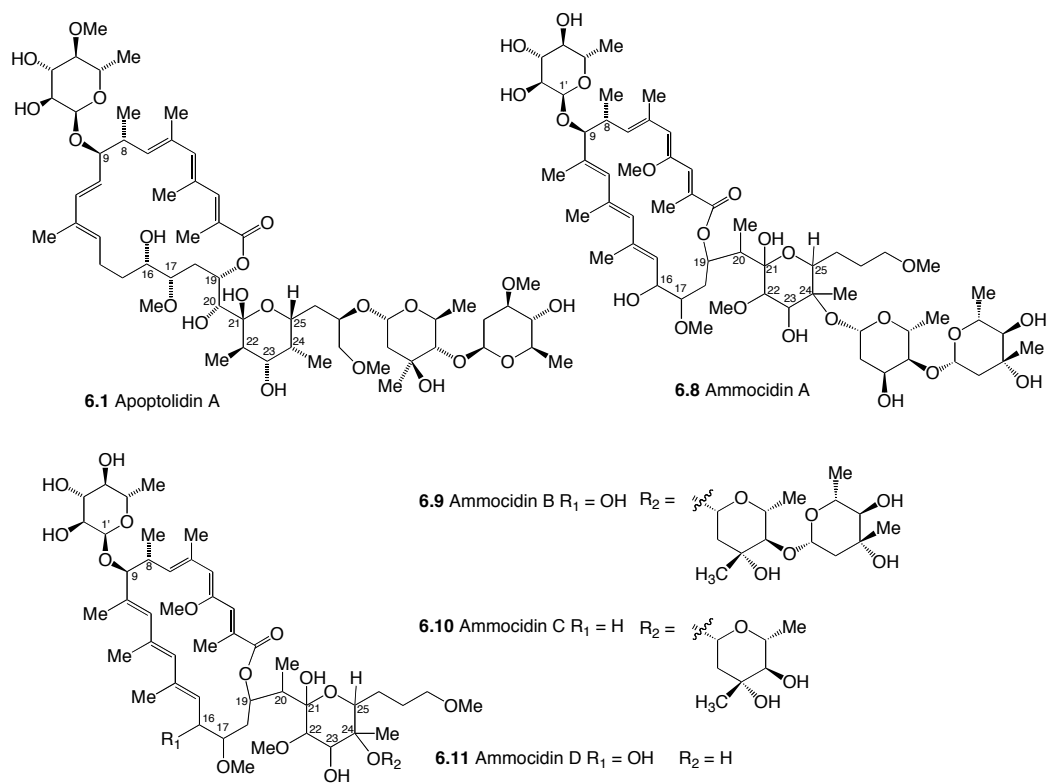


Figure 6.8 Structures of Ammocidin A-D and apoptolidin A

Table 6.1 Antiproliferative activities of ammocidins

	A549 (IC ₅₀ (μM))	MCF-7 (IC ₅₀ (μM))	HCT116(IC ₅₀ (μM))
Ammocidin A	0.058	0.14	0.11
Ammocidin B	0.073	0.10	0.38
Ammocidin C	2.1	1.8	8.4
Ammocidin D	6.4	5.0	23

Although the exact cellular action mechanism is still unknown, the important role of disaccharides displayed in both apoptolidin A **6.1** and ammocidin A **6.8** cytotoxicity has suggested that disaccharide is a crucial structural feature for their anti-tumor activity. This result is an important basis for future design of apoptolidin probes to study both the action mechanism and structure optimization to improve desired biological effects.

6.4 Apoptolidin Probe Design and Future Directions

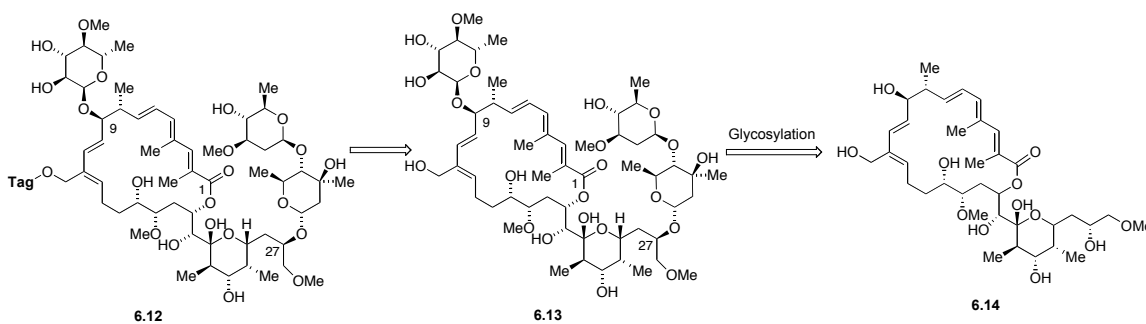
In order to identify the cellular target of apoptolidin A, Wender's group synthesized several biotinylated photoaffinity apoptolidin probes (See details in Chapter III).⁵⁸ Since apoptolidin A is not stable under photo irradiation conditions, the reactive species generated from irradiation with specific wavelength ($\lambda = 254$ nm) result in extensive and apoptolidin independent labeling of proteins in cell lysate. This finding suggests that apoptolidin photoaffinity conjugates are not suitable for elucidation of the specific protein binding in apoptolidin biological

activity.⁵⁸ There are two contributors to the success of target identification using an affinity chromatography: strong affinity in natural product-protein interaction and high abundance of the target protein(s).¹¹⁸ Considering the trienoate moiety in apoptolidin A may act as a Michael receptor to covalently bind to the target protein with sufficient strength, fluorescent tag labeled apoptolidin and a three-hybrid system of apoptolidin may be used for target identification.

Several factors need to be taken into consideration when designing a apoptolidin probe.^{128,129,130} First, the tag should have no effect or minimal effect on apoptolidin's biological activity (i.e. apoptosis). Second, the linker that connects the tag and apoptolidin, should be stable enough to tolerate the assay conditions. Third, the tag should be readily available either commercially or by simple chemical synthesis. Fourth, the tag should be readily conjugated to apoptolidin under mild reaction conditions.

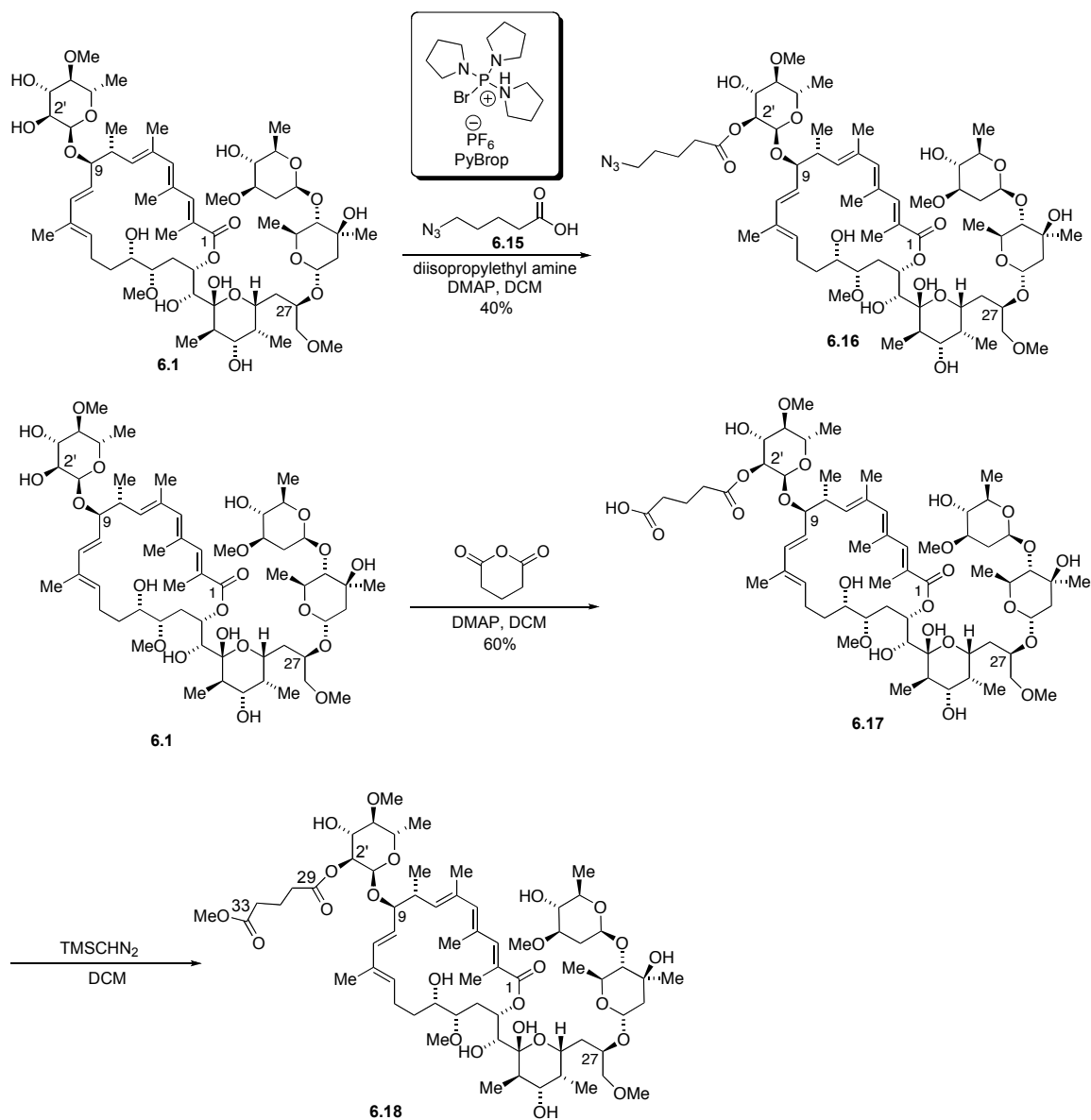
To minimize the effects on apoptolidin biological activity, choosing a right site for tag attachment is very important. Based on previous SAR studies conducted by several groups,^{14,15,19} we assumed that all sugar moieties in apoptolidin A are equally important for target recognition. Therefore, initial experiments were designed to incorporate a rhodamine based fluorescent tag at the C-12 methyl group of apoptolidin as shown in Scheme **6.1**. This strategy required functionalization of the methyl group at C-12 position of apoptolidin with a hydroxyl functionality, oxy-apoptolidin **6.13**. Although apoptolidin A **6.1** can be isolated from fermentation broth of *Nocardioopsis sp.* in moderate yield, due to the instability of apoptolidin, modification of its structure by chemical method,

especially on the macrolide core structure, was thought to be difficult. Therefore, oxy-apoptolidinone D **6.14** were synthesized based on our previous successful experience in the total synthesis of apoptolidinone A and relied on precursor directed bioglycosylation using apoptolidin producer (*Nocardioopsis sp.*) to attach the sugars to oxy-aglycone **6.14** and prepare oxy-apoptolidin **6.13**. As described in Chapter V, installation of sugar units using biological method was not succeeded, which led us to seek an alternative method to synthesize apoptolidin probe.



Scheme 6.1 Initial apoptolidin probe design

In the bioglycosylation experiments, we found that the fermentation yield of apoptolidin A **6.1** could be increased significantly from 110 mg/L (as reported by Seto's group) to 250-300 mg/L by scaling down the fermentation volume to 50 mL in 250 mL erlenmeyer flask and elongating the time of production fermentation from 5 days to 6 day (See Chapter V for details). Therefore, attention was turned to developing apoptolidin probes from natural apoptolidin A **6.1** via semi-synthesis.



Scheme 6.2 Synthesis of apoptolidin derivatives **6.16**, **6.17** and **6.18**

In Wender's SAR study, a series of hydroxyl group derivatives were synthesized from apoptolidin A.⁵⁷ Their work demonstrated that C-2' alcohol is the most reactive among eight hydroxyl groups in apoptolidin A. Based on this

finding, we decided to incorporate a fluorescent tag or a hybrid system at the C-2' position of apoptolidin A **6.1** with the hope that the tag attachment at this position would not interfere with the binding to the cellular target. Towards this goal, apoptolidin derivative **6.16** was synthesized via esterification of apoptolidin A **6.1** with azido acid **6.15** in the presence of PyBrop, Hunig's base, and DMAP. Azido acid **6.15** was prepared from methyl 5-bromopentanoate in two steps.¹³¹ Apoptolidin derivative **6.17** was synthesized via esterification of apoptolidin A **6.1** with glutaric anhydride and catalytic amount of DMAP in dichloromethane. Further methylation of apoptolidin derivative **6.17** with trimethylsilyldiazomethane provided apoptolidin derivative **6.18**. From the HMBC spectrum of **6.18**, strong correlation between H-2' and C-29 was observed. Abeit with NMR analysis of HSQC, COSY, ¹H and ¹³C spectra, the position of esterification was confirmed at C-2' position. The terminal carboxylic acid functionality in **6.17** and terminal azide functionality in **6.16** could be further derivatized and conjugated with pre-defined tags.

At this stage, the cytotoxicity of apoptolidin derivative **6.18** was screened against H292 cell line. The results showed that **6.18** (EC₅₀=125 nM) retained most of the cytotoxicity of apoptolidin A (EC₅₀=25 nM) in H292 cells, which indicated that modification at C-2' position did not block the binding with target protein(s). Since modification on C-2' position did not affect apoptolidin cytotoxicity significantly, we then tried to construct apoptolidin probes with tags attached on C-2' position. Apoptolidin fluorescent probe **6.19** and MTX probe **6.20** are promising options for further investigation.

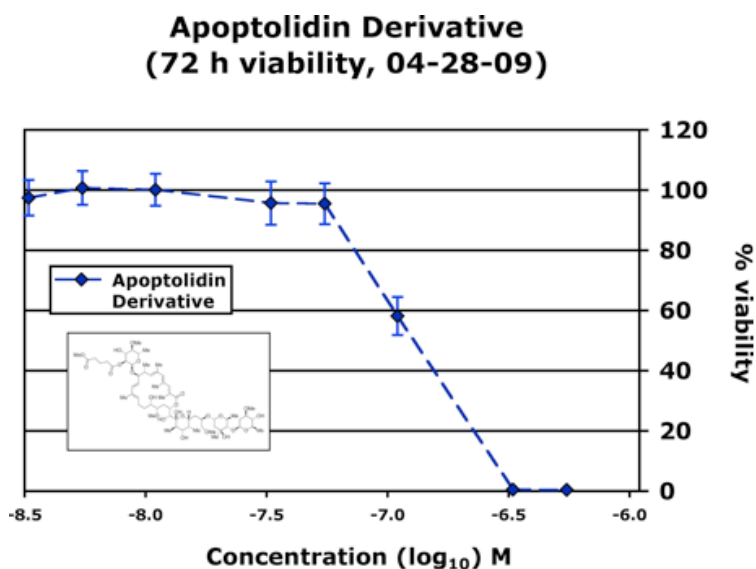


Figure 6.9 Cytotoxicity of apoptolidin derivative **6.18** in H292 cells

Because of the high absorption and emission, rhodamine dyes have been successfully used for imaging of living cells and live animals.¹³² Thus, we anticipated that 5-carboxy-X-rhodamine apoptolidin conjugate **6.19** would reveal the cellular location of apoptolidin. Three-hybrid systems were recently developed for efficient identification of interactions between small molecules and protein receptors.^{120,121} The MTX (methotrexate) three-hybrid system has been proven to be a powerful tool for target identification.^{133,134,135,136} There are three components in the three-hybrid system including a DNA-binding domain fused to a ligand-binding domain (i.e. DHFR), a ligand molecule (i. e. MTX) linked to a small molecule (i.e. natural products), and a transcriptional activation domain fused to a protein from a cDNA library. The interaction between small molecule and protein target(s) results in the formation of a trimeric complex, which can

activate the expression of reporter gene(s). Taking advantage the efficiency of MTX three-hybrid system in target identification, a MTX-apoptolidin dimerizer **6.20** will be synthesized.

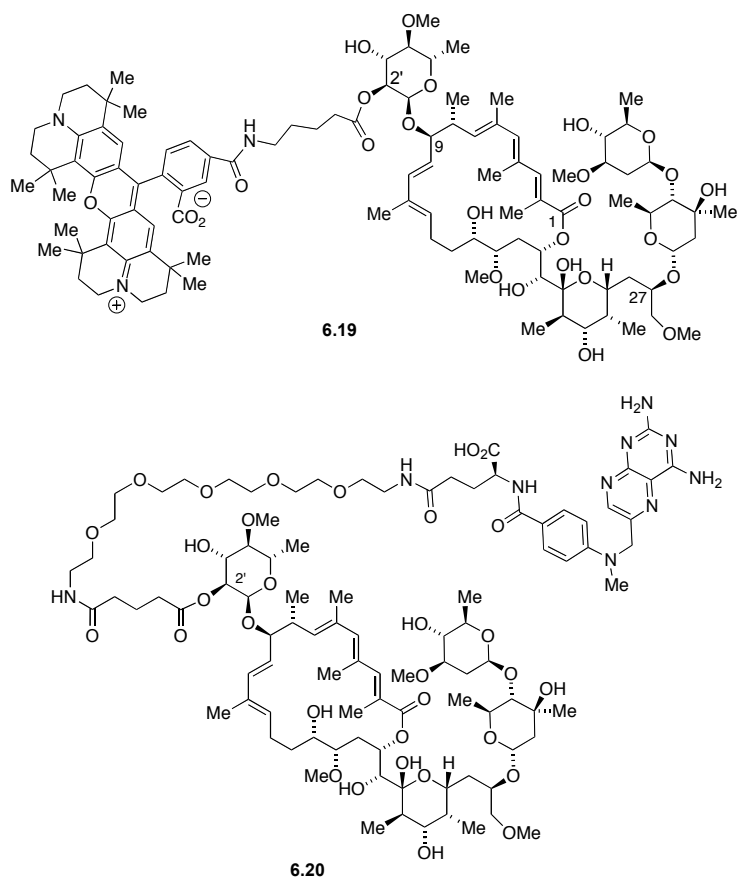


Figure 6.10 Structures of apoptolidin probes **6.19** and **6.20**

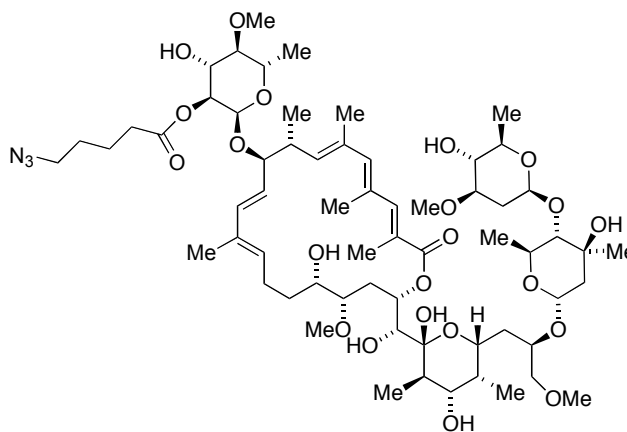
6.5 Summary

Apoptolidin A can selectively induce apoptosis in E1A transformed glia cells with minimal effects on normal glia cells. This distinguished feature makes apoptolidin A a promising lead for the development of new anticancer agents. In order to understand the action mechanism of apoptolidin A and identify its protein

target, the synthesis of an effective apoptolidin probe was explored. In this progress, 3 unnatural apoptolidinones including 6-normethyl apoptolidinone A, 2,6-dinormethyl apoptolidinone A and oxy-apoptolidinone D were synthesized via modifying the synthetic routes for several small building fragments based on our convergent synthetic strategy developed for the total synthesis of apoptolidinone A in 2004. Since apoptolidinones without sugar units displayed no cytotoxicity, precursor directed bioglycosylation was employed for the installation of sugar units. In this biotransformation process, we successfully purified and identified a new partially glycosylated apoptolidin congener, apoptolidin D C-27 disaccharide, which is only 10 fold less active than apoptolidin A. However, oxy-apoptolidinone D, featured a hydroxyl group at C-12 methyl position, was not a competitive substrate for this bioglycosylation. The C-12 hydroxyl group in oxy-apoptolidinone D was initially designed as an attachment point of a fluorescent or affinity reagent to synthesize a biological probe of apoptolidin. In the bioglycosylation study, we found that the production yield of apoptolidin A could be significantly increased by 2 to 3 folds by decreasing the fermentation volume and elongating the fermentation time. As SAR studies of sugars of apoptolidin A revealed that the C-9 monosaccharide was not important to apoptolidin cytotoxicity, and esterification at C-2' hydroxyl group was proven to have minimal effects on apoptolidin cytotoxicity, future direction in the construction of an apoptolidin probe will concentrate on the attachment of a fluorescent or affinity reagent on C-2' position.

6.6 Experimental Section

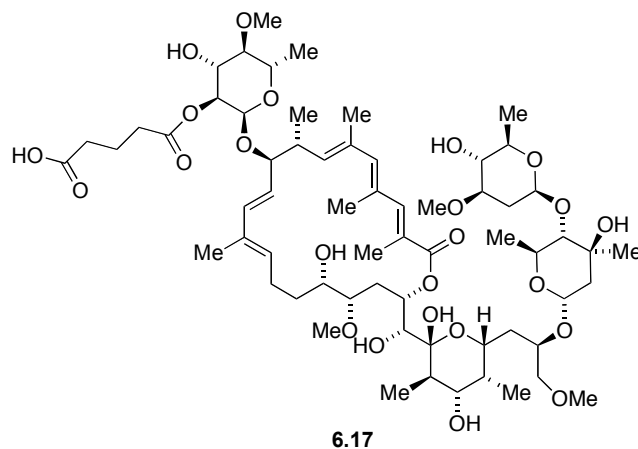
General Procedures: Unless indicated, all commercial reagents were used as received without further purification. All reactions were carried out under a nitrogen or argon atmosphere using dry glassware that had been flame-dried under a stream of nitrogen, unless otherwise noted. All solvents were purified prior to use. Dichloromethane was distilled from calcium hydride. Reactions were monitored by thin-layer chromatography (TLC) using 0.25-mm E. Merck precoated silica gel plates. Visualization was accomplished with UV light ($\lambda = 254$ nm) and aqueous anisaldehyde stain or KMnO_4 followed by charring on a silica gel 60 (particle size 230-400 mesh) with the indicated solvent. Flash chromatography was performed with the indicated solvents using mesh) with the indicated solvent. An automated chromatography system was also employed. Chromatography methods were created based on R_f values. Yields refer to chromatographically and spectroscopically pure compounds unless otherwise stated. Melting points are uncorrected unless otherwise noted. ^1H and ^{13}C NMR data are reported as δ values relative to residual non-deuterated solvent δ 3.31 ppm from CH_3OD . For ^{13}C spectra, chemical shifts are reported relative to the δ 49.0 ppm resonance of CD_3OD . High-resolution mass spectra were conducted at the Department of Chemistry and Biochemistry, University of Notre Dame on a JEOL AX505HA or JEOL JMS-GCmate mass spectrometer. Infrared (IR) spectra were recorded as thin films or solutions in the indicated solvent.



6.16

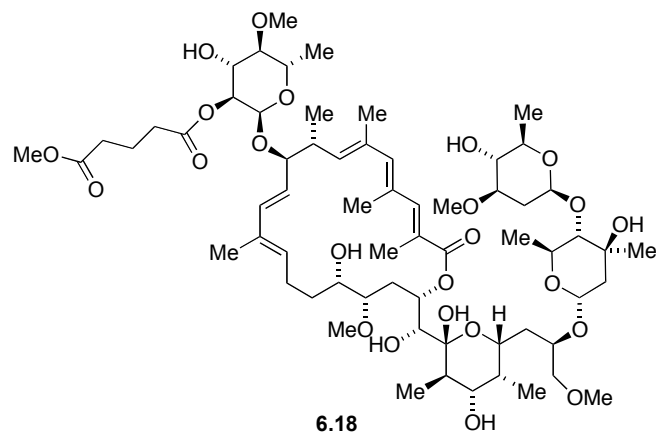
Azidoapoptolidin A 6.16: To a solution of azido acid **6.15** (50 mg, 44.30 μmol) in dichloromethane (8.8 mL) was added diisopropylethylamine (77 μL , 443.0 μmol) and PyBroP (61.9 mg, 132.9 μmol) at room temperature. The resulted solution was stirred for 10 min at room temperature and then transferred to a solution of **6.1** (19 mg, 132.9 μmol) and DMAP (3.78 mg, 31.0 μmol) in dichloromethane (1.5 mL) in a separate flask. After being stirred for 1 hour at room temperature, the reaction mixture was poured into aqueous 5% HCl (4 mL), and extracted with dichloromethane (3 X 10 mL). The organic fractions were washed with saturated aqueous NaHCO_3 (1 X 10 mL) and further washed with brine (1 X 10 mL). The organic layer was dried (Na_2SO_4), filtered and concentrated *in vacuo*. The residue was purified by Biotage chromatography (2%-18% methanol in dichloromethane) to afford azidoapoptolidin A **6.16** (28.4 mg, 52%) as a white solid: IR (neat) 3408, 2931, 2098, 1736, 1666, 1387, 1258, 1079, 846; ^1H NMR (500 MHz, CD_3OD): δ 7.38 (s, 1H), 6.19 (s, 1H), 6.14 (d, $J = 16.0$ Hz, 1H), 5.65 (t, $J = 7.5$ Hz, 1H), 5.29 (dt, $J = 11.0, 0.0$ Hz, 1H), 5.21 (d, $J = 10.5$ Hz, 1H), 5.05 (dd, $J = 16.0, 9.0$ Hz, 1H), 4.98 (d, $J = 4.0$ Hz, 1H), 4.94 (d, J

= 4.5 Hz, 1H), 4.83 (dd, $J = 10.0, 1.5$ Hz, 1H), 4.55 (dd, $J = 10.0, 4.0$ Hz, 1H), 3.95-3.93 (m, 1H), 3.92-3.74 (m, 3H), 3.71 (dd, $J = 11.5, 5.0$ Hz, 1H), 3.67 (dd, $J = 9.5, 6.0$ Hz, 1H), 3.60 (s, 3H), 3.58 (d, $J = 3.5$ Hz, 1H), 3.48-3.44 (m, 1H), 3.42 (s, 3H), 3.42-3.38 (m, 1H), 3.36 (s, 3H), 3.34-3.32 (m, 3H), 3.27 (s, 3H), 3.24-3.15 (m, 2H), 2.97 (t, $J = 9.0$ Hz, 1H), 2.81 (t, $J = 9.0$ Hz, 1H), 2.71 (dd, $J = 9.5, 4.5$ Hz, 1H), 2.68-2.64 (m, 1H), 2.47-2.39 (m, 4H), 2.19 (s, 3H), 2.11 (s, 3H), 2.10-2.01 (m, 3H), 1.95 (s, 3H), 1.94-1.87 (m, 1H), 1.82-1.63 (m, 8H), 1.65 (s, 3H), 1.63-1.55 (m, 2H), 1.54-1.43 (m, 2H), 1.32 (s, 3H), 1.30-1.27 (m, 1H), 1.28 (d, $J = 6.0$ Hz, 3H), 1.27 (d, $J = 6.0$ Hz, 3H), 1.21 (d, $J = 6.5$ Hz, 3H), 1.13 (d, $J = 6.5$ Hz, 3H), 1.02 (d, $J = 6.5$ Hz, 3H), 0.89 (d, $J = 7.0$ Hz, 3H).



Carboxylic Acid 6.17: To a solution of apoptolidin A **6.1** (50 mg, 44.70 μmol) in dichloromethane (8.8 mL) was added glutaric anhydride (15.1 mg, 132.9 μmol) and DMAP (5.9 mg, 48.73 μmol) at room temperature. The resulted solution was continuously stirred for 48 hours at room temperature and then concentrated *in vacuo*. The residue was purified by Biotage chromatography (5%-25% methanol

in dichloromethane) to afford carboxylic acid **6.17** (20.7 mg, 37%) as a white solid: ^1H NMR (400 MHz, CD_3OD): δ 7.38 (s, 1H), 6.19 (s, 1H), 6.14 (d, $J = 16.0$ Hz, 1H), 5.65 (t, $J = 8.0$ Hz, 1H), 5.32 (dt, $J = 11.4, 0.0$ Hz, 1H), 5.21 (d, $J = 8.0$ Hz, 1H), 5.06 (dd, $J = 16.0, 8.0$ Hz, 1H), 4.99 (d, $J = 4.0$ Hz, 1H), 4.94 (d, $J = 4.0$ Hz, 1H), 4.83-4.82 (m, 1H), 4.55 (dd, $J = 12.0, 4.0$ Hz, 1H), 3.95-3.92 (m, 1H), 3.92 (dd, $J = 8.0, 0$ Hz, 1H), 3.82 (dd, $J = 8.0, 0$ Hz, 1H), 3.80-3.63 (m, 3H), 3.60 (s, 3H), 3.59 (d, $J = 4.0$ Hz, 1H), 3.48-3.44 (m, 1H), 3.42 (s, 3H), 3.42-3.38 (m, 1H), 3.36 (s, 3H), 3.34-3.32 (m, 3H), 3.27 (s, 3H), 3.22-3.15 (m, 2H), 2.97 (t, $J = 8.0$ Hz, 1H), 2.82 (t, $J = 8.0$ Hz, 1H), 2.71 (dd, $J = 8.0, 4.0$ Hz, 1H), 2.70-2.64 (m, 1H), 2.47-2.39 (m, 5H), 2.39-2.33 (m, 1H), 2.35 (t, $J = 8.0$ Hz, 2H), 2.18 (s, 3H), 2.10 (s, 3H), 2.10-2.01 (m, 3H), 1.94 (s, 3H), 1.94-1.87 (m, 1H), 1.82-1.67 (m, 3H), 1.65 (s, 3H), 1.62-1.55 (m, 2H), 1.54-1.45 (m, 2H), 1.32 (s, 3H), 1.30-1.27 (m, 1H), 1.28 (d, $J = 6.0$ Hz, 3H), 1.27 (d, $J = 6.0$ Hz, 3H), 1.22 (d, $J = 4.0$ Hz, 3H), 1.13 (d, $J = 4.0$ Hz, 3H), 1.02 (d, $J = 8.0$ Hz, 3H), 0.89 (d, $J = 8.0$ Hz, 3H); ^{13}C NMR (150 MHz, CD_3OD) δ 175.5, 174.5, 172.7, 172.7, 149.3, 147.0, 142.7, 141.4, 134.6, 133.8, 133.7, 133.1, 125.5, 123.8, 101.9, 101.3, 99.5, 93.6, 87.3, 85.9, 84.4, 83.9, 82.0, 77.1, 76.9, 76.8, 75.4, 75.2, 74.6, 73.9, 73.2, 73.0, 72.4, 72.2, 69.4, 68.2, 67.4, 61.3, 61.2, 59.5, 57.3, 52.0, 45.5, 40.6, 39.1, 38.4, 37.2, 36.4, 34.4, 34.1, 24.6, 22.8, 22.1, 18.9, 18.3, 18.2, 18.1, 17.9, 16.5, 14.5, 12.2, 12.1, 5.2.



Methyl Ester 6.18: To a solution of apoptolidin A **6.1** (15 mg, 13.29 μmol) in dichloromethane (2.5 mL) was added glutaric anhydride (3.1 mg, 25.58 μmol) and DMAP (1.7 mg, 13.29 μmol) at room temperature. After the resulted solution was stirred for 48 hours at room temperature, 2M trimethylsilyldiazomethane in diethyl ether (13 μL , 25.58 μmol) was added. The reaction mixture was stirred for another 2 hours and then quenched with H_2O , extracted with dichloromethane (3 X 4 mL). The organic layer was dried (Na_2SO_4), filtered and concentrated *in vacuo*. The residue was purified by flash chromatography (dichloromethane/methanol 10:1) to afford methyl ester **6.18** (4.5 mg, 36% over 2 steps) as a white solid: IR (neat) 3428, 2931, 1738, 1668, 1385, 1252, 1102, 1066, 1008; ^1H NMR (600 MHz, CD_3OD): δ 7.38 (s, 1H), 6.19 (s, 1H), 6.14 (d, $J = 15.6$ Hz, 1H), 5.65 (t, $J = 7.8$ Hz, 1H), 5.25 (dt, $J = 11.4, 0.0$ Hz, 1H), 5.21 (d, $J = 9.6$ Hz, 1H), 5.06 (dd, $J = 15.6, 9.0$ Hz, 1H), 4.99 (d, $J = 4.2$ Hz, 1H), 4.94 (d, $J = 4.2$ Hz, 1H), 4.83 (dd, $J = 9.6, 1.8$ Hz, 1H), 4.55 (dd, $J = 10.2, 3.6$ Hz, 1H), 3.95 (ddd, $J = 8.4, 4.2, 2.4$ Hz, 1H), 3.92-3.89 (m, 1H), 3.90 (dd, $J = 9.0, 0$ Hz, 1H), 3.83 (dd, $J = 8.4$ Hz, 1H), 3.78-3.74 (m, 1H), 3.76 (dd, $J = 9.6, 6.6$ Hz, 1H), 3.71

(dd, $J = 10.8, 4.8$ Hz, 1H), 3.66 (s, 3H), 3.60 (s, 3H), 3.58 (d, $J = 3.6$ Hz, 1H), 3.55-3.53 (m, 1H), 3.42 (s, 3H), 3.42-3.39 (m, 1H), 3.36 (s, 3H), 3.34-3.32 (m, 3H), 3.27 (s, 3H), 3.22-3.15 (m, 2H), 2.97 (t, $J = 9.0$ Hz, 1H), 2.81 (t, $J = 9.0$ Hz, 1H), 2.71 (dd, $J = 9.6, 4.8$ Hz, 1H), 2.68-2.64 (m, 1H), 2.46-2.37 (m, 8H), 2.19 (s, 3H), 2.10 (s, 3H), 2.10-2.03 (m, 3H), 1.94 (s, 3H), 1.94-1.87 (m, 1H), 1.82-1.67 (m, 3H), 1.65 (s, 3H), 1.62-1.55 (m, 2H), 1.54-1.45 (m, 2H), 1.32 (s, 3H), 1.30-1.27 (m, 1H), 1.28 (d, $J = 6.0$ Hz, 3H), 1.27 (d, $J = 6.0$ Hz, 3H), 1.22 (d, $J = 6.0$ Hz, 3H), 1.13 (d, $J = 6.6$ Hz, 3H), 1.02 (d, $J = 7.2$ Hz, 3H), 0.89 (d, $J = 7.2$ Hz, 3H); ^{13}C NMR (150 MHz, CD_3OD) δ 175.0, 174.2, 172.7, 149.3, 147.0, 142.7, 141.4, 134.6, 133.8, 133.7, 133.1, 125.5, 123.8, 101.9, 101.3, 99.5, 93.5, 87.4, 85.9, 84.3, 83.9, 82.0, 77.1, 76.9, 76.8, 75.4, 75.2, 74.6, 73.9, 73.2, 73.0, 72.4, 72.3, 69.4, 68.2, 67.4, 61.3, 61.2, 59.5, 57.3, 52.1, 52.0, 45.5, 40.6, 39.1, 38.4, 37.2, 36.4, 34.2, 34.0, 33.8, 24.6, 22.8, 21.3, 18.9, 18.3, 18.2, 18.1, 17.9, 16.5, 14.5, 12.2, 12.1, 5.2.

Table 6.2 NMR spectroscopic data for apoptolidin A congeners in CD₃OD^a

Apop A	δ_{H}	6.16 δ_{H} (J in Hz)	6.17 δ_{H} (J in Hz)	6.18 δ_{H} (J in Hz)
3	7.41	s, 7.38	s, 7.38	s, 7.38
5	6.23	s, 6.19	s, 6.19	s, 6.19
7	5.27	d, 5.21 (10.5)	d, 5.21 (8.0)	d, 5.21 (9.6)
8	2.79	m, 2.68-2.64	m, 2.70-2.64	m, 2.68-2.64
9	3.87	m, 3.86-3.81	m, 3.92-3.89	dd, 3.83 (8.4, 0)
10	5.26	dd, 5.05 (16.0, 9.0)	dd, 5.06 (16.0, 8.0)	dd, 5.06 (15.6, 9.0)
11	6.21	d, 6.14 (16.0)	d, 6.14 (16.0)	d, 6.14 (15.6)
13	5.71	t, 5.65 (7.5)	t, 5.65 (8.0)	t, 5.65 (7.8)
14	2.50,2.09	m, 2.47-2.41, 2.10-2.01	m, 2.47-2.40, 2.10-2.06	m, 2.47-2.40, 2.10-2.06
15	1.52,1.44	m, 1.63-1.55, 1.48-1.43	m, 1.61-1.54, 1.51-1.41	m, 1.61-1.54, 1.51-1.41
16	3.47	m, 3.48-3.40	m, 3.42-3.39	m, 3.42-3.39
17	2.75	dd, 2.71 (9.5, 4.5)	dd, 2.71 (8.0, 4.0)	dd, 2.71 (9.6, 4.8)
18	2.20,1.78	m, 2.12-2.03, 1.82-1.78	m, 2.06-2.03, 1.82-1.78	m, 2.06-2.03, 1.82-1.78
19	5.32	dt, 5.29 (11.0, 0)	dt, 5.32 (12.0, 0)	dt, 5.25 (11.4, 0)
20	3.57	d, 3.58 (3.5)	d, 3.59 (4.0)	d, 3.58 (3.6)
22	2.08	m, 2.71-2.01	m, 2.07-2.05	m, 2.07-2.05
23	3.76	m, 3.80-3.75	m, 3.78-3.74	m, 3.78-3.74
24	1.76	m, 1.75-1.69	m, 1.75-1.73	m, 1.75-1.73
25	3.99	m, 3.95-3.93	m, 3.95-3.92	ddd, 3.95 (8.4, 4.2, 2.4)
26	1.62,1.49	m, 1.67-1.63, 1.54-1.47	m, 1.61-1.54, 1.53-1.51	m, 1.61-1.54, 1.53-1.51
27	3.48	m, 3.56-3.53	m, 3.48-3.44	m, 3.55-3.53
28	3.36	m, 3.34-3.31	m, 3.34-3.32	m, 3.34-3.32
2-Me	2.14	s, 2.11	s, 2.11	s, 2.11
4-Me	2.21	s, 2.19	s, 2.18	s, 2.19
6-Me	1.97	s, 1.95	s, 1.94	s, 1.94
8-Me	1.17	d, 1.13 (6.5)	d, 1.13 (4.0)	d, 1.13 (6.6)
12-Me	1.71	s, 1.65	s, 1.65	s, 1.65
22-Me	1.06	d, 1.02 (6.5)	d, 1.02 (8.0)	d, 1.02 (7.2)
24-Me	0.92	d, 0.89 (7.0)	d, 0.89 (8.0)	d, 0.89 (7.2)
1 [*]	4.85	d, 4.98 (4.0)	d, 4.99 (4.0)	d, 4.99 (4.2)
2 [*]	3.44	dd, 4.55 (10.0, 4.0)	dd, 4.55 (12.0, 4.0)	dd, 4.55 (10.2, 3.6)
3 [*]	3.76	m, 3.83 (9.0)	t, 3.92 (8.0)	dd, 3.91 (9.0, 0)
4 [*]	2.76	t, 2.81 (9.0)	t, 2.82 (8.0)	t, 2.81 (9.0)
5 [*]	3.73	dd, 3.67 (9.5, 6.0)	m, 3.78-3.74	dd, 3.76 (9.6, 6.6)
6 [*]	1.25	d, 1.27 (6.0)	d, 1.27 (6.0)	d, 1.27 (6.0)
1 ^{**}	4.97	d, 4.94 (4.5)	d, 4.94 (4.0)	d, 4.94 (4.2)
2 ^{**}	1.96,1.84	m, 1.97-1.90, 1.70-1.65	m, 1.95-1.90, 1.77-1.74	m, 1.95-1.90, 1.77-1.74
4 ^{**}	3.37	m, 3.34-3.31	m, 3.34-3.32	m, 3.34-3.32
5 ^{**}	3.70	dd, 3.71 (11.5, 5.0)	dd, 3.71 (12.0, 4.0)	dd, 3.71 (10.8, 4.8)
6 ^{**}	1.22	d, 1.21 (6.5)	d, 1.22 (4.0)	d, 1.22 (6.0)
3 ^{**} -Me	1.36	s, 1.32	s, 1.32	s, 1.32
1 ^{***}	4.86	dd, 4.83 (10.0, 1.5)	m, 4.83-4.82	dd, 4.83 (9.6, 1.8)
2 ^{***}	2.47,1.32	m, 2.46-2.42, 1.30-1.26	m, 2.46-2.42, 1.30-1.26	m, 2.46-2.42, 1.30-1.26
3 ^{***}	3.21	m, 3.24-3.15	m, 3.22-3.19	m, 3.22-3.19
4 ^{***}	3.01	t, 2.97 (9.0)	t, 2.97 (8.0)	t, 2.97 (9.0)
5 ^{***}	3.24	m, 3.24-3.15	m, 3.22-3.19	m, 3.22-3.19
6 ^{***}	1.27	d, 1.27 (6.0)	d, 1.28 (8.0)	d, 1.28 (6.0)
4 [*] -OMe	3.61	s, 3.60	s, 3.59	s, 3.59
3 ^{***} -OMe	3.46	s, 3.42	s, 3.42	s, 3.42
17-OMe	3.40	s, 3.36	s, 3.36	s, 3.36
28-OMe	3.30	s, 3.27	s, 3.27	s, 3.27
OMe				s, 3.66
30-33 CH ₂		m, 2.46-2.37, 1.76-1.69	m, 2.47-2.43, t, 2.35 (8.0)	m, 2.46-2.37

^a ¹H NMR for congener **6.16** was obtained on 500 MHz NMR spectrometer; ¹H NMR for congener **6.17** was obtained on 400 MHz NMR spectrometer; ¹H NMR for congener **6.18** was obtained on 600 MHz NMR spectrometer; ¹H NMR data for apoptolidin A was modified from ref 3.

6.7 Materials and Methods for Biological Activity Studies

6.7.1 Synthesis of Apoptolidin Sugar Analogues:

The synthesis of apoptolidinone A **6.3** and apoptolidinone D **6.4** was described in Chapter III and IV. Biosynthesis of apoptolidinone D disaccharide **6.5** was described in Chapter V. Apoptolidin A **6.1** and isoapoptolidin A **6.2** were isolated from fermentation broth of *Nocardioopsis sp.* as described in Chapter V. Stock solutions were prepared by using DMSO as solvent. It was further diluted in DMSO to the desired concentrations for experimental use.

6.7.2 Cell Assay:

In our study, we used H292 lung carcinoma cells assay, which were purchased from ATCC (CRL-1848). H292 cells were cultured at 37 °C, 5% CO₂ in air in a humidified incubator. Generally, H292 cells were maintained in RPMI 1640 medium supplemented with 10% fetal bovine serum (FBS) and 1% (1:100 dilution) of antibiotic-antimycotic (Invitrogen, 15240-062) for compounds activity screening. MEM and DMEM medium were chose for observation of glucose-starvation effects and density effect.

6.7.3 Cell Viability Analysis:

H292 cells were plated at a density of 500/well or 5000/well in 96-well plates, and cell viability was measured after 7 or 3 days by adding 2 μM Calcein-AM, and measuring fluorescence on a Spectramax (Molecular Dynamics) plate

reader, $\lambda_{\text{abs}} = 494$; $\lambda_{\text{em}} = 517$. Effective concentration 50 (EC_{50}) values are defined as the concentration of compound at which Calcein-AM fluorescence is inhibited by 50%.

APPENDIX

SPECTRA RELEVANT TO CHAPTER IV AND CHAPTER V

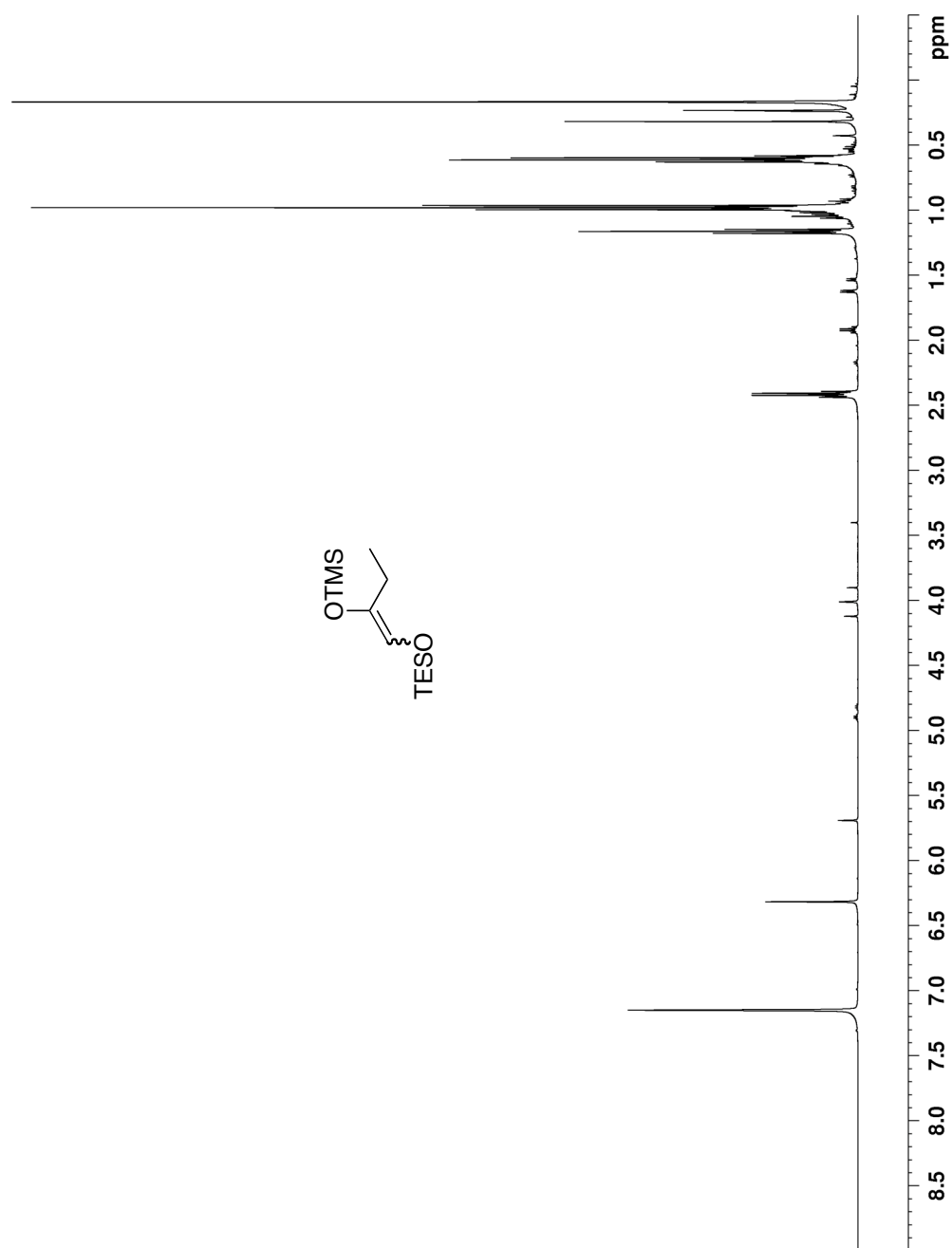


Figure A1a The 500 MHz ¹H NMR spectrum of silyl enol ether **4.9** in C₆D₆

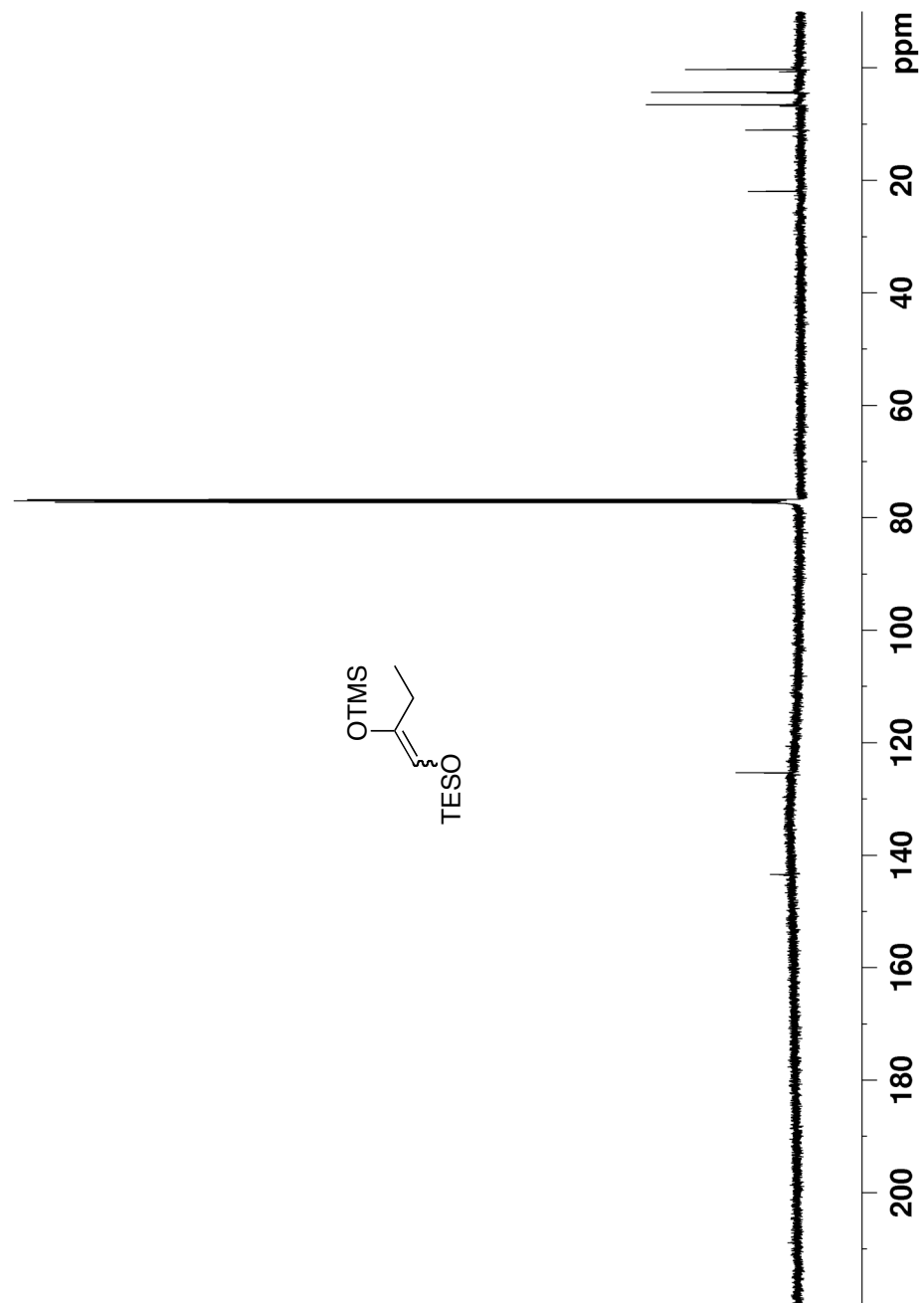


Figure A1b The 125 MHz ^{13}C NMR spectrum of silyl enol ether **4.9** in CDCl_3

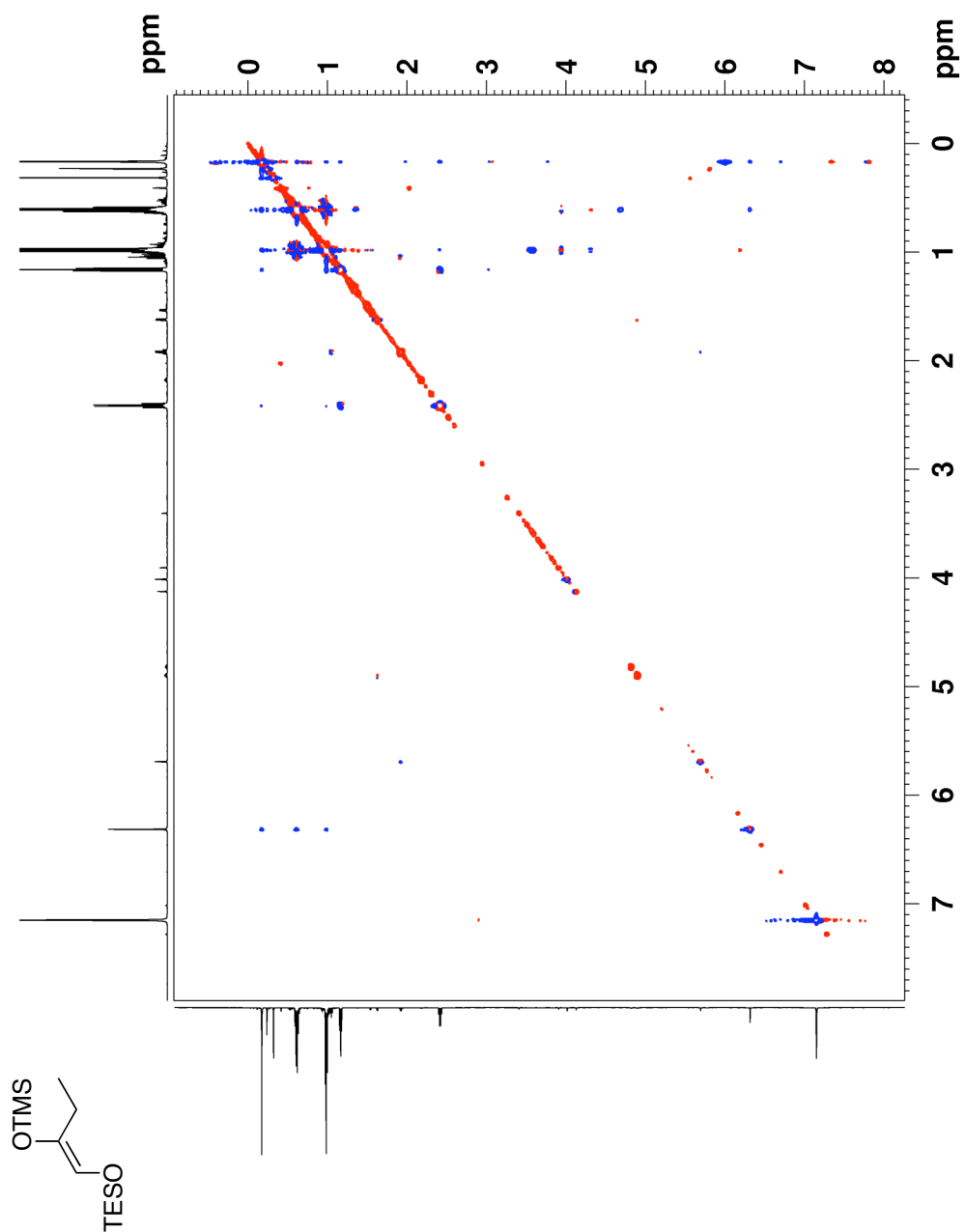


Figure A1c The 600 MHz NOESY NMR spectrum of silyl enol ether **4.9** in C_6D_6

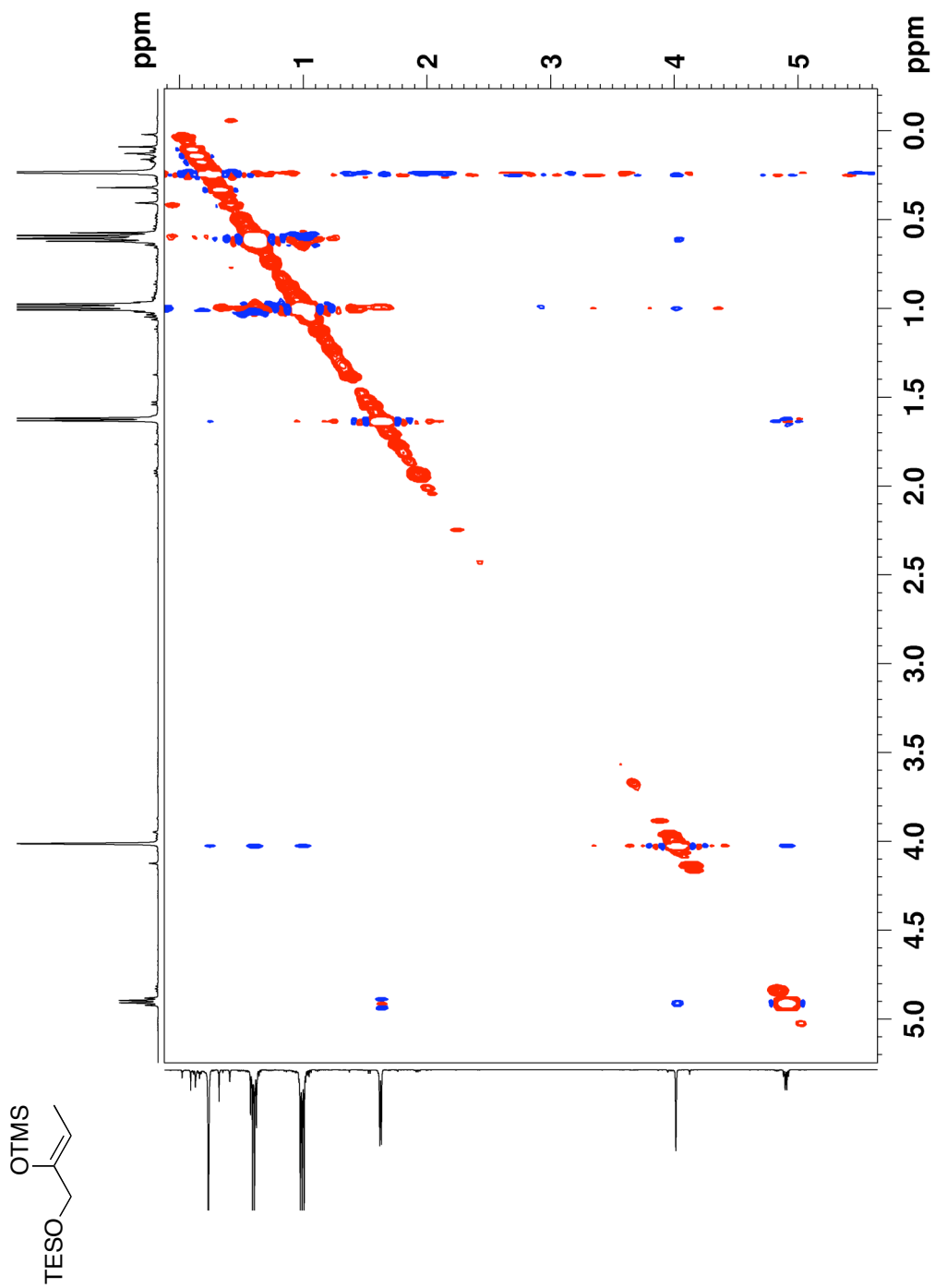


Figure A2a The 500 MHz NOESY NMR spectrum of silyl enol ether **4.29** in CDCl_3

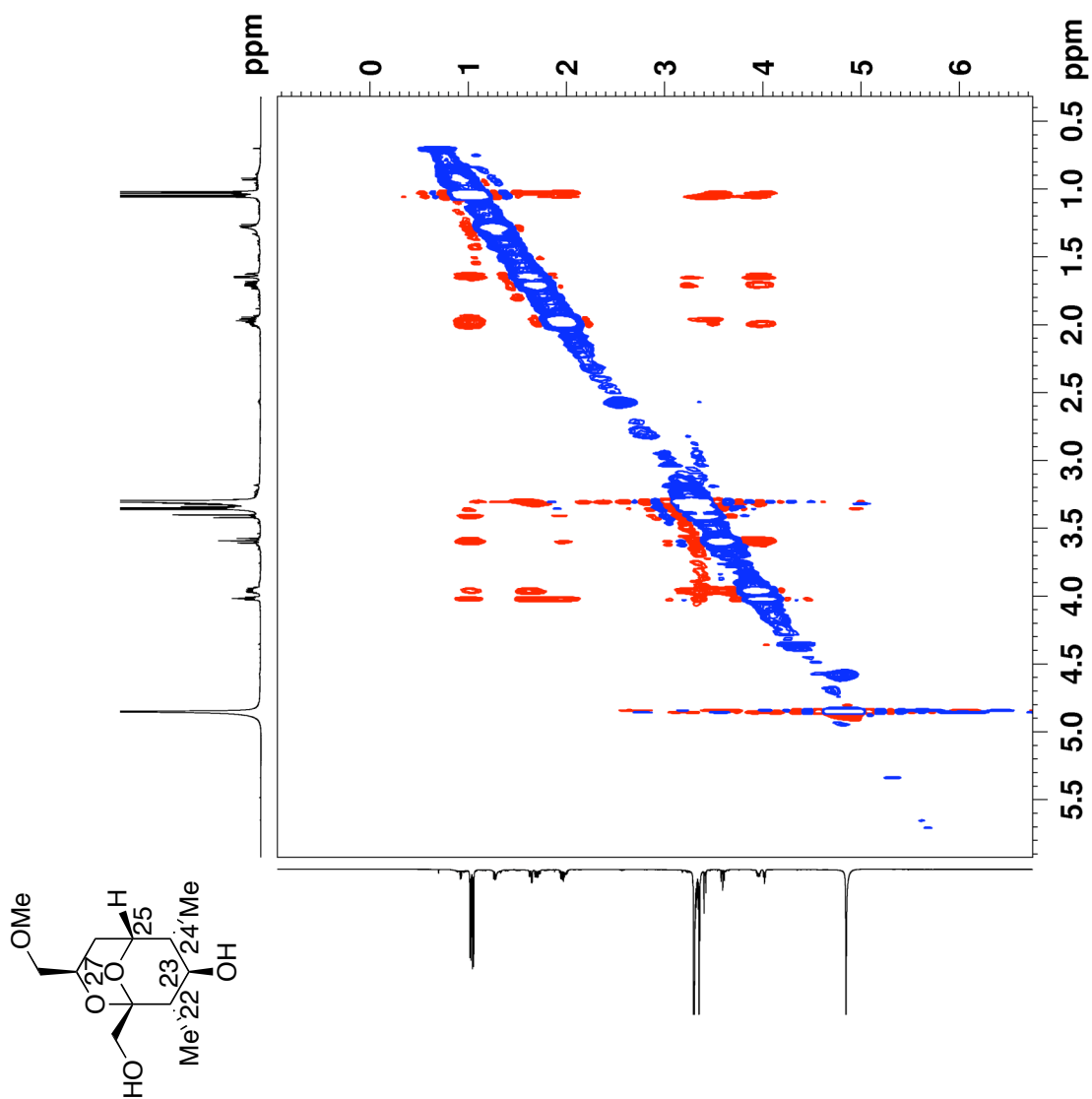


Figure A3a The 600 MHz NOESY NMR spectrum of pyran **4.32** in CD₃OD

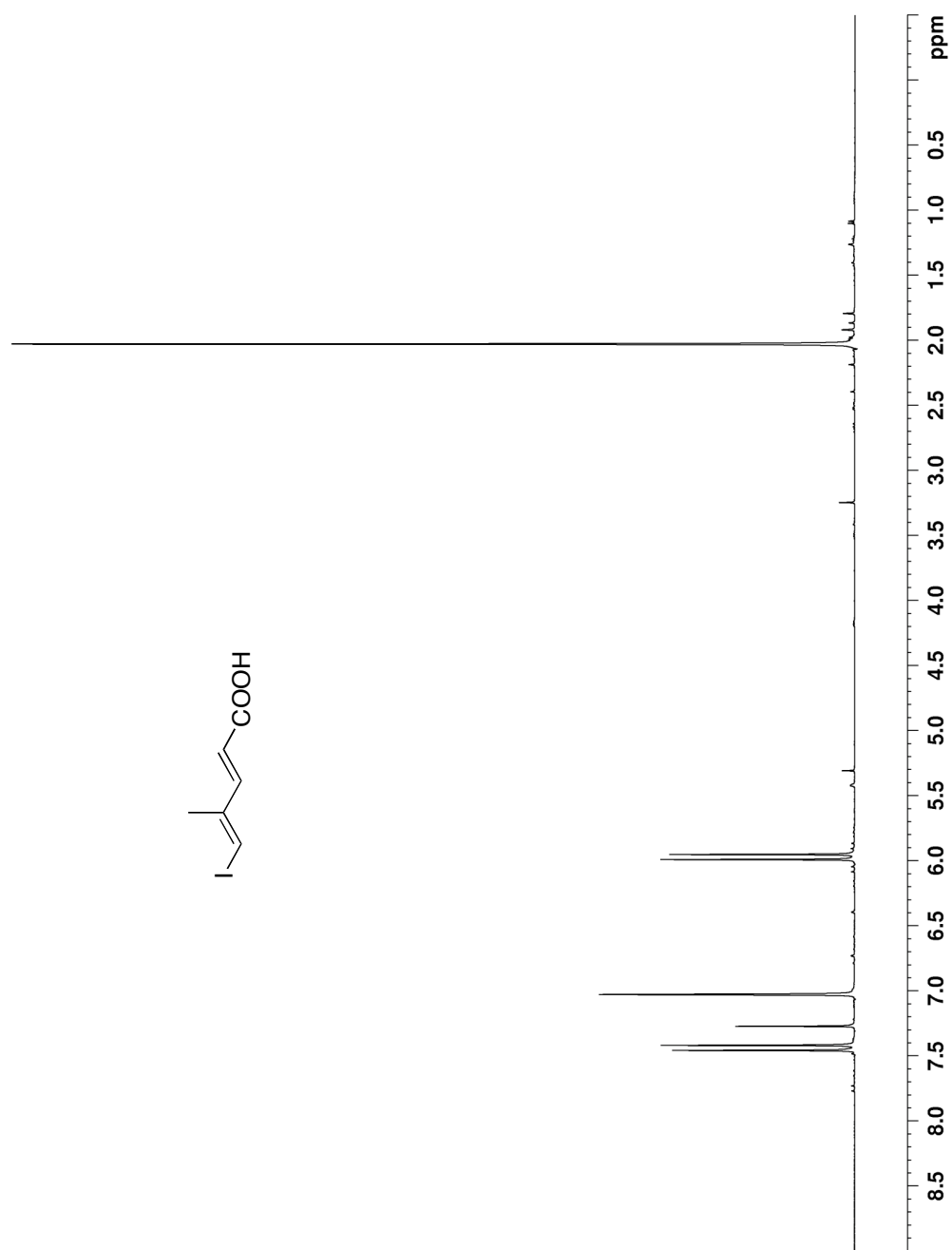


Figure A4a The 400 MHz $^1\text{H NMR}$ spectrum of carboxylic acid **4.37** in CDCl_3

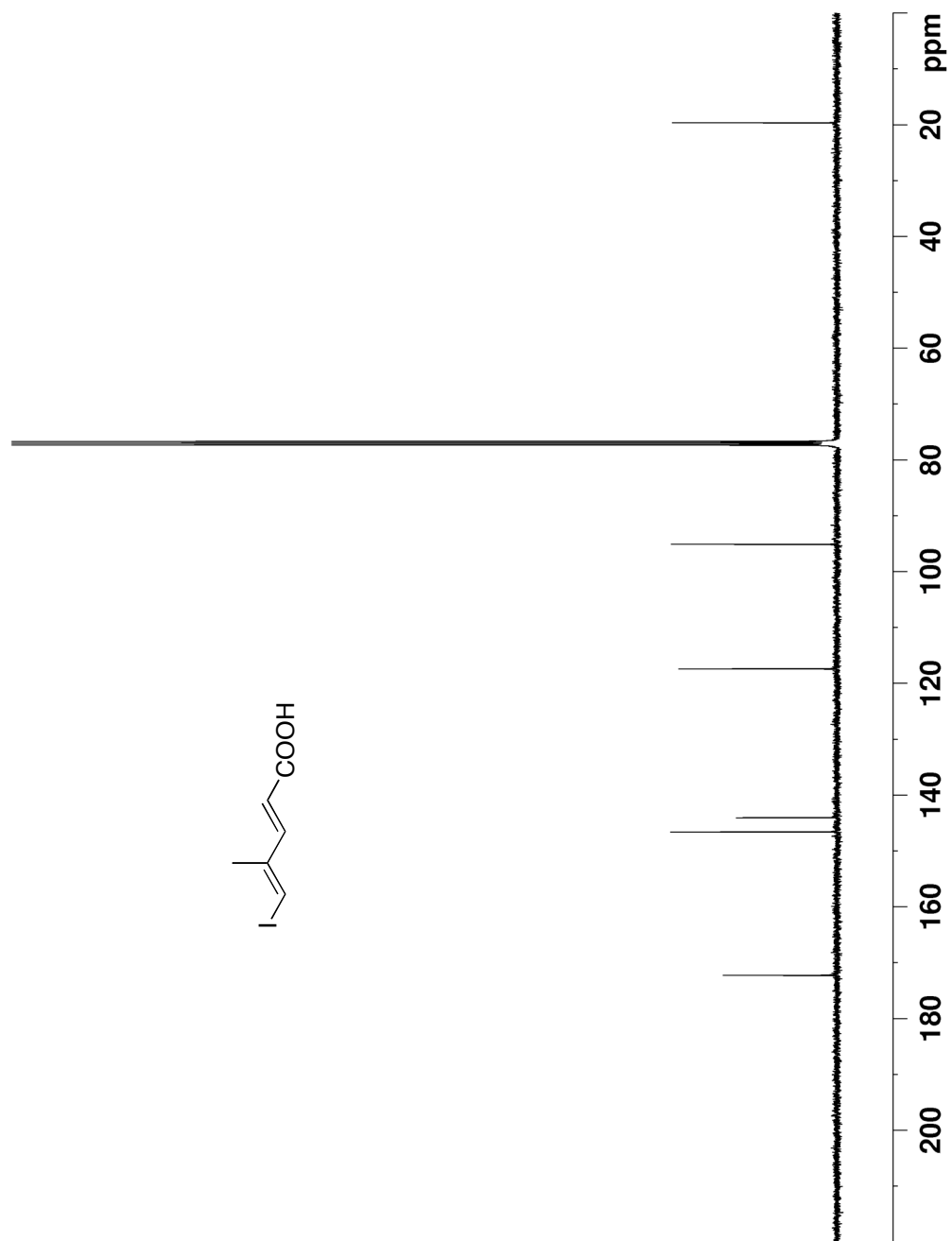


Figure A4b The 100 MHz ^{13}C NMR spectrum of carboxylic acid **4.37** in CDCl_3

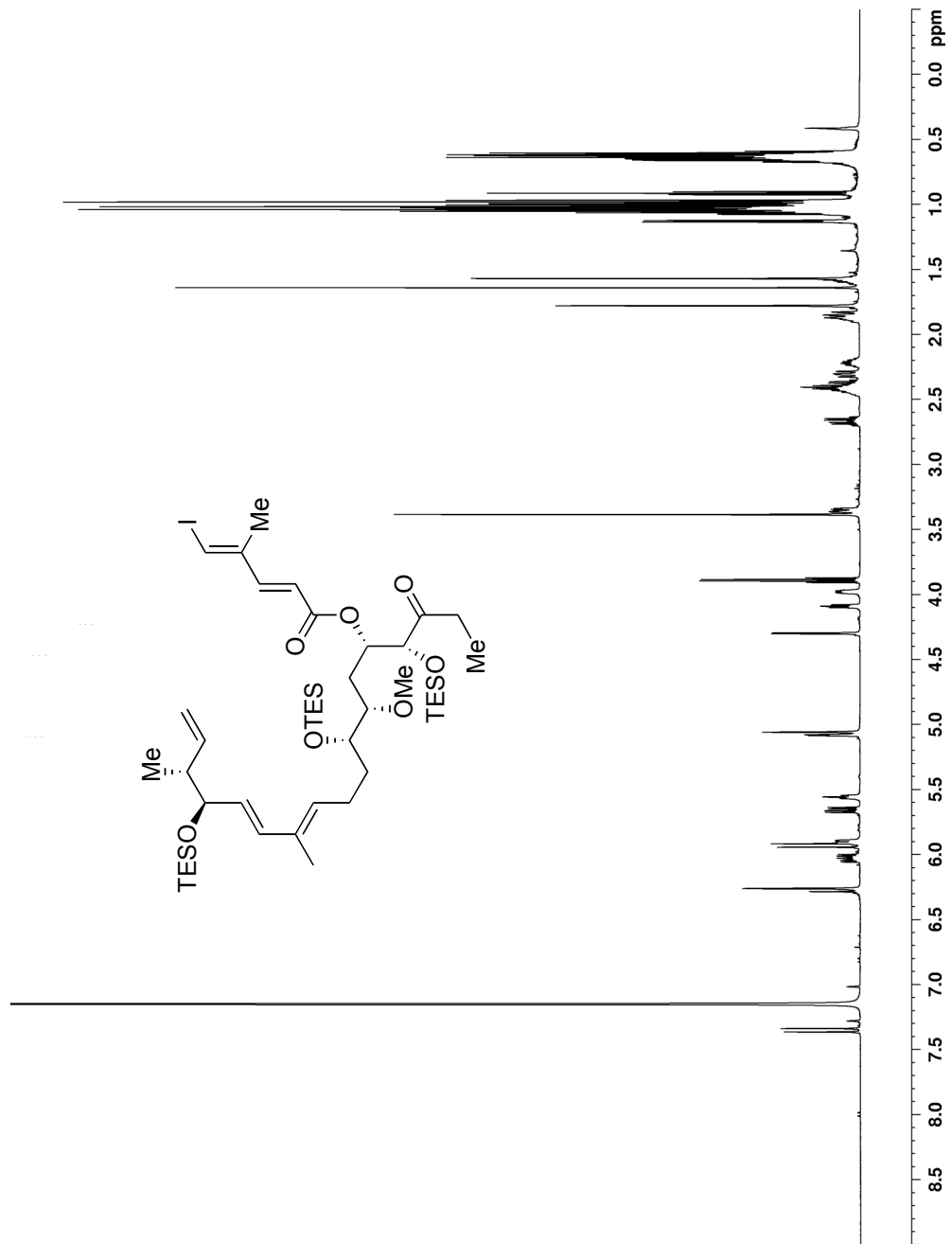


Figure A5a The 600 MHz ^1H NMR spectrum of ester **4.43** in C_6D_6

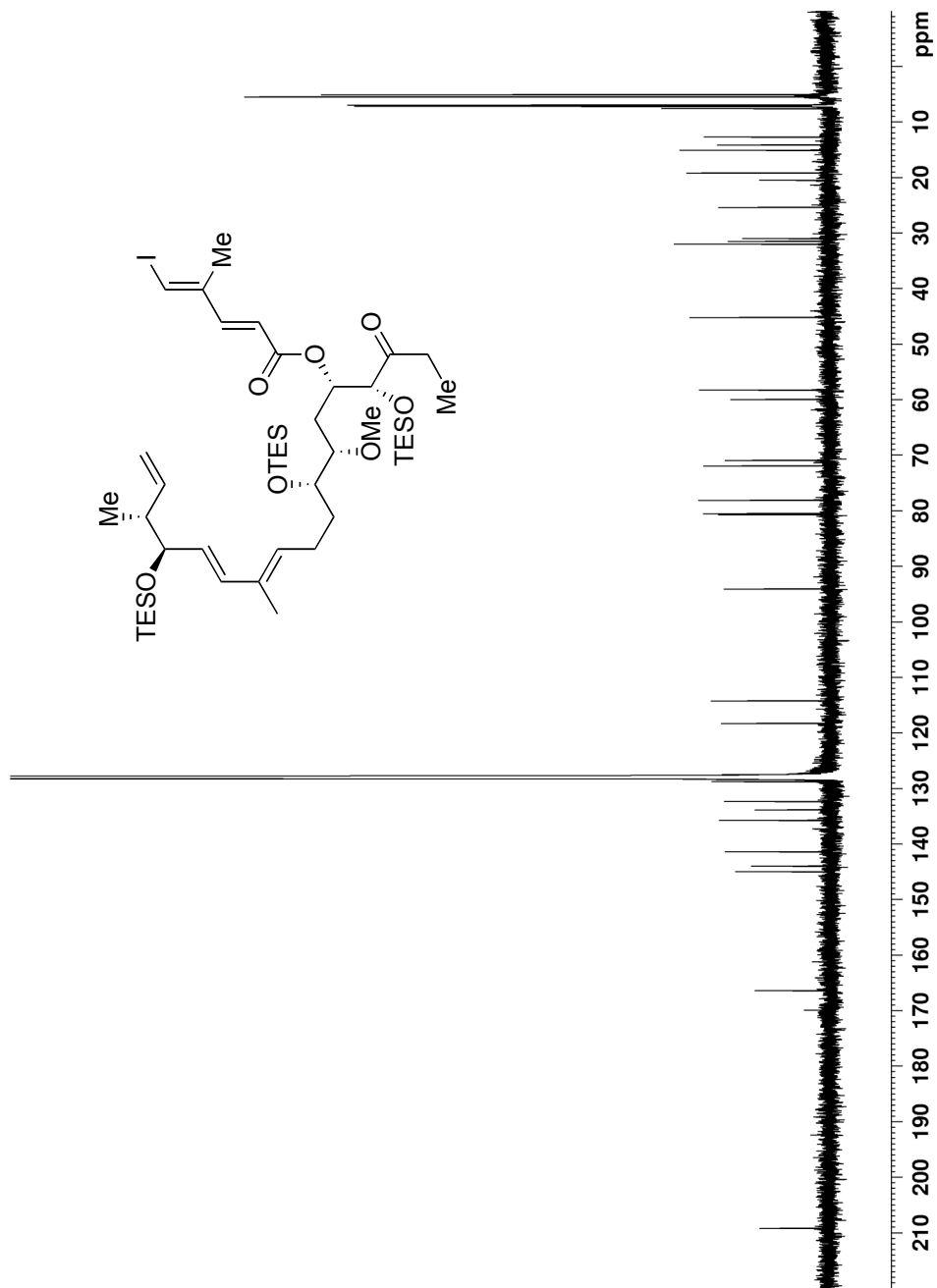


Figure A5b The 150 MHz ^{13}C NMR Spectrum of Ester **4.43** in C_6D_6

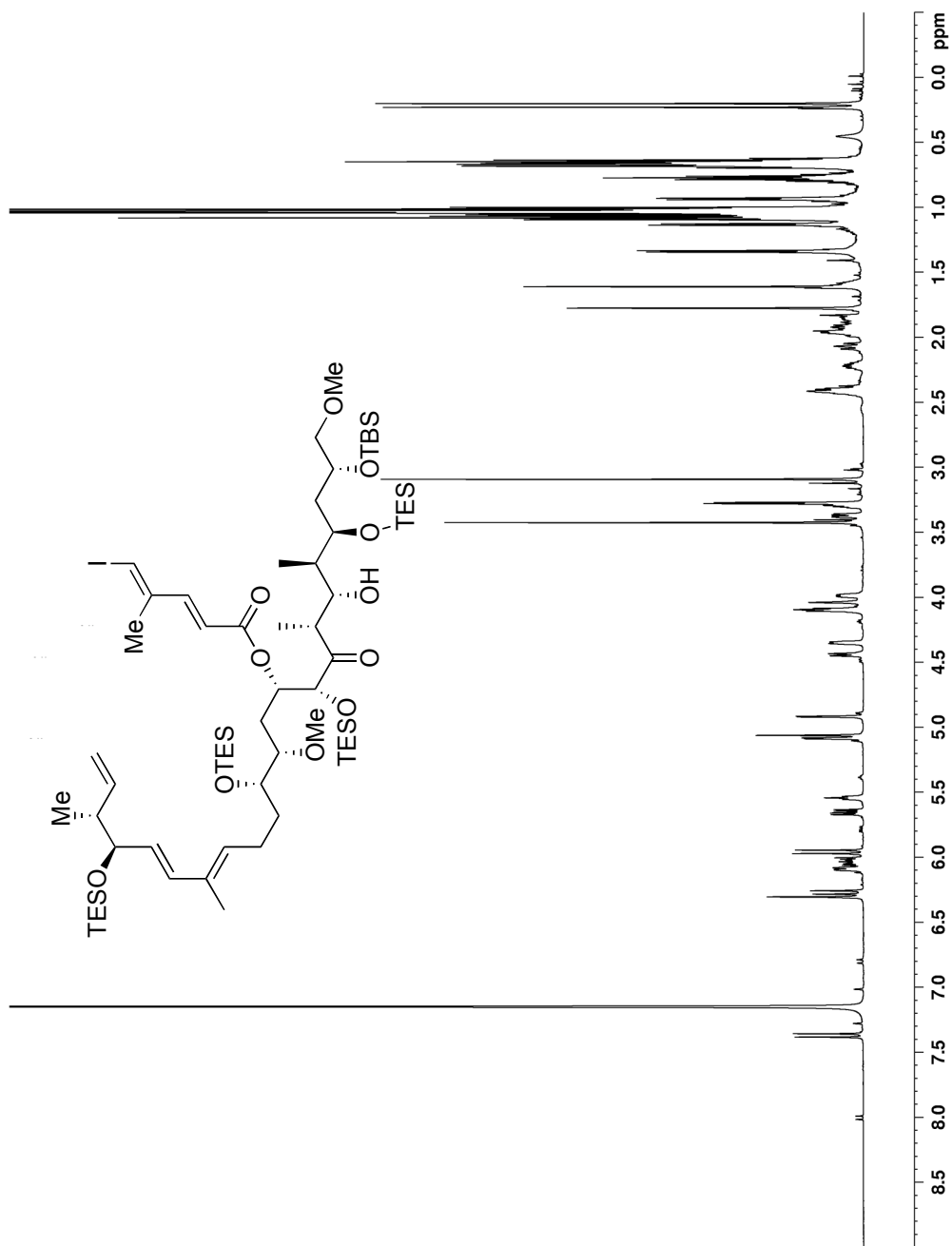


Figure A6a The 600 MHz ^1H NMR spectrum of alcohol **4.44** in C_6D_6

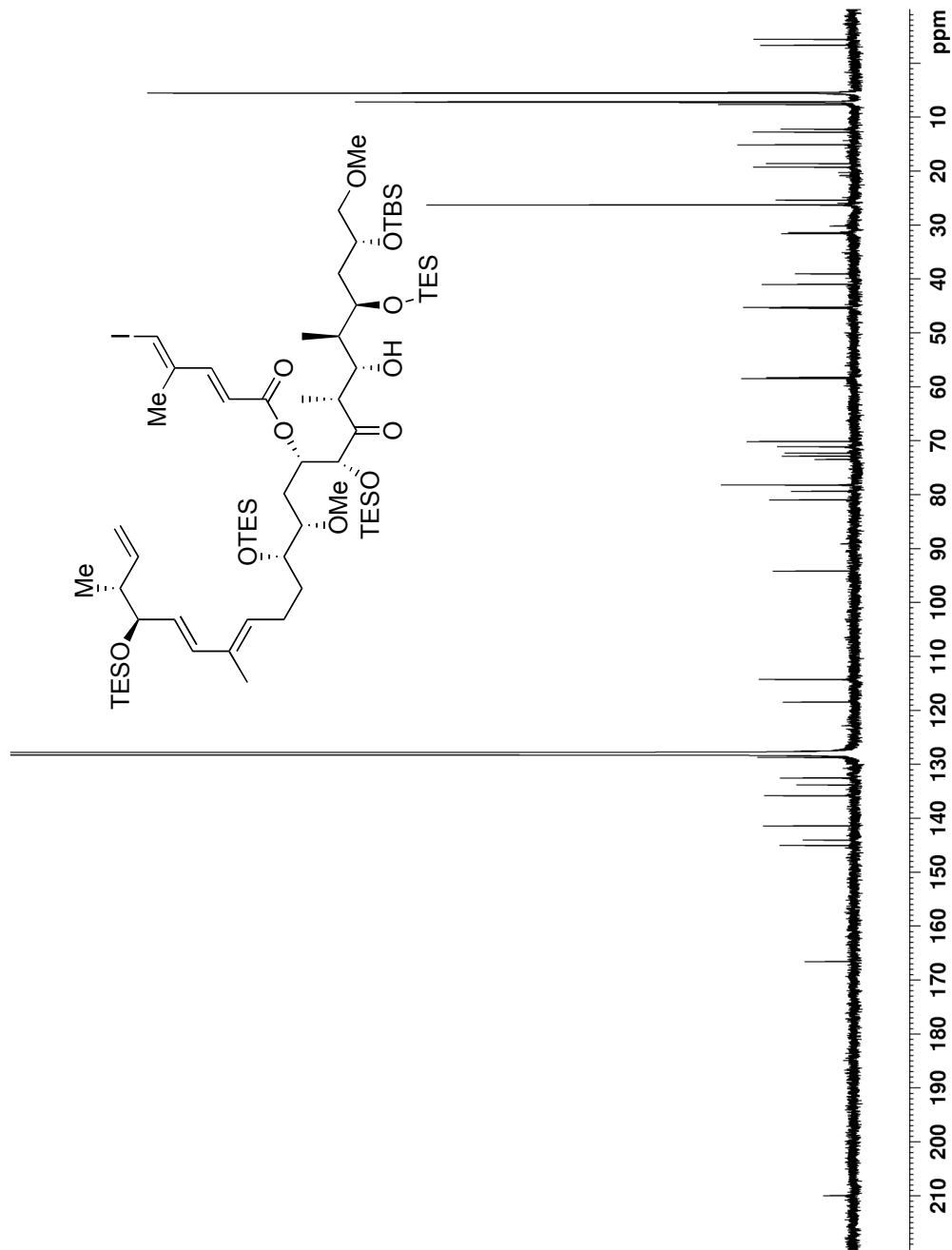


Figure A6b The 150 MHz ¹³C NMR spectrum of alcohol **4.44** in C₆D₆

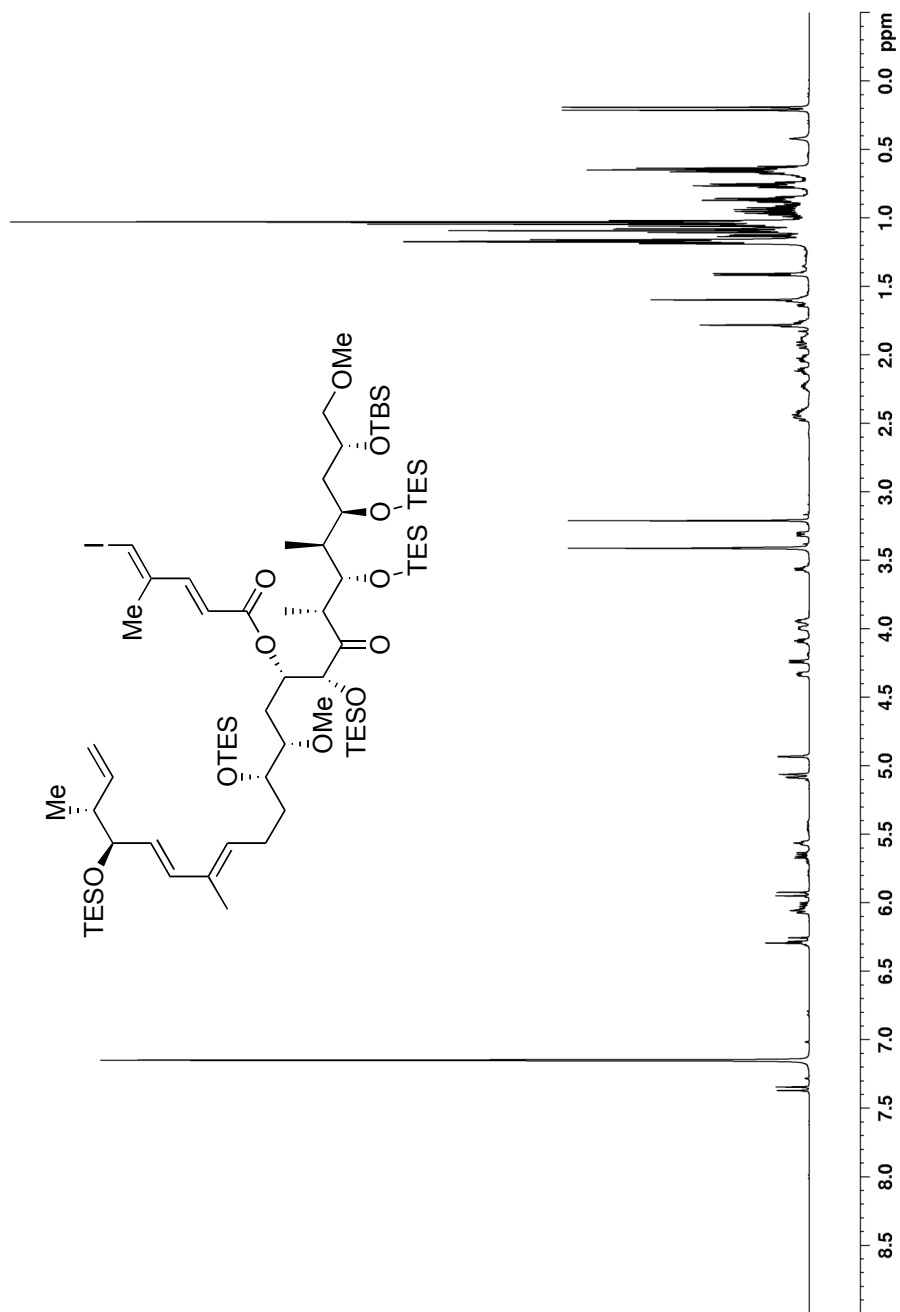


Figure A7a The 600 MHz ^1H NMR spectrum of TES ether **4.45** in C_6D_6

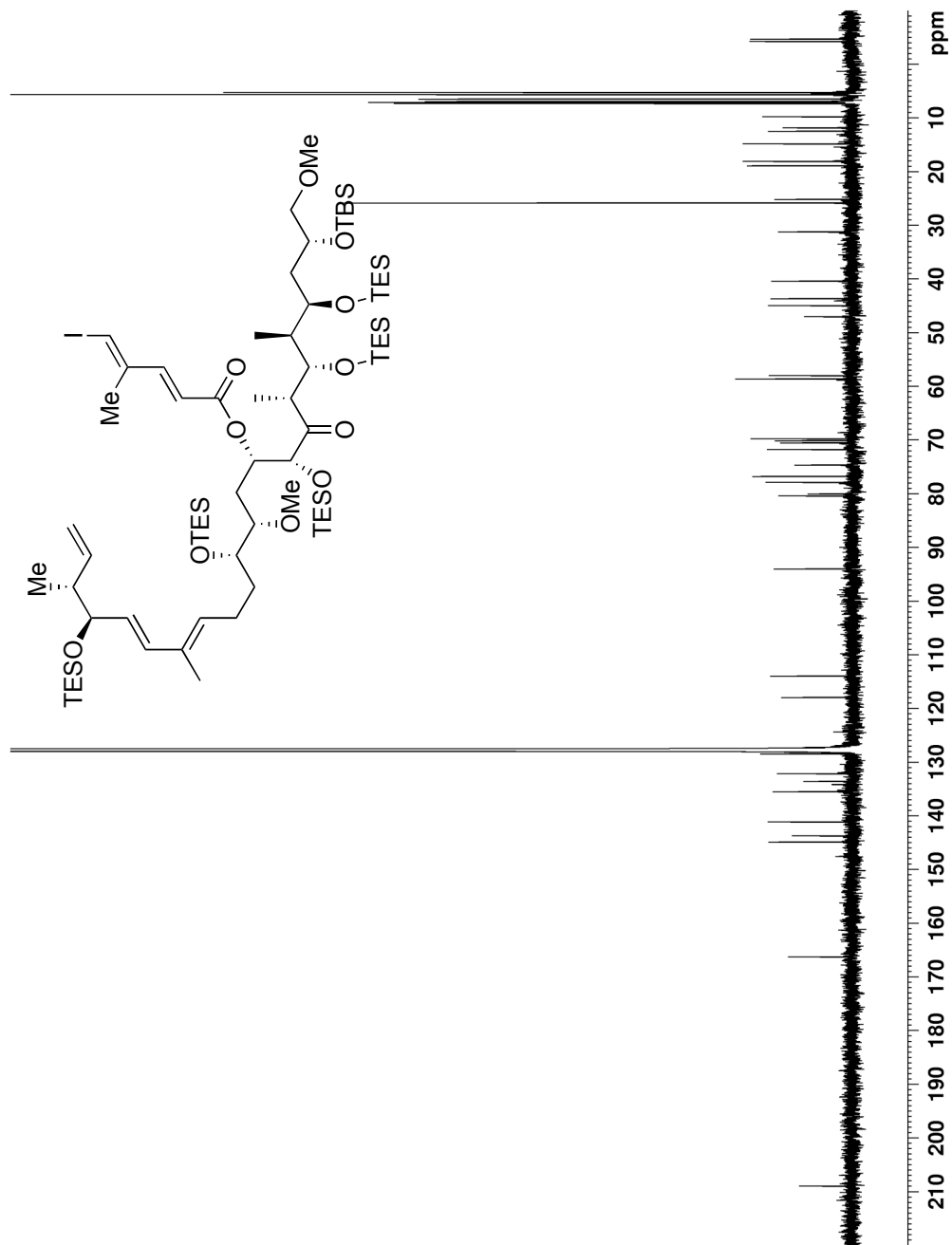


Figure A7b The 150 MHz ¹³C NMR spectrum of TES ether **4.45** in C₆D₆

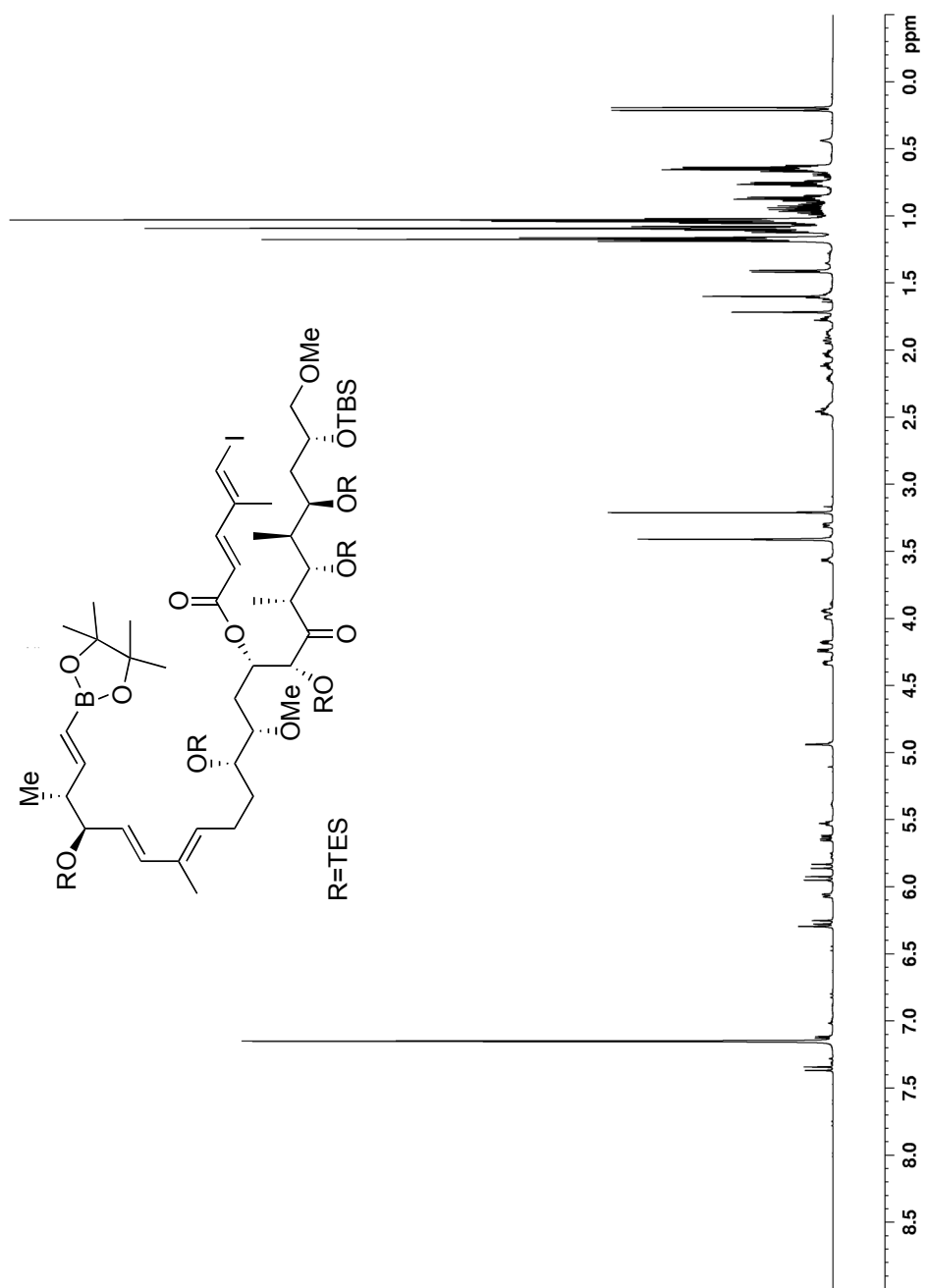


Figure A8a The 600 MHz ^1H NMR spectrum of vinyl borate **4.46** in C_6D_6

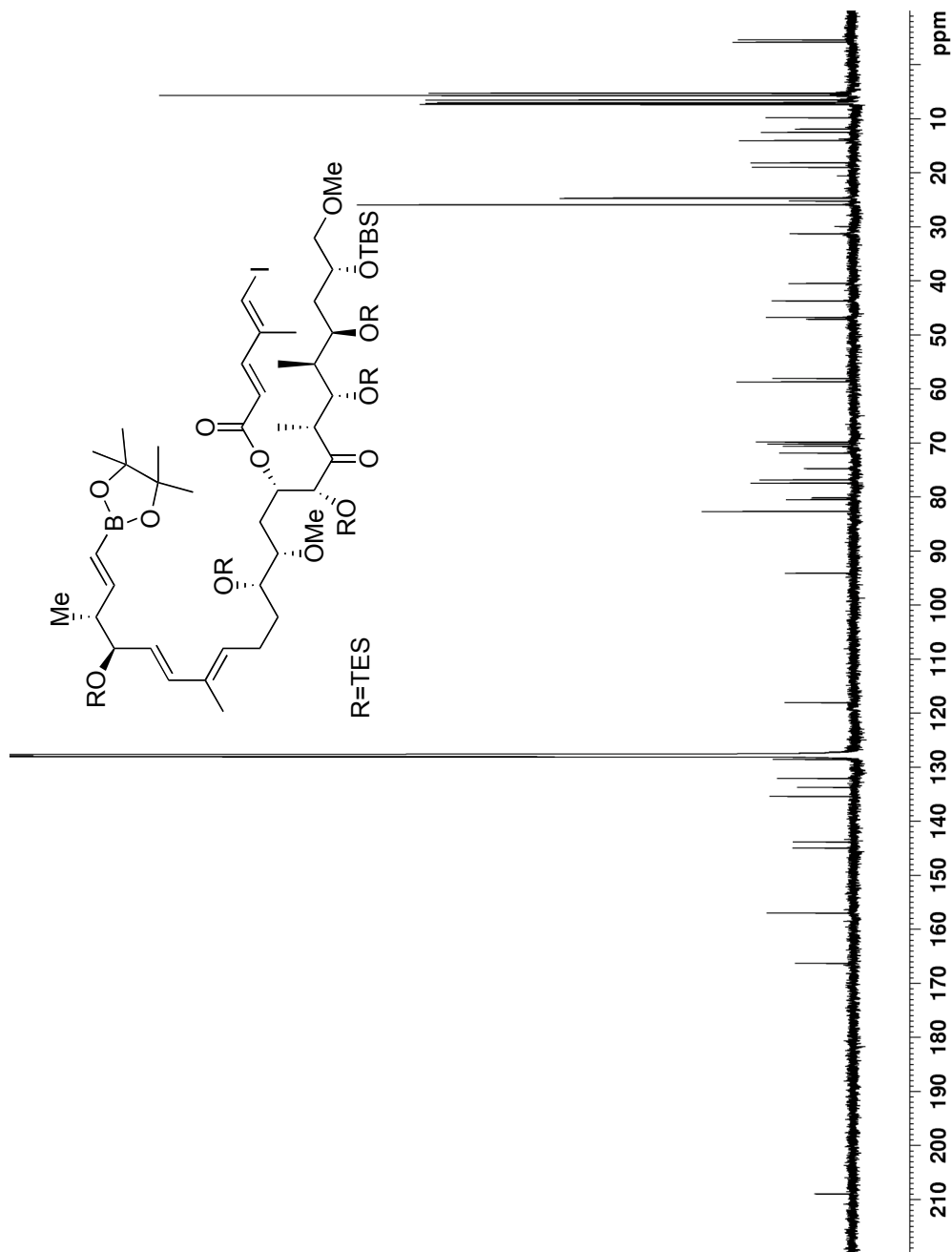


Figure A8b The 150 MHz ¹³C NMR spectrum of vinyl borate **4.46** in C₆D₆

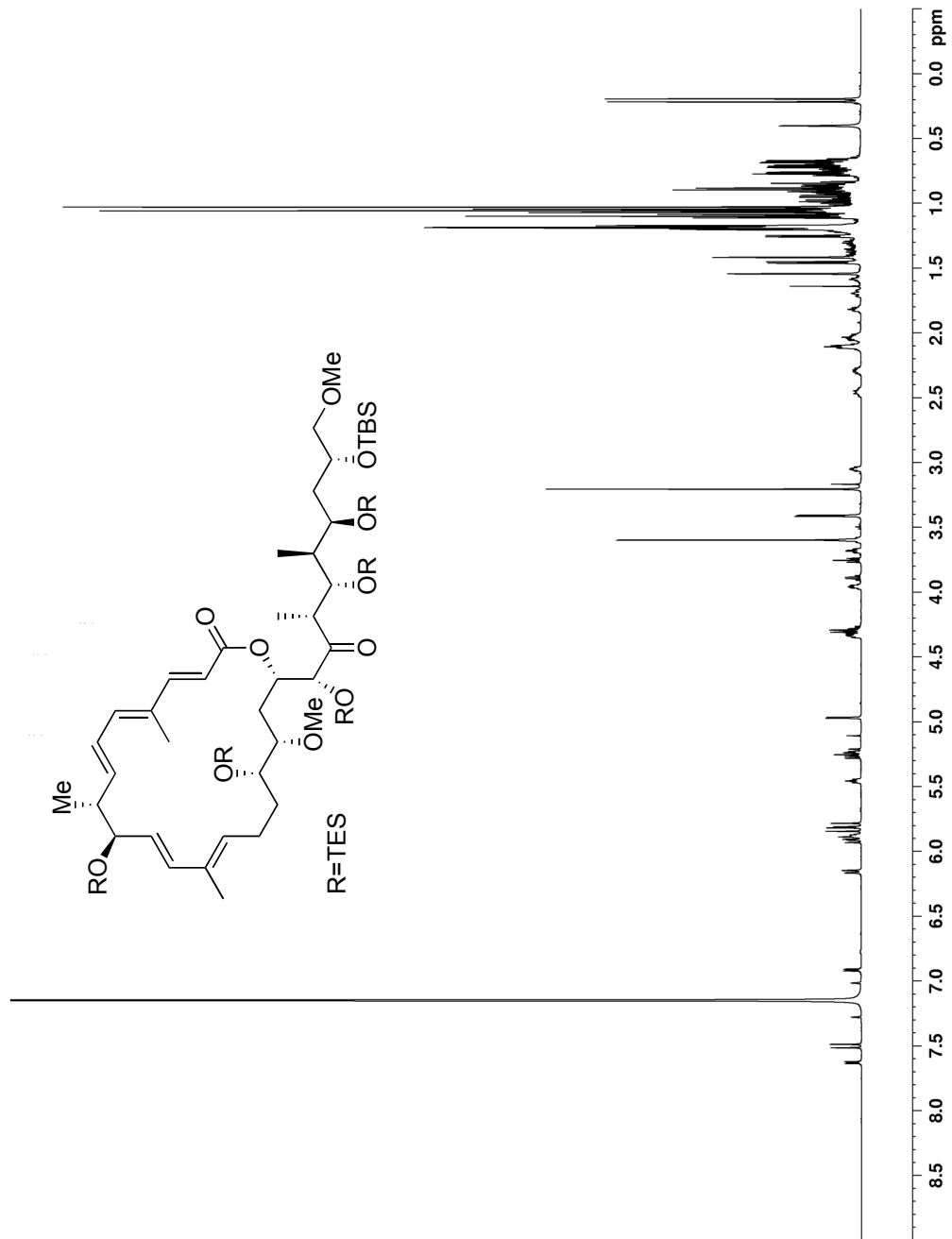


Figure A9a The 600 MHz ^1H NMR spectrum of macrolactone **4.36** in C_6D_6

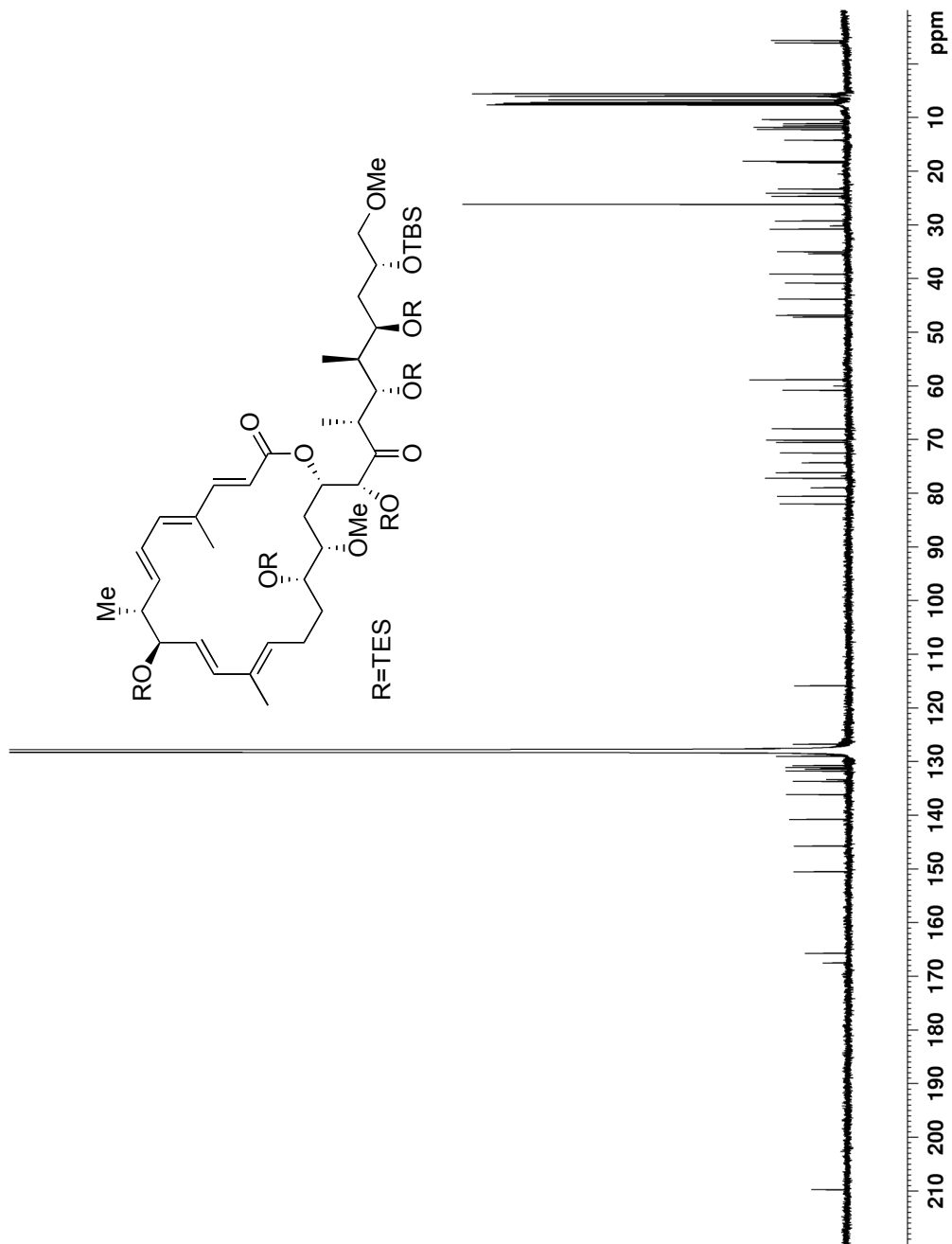


Figure A9b The 150 MHz ^{13}C NMR spectrum of macrolactone **4.36** in C_6D_6

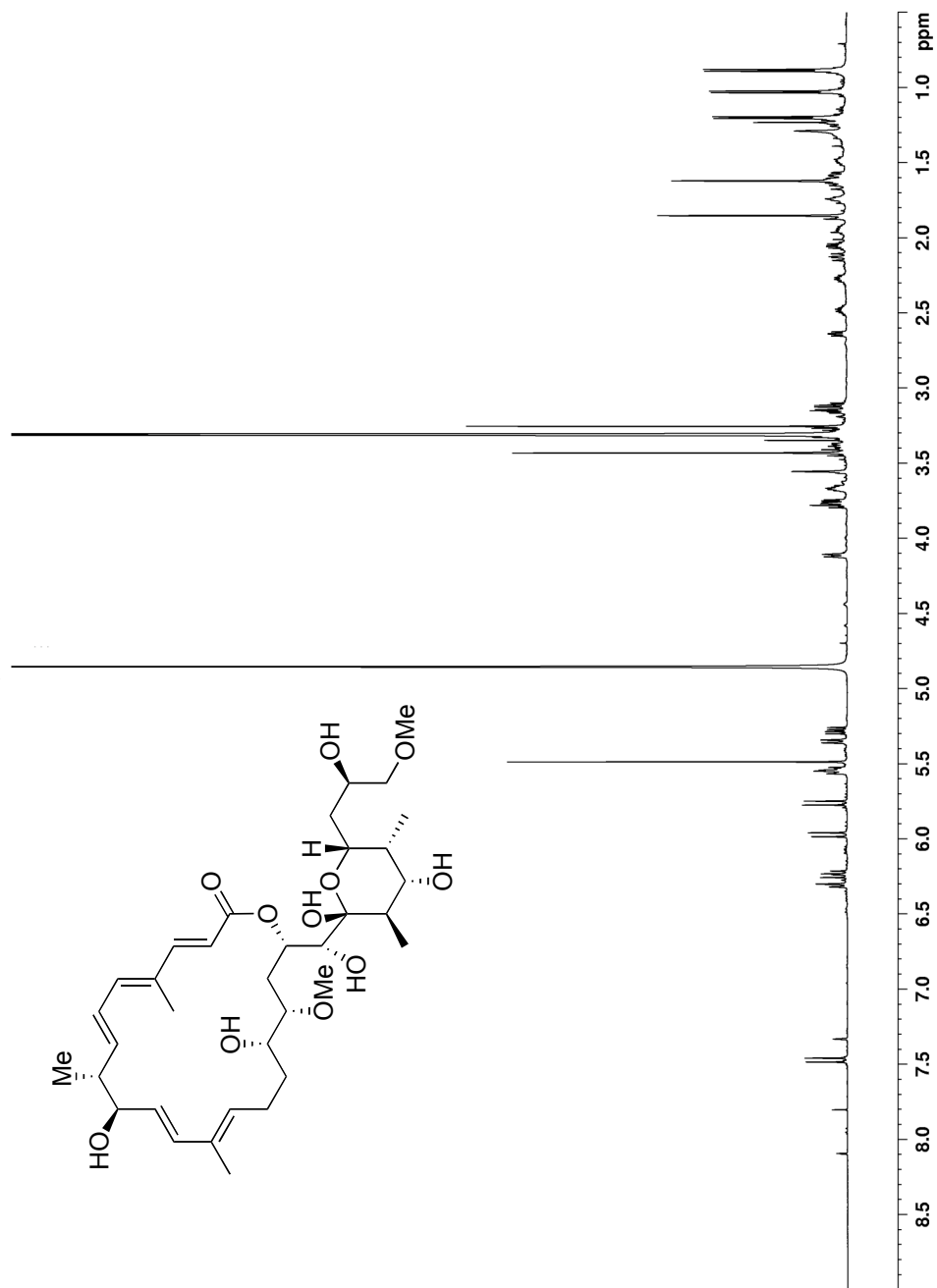


Figure A10a The 600 MHz ^1H NMR spectrum of 2,6 normethyl apoptolidinone A **4.3** in CD_3OD

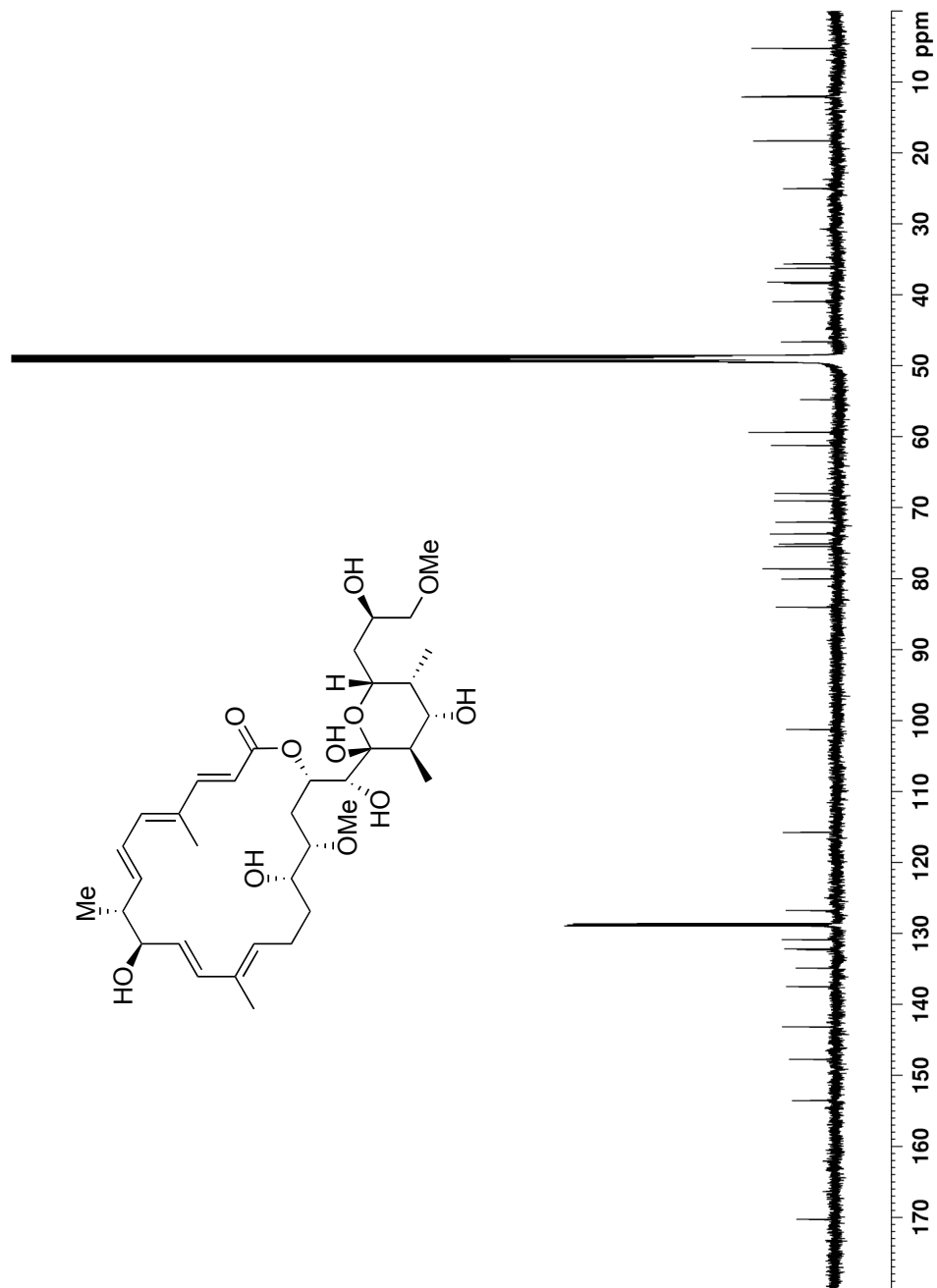


Figure A10b The 150 MHz ^{13}C NMR spectrum of 2,6 normethyl apoptolidinone A **4.3** in CD_3OD

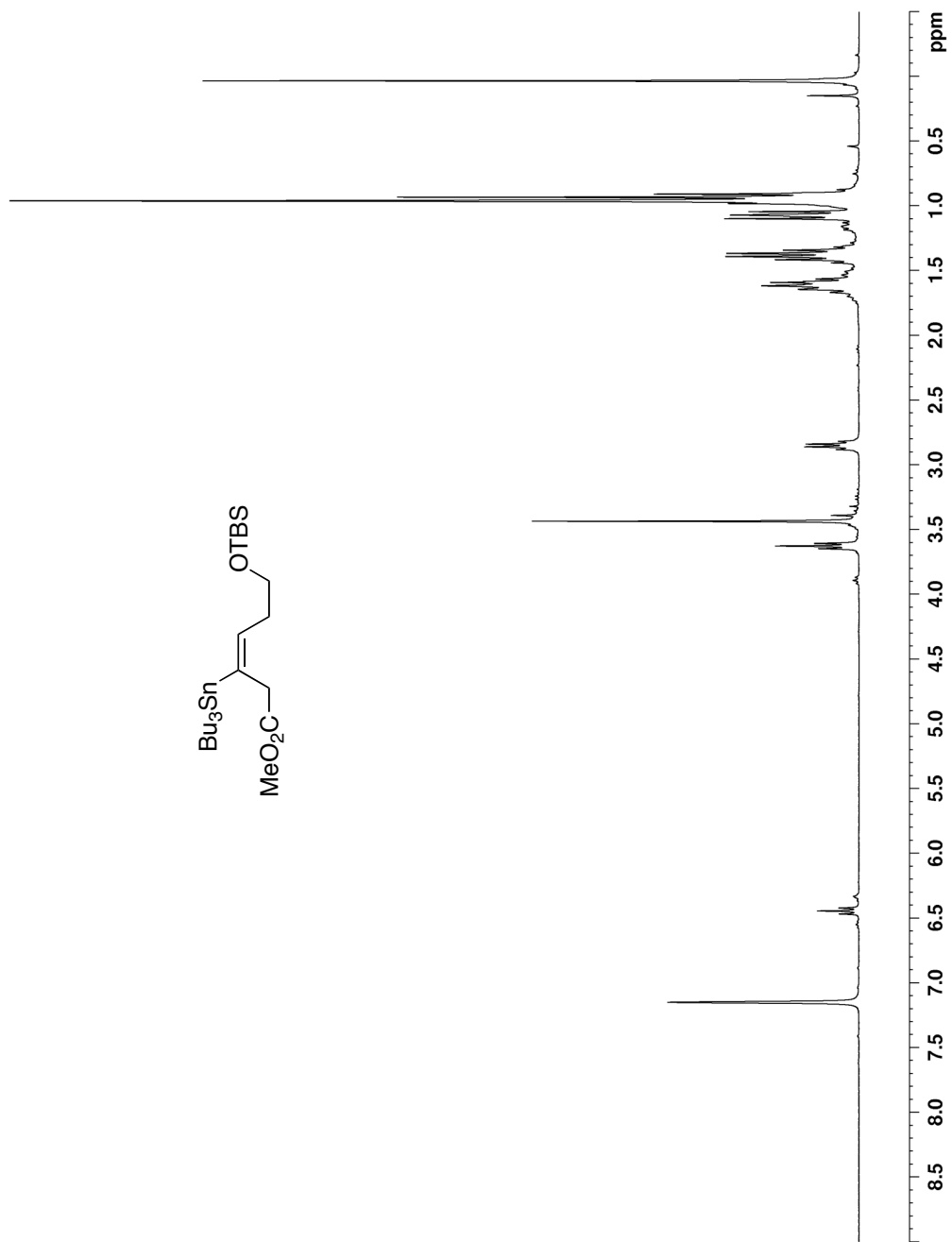


Figure A11a The 300 MHz ^1H NMR spectrum of vinyl tin **4.53** in C_6D_6

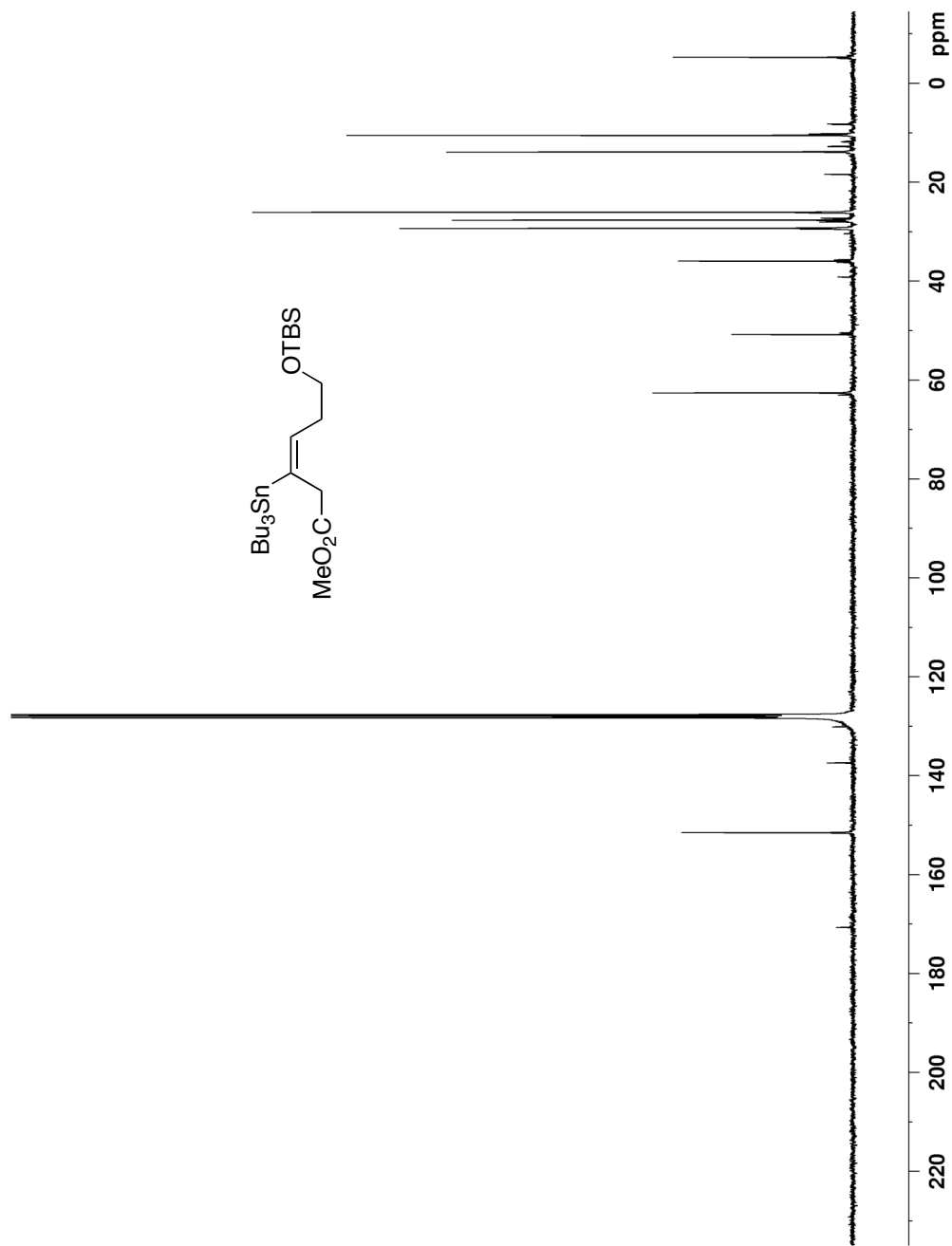


Figure A11b The 75 MHz ^{13}C NMR spectrum of vinyl tin **4.53** in C_6D_6

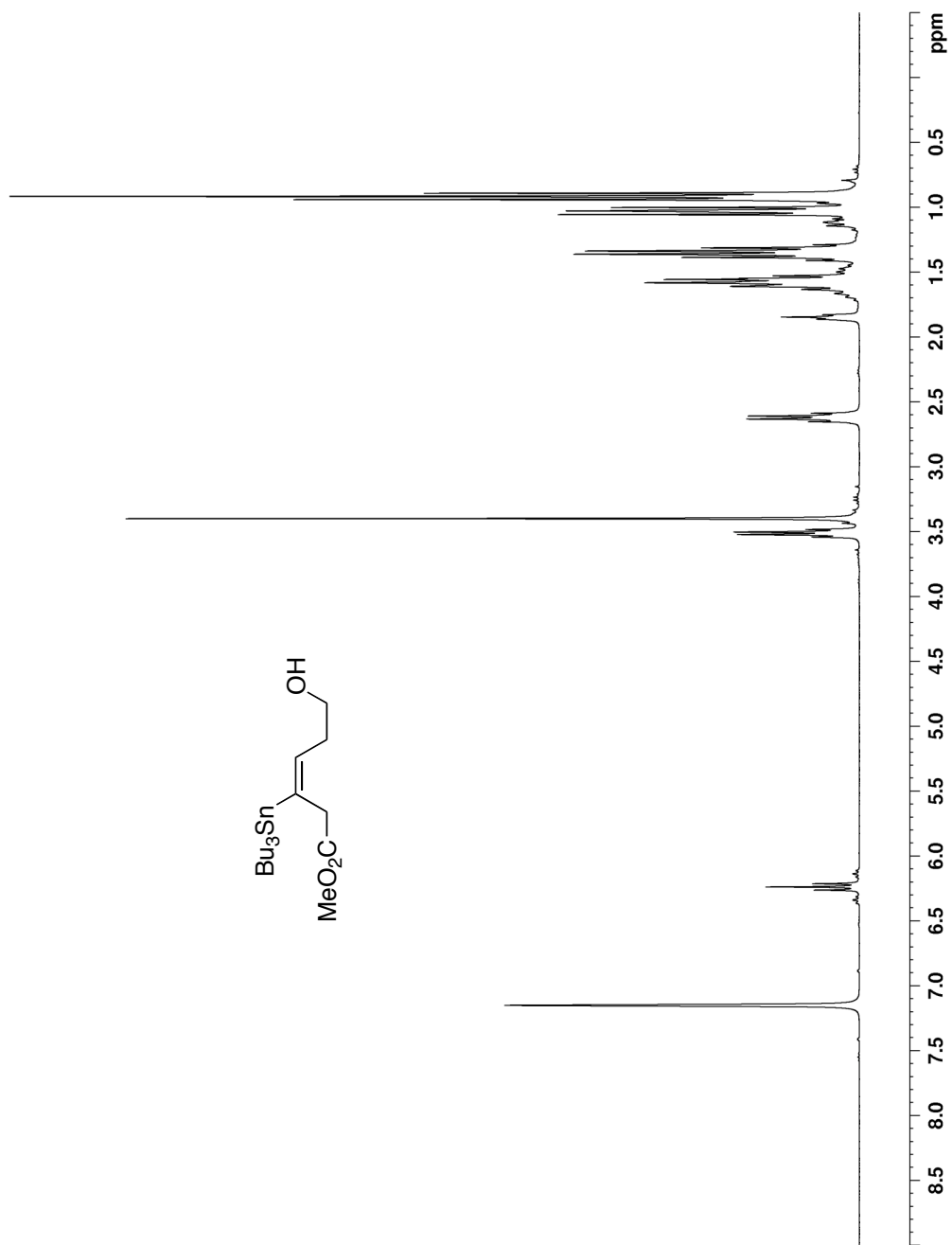


Figure A12a The 300 MHz ^1H NMR spectrum of alcohol **4.54** in C_6D_6

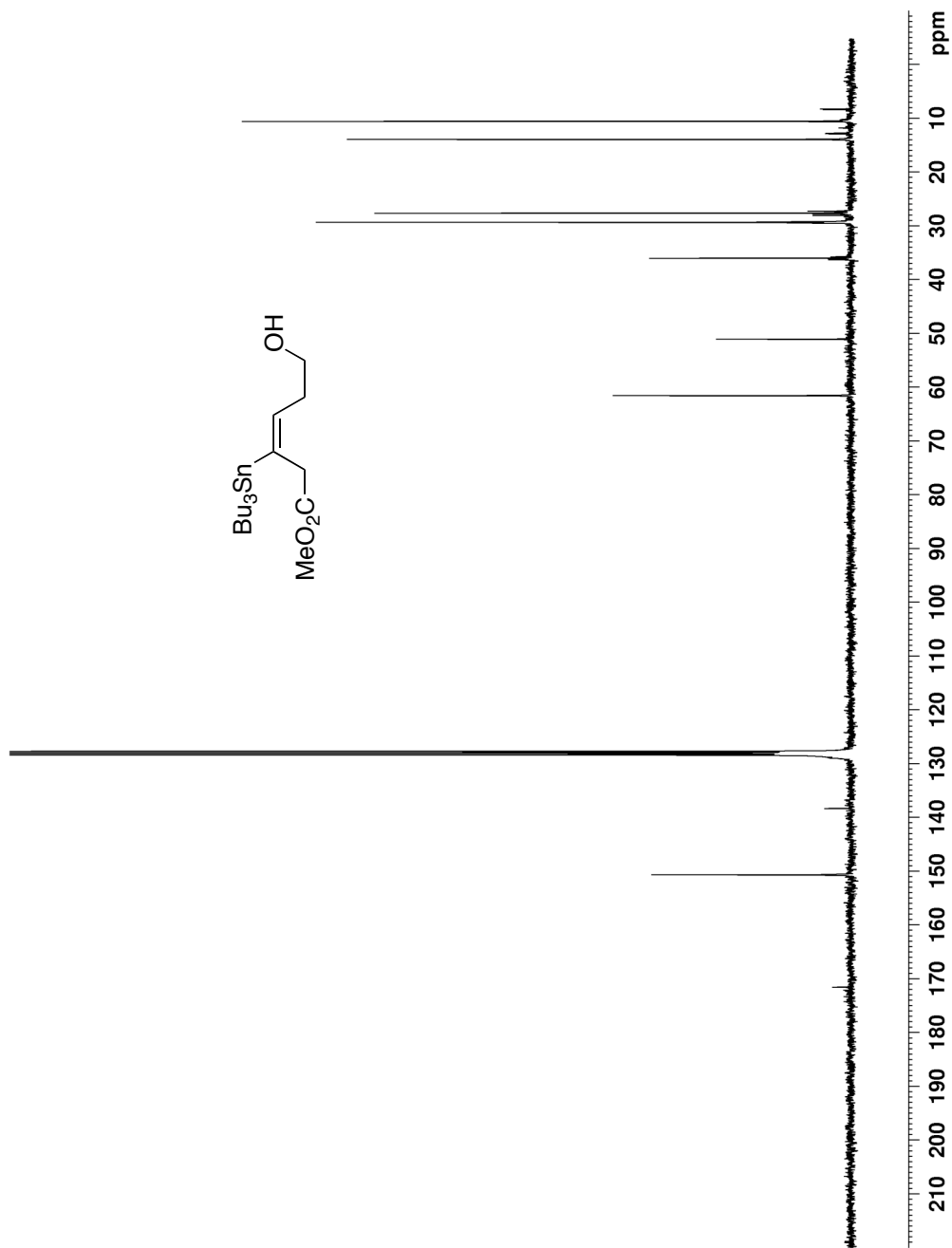


Figure A12b The 75 MHz ^{13}C NMR spectrum of alcohol **4.54** in C_6D_6

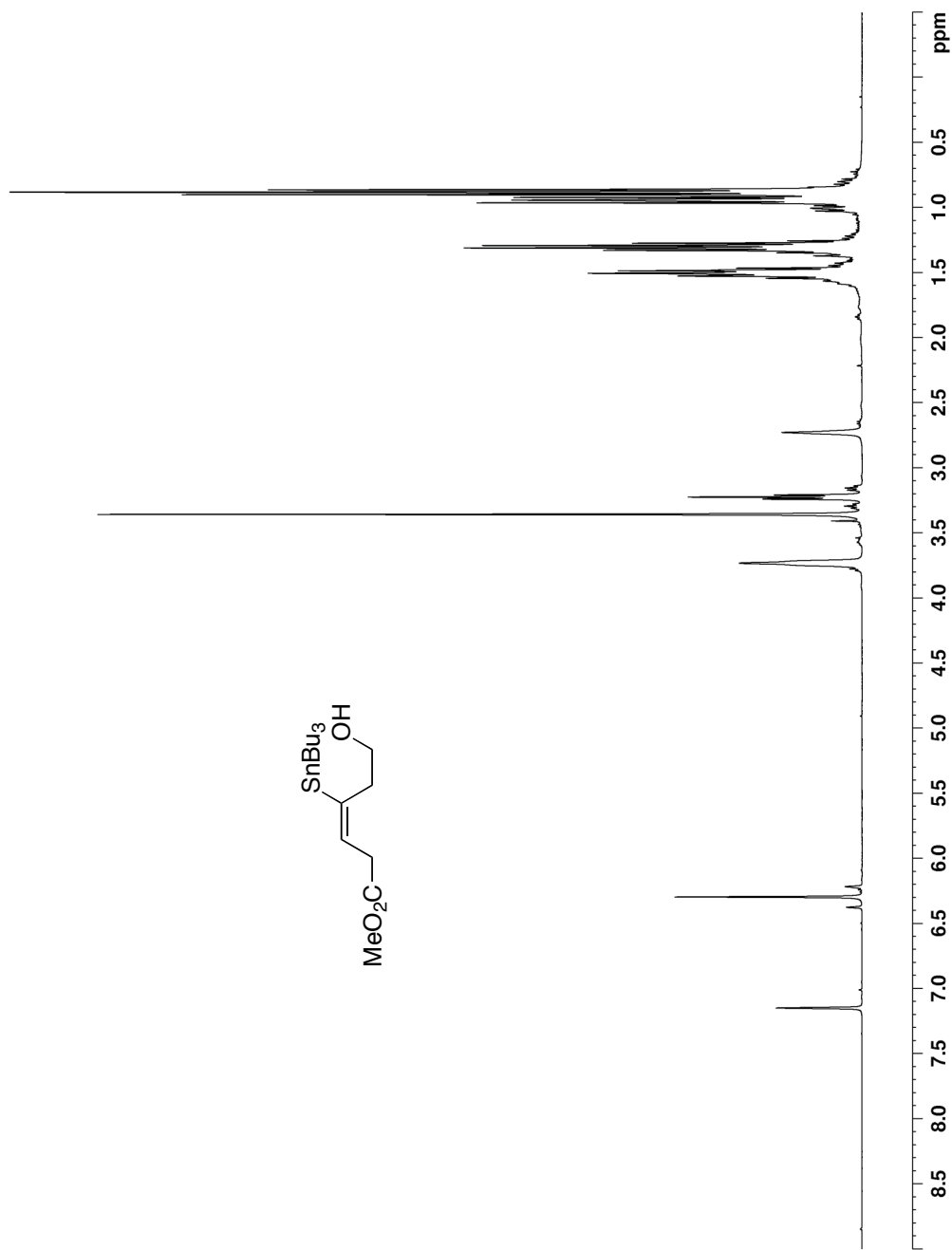


Figure A13a The 400 MHz ^1H NMR spectrum of alcohol **4.54b** in C_6D_6

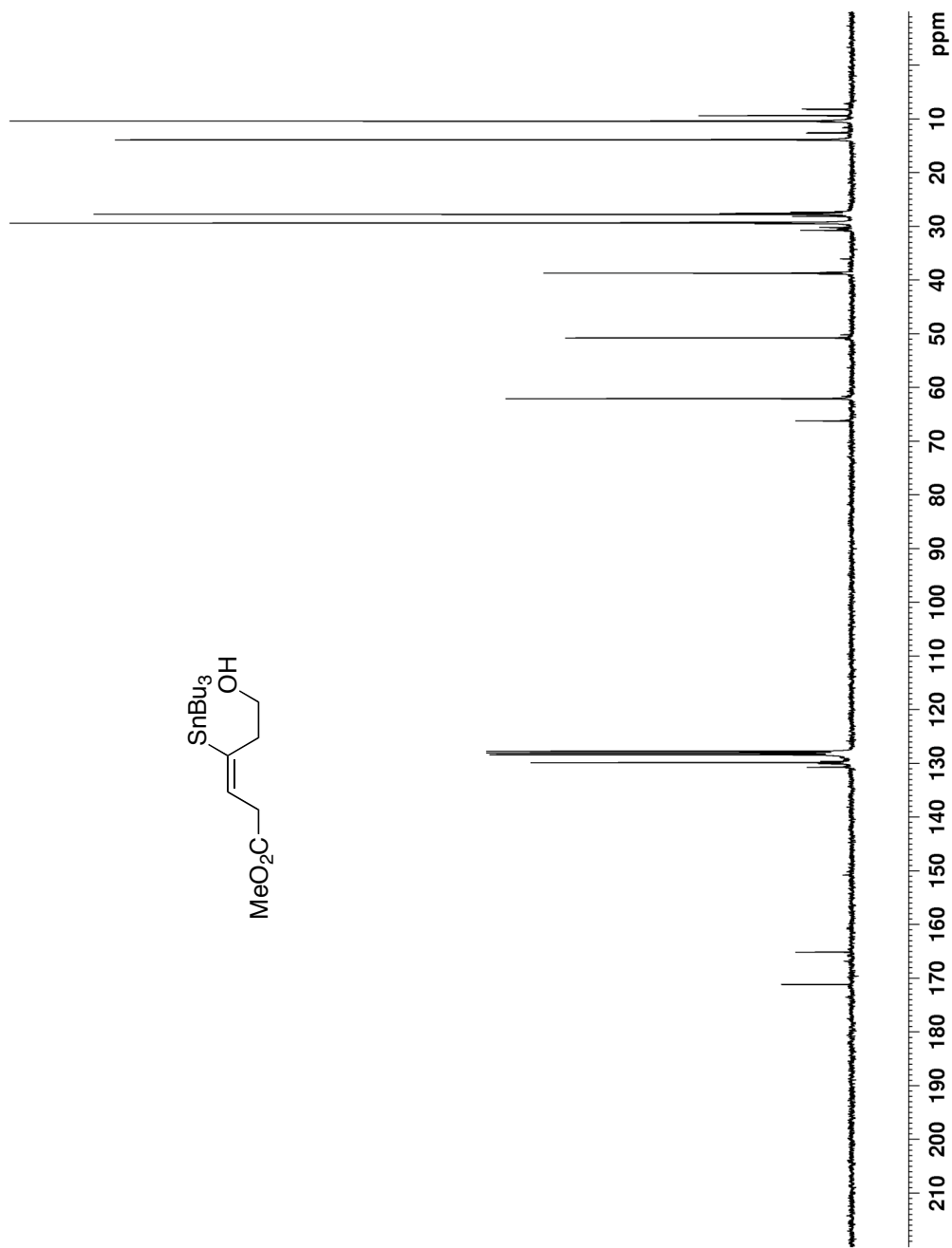


Figure A13b The 75 MHz ^{13}C NMR spectrum of alcohol **4.54b** in C_6D_6

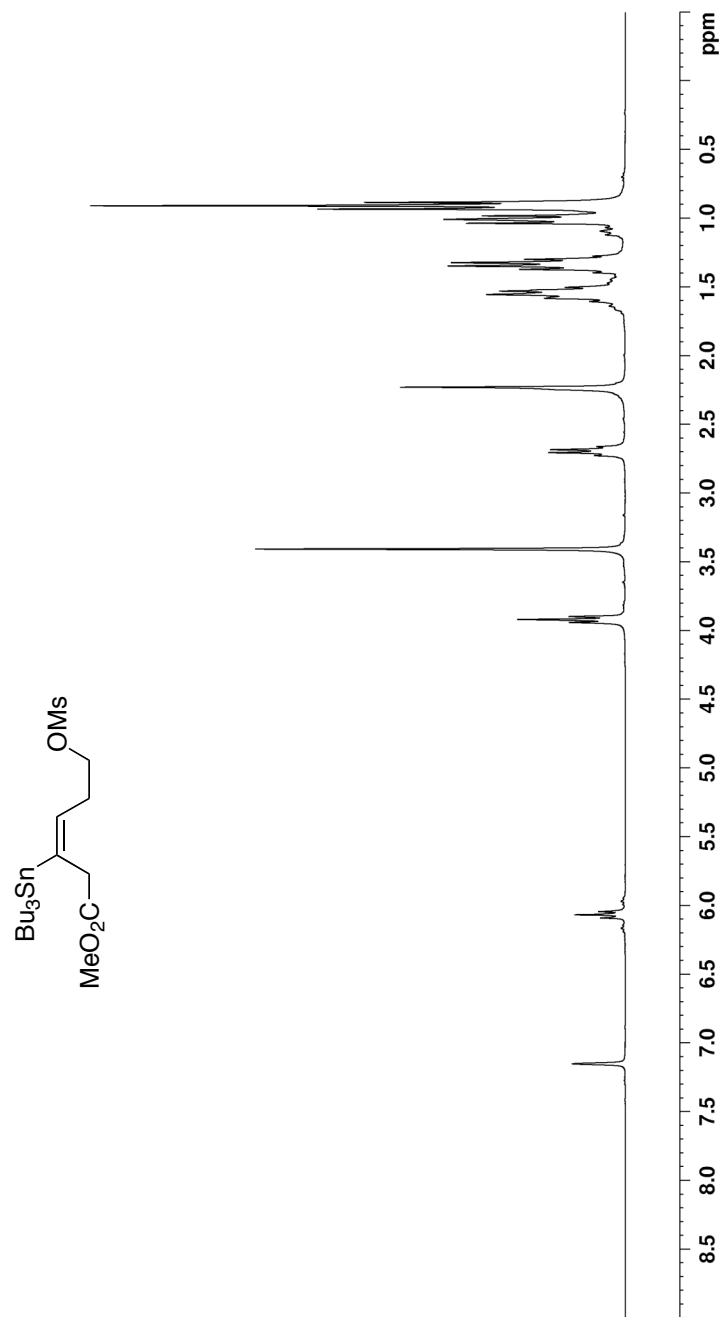


Figure A14a The 400 MHz ¹H NMR spectrum of mesylate **4.55** in C₆D₆

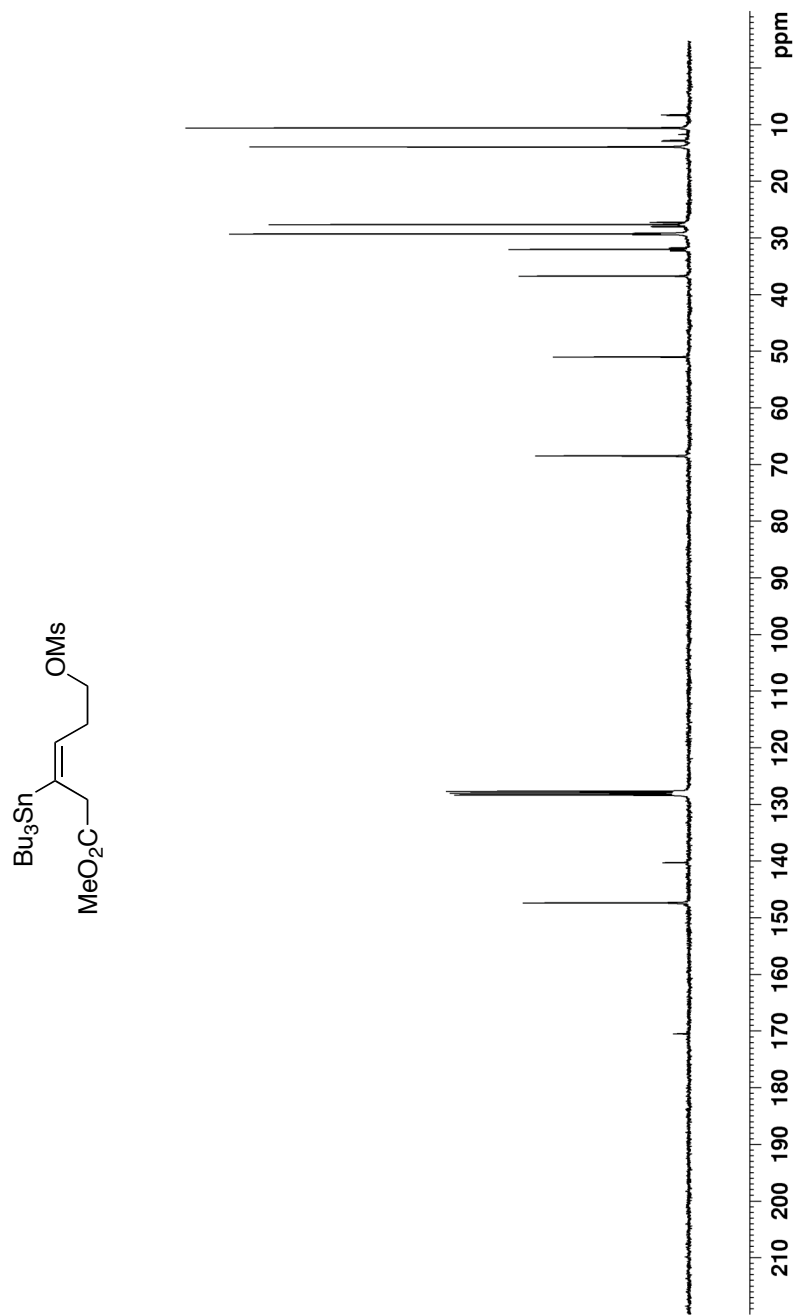


Figure A14b The 75 MHz ^{13}C NMR Spectrum of mesylate **4.55** in C_6D_6

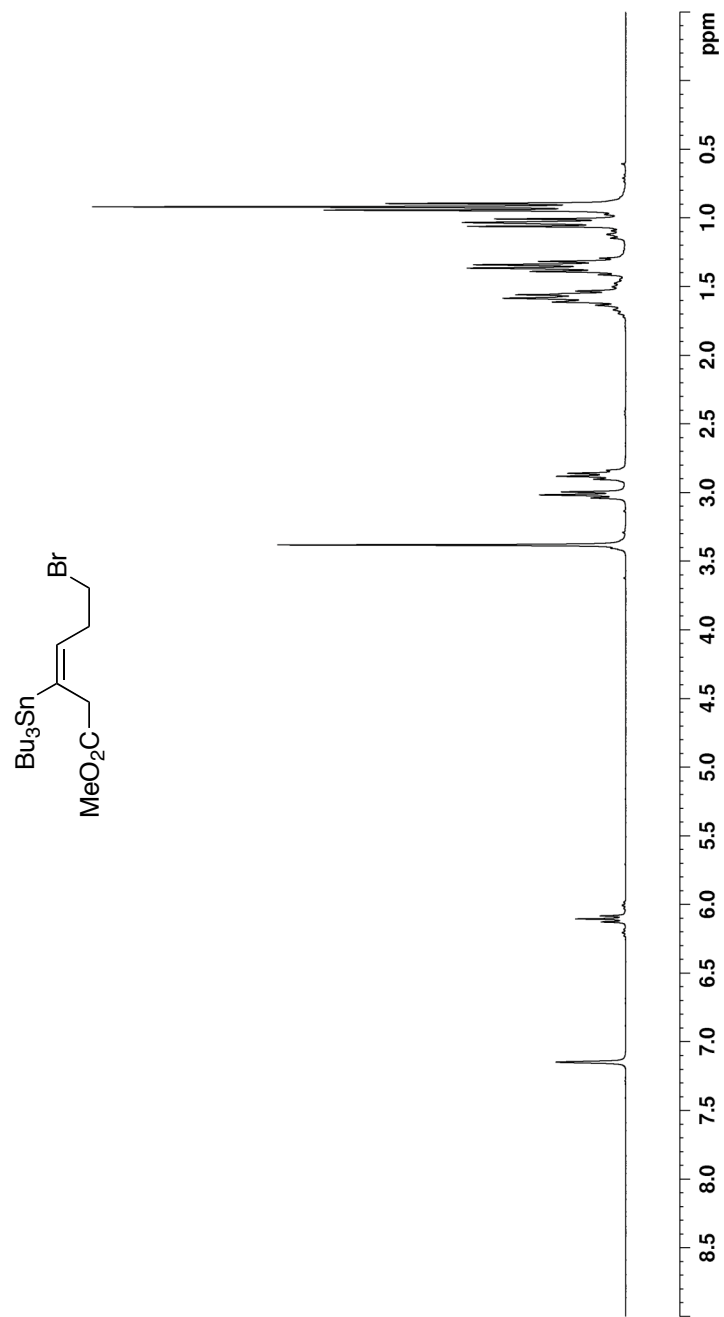


Figure A15a The 300 MHz ^1H NMR spectrum of bromide **4.56** in C_6D_6

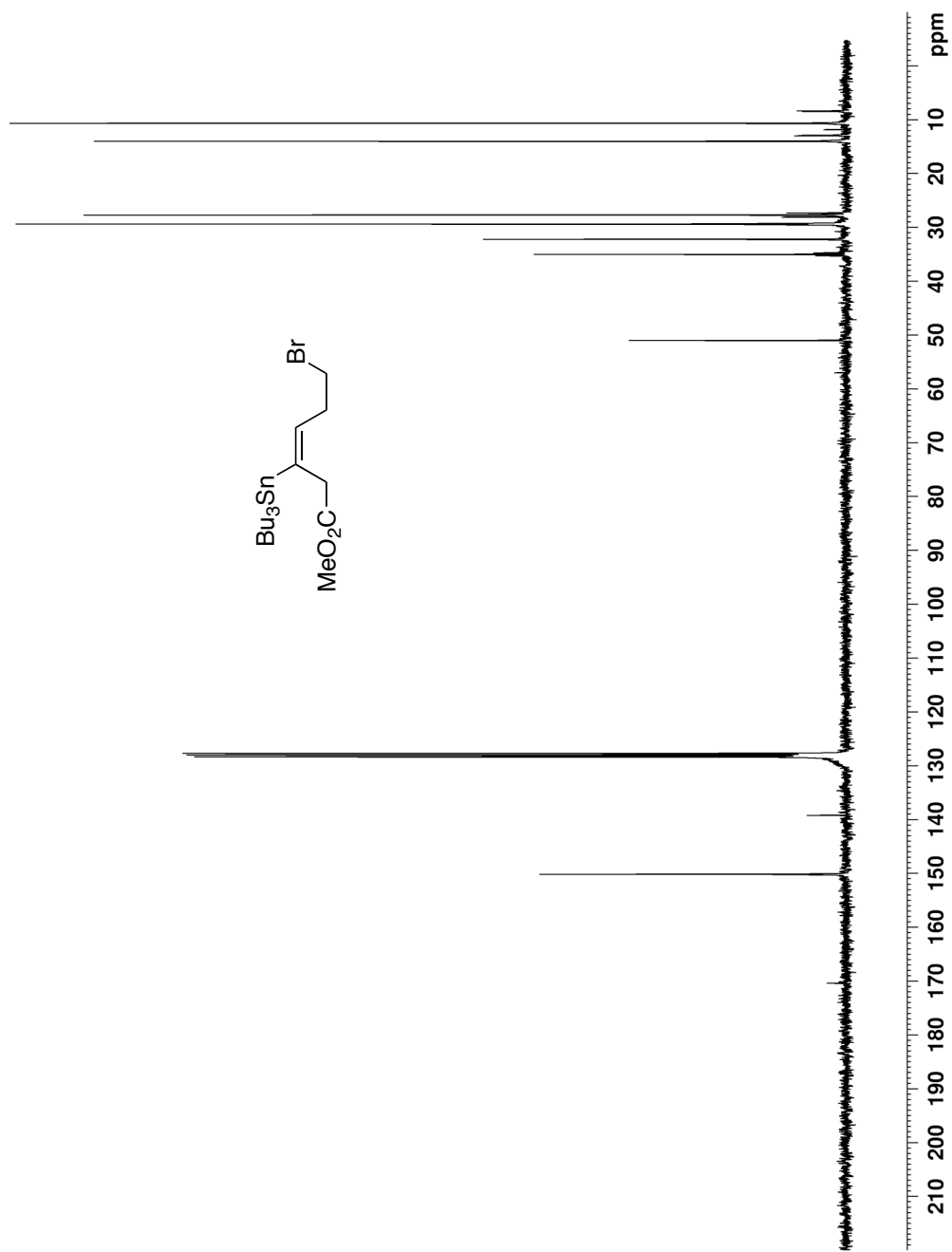


Figure A15b The 75 MHz ^{13}C NMR spectrum of bromide **4.56** in C_6D_6

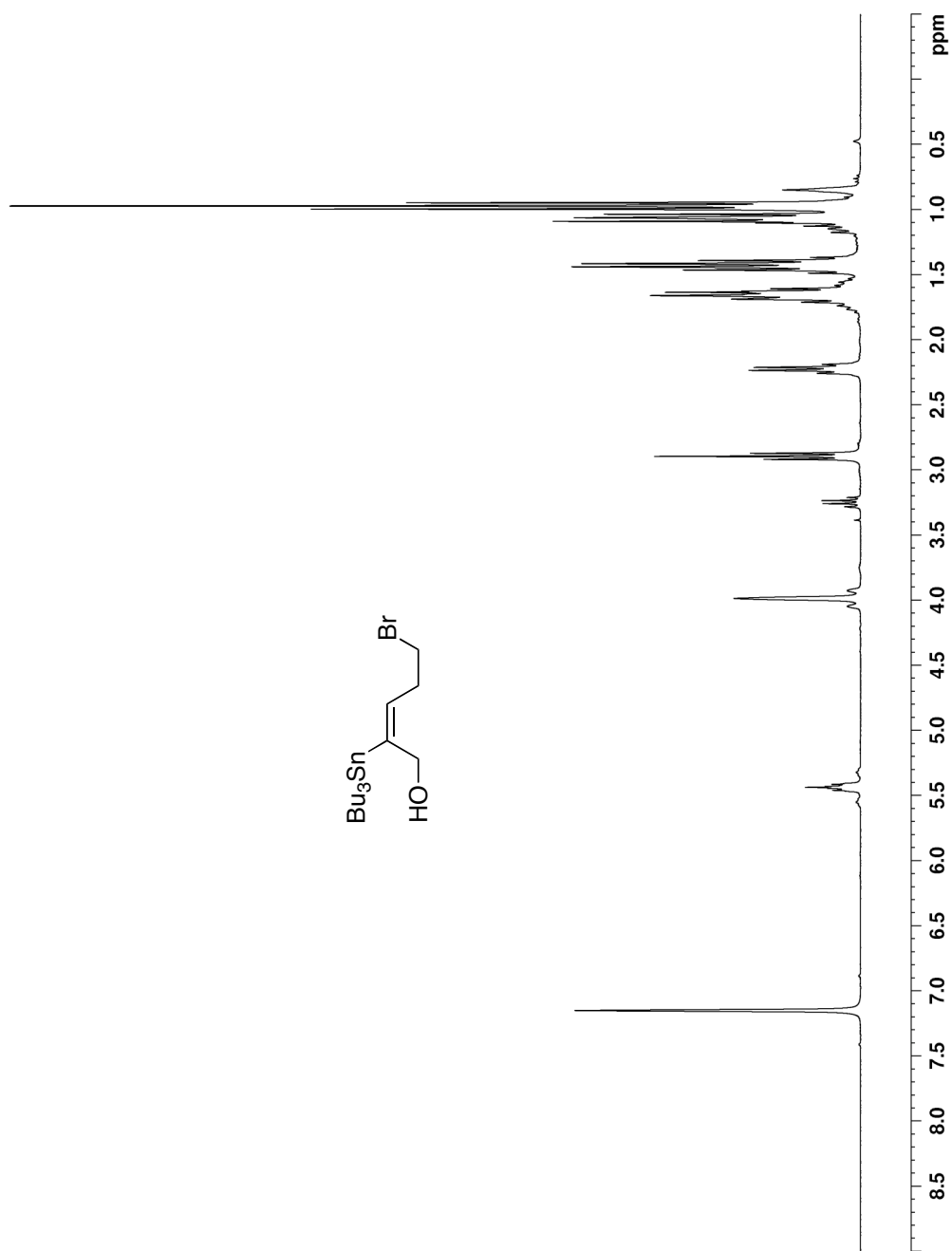


Figure A16a The 300 MHz ^1H NMR spectrum of alcohol **4.57** in C_6D_6

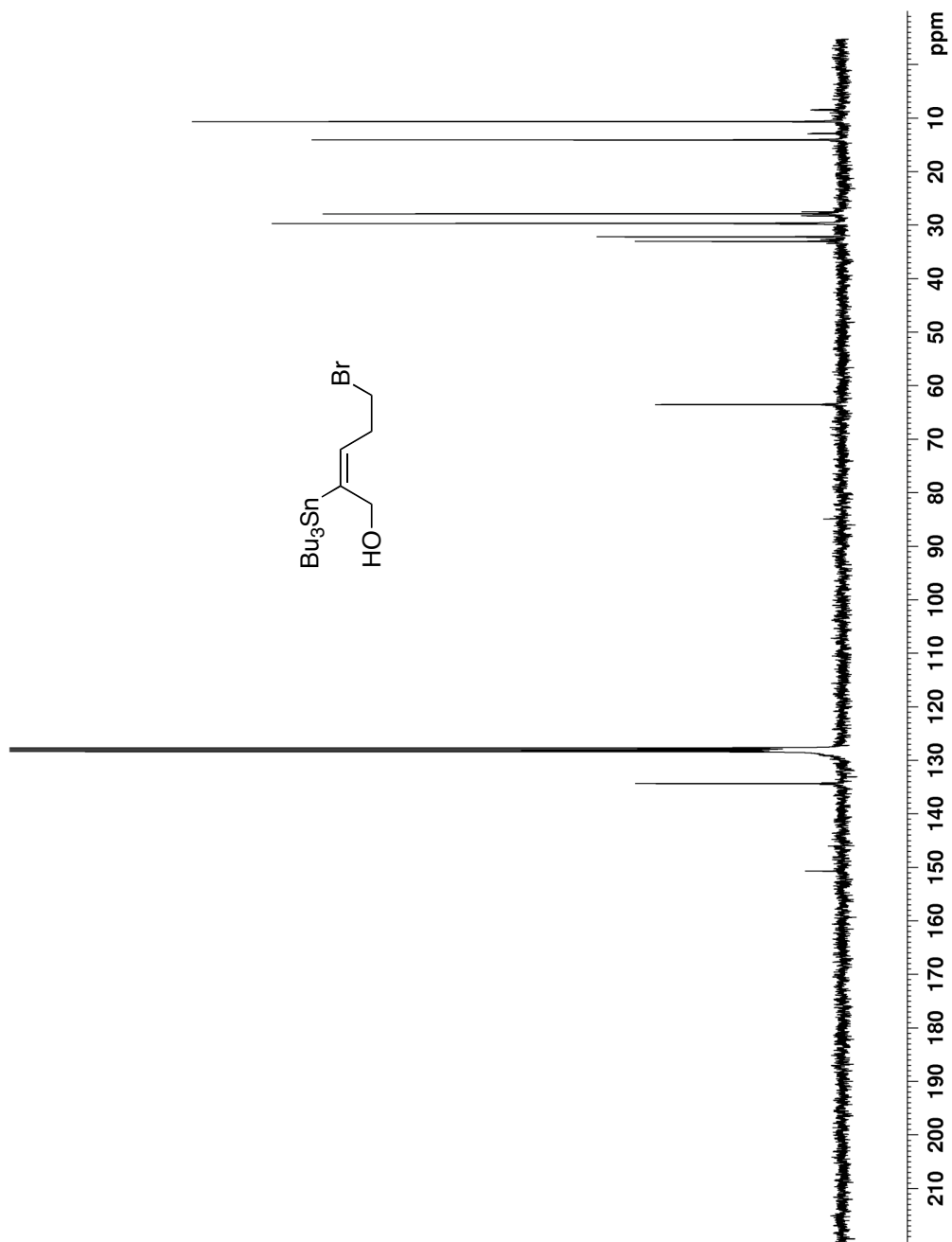


Figure A16b The 75 MHz ^{13}C NMR spectrum of alcohol **4.57** in C_6D_6

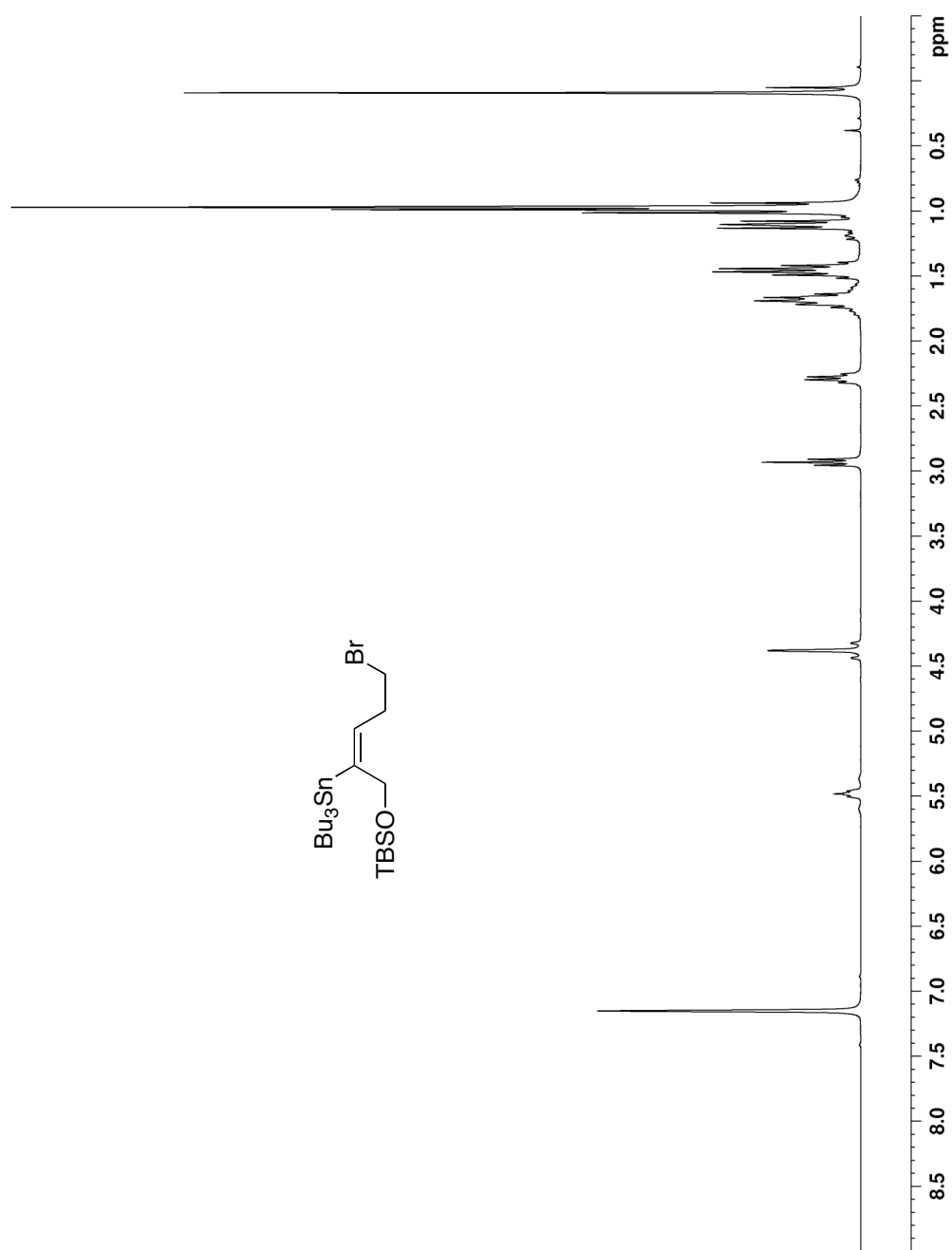


Figure A17a The 300 MHz ^1H NMR spectrum of bromide **4.48** in C_6D_6

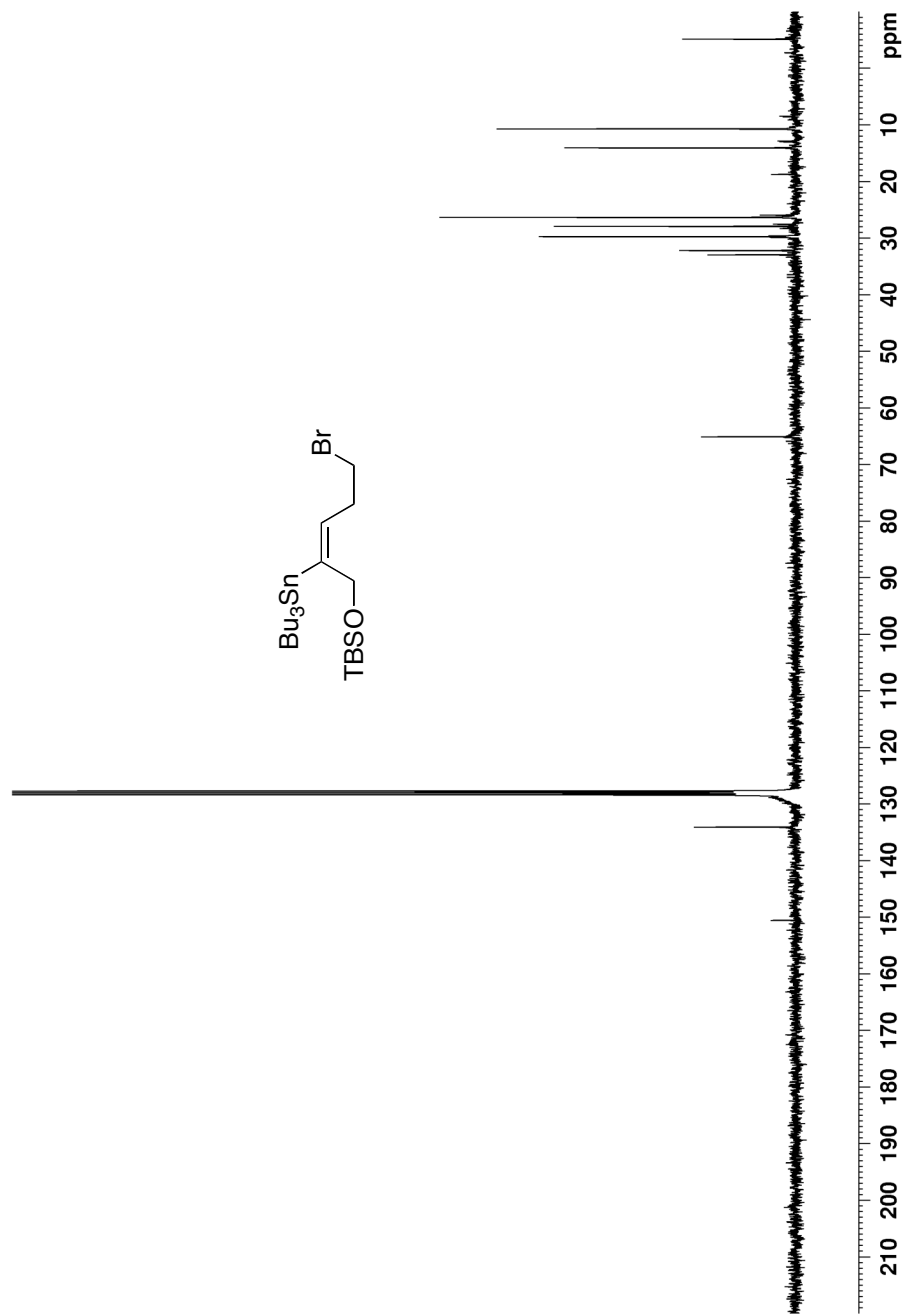


Figure A17b The 75 MHz ^{13}C NMR spectrum of bromide **4.48** in C_6D_6

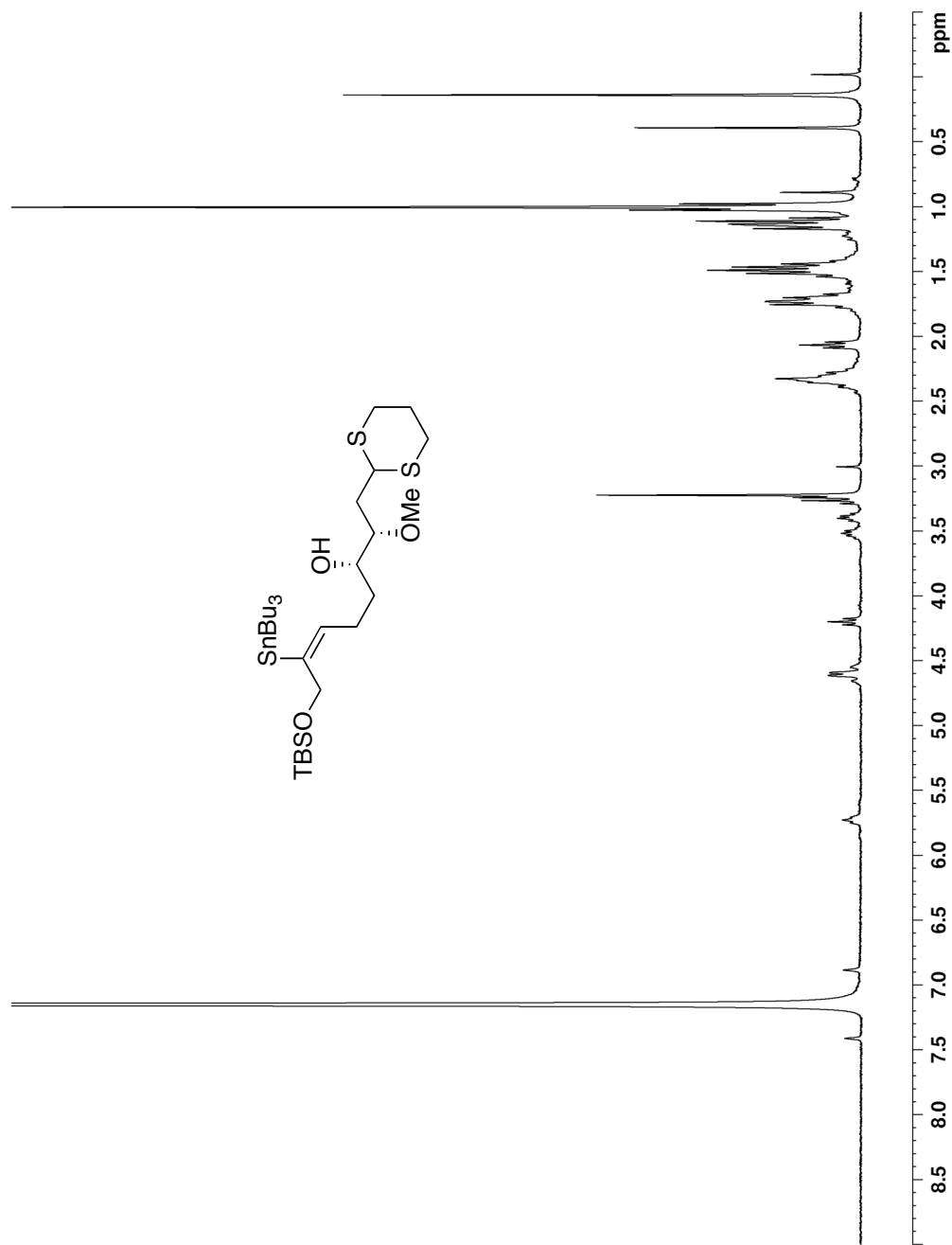


Figure A18a The 300 MHz ^1H NMR spectrum of alcohol **4.58** in C_6D_6

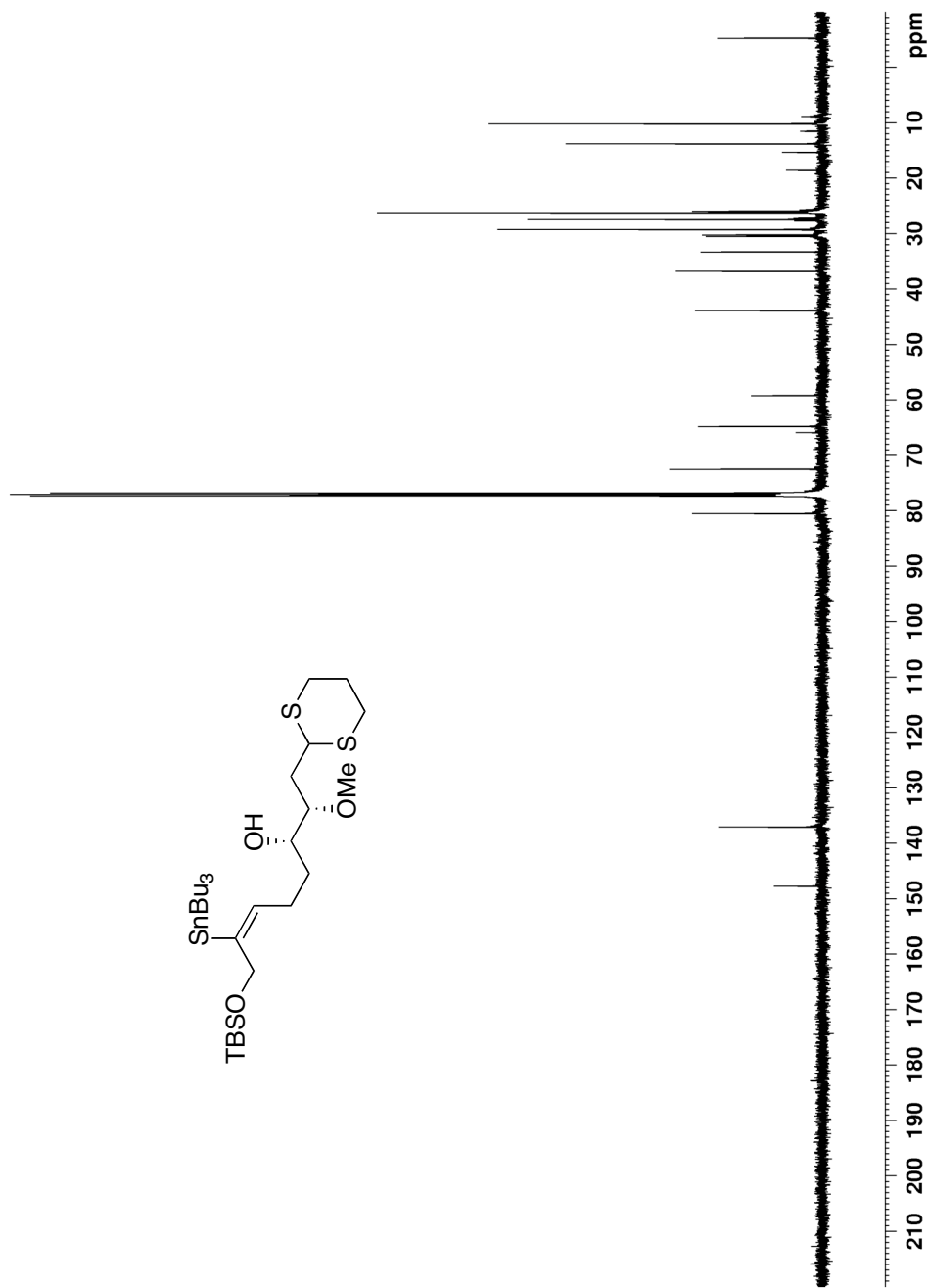


Figure A18b The 125 MHz ^{13}C NMR spectrum of alcohol **4.58** in CDCl_3

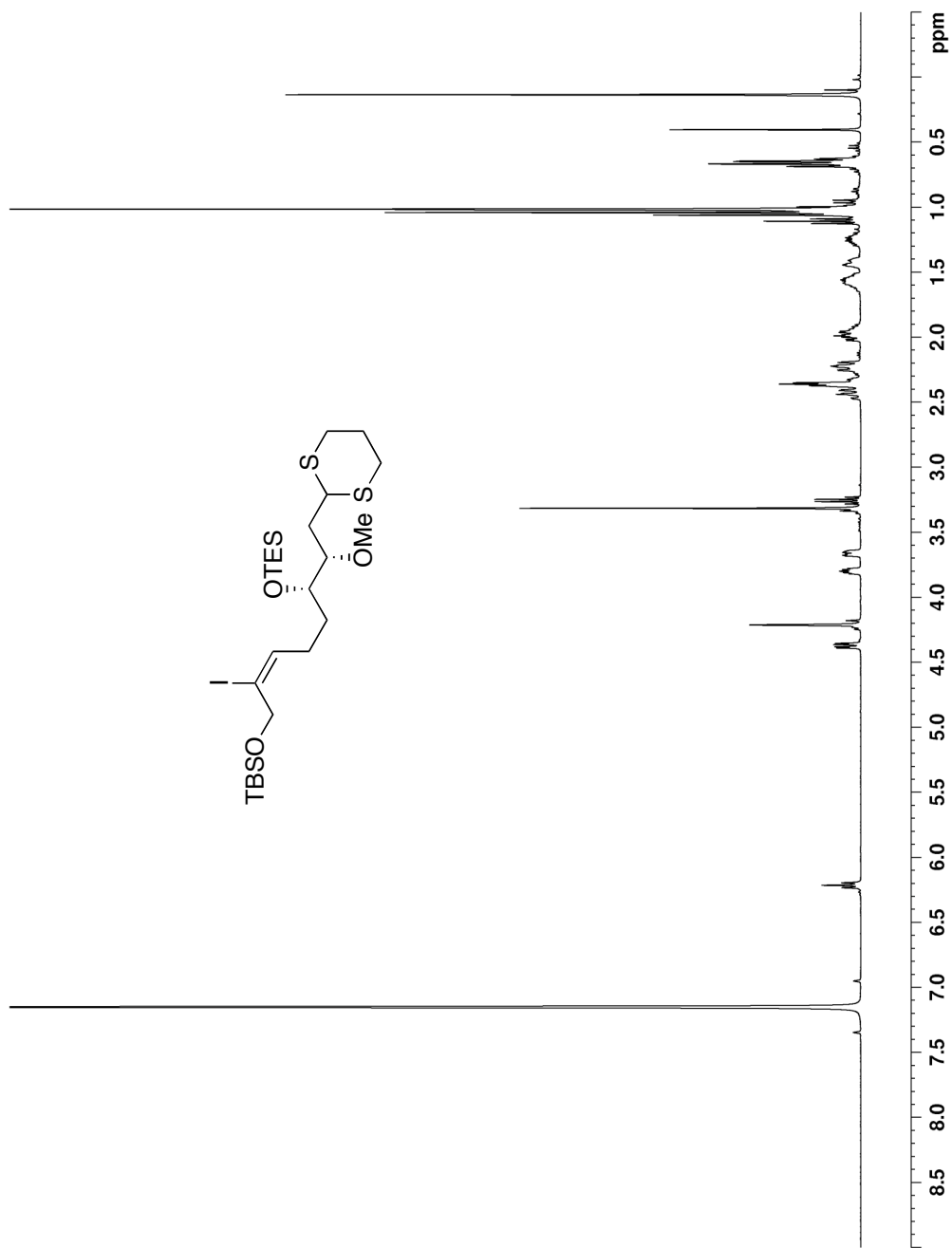


Figure A19a The 400 MHz ^1H NMR spectrum of vinyl iodide **4.59** in C_6D_6

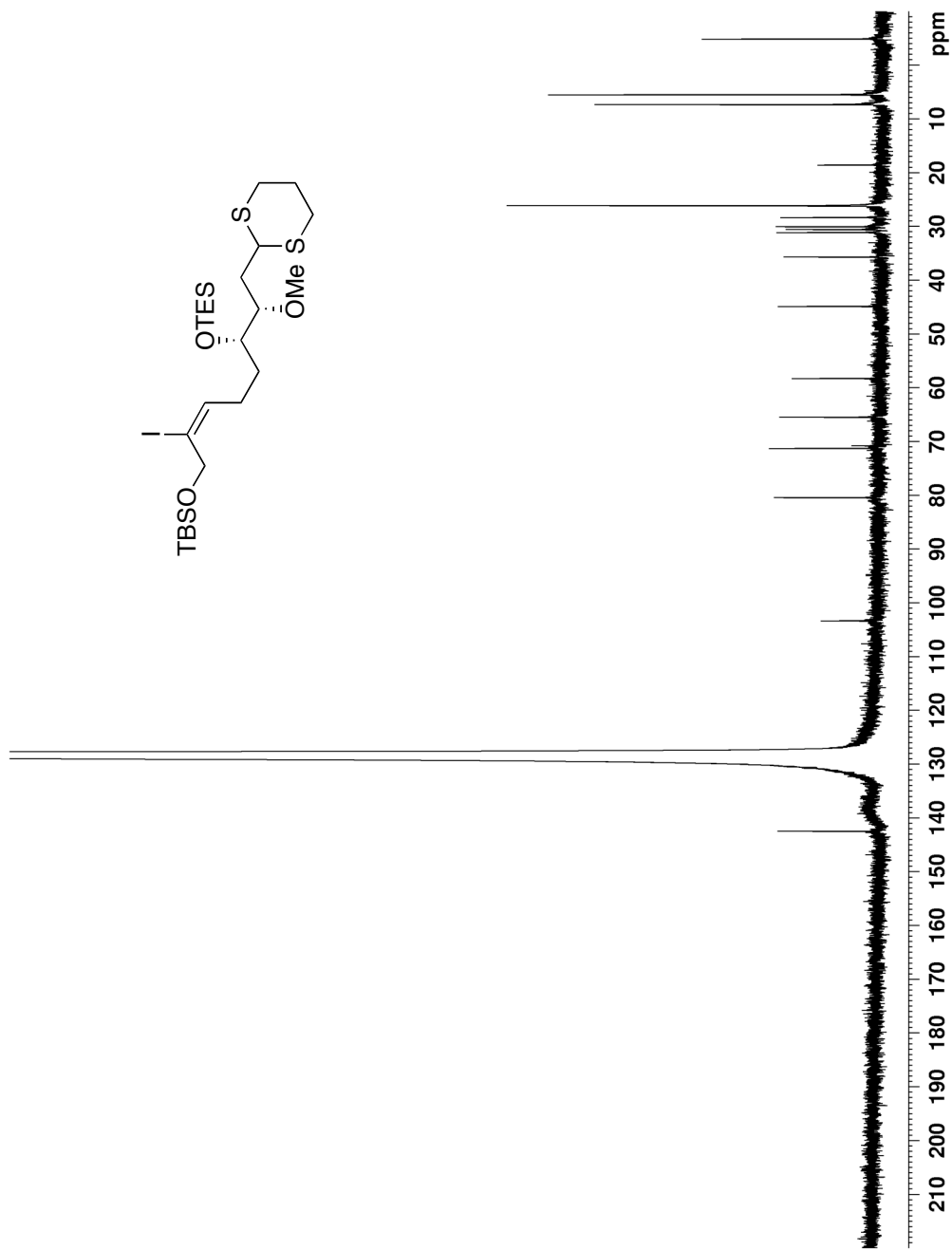


Figure A19b The 125 MHz ^{13}C NMR spectrum of vinyl iodide **4.59** in C_6D_6

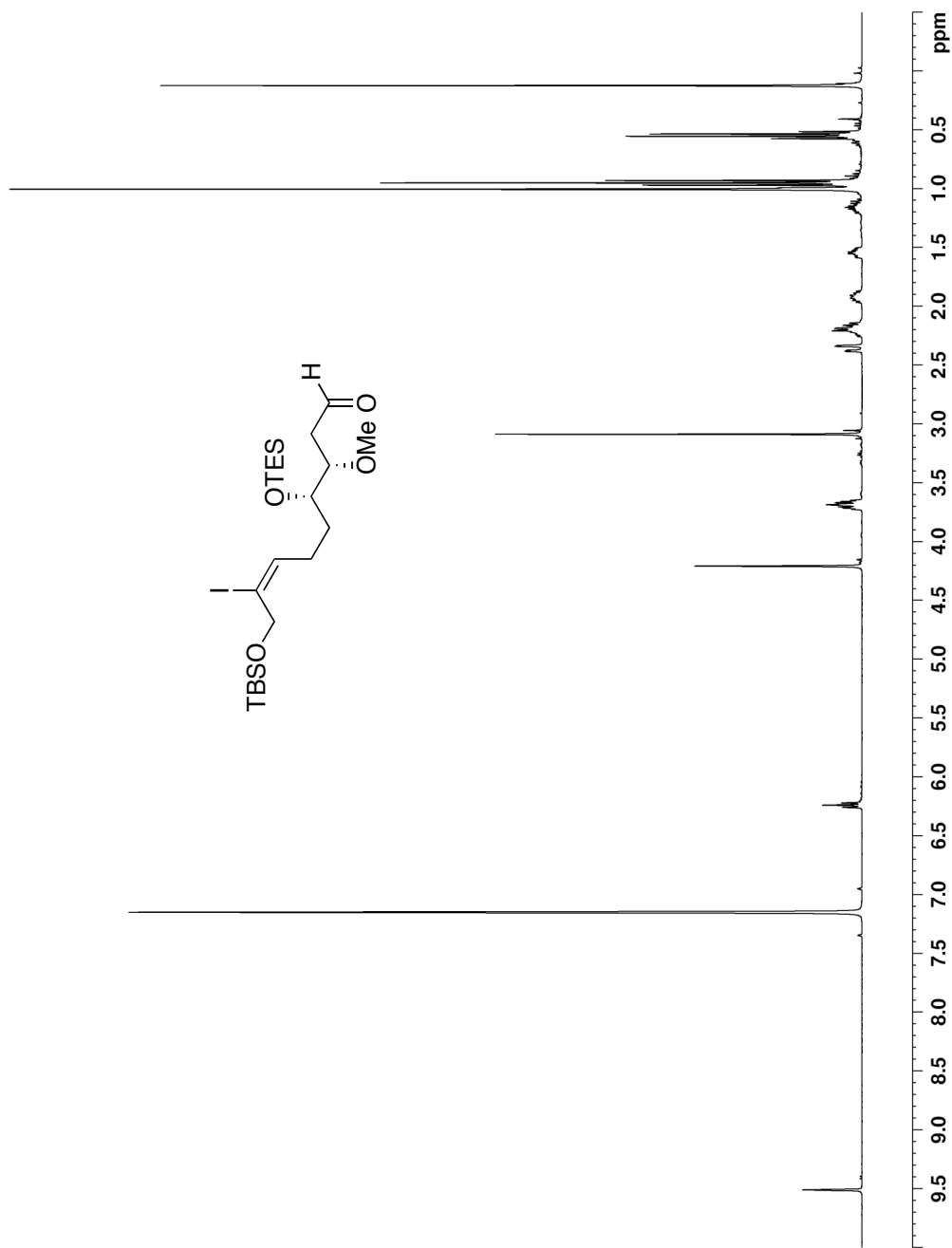


Figure A20a The 400 MHz ^1H NMR spectrum of aldehyde **4.60** in C_6D_6

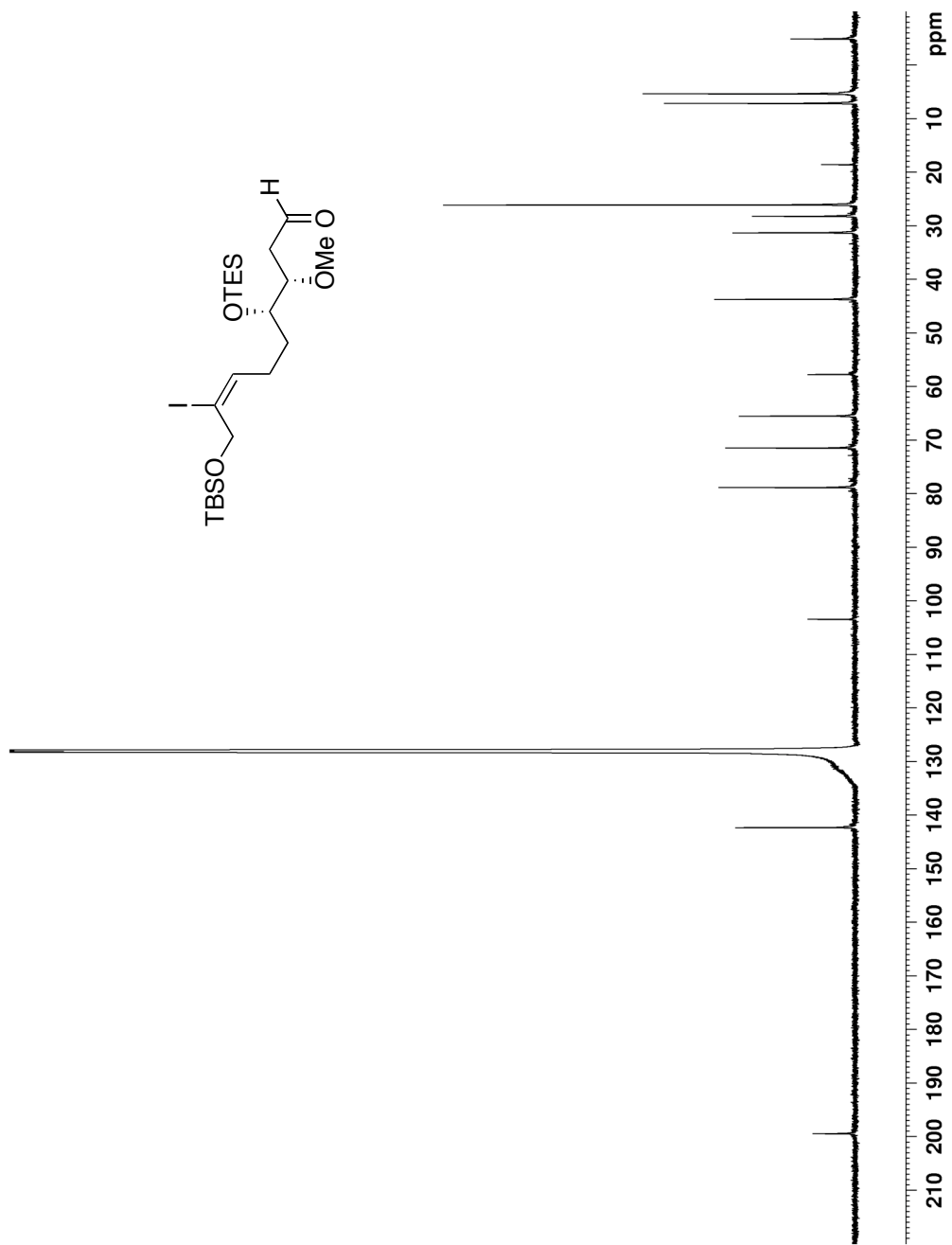


Figure A20b The 125 MHz ^{13}C NMR spectrum of aldehyde **4.60** in C_6D_6

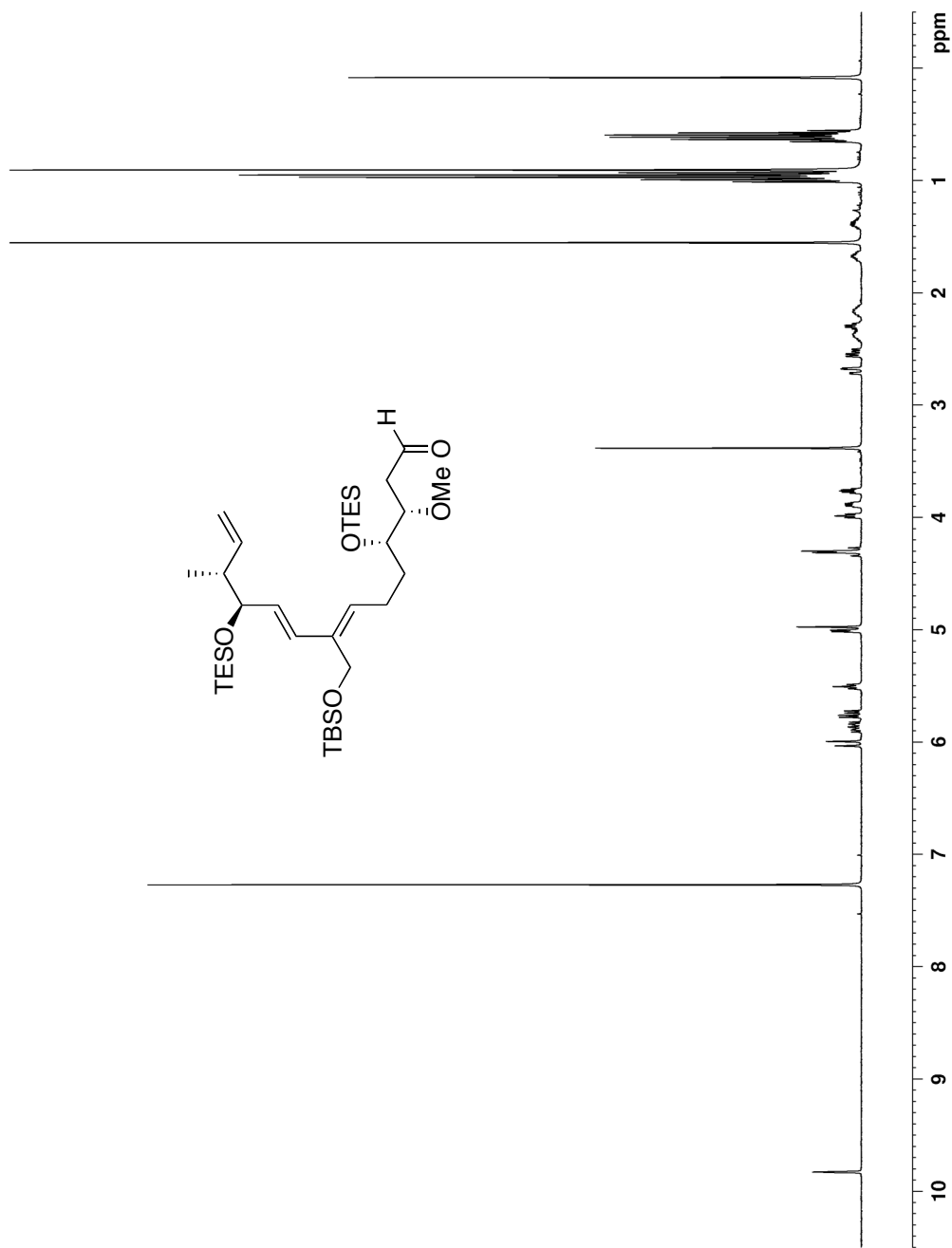


Figure A21a The 400 MHz ^1H NMR spectrum of triene **4.61** in CDCl_3

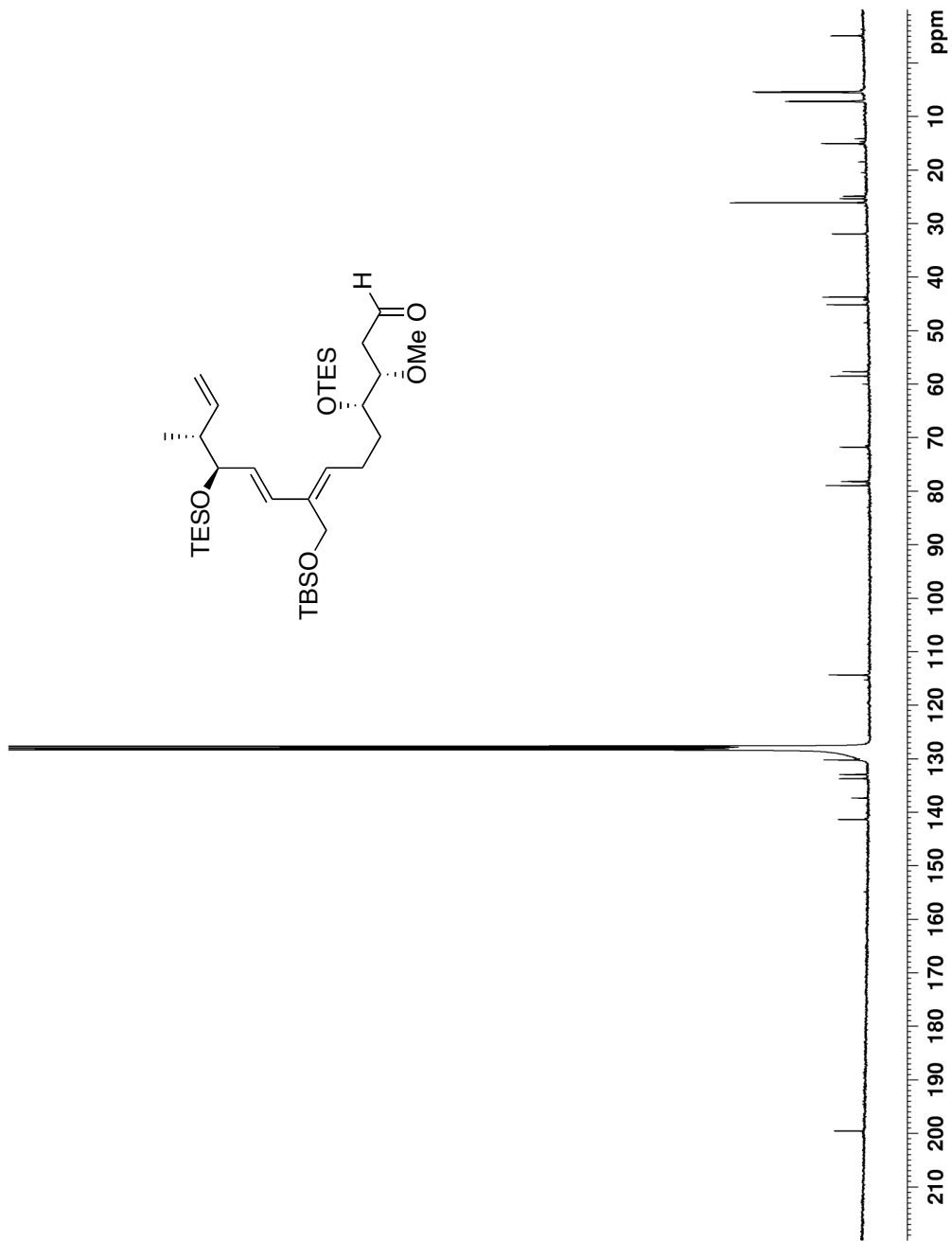


Figure A21b The 75 MHz ^{13}C NMR spectrum of triene **4.61** in C_6D_6

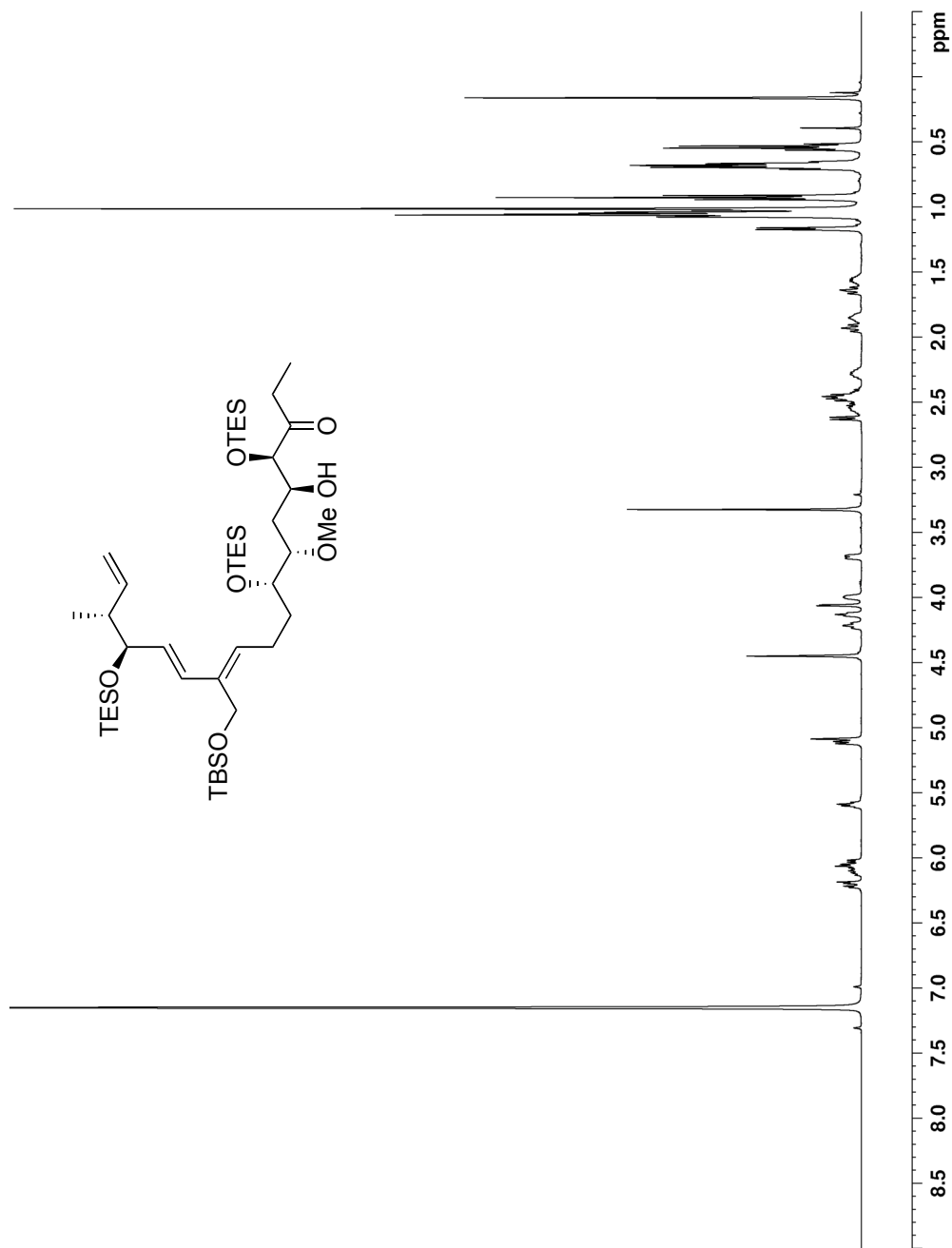


Figure A22a The 500 MHz ^1H NMR spectrum of aldol **4.62** in C_6D_6

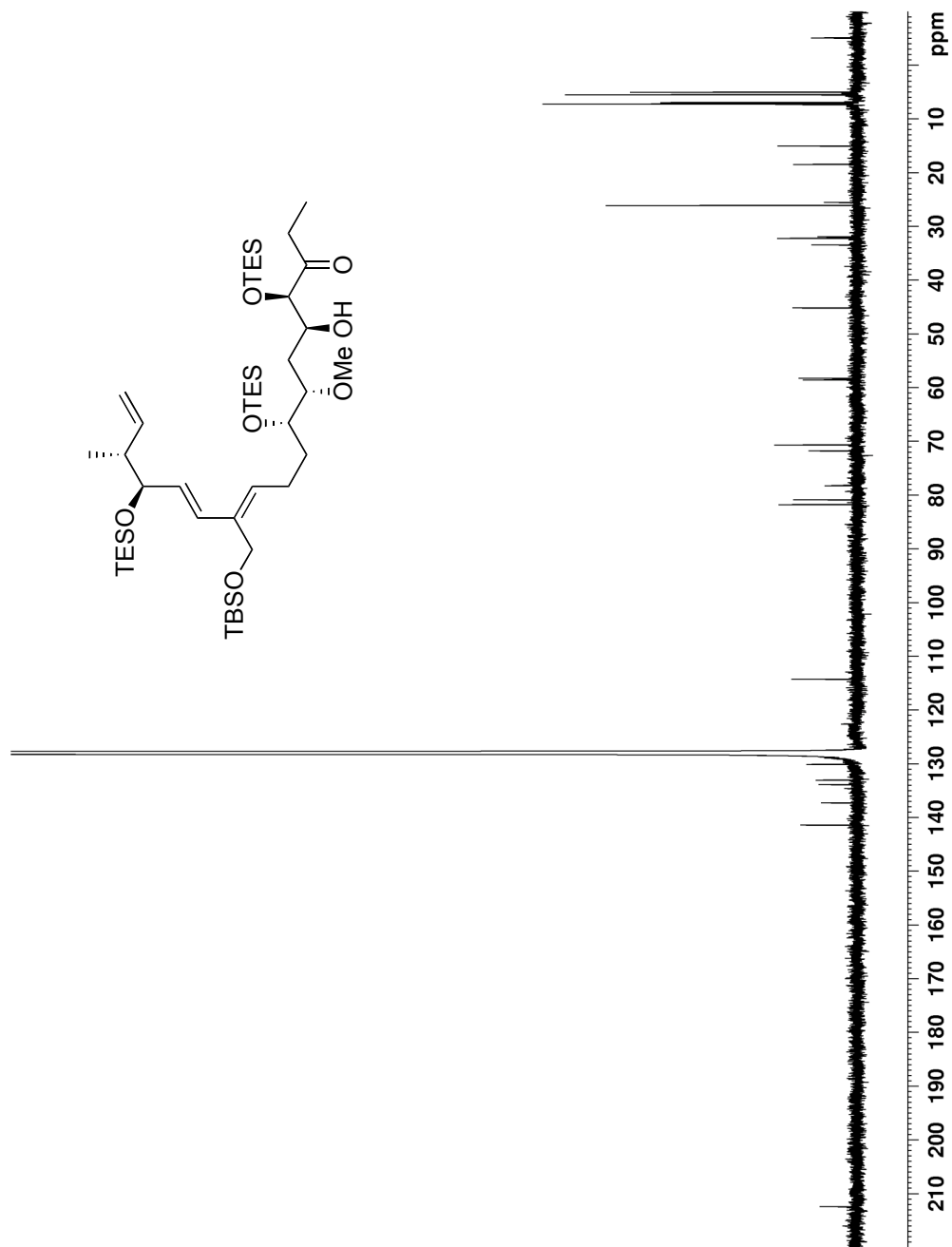


Figure A22b The 125 MHz ^{13}C NMR spectrum of aldol **4.62** in C_6D_6

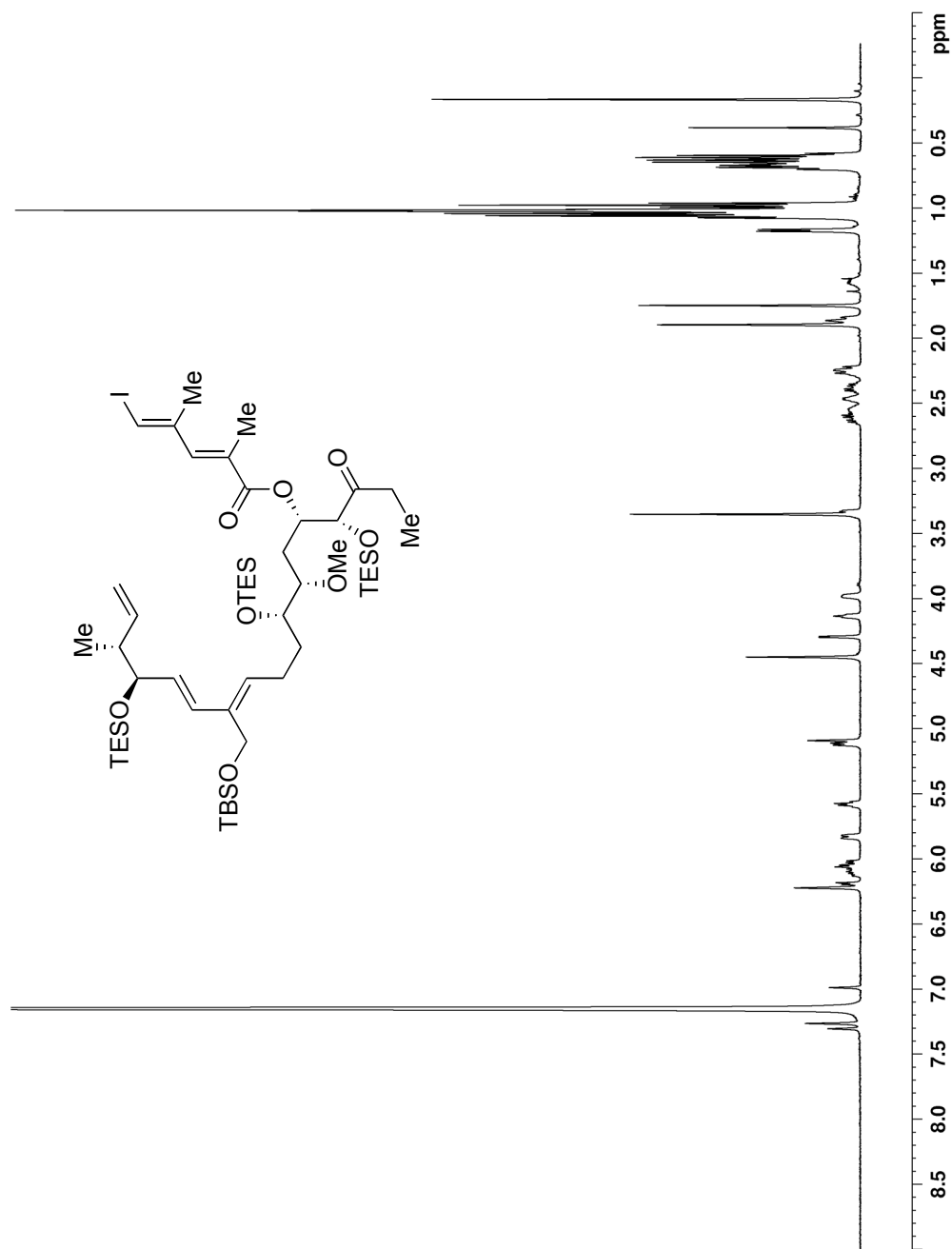


Figure A23a The 300 MHz ^1H NMR spectrum of ester **4.63** in C_6D_6

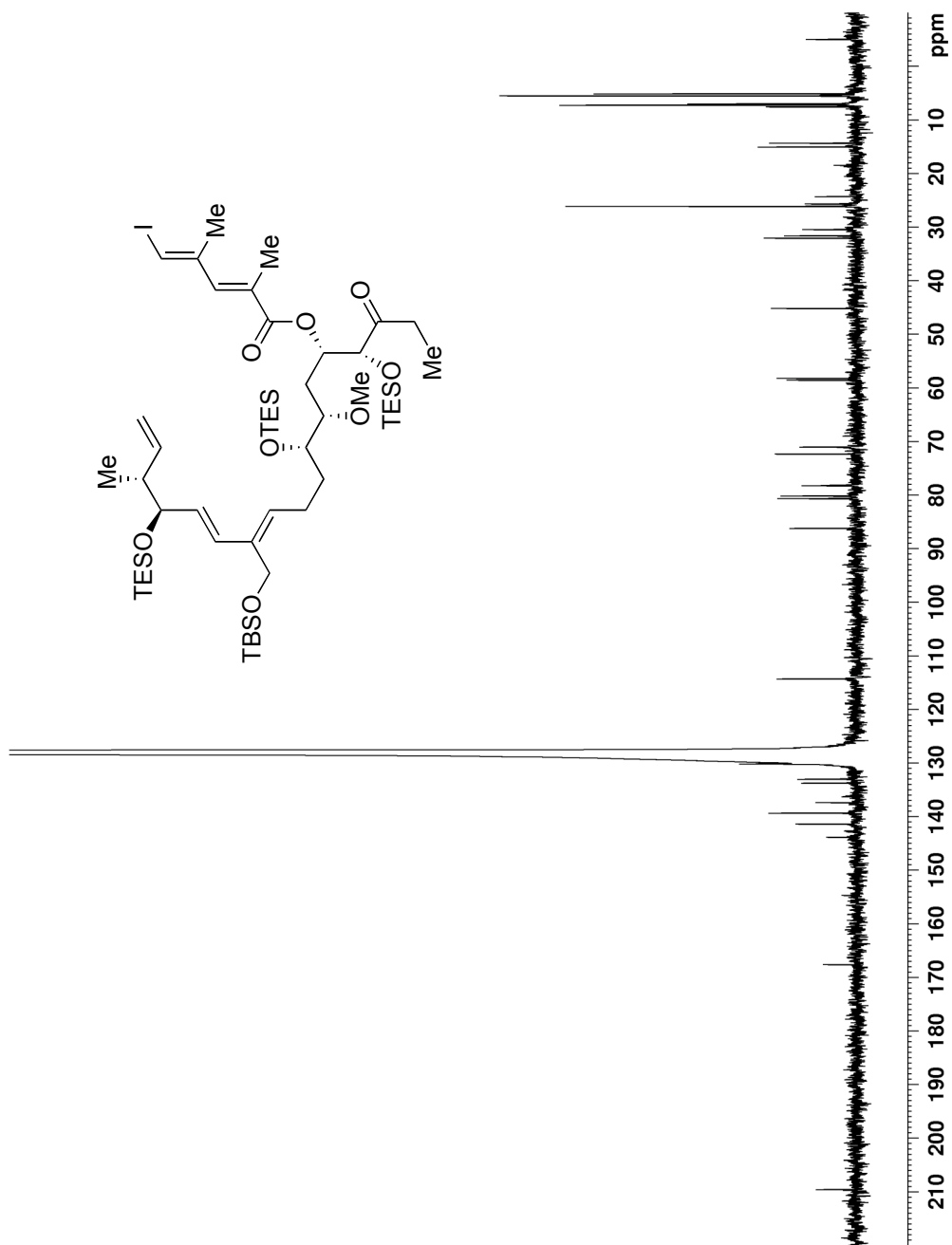


Figure A23b The 125 MHz ^{13}C NMR spectrum of ester **4.63** in C_6D_6

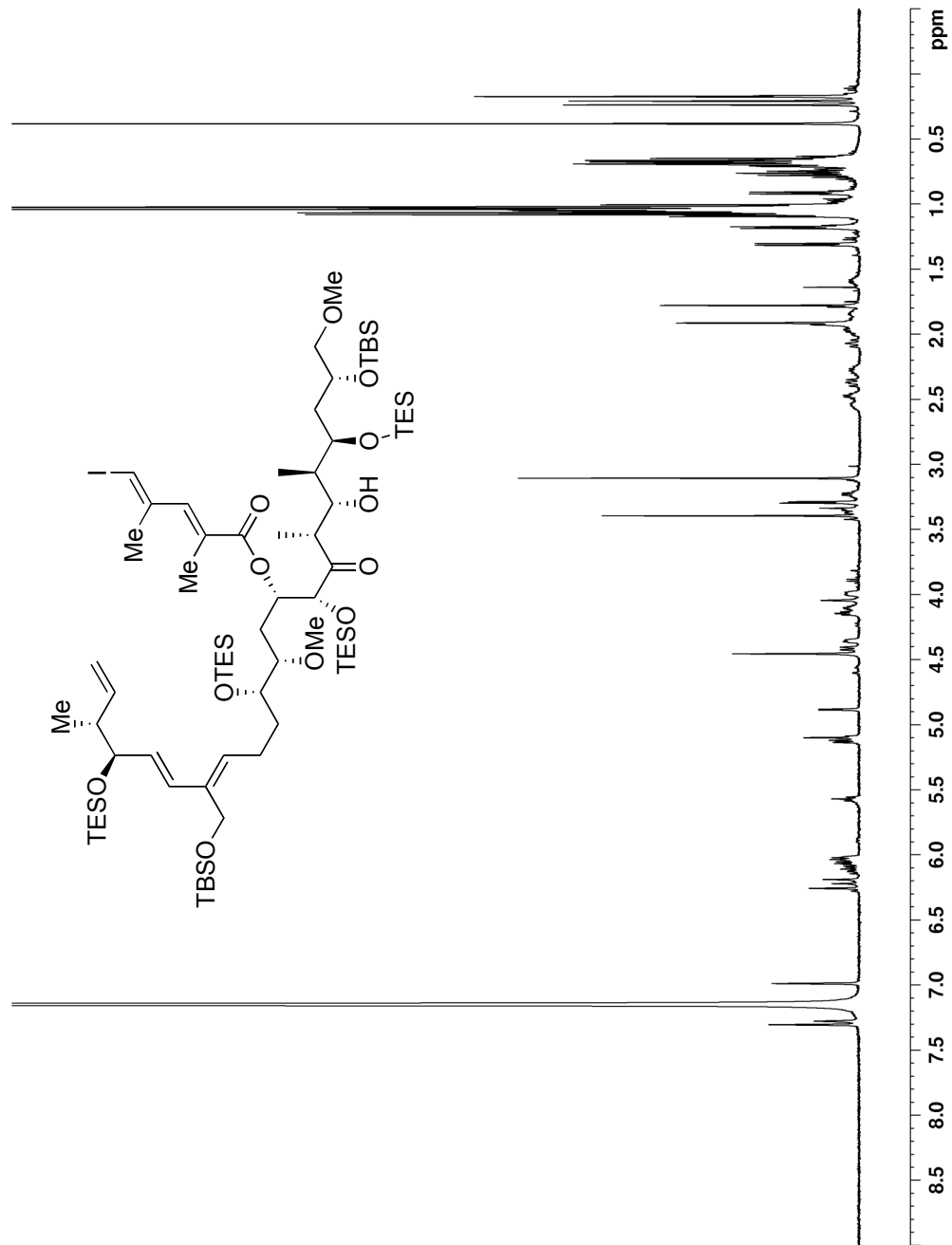


Figure A24a The 500 MHz ^1H NMR spectrum of alcohol **4.64** in C_6D_6

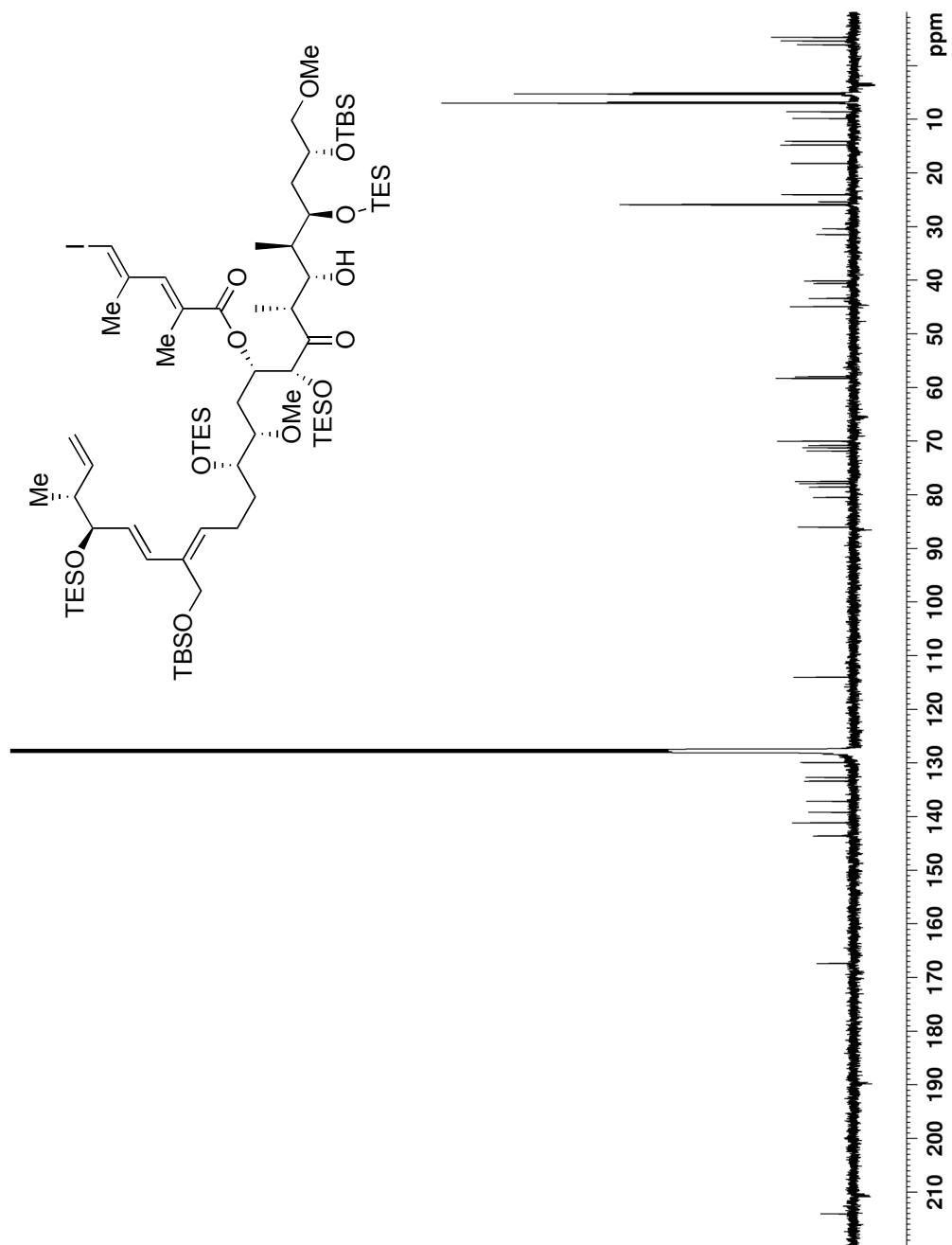


Figure A24b The 100 MHz ^{13}C NMR spectrum of alcohol **4.64** in C_6D_6

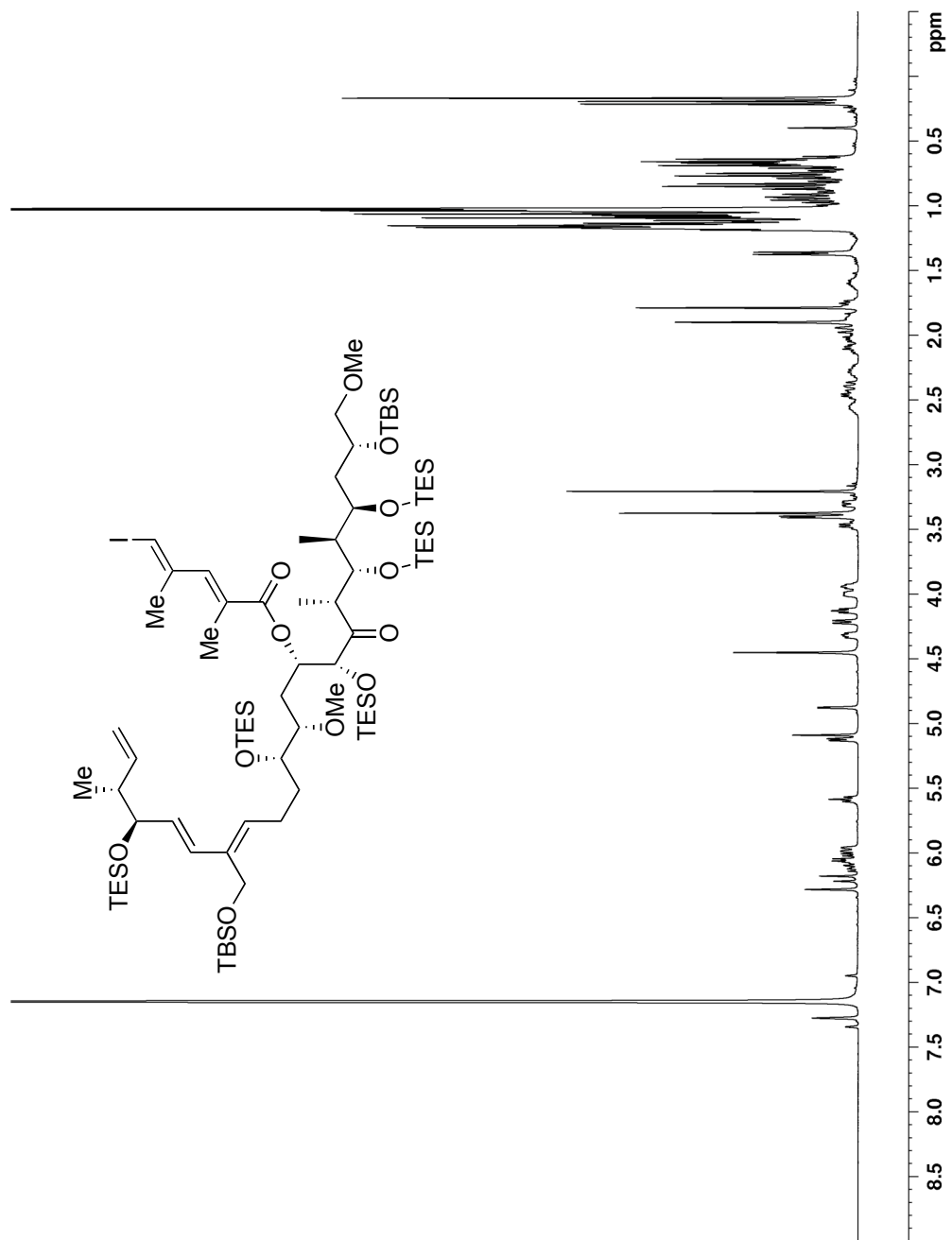


Figure A25a The 400 MHz ¹H NMR spectrum of TES ether **4.65** in C₆D₆

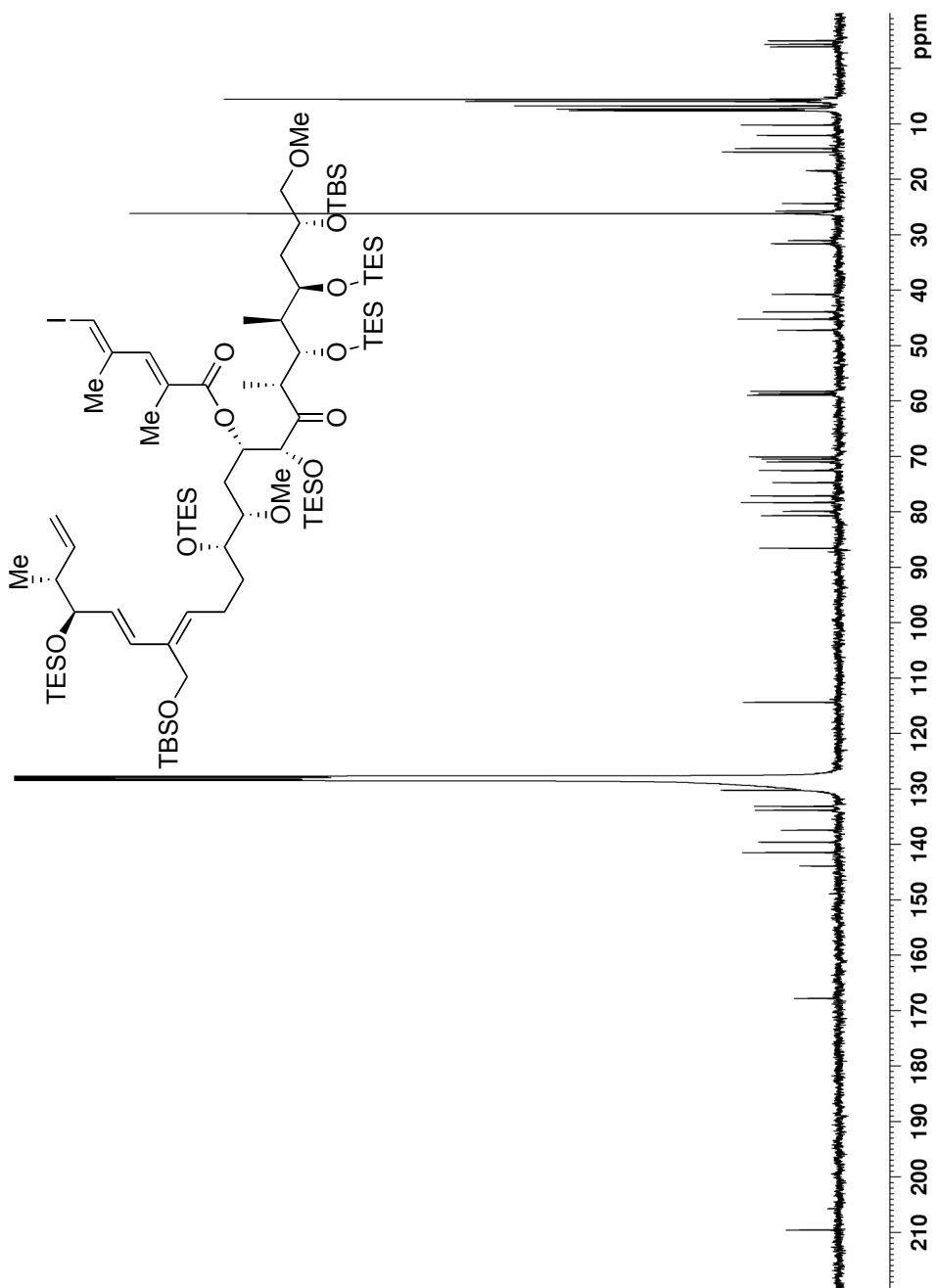


Figure A25b The 75 MHz ^{13}C NMR spectrum of TES ether **4.65** in C_6D_6

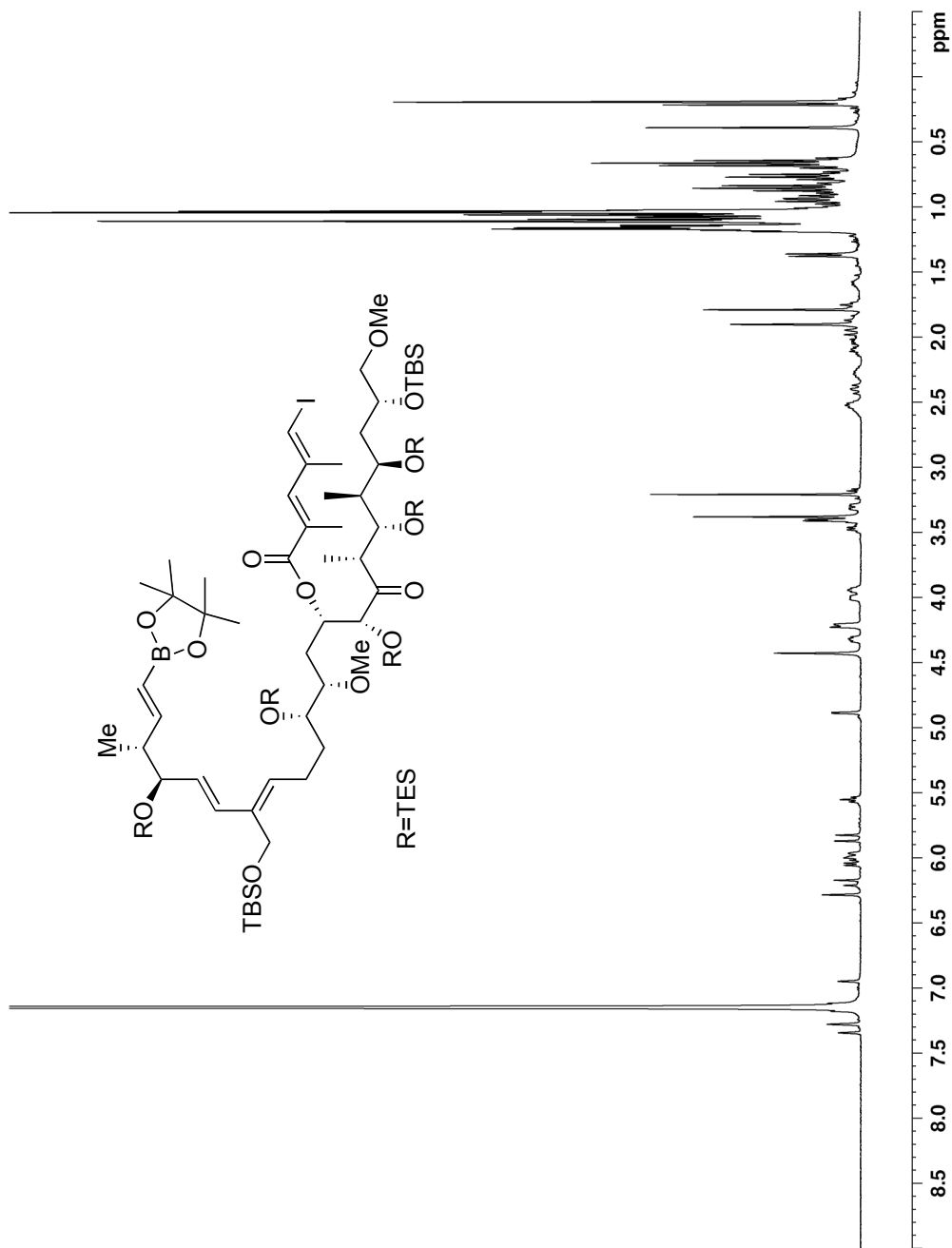


Figure A26a The 400 MHz ^1H NMR spectrum of vinyl borate **4.66** in C_6D_6

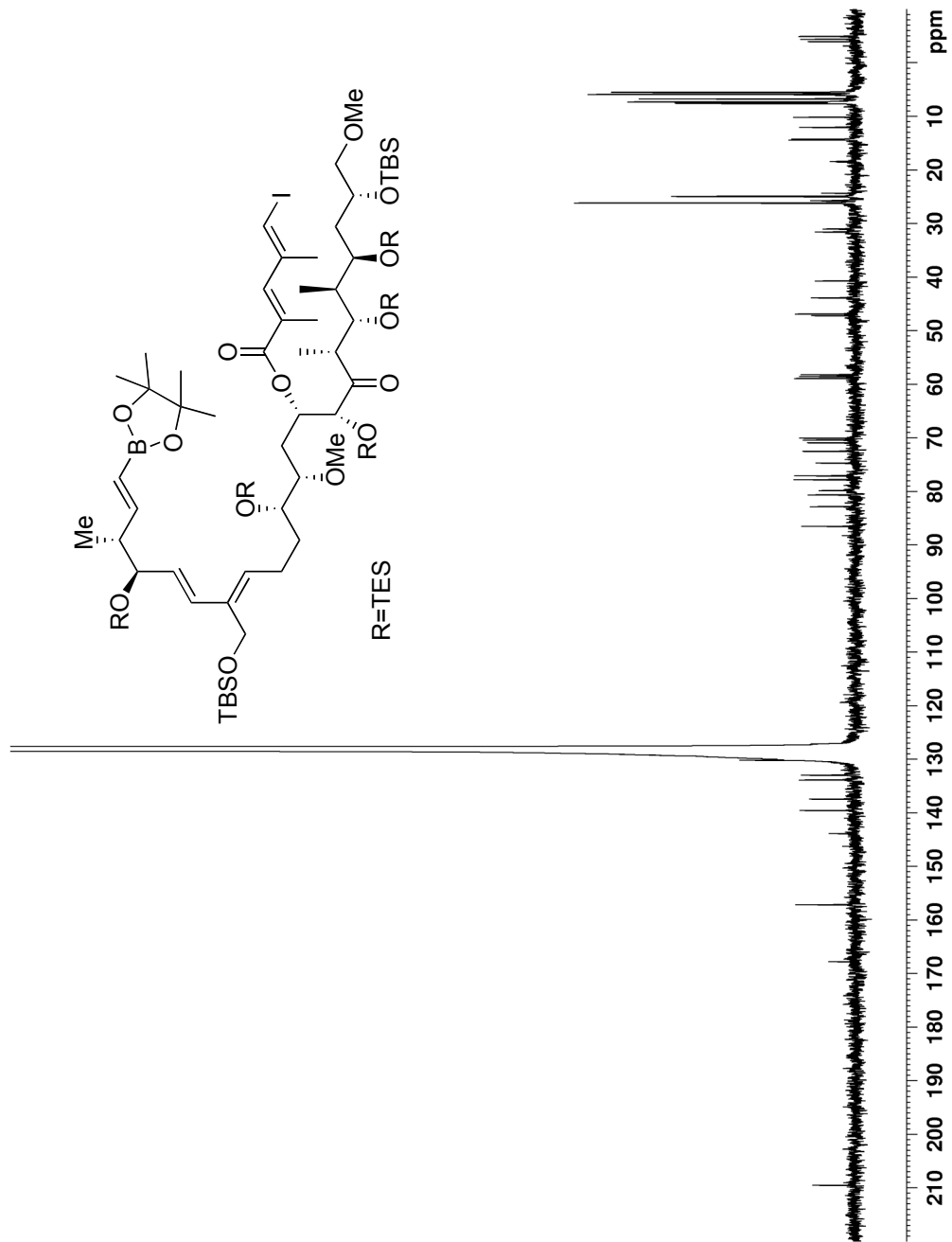


Figure A26b The 75 MHz ^{13}C NMR Spectrum of vinyl borate **4.66** in C_6D_6

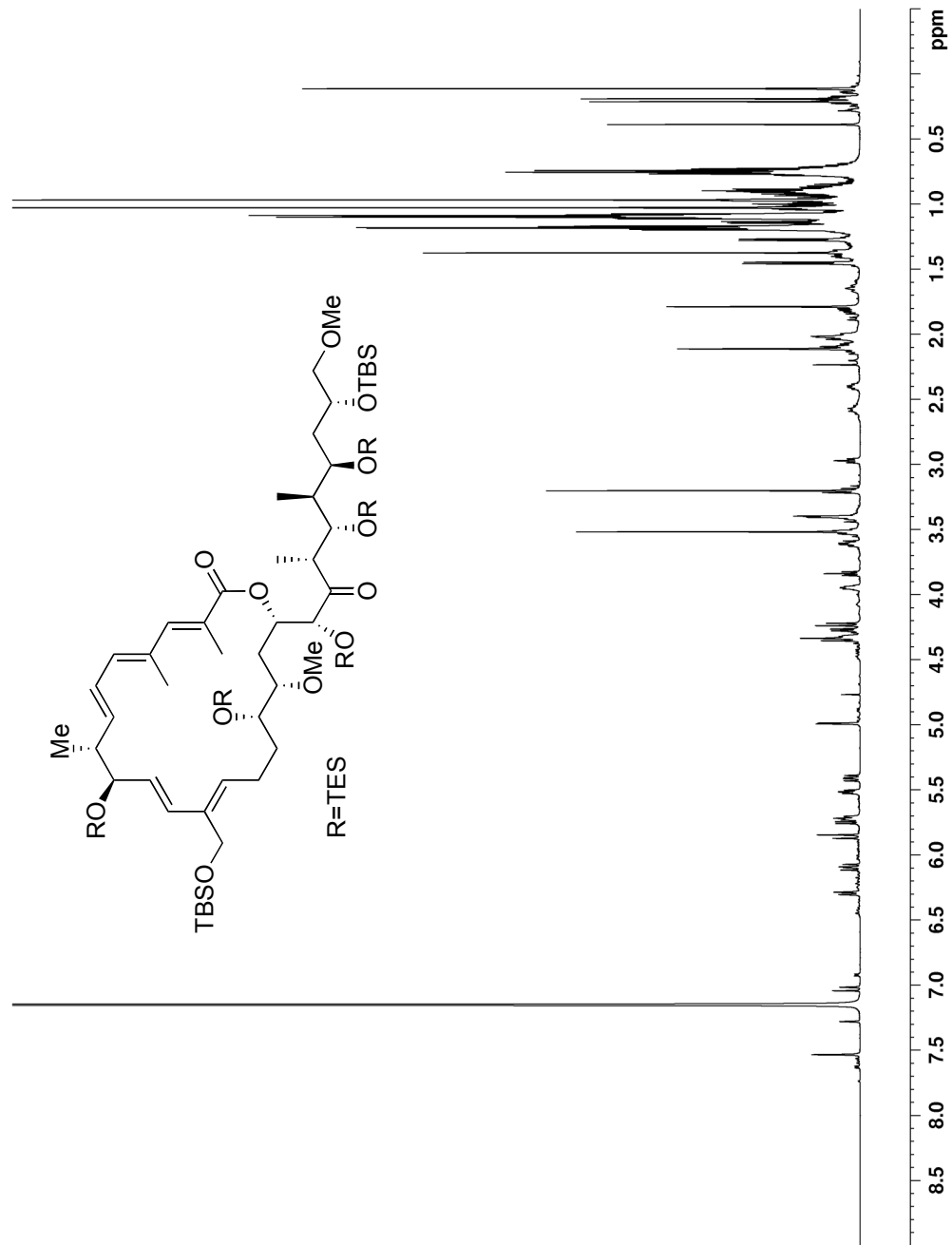


Figure A27a The 600 MHz ^1H NMR spectrum of macrolactone **4.47** in C_6D_6

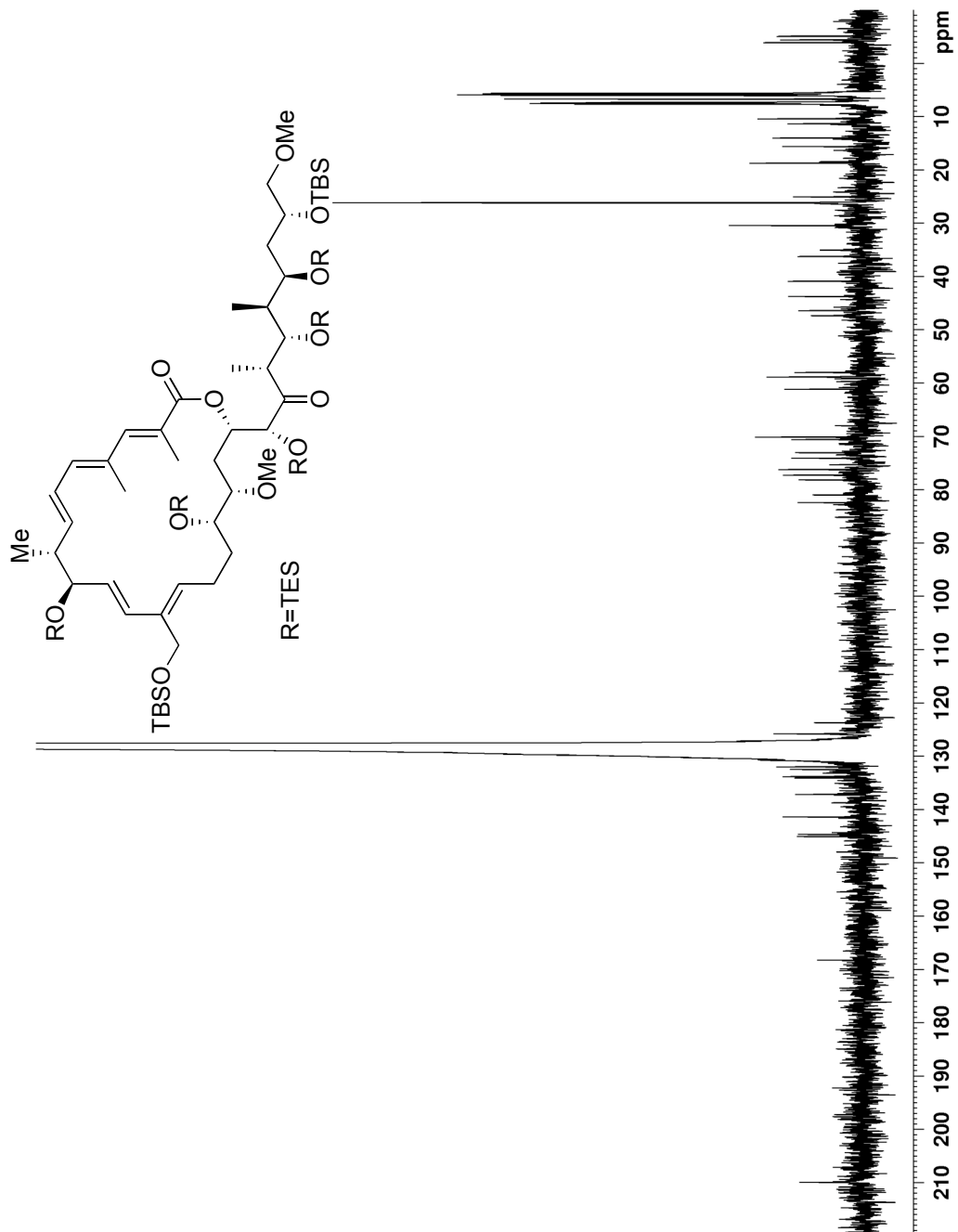


Figure A27b The 75 MHz ^{13}C NMR spectrum of macrolactone **4.47** in C_6D_6

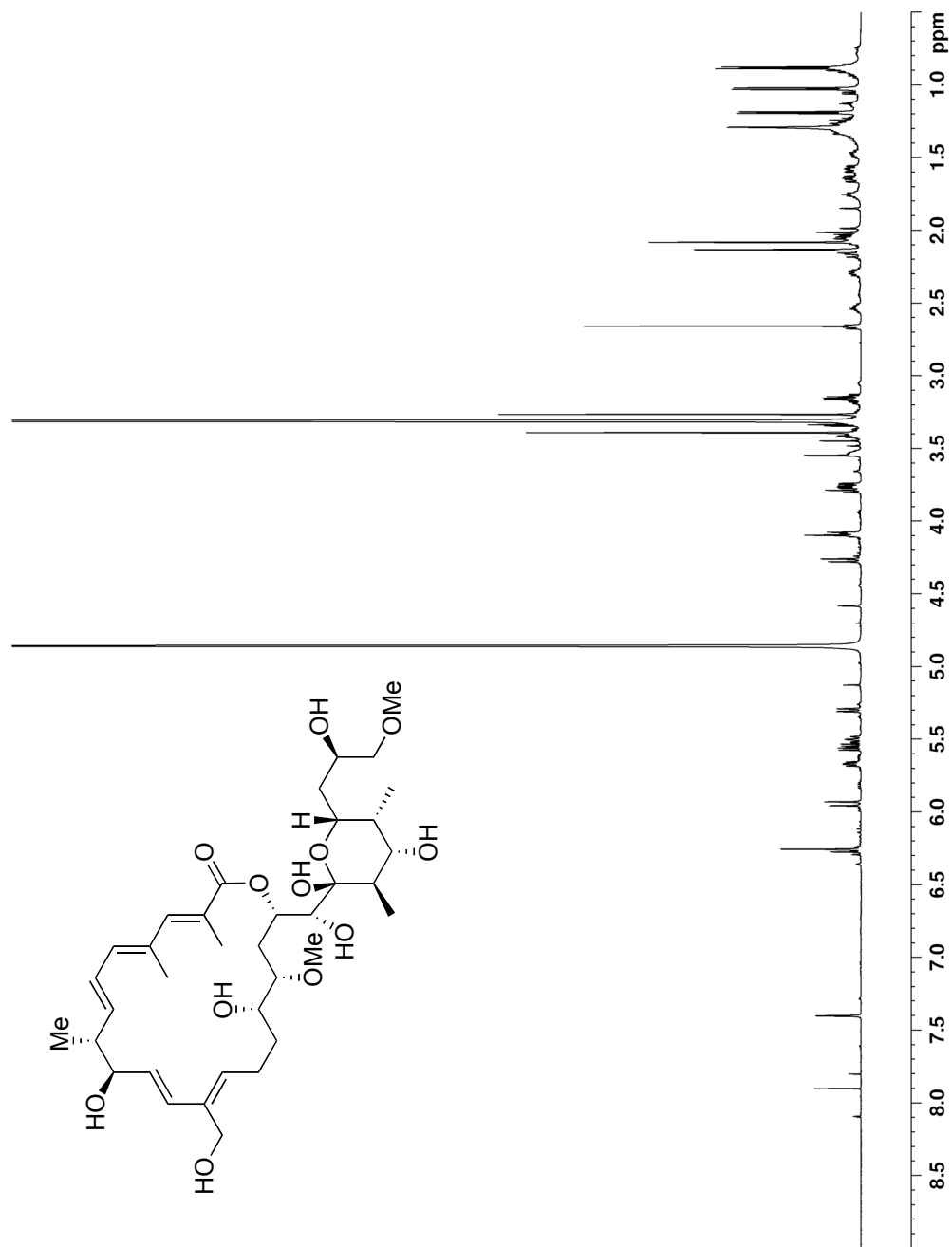


Figure A28a The 600 MHz ¹H NMR spectrum of oxy-apoptolidinone D 4.4 in CD₃OD

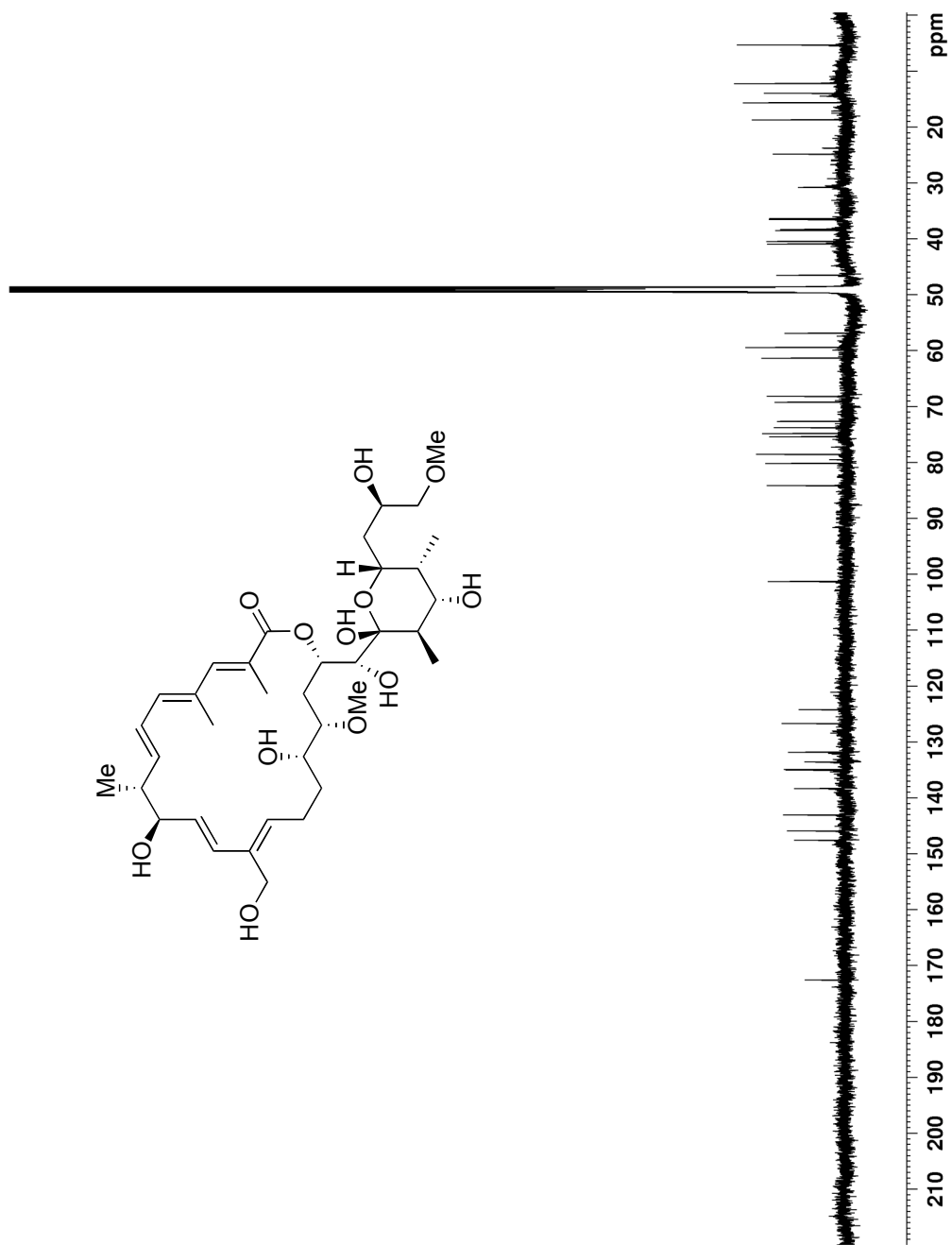


Figure A28b The 150 MHz ^{13}C NMR spectrum of oxy-apoptolidinone D 4.4 in CD_3OD

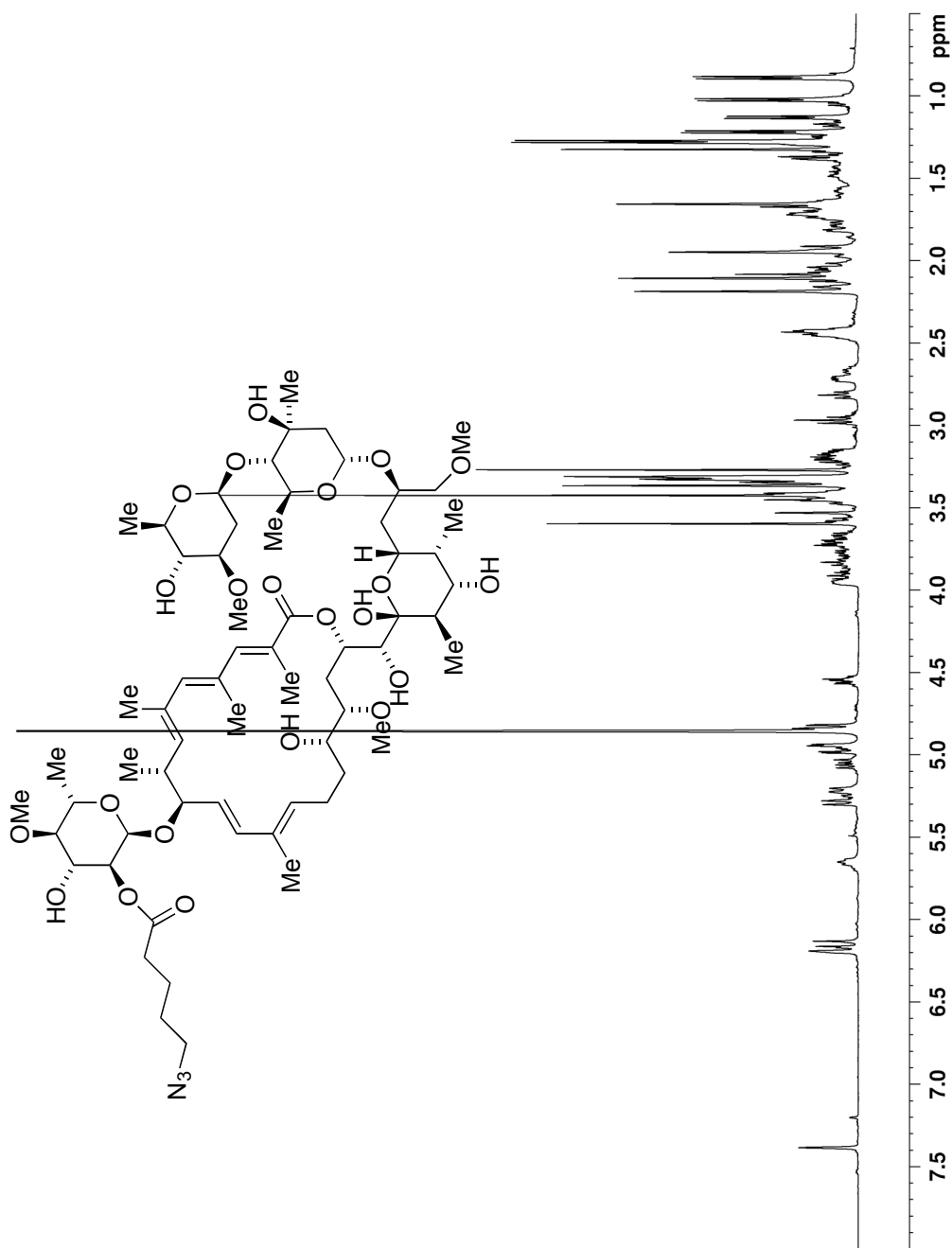


Figure A29a The 500 MHz ¹H NMR spectrum of apoptolidin A congener **6.16** in CD₃OD

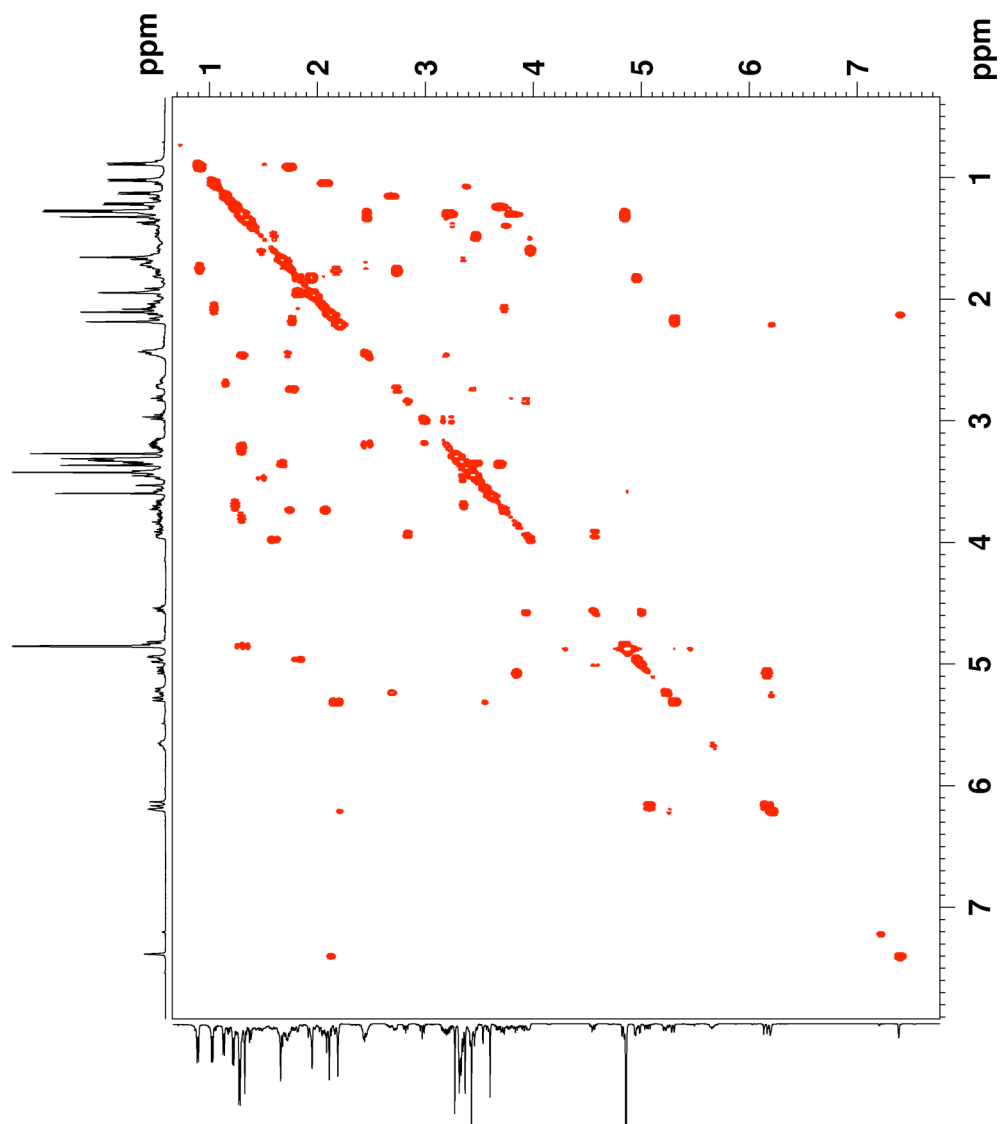


Figure A29b The 500 MHz COSY NMR spectrum of apoptolidin A congener **6.16** in CD₃OD

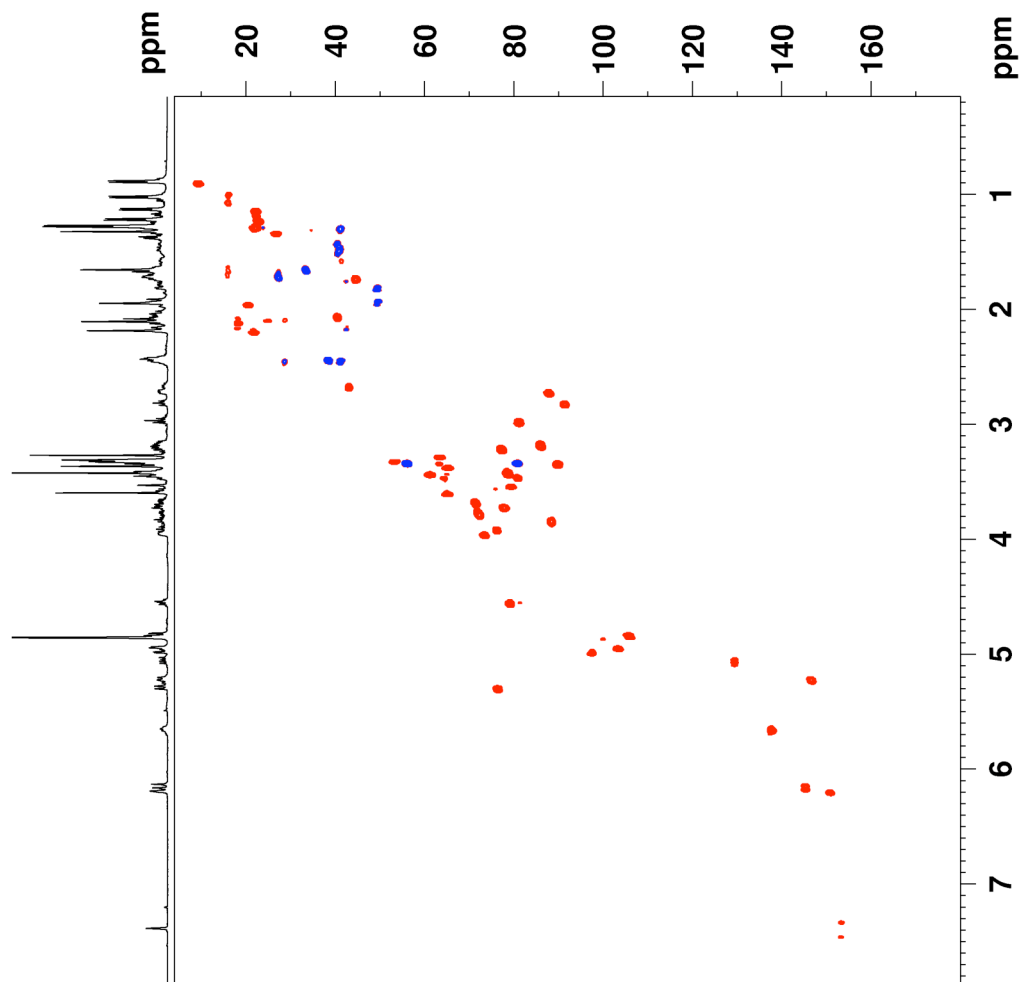


Figure A29c The 500 MHz HSQC NMR spectrum of apoptolidin A congener **6.16** in CD_3OD

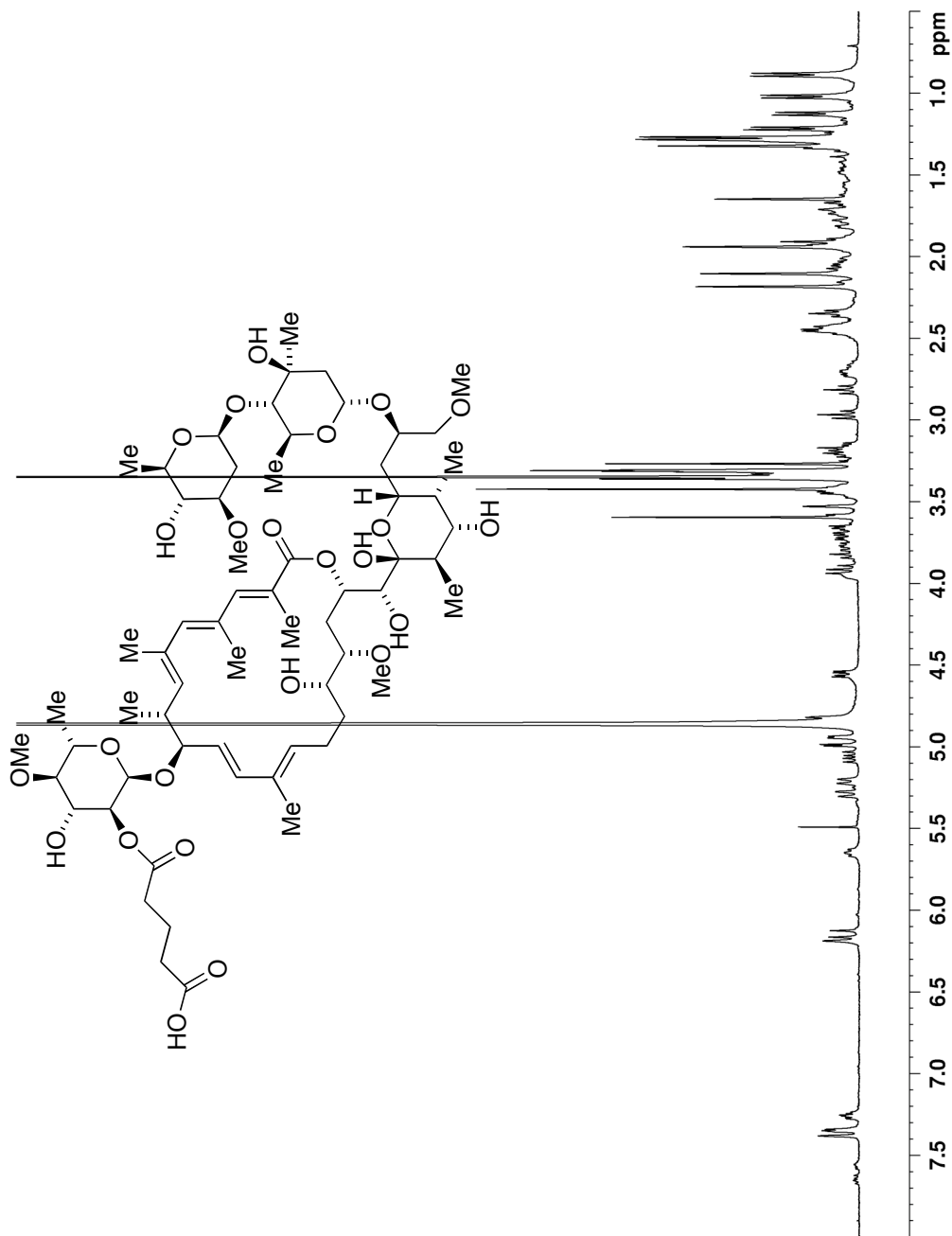


Figure A30a The 400 MHz ¹H NMR spectrum of apoptolidin A congener **6.17** in CD₃OD

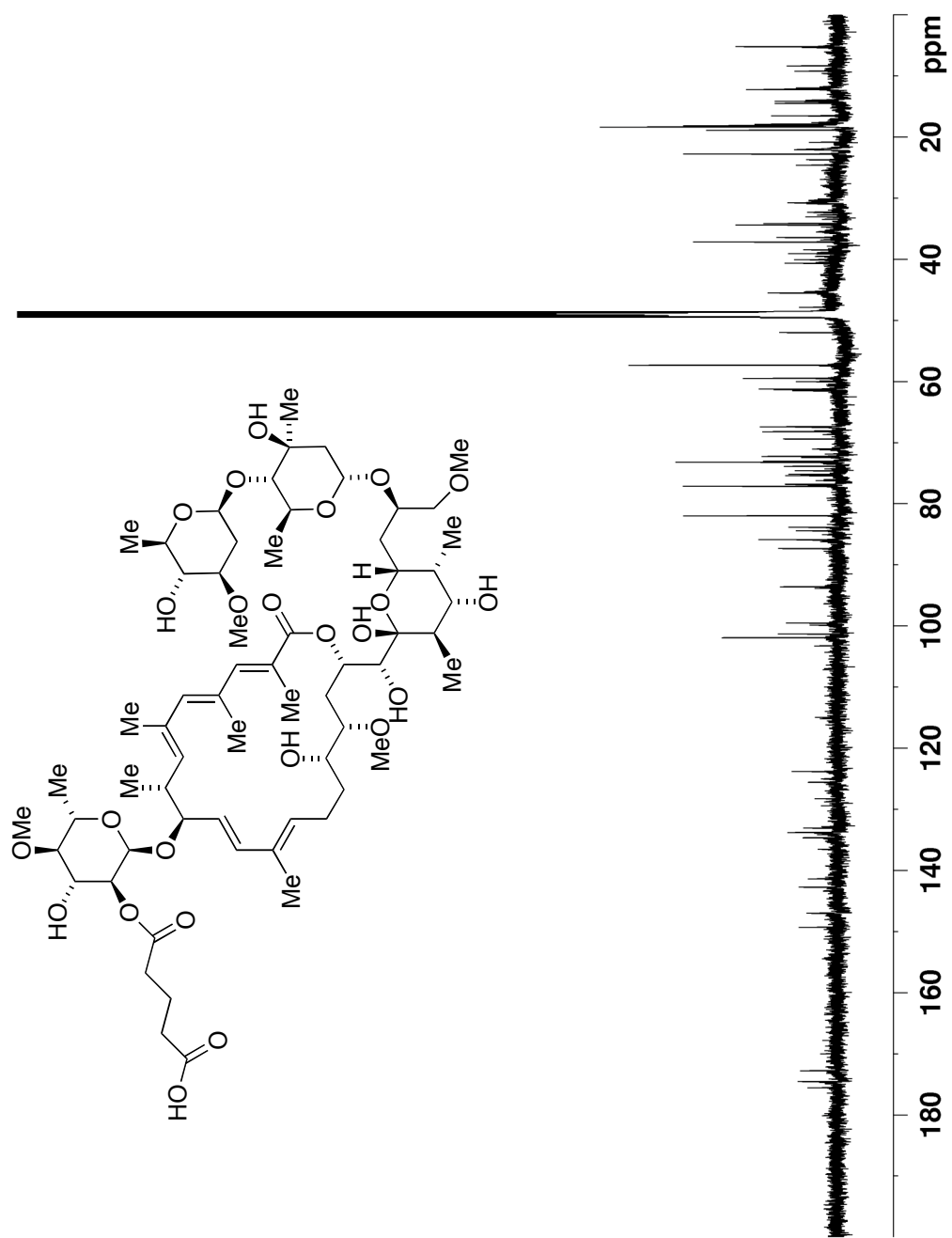


Figure A30b The 125 MHz ^{13}C NMR spectrum of apoptolidin A congener **6.17** in CD_3OD

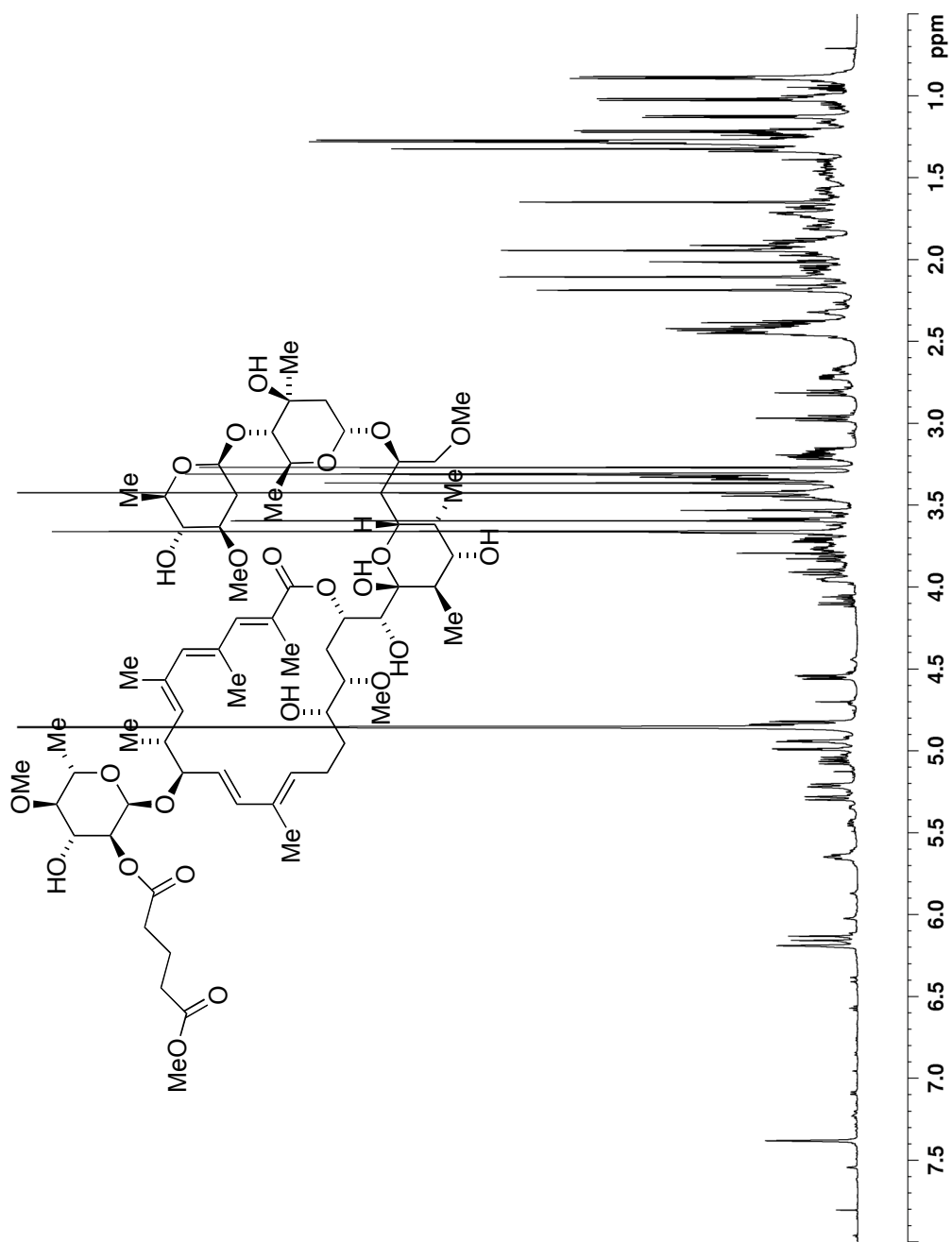


Figure A31a The 600 MHz ^1H NMR spectrum of apoptolidin A congener **6.18** in CD_3OD

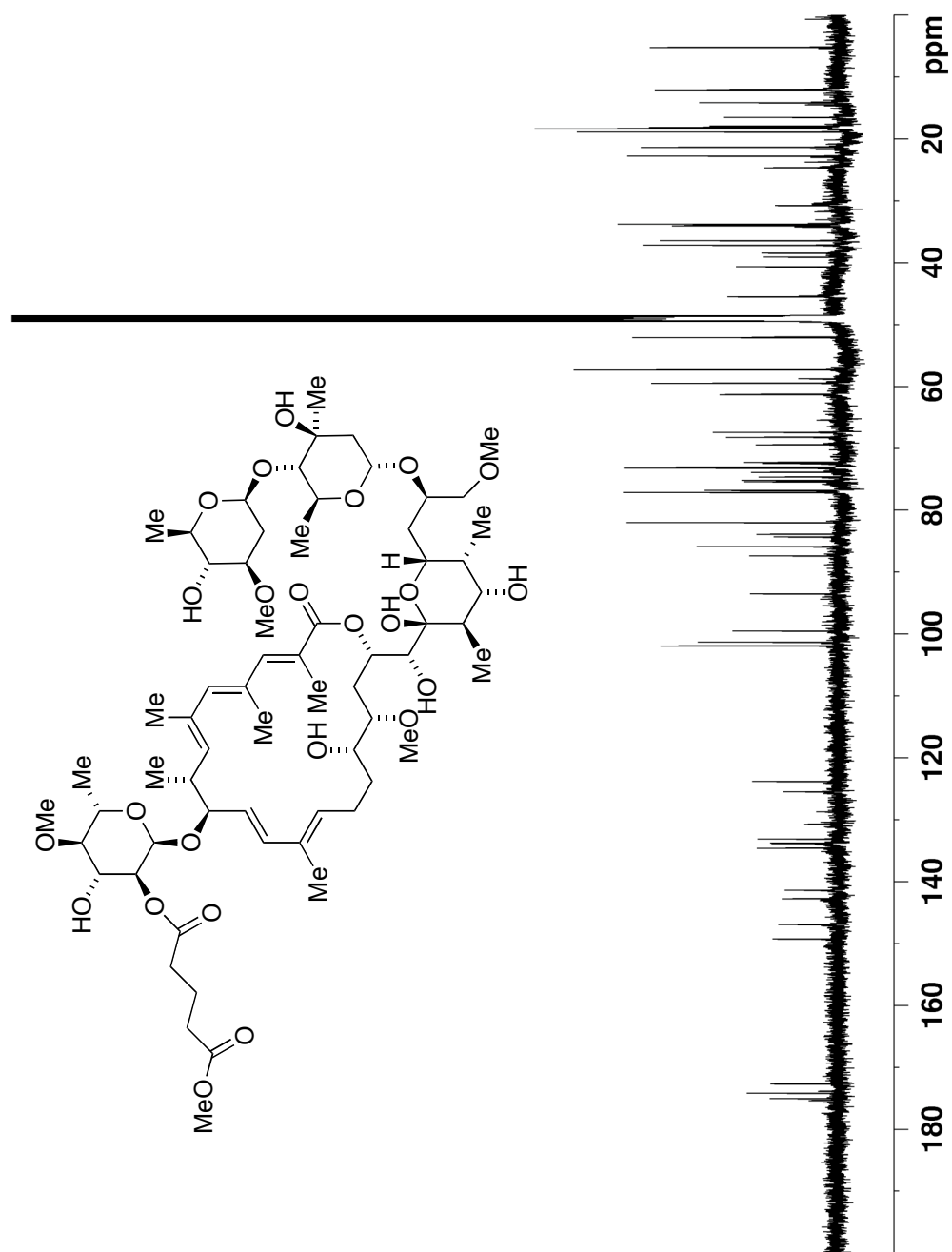


Figure A31b The 125 MHz ¹H NMR spectrum of apoptolidin A congener **6.18** in CD₃OD

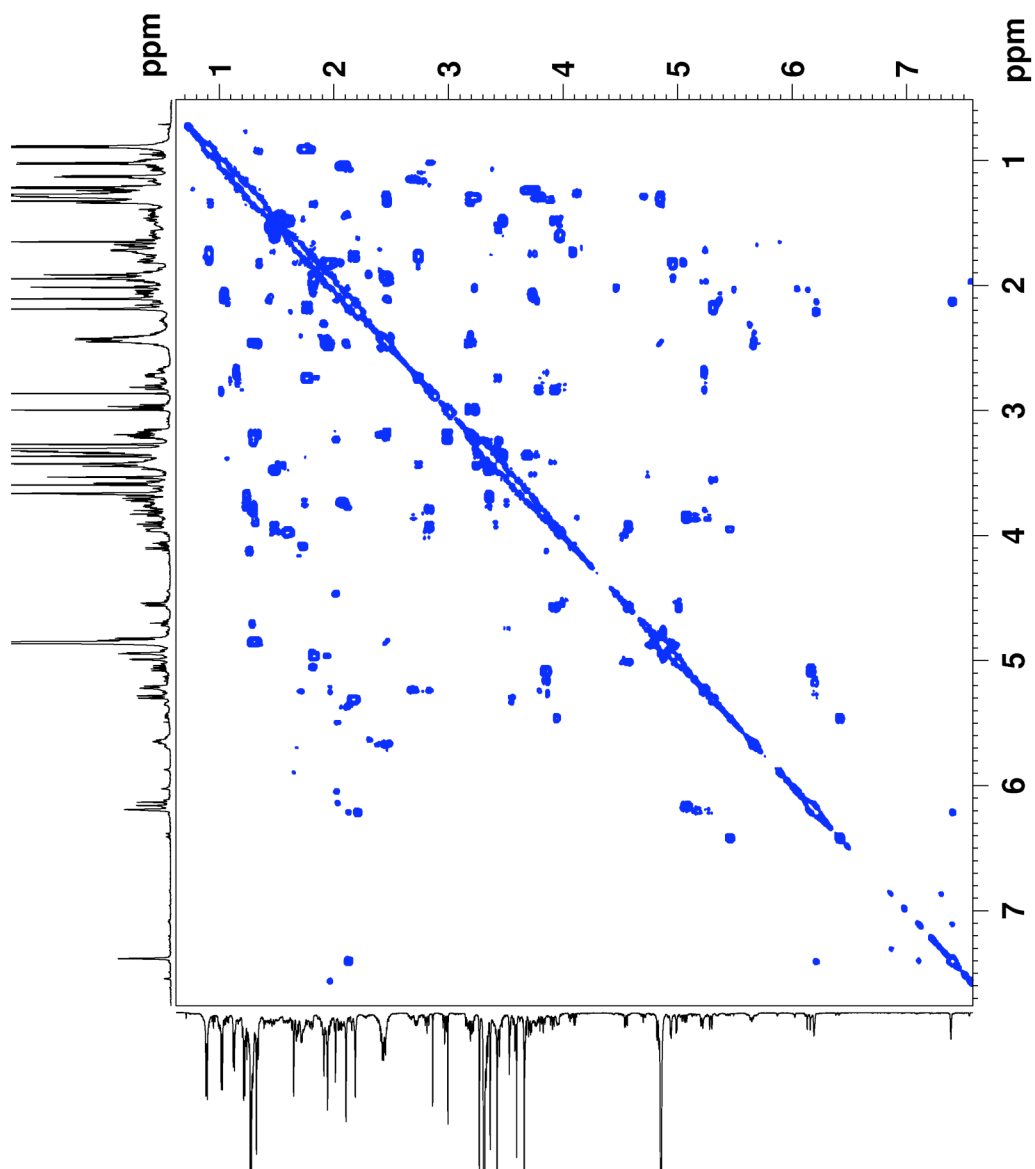


Figure A31c The 600 MHz COSY NMR spectrum of apoptolidin A congener **6.18** in CD₃OD

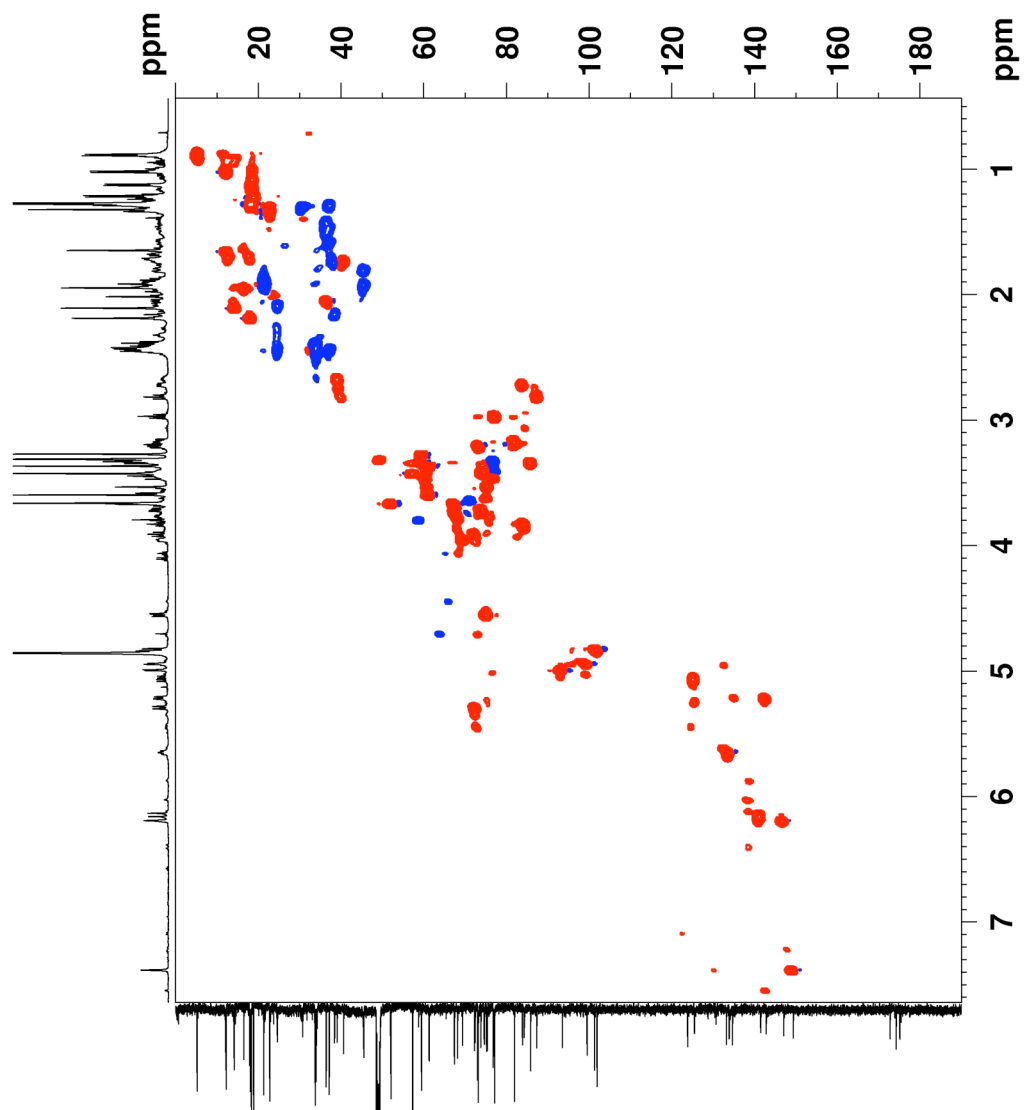


Figure A31d The 600 MHz HSQC NMR spectrum of apoptolidin A congener **6.18** in CD_3OD

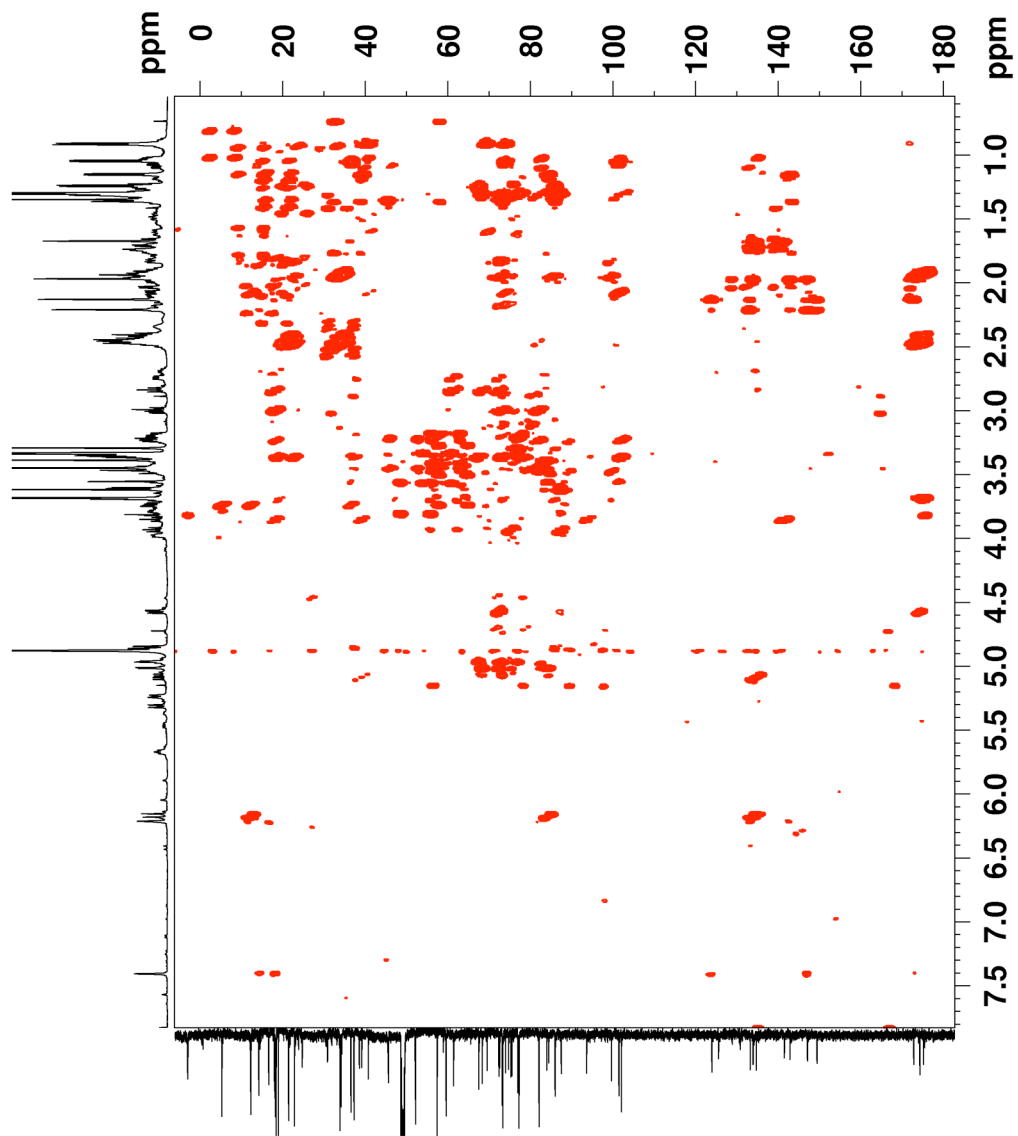


Figure A31e The 600 MHz HMBC NMR spectrum of apoptolidin A congener **6.18** in CD_3OD

REFERENCES

1. Croce, C. M., Molecular origins of cancer: Oncogenes and cancer. *N. Engl. J. Med.* **2008**, 358, 502.
2. Newman, D. J.; Cragg, G. M.; Snader, K. M., Natural products as sources of new drugs over the period 1981-2002. *J. Nat. Prod.* **2003**, 66, 1022.
3. Kim, J. W.; Adachi, H.; ShinYa, K.; Hayakawa, Y.; Seto, H., Apoptolidin, a new apoptosis inducer in transformed cells from *Nocardiosis* sp. *J. Antibiot.* **1997**, 50, 628.
4. Hayakawa, Y.; Kim, J. W.; Adachi, H.; Shin-ya, K.; Fujita, K.; Seto, H., Structure of apoptolidin, a specific apoptosis inducer in transformed cells. *J. Am. Chem. Soc.* **1998**, 120, 3524.
5. Wender, P. A.; Sukopp, M.; Longcore, K., Apoptolidins B and C: Isolation, structure determination, and biological activity. *Org. Lett.* **2005**, 7, 3025.
6. Wender, P. A.; Longcore, K. E., Isolation, structure determination, and anti-cancer activity of apoptolidin D. *Org. Lett.* **2007**, 9, 691.
7. Moore, B. S.; Hertweck, C., Biosynthesis and attachment of novel bacterial polyketide synthase starter units. *Nat. Prod. Rep.* **2002**, 19, 70.
8. Wender, P. A.; Gullledge, A. V.; Jankowski, O. D.; Seto, H., Isoapoptolidin: Structure and activity of the ring-expanded isomer of apoptolidin. *Org. Lett.* **2002**, 4, 3819.
9. Pennington, J. D.; Williams, H. J.; Salomon, A. R.; Sulikowski, G. A., Toward a stable apoptolidin derivative: Identification of isoapoptolidin and selective deglycosylation of apoptolidin. *Org. Lett.* **2002**, 4, 3823.
10. Hanessian, S.; Meng, Q. C.; Olivier, E., An Unprecedented Ring Expansion in the Macrolide Series - Synthesis of Iso-Bafilomycin a(1). *Tetrahedron Lett.* **1994**, 35, 5393.
11. Developmental Therapeutics Program NCI/NIH, <http://dtp.nci.nih.gov> (accessed July 2002)
12. Salomon, A. R.; Voehringer, D. W.; Herzenberg, L. A.; Khosla, C., Understanding and exploiting the mechanistic basis for selectivity of polyketide inhibitors of F0F1-ATPase. *Proc. Natl. Acad. Sci. U. S. A.* **2000**, 97, 14766.

13. Salomon, A. R.; Voehringer, D. W.; Herzenberg, L. A.; Khosla, C., Apoptolidin, a selective cytotoxic agent, is an inhibitor of F₀F₁-ATPase. *Chem. Biol.* **2001**, 8, 71.
14. Salomon, A. R.; Zhang, Y. B.; Seto, H.; Khosla, C., Structure-activity relationships within a family of selectively cytotoxic macrolide natural products. *Org. Lett.* **2001**, 3, 57.
15. Wender, P. A.; Jankowski, O. D.; Longcore, K.; Tabet, E. A.; Seto, H.; Tomikawa, T., Correlation of F₀F₁-ATPase inhibition and antiproliferative activity of apoptolidin analogues. *Org. Lett.* **2006**, 8, 589.
16. Nicolaou, K. C.; Li, Y.; Fylaktakidou, K. C.; Mitchell, H. J.; Weyershausen, B.; Wei, H.; Weyershausen, B., Total synthesis of spoptolidin: Part 1. retrosynthetic analysis and construction of building blocks. *Angew. Chem. Int. Ed.* **2001**, 40, 3849.
17. Nicolaou, K. C.; Li, Y.; Fylaktakidou, K. C.; Mitchell, H. J.; Sugita, K., Total synthesis of apoptolidin: Part 2. coupling of key building blocks and completion of the synthesis. *Angew. Chem. Int. Ed.* **2001**, 40, 3854.
18. Nicolaou, K. C.; Fylaktakidou, K. C.; Monenschein, H.; Li, Y. W.; Weyershausen, B.; Mitchell, H. J.; Wei, H. X.; Guntupalli, P.; Hepworth, D.; Sugita, K., Total synthesis of apoptolidin: Construction of enantiomerically pure fragments. *J. Am. Chem. Soc.* **2003**, 125, 15433.
19. Nicolaou, K. C.; Li, Y. W.; Sugita, K.; Monenschein, H.; Guntupalli, P.; Mitchell, H. J.; Fylaktakidou, K. C.; Vourloumis, D.; Giannakakou, P.; O'Brate, A., Total synthesis of apoptolidin: Completion of the synthesis and analogue synthesis and evaluation. *J. Am. Chem. Soc.* **2003**, 125, 15443.
20. Wehlan, H.; Dauber, M.; Fernaud, M. T. M.; Schuppan, J.; Mahrwald, R.; Ziemer, B.; Garcia, M. E. J.; Koert, U., Total synthesis of apoptolidin. *Angew. Chem. Int. Edit.* **2004**, 43, 4597.
21. Daniel, P. T.; Koert, U.; Schuppan, J., Apoptolidin: Induction of Apoptosis by a Natural Product. *Angew. Chem. Int. Ed.* **2006**, 45, 872.
22. Crimmins, M. T.; Christie, H. S.; Long, A.; Chaudhary, K., Total Synthesis of Apoptolidin A. *Org. Lett.* **2009**, 11, 831.
23. Schuppan, J.; Wehlan, H.; Keiper, S.; Koert, U., Synthesis of apoptolidinone. *Angew. Chem. Int. Ed.* **2001**, 40, 2063.

24. Wu, B.; Liu, Q. S.; Sulikowski, G. A., Total synthesis of apoptolidinone. *Angew. Chem.Int. Edit.* **2004**, 43, 6673.
25. Crimmins, M. T.; Christie, H. S.; Chaudhary, K.; Long, A., Enantioselective synthesis of apoptolidinone: Exploiting the versatility of thiazolidinethione chiral auxiliaries. *J. Am. Chem. Soc.* **2005**, 127, 13810.
26. Nicolaou, K. C.; Li, Y.; Weyershausen, B.; Wei, H., Synthesis of the macrocyclic core of apoptolidin. *Chem. Commun.* **2000**, 307.
27. Sulikowski, G. A.; Lee, W.; Jin, B.; Wu, B., Synthesis of the apoptosis inducing agent apoptolidin. Assembly of the C(16)-C(28) fragment. *Org. Lett.* **2000**, 2, 1439.
28. Toshima, K.; Arita, T.; Kato, K.; Tanaka, D.; Matsumura, S., Synthetic studies on apoptolidin: synthesis of the C1-C21 macrolide fragment. *Tetrahedron Lett.* **2001**, 42, 8873.
29. Abe, K.; Kato, K.; Arai, T.; Rahim, M. A.; Sultana, I.; Matsumura, S.; Toshima, K., Synthetic studies on apoptolidin: synthesis of C12-C28 fragment via a highly stereoselective aldol reaction. *Tetrahedron Lett.* **2004**, 45, 8849.
30. Paquette, W. D.; Taylor, R. E., Enantioselective Preparation of the C1-C11 Fragment of Apoptolidin. *Org. Lett.* **2004**, 6, 103.
31. Bouchez, L. C.; Vogel, P., Synthesis of C(1)-C(11) polyene fragment of apoptolidin with a new sulfur dioxide-based organic chemistry. *Chem. Eur. J.* **2005**, 11, 4609.
32. Crimmins, M. T.; Long, A., Enantioselective synthesis of apoptolidin sugars. *Org. Lett.* **2005**, 7, 4157.
33. Wu, B.; Liu, Q. S.; Jin, B. H.; Qu, T.; Sulikowski, G. A., Studies on the synthesis of apoptolidin: Progress on the stereocontrolled assembly of the pseudo aglycone of apoptolidin. *Eur. J. Org. Chem.* **2006**, 277.
34. Handa, M.; Scheidt, K. A.; Bossart, M.; Zheng, N.; Roush, W. R., Studies on the synthesis of apoptolidin A. 1. Synthesis of the C(1)-C(11) fragment. *J. Org. Chem.* **2008**, 73, 1031.
35. Handa, M.; Smith, W. J.; Roush, W. R., Studies on the synthesis of apoptolidin A. 2. Synthesis of the disaccharide unit. *J. Org. Chem.* **2008**, 73, 1036.

36. Chng, S. S.; Xu, J.; Loh, T. P., A divergent approach to apoptolidin and FD-891: asymmetric preparation of a common intermediate. *Tetrahedron Lett.* **2003**, 44, 4997.
37. Craita, C.; Didier, C.; Vogel, P., Short synthesis of the C-16-C-28 polyketide fragment of apoptolidin A aglycone. *Chem. Commun.* **2007**, 2411.
38. Jin, B. H.; Liu, Q. S.; Sulikowski, G. A., Development of an end-game strategy towards apoptolidin: a sequential Suzuki coupling approach. *Tetrahedron* **2005**, 61, 401.
39. Schuppan, J.; Ziemer, B.; Koert, U., Stereoselective synthesis of the C18-C28 fragment of apoptolidin. *Tetrahedron Lett.* **2000**, 41, 621.
40. Wu, B.; Liu, Q. S.; Sulikowski, G. A., Total synthesis of apoptolidinone. *Angew. Chem.Int. Edit.* **2004**, 43, 6673.
41. Handa, M.; Scheidt, K. A.; Bossart, M.; Zheng, N.; Roush, W. R., Studies on the synthesis of apoptolidin A. 1. Synthesis of the C(1)-C(11) fragment. *J. Org. Chem.* **2008**, 73, 1031.
42. Toshima, K.; Arita, T.; Kato, K.; Tanaka, D.; Matsumura, S., Synthetic studies on apoptolidin: synthesis of the C1-C21 macrolide fragment. *Tetrahedron Lett.* **2001**, 42, 8873.
43. Reed, J. C., Apoptosis-based therapies. *Nat. Rev. Drug Discov.* **2002**, 1, 111.
44. Kondo, Y.; Kanzawa, T.; Sawaya, R.; Kondo, S., The role of autophagy in cancer development and response to therapy. *Nat. Rev. Cancer* **2005**, 5, 726.
45. Moretti, L.; Yang, E. S.; Kim, K. W.; Lu, B., Autophagy signaling in cancer and its potential as novel target to improve anticancer therapy. *Drug Resist. Update* **2007**, 10, 135.
46. Kerr, J. F. R.; Wyllie, A. H.; Currie, A. R., Apoptosis - Basic Biological Phenomenon with Wide-Ranging Implications in Tissue Kinetics. *Br. J. Cancer* **1972**, 26, 239.
47. Reed, J. C., Mechanisms of apoptosis. *Am. J. Pathol.* **2000**, 157, 1415.
48. Kim, R., Recent advances in understanding the cell death pathways activated by anticancer therapy. *Cancer* **2005**, 103, 1551.
49. Reed, J. C., Mechanisms of apoptosis regulation. *Cytometry* **2002**, 26.

50. Schweich, J.; Merker, H. J., Morphology of Various Types of Cell Death in Prenatal Tissues. *Teratology* **1973**, *7*, 253.
51. Gozuacik, D.; Kimchi, A., Autophagy and cell death. In *Current Topics in Developmental Biology*, Vol 78, Elsevier Academic Press Inc: San Diego, 2007; Vol. 78, pp 217.
52. Salomon, A. R.; Voehringer, D. W.; Herzenberg, L. A.; Khosla, C., Understanding and exploiting the mechanistic basis for selectivity of polyketide inhibitors of F₀F₁-ATPase. *Proc. Natl. Acad. Sci. U. S. A.* **2000**, *97*, 14766.
53. Salomon, A. R.; Voehringer, D. W.; Herzenberg, L. A.; Khosla, C., Apoptolidin, a selective cytotoxic agent, is an inhibitor of F₀F₁-ATPase. *Chem. Biol.* **2001**, *8*, 71.
54. Salomon, A. R.; Zhang, Y. B.; Seto, H.; Khosla, C., Structure-activity relationships within a family of selectively cytotoxic macrolide natural products. *Org. Lett.* **2001**, *3*, 57.
55. Warburg, O., On the origin of cancer cells. *Science* **1956**, *123*, 309.
56. Kim, J. W.; Dang, C. V., Cancer's molecular sweet tooth and the Warburg effect. *Cancer Research* **2006**, *66*, 8927.
57. Wender, P. A.; Jankowski, O. D.; Tabet, E. A.; Seto, H., Toward a structure-activity relationship for apoptolidin: selective functionalization of the hydroxyl group array. *Org. Lett.* **2003**, *5*, 487.
58. Jankowski, O. D., Ph.D. Dissertation, Thesis, Exploring the chemistry and biology of apoptolidin, Stanford University, . **2004**.
59. Hagenstein, M. C.; Mussgnug, J. H.; Lotte, K.; Plessow, R.; Brockhinke, A.; Kruse, O.; Sewald, N., Affinity-based tagging of protein families with reversible inhibitors: A concept for functional proteomics. *Angew. Chem.Int. Edit.* **2003**, *42*, 5635.
60. Tomohiro, T.; Hashimoto, M.; Hatanaka, Y., Cross-linking chemistry and biology: Development of multifunctional photoaffinity probes. *Chem. Rec.* **2005**, *5*, 385.
61. Carboni, J. M.; Farina, V.; Rao, S.; Hauck, S. I.; Horwitz, S. B.; Ringel, I., Use of photoaffinity analogues of taxol as an approach to identifying the taxol binding sites on microtubules. *Cellular Pharmacology* **1993**, *1*, S118.

62. Sydnnes, M. O.; Kuse, M.; Kurono, M.; Shimomura, A.; Ohinata, H.; Takai, A.; Isobe, M., Protein phosphatase inhibitory activity of tautomycin photoaffinity probes evaluated at femto-molar level. *Bioorg. Med. Chem.* **2008**, *16*, 1747.
63. Qiu, W. W.; Xu, J.; Liu, D. Z.; Li, J. Y.; Ye, Y.; Zhu, X. Z.; Li, J.; Nan, F. J., Design and synthesis of a biotin-tagged photoaffinity probe of paeoniflorin. *Bioorg. Med. Chem. Lett.* **2006**, *16*, 3306.
64. Kanoh, N.; Kumashiro, S.; Simizu, S.; Kondoh, Y.; Hatakeyama, S.; Tashiro, H.; Osada, H., Immobilization of natural products on glass slides by using a photoaffinity reaction and the detection of protein-small-molecule interactions. *Angew. Chem.Int. Edit.* **2003**, *42*, 5584.
65. Andrus, M. B.; Turner, T. M.; Sauna, Z. E.; Ambudkar, S. V., Synthesis and preliminary analysis of a P-glycoprotein-specific [H-3]-benzophenone photoaffinity label based on (-)-stipiamide. *Bioorg. Med. Chem. Lett.* **2000**, *10*, 2275.
66. Radeke, H. S.; Snapper, M. L., Photoaffinity study of the cellular interactions of ilimaquinone. *Bioorg. Med. Chem.* **1998**, *6*, 1227.
67. Gullledge, A. V., Synthesis, characterization, and biological evaluation of apoptolidin derivatives *Chemistry, Stanford University: Stanford* **2001**.
68. Ghidu, V. P.; Wang, J. Q.; Wu, B.; Liu, Q. S.; Jacobs, A.; Marnett, L. J.; Sulikowski, G. A., Synthesis and evaluation of the cytotoxicity of apoptolidinones A and D. *J. Org. Chem.* **2008**, *73*, 4949.
69. Roush, W. R.; Ando, K.; Powers, D. B.; Palkowitz, A. D.; Halterman, R. L., Asymmetric-Synthesis Using Diisopropyl Tartrate Modified (E)-Crotylboronates and (Z)-Crotylboronates - Preparation of the Chiral Crotylboronates and Reactions with Achiral Aldehydes. *J. Am. Chem. Soc.* **1990**, *112*, 6339.
70. White, J. D.; Hanselmann, R.; Jackson, R. W.; Porter, W. J.; Ohba, Y.; Tiller, T.; Wang, S., Total synthesis of rutamycin B, a macrolide antibiotic from *Streptomyces aureofaciens*. *J. Org. Chem.* **2001**, *66*, 5217.
71. Liu, Q., Large scale total synthesis of apoptolidinone and progress towards the total synthesis of ammocidin. *Texas A and M University* **2006**.
72. Marek, I.; Meyer, C.; Normant, J.-F., A Simple and Convenient Method for The Preparation of (Z)- β -Iodoacrolein and of (Z)- or (E)- γ -Iodo Allylic Alcohols: (Z)- and (E)-1-Iodohept-1-en-3-ol. *Org. Syn.* **1998**, *9*, 510.

73. Trost, B. M.; Frederiksen, M. U.; Papillon, J. P. N.; Harrington, P. E.; Shin, S.; Shireman, B. T., Dinuclear asymmetric Zn aldol additions: Formal asymmetric synthesis of fostriecin. *J. Am. Chem. Soc.* **2005**, 127, 3666.
74. Brown, H. C.; Jadhav, P. K., Asymmetric Carbon Carbon Bond Formation Via Beta-Allyldiisopinocampheylborane - Simple Synthesis of Secondary Homoallylic Alcohols with Excellent Enantiomeric Purities. *J. Am. Chem. Soc.* **1983**, 105, 2092.
75. Brown, H. C.; Bhat, K. S., Chiral Synthesis Via Organoboranes .7. Diastereoselective and Enantioselective Synthesis of Erythro-Beta-Methylomoallyl and Threo-Beta-Methylhomoallyl Alcohols Via Enantiomeric (Z)-Crotylborane and (E)-Crotylborane. *J. Am. Chem. Soc.* **1986**, 108, 5919.
76. Cho, B. T.; Chun, Y. S., Facile synthesis of terminal 1,2-diols with high optical purity via oxazaborolidine-catalyzed asymmetric borane reduction. *J. Org. Chem.* **1998**, 63, 5280.
77. Paquette, L. A.; O'Neil, S. V.; Guillo, N.; Zeng, Q. B.; Young, D. G., The need for an incisive analysis of the regioselectivity associated with the deprotonation of alpha-alkoxy and alpha-acyloxy ketones. *Synlett* **1999**, 1857.
78. Evans, D. A.; Yang, M. G.; Dart, M. J.; Duffy, J. L.; Kim, A. S., Double Stereodifferentiating Lewis Acid-Promoted (Mukaiyama) Aldol Bond Constructions. *J. Am. Chem. Soc.* **1995**, 117, 9598.
79. Heathcock, C. H.; Buse, C. T.; Kleschick, W. A.; Pirrung, M. C.; Sohn, J. E.; Lampe, J., Acyclic Stereoselection .7. Stereoselective Synthesis of 2-Alkyl-3-Hydroxy Carbonyl-Compounds by Aldol Condensation. *J. Org. Chem.* **1980**, 45, 1066.
80. Heathcock, C. H.; Flippin, L. A., Acyclic Stereoselection .16. High Diastereofacial Selectivity in Lewis Acid Mediated Additions of Enolsilanes to Chiral Aldehydes. *J. Am. Chem. Soc.* **1983**, 105, 1667.
81. Heathcock, C. H.; Hug, K. T.; Flippin, L. A., Acyclic Stereoselection .27. Simple Diastereoselection in the Lewis Acid Mediated Reactions of Enolsilanes with Aldehydes. *Tetrahedron Lett.* **1984**, 25, 5973.
82. Heathcock, C. H.; Davidsen, S. K.; Hug, K. T.; Flippin, L. A., Acyclic Stereoselection .36. Simple Diastereoselection in the Lewis Acid Mediated Reactions of Enol Silanes with Aldehydes. *J. Org. Chem.* **1986**, 51, 3027.
83. Evans, D. A.; Duffy, J. L.; Dart, M. J., 1,3-Asymmetric Induction in the Aldol Addition-Reactions of Methyl Ketone Enolates and Enolsilanes to Beta-

Substituted Aldehydes - a Model for Chirality Transfer. *Tetrahedron Lett.* **1994**, 35, 8537.

84. Evans, D. A.; Dart, M. J.; Duffy, J. L.; Yang, M. G., A stereochemical model for merged 1,2- and 1,3-asymmetric induction in diastereoselective Mukaiyama aldol addition reactions and related processes. *J. Am. Chem. Soc.* **1996**, 118, 4322.

85. Evans, D. A.; Yang, M. G.; Dart, M. J.; Duffy, J. L.; Kim, A. S., Double Stereodifferentiating Lewis Acid-Promoted (Mukaiyama) Aldol Bond Constructions. *J. Am. Chem. Soc.* **1995**, 117, 9598.

86. Evans, D. A.; Dart, M. J.; Duffy, J. L.; Yang, M. G.; Livingston, A. B., Diastereoselective Aldol and Allylstannane Addition-Reactions - the Merged Stereochemical Impact of Alpha-Aldehyde and Beta-Aldehyde Substituents. *J. Am. Chem. Soc.* **1995**, 117, 6619.

87. Evans, D. A.; Dart, M. J.; Duffy, J. L.; Rieger, D. L., Double Stereodifferentiating Aldol Reactions - the Documentation of Partially Matched Aldol Bond Constructions in the Assemblage of Polypropionate Systems. *J. Am. Chem. Soc.* **1995**, 117, 9073.

88. Ruck, R. T.; Jacobsen, E. N., Asymmetric hetero-ene reactions of trimethylsilyl enol ethers catalyzed by tridentate Schiff base chromium(III) complexes. *Angew. Chem.Int. Edit.* **2003**, 42, 4771.

89. Baker, R.; Castro, J. L., Total Synthesis of (+)-Macbecin-I. *J. Chem. Soc., Perkin Trans. 1* **1990**, 47.

90. Fargeas, V.; LeMenez, P.; Berque, I.; Ardisson, J.; Pancrazi, A., Studies in cuprate rearrangement and stannylicupration: Application to the stereo- and enantiospecific synthesis of a stannyldiene C-10-C-15 fragment of des-epoxy-rosaramycin. *Tetrahedron* **1996**, 52, 6613.

91. Bellina, F.; Carpita, A.; Desantis, M.; Rossi, R., Synthesis of Various 2-Substituted Alkyl (Z)-2-Alkenoate and (E)-2-Alkenoate and (Z)-Alpha-Ylidene-Gamma-Butyrolactone and (E)-Alpha-Ylidene-Gamma-Butyrolactone Via Palladium-Mediated Cross-Coupling Reactions between Organostannanes and Organic Halides. *Tetrahedron* **1994**, 50, 12029.

92. Schmidt-Leithoff, J.; Bruckner, R., Synthesis of the 2-alkenyl-4-alkylidenebut-2-eno-4-lactone (=alpha-alkenyl-gamma-alkylidenebutenolide) core structure of the carotenoid pyrroxanthin via the regioselective dihydroxylation of hepta-2,4-diene-5-ynoic acid esters. *Helv. Chim. Acta* **2005**, 88, 1943.

93. Staunton, J.; Weissman, K. J., Polyketide biosynthesis: a millennium review. *Nat. Prod. Rep.* **2001**, 18, 380.
94. Thibodeaux, C. J.; Melancon, C. E.; Liu, H. W., Natural-Product Sugar Biosynthesis and Enzymatic Glycodiversification. *Angew. Chem.Int. Edit.* **2008**, 47, 9814.
95. Mendez, C.; Luzhetskyy, A.; Bechthold, A.; Salas, J. A., Deoxysugars in bioactive natural products: Development of novel derivatives by altering the sugar pattern. *Current Topics in Medicinal Chemistry* **2008**, 8, 710.
96. Luzhetskyy, A.; Mendez, C.; Salas, J. A.; Bechthold, A., Glycosyltransferases, important tools for drug design. *Curr. Top. Med. Chem.* **2008**, 8, 680.
97. Walsh, C.; Meyers, C. L. F.; Losey, H. C., Antibiotic glycosyltransferases: Antibiotic maturation and prospects for reprogramming. *J. Med. Chem.* **2003**, 46, 3425.
98. Thorson, J. S.; Hosted, T. J.; Jiang, J. Q.; Biggins, J. B.; Ahlert, J., Nature's carbohydrate chemists: The enzymatic glycosylation of bioactive bacterial metabolites. *Curr. Org. Chem.* **2001**, 5, 139.
99. Kennedy, J., Mutasynthesis, chemobiosynthesis, and back to semi-synthesis: combining synthetic chemistry and biosynthetic engineering for diversifying natural products. *Nat. Prod. Rep.* **2008**, 25, 25.
100. Venkatraman, L.; Salomon, C. E.; Sherman, D. H.; Fecik, R. A., Total synthesis of narbonolide and biotransformation to pikromycin. *J. Org. Chem.* **2006**, 71, 9853.
101. Ashley, G. W.; Burlingame, M.; Desai, R.; Fu, H.; Leaf, T.; Licari, P. J.; Tran, C.; Abbanat, D.; Bush, K.; Macielag, M., Preparation of erythromycin analogs having functional groups at C-15. *J. Antibiot.* **2006**, 59, 392.
102. Thiericke, R., Biological Variation of Microbial Metabolites by Precursor-Directed Biosynthesis. *Nat. Prod. Rep.* **1993**, 10, 265.
103. Nakagawa, A.; Omura, S., Biosynthesis of bioactive microbial metabolites and its application to the structural studies and production of hybrid compounds. *J. Antibiot.* **1996**, 49, 717, Hata, T.; Sano, Y.; Matsumae, A.; Kamio, Y.; Nomura, S.; Sugawara, R., Study of New Antifungal Antibiotic. *J. Bacteriol.* **1960**, 15, 1075.

104. Omura, S.; Sadakane, N.; Tanaka, Y.; Matsubara, H., Bioconversion and Biosynthesis of 16-Membered Macrolide Antibiotics .26. Chimeramycins - New Macrolide Antibiotics Produced by Hybrid Biosynthesis. *J. Antibiot.* **1983**, 36, 927.
105. Sadakane, N.; Tanaka, Y.; Omura, S., Bioconversion and Biosynthesis of 16-Membered Macrolide Antibiotics .23. Hybrid Biosynthesis of Derivatives of Protylonolide and M-4365 by Macrolide-Producing Microorganisms. *J. Antibiot.* **1982**, 35, 680.
106. Sadakane, N.; Tanaka, Y.; Omura, S., Bioconversion and Biosynthesis of 16-Membered Vo Macrolide Antibiotics .25. Hybrid Biosynthesis of a New Macrolide Antibiotic by a Daunomycin-Producing Microorganism. *J. Antibiot.* **1983**, 36, 921.
107. Ghidu, V. P.; Ntai, I.; Wang, J. Q.; Jacobs, A. T.; Marnett, L. J.; Bachmann, B. O.; Sulikowski, G. A., Combined Chemical and Biosynthetic Route to Access a New Apoptolidin Congener. *Org. Lett.* **2009**, 11, 3032.
108. Hata, T.; Sano, Y.; Matsumae, A.; Kamio, Y.; Nomura, S.; Sugawara, R., Study of New Antifungal Antibiotic. *J. Bacteriol.* **1960**, 15, 1075.
109. Price, A. C.; Choi, K. H.; Heath, R. J.; Li, Z. M.; White, S. W.; Rock, C. O., Inhibition of beta-ketoacyl-acyl carrier protein syntheses by thiolactomycin and cerulenin - Structure and mechanism. *J. Biol. Chem.* **2001**, 276, 6551.
110. Omura, S.; Takeshim.H, Inhibition of Biosynthesis of Leucomycin, a Macrolide Antibiotic, by Cerulenin. *J. Biochem.* **1974**, 75, 193.
111. Kao, C. L.; Borisova, S. A.; Kim, H. J.; Liu, H. W., Linear aglycones are the substrates for glycosyltransferase DesVII in methymycin biosynthesis: Analysis and implications. *J. Am. Chem. Soc.* **2006**, 128, 5606.
112. Borisova, S. A.; Kim, H. J.; Pu, X. T.; Liu, H. W., Glycosylation of acyclic and cyclic aglycone substrates by macrolide glycosyltransferase DesVII/DesVIII: Analysis and implications. *ChemBiochem* **2008**, 9, 1554.
113. Pucheault, M., Natural products: chemical instruments to apprehend biological symphony. *Org. Biomol. Chem.* **2008**, 6, 424.
114. Drahl, C.; Cravatt, B. F.; Sorensen, E. J., Protein-reactive natural products. *Angew. Chem. Int. Ed.* **2005**, 44, 5788.
115. Wang, S. L.; Sim, T. B.; Chang, Y. T., Tools for target identification and validation. *Curr. Opinion in Chem. Biol.* **2004**, 8, 371.

116. Burdine, L.; Kodadek, T., Target identification in chemical genetics: The (often) missing link. *Chem. Biol.* **2004**, 11, 593.
117. Terstappen, G. C.; Schlupen, C.; Raggiaschi, R.; Gaviraghi, G., Target deconvolution strategies in drug discovery. *Nat. Rev. Drug Discov.* **2007**, 6, 891.
118. Leslie, B. J.; Hergenrother, P. J., Identification of the cellular targets of bioactive small organic molecules using affinity reagents. *Chem. Soc. Rev.* **2008**, 37, 1347.
119. Huebel, K.; Lessmann, T.; Waldmann, H., Chemical biology - identification of small molecule modulators of cellular activity by natural product inspired synthesis. *Chem. Soc. Rev.* **2008**, 37, 1361.
120. Licitra, E. J.; Liu, J. O., A three-hybrid system for detecting small ligand-protein receptor interactions. *Proc. Natl. Acad. Sci. U. S. A.* **1996**, 93, 12817.
121. Becker, F.; Murthi, K.; Smith, C.; Come, J.; Costa-Roldan, N.; Kaufmann, C.; Hanke, U.; Degenhart, C.; Baumann, S.; Wallner, W.; Huber, A.; Dedier, S.; Dill, S.; Kinsman, D.; Hediger, M.; Bockovich, N.; Meier-Ewert, S.; Kluge, A. F.; Kley, N., A three-hybrid approach to scanning the proteome for targets of small molecule kinase inhibitors. *Chem. Biol.* **2004**, 11, 211.
122. Baryza, J., I. Design, synthesis, and biological evaluation of new analogs of bryostatin. II. Investigations into the mode of action of apoptolidin A. *Stanford Univ.* **2005**.
123. Arkin, H.; Ohnuma, T.; Holland, J. F.; Gailani, S. D., Effects of Cell-Density on Drug-Induced Cell Kill Kinetics In vitro (Inoculum Effect). *Proc. Amer. Assoc. Cancer Res.* **1984**, 25, 315.
124. WeymouthWilson, A. C., The role of carbohydrates in biologically active natural products. *Nat. Prod. Rep.* **1997**, 14, 99.
125. Murakami, R.; Shinozaki, J.; Kajiura, T.; Kozono, I.; Takagi, M.; Shin-Ya, K.; Seto, H.; Hayakawa, Y., Ammocidins B, C and D, new cytotoxic 20-membered macrolides from *Saccharothrix* sp. AJ9571. *J. Antibiot.* **2009**, 62, 123.
126. Murakami, R.; Tomikawa, T.; Shin-Ya, K.; Shinozaki, J.; Kajiura, T.; Kinoshita, T.; Miyajima, A.; Seto, H.; Hayakawa, Y., Ammocidin, a new apoptosis inducer in Ras-dependent cells from *Saccharothrix* sp. I. Production, isolation and biological activity. *J. Antibiot.* **2001**, 54, 710.

127. Murakami, R.; Tomikawa, T.; Shin-Ya, K.; Shinozaki, J.; Kajiura, T.; Seto, H.; Hayakawa, Y., Ammocidin, a new apoptosis inducer in Ras-dependent cells from *Saccharothrix* sp - II. Physico-chemical properties and structure elucidation. *J. Antibiot.* **2001**, 54, 714.
128. Adam, G. C.; Sorensen, E. J.; Cravatt, B. F., Chemical strategies for functional proteomics. *Molecular & Cellular Proteomics* **2002**, 1, 781.
129. Adam, G. C.; Sorensen, E. J.; Cravatt, B. F., Trifunctional chemical probes for the consolidated detection and identification of enzyme activities from complex proteomes. *Molecular & Cellular Proteomics* **2002**, 1, 828.
130. Adam, G. C.; Sorensen, E. J.; Cravatt, B. F., Proteomic profiling of mechanistically distinct enzyme classes using a common chemotype. *Nat. Biotechnol.* **2002**, 20, 805.
131. Khoukhi, N.; Vaultier, M.; Carrie, R., Synthesis and Reactivity of Methyl Gamma-Azido Butyrates and Ethyl Delta-Azido Valerates and of the Corresponding Acid-Chlorides as Useful Reagents for the Aminoalkylation. *Tetrahedron* **1987**, 43, 1811.
132. Johnson, L. V.; Walsh, M. L.; Chen, L. B., Localization of Mitochondria in Living Cells with Rhodamine-123. *Proc. Natl. Acad. Sci. U. S. A.* **1980**, 77, 990.
133. Lin, H. N.; Abida, W. M.; Sauer, R. T.; Cornish, V. W., Dexamethasone-methotrexate: An efficient chemical inducer of protein dimerization in vivo. *J. Am. Chem. Soc.* **2000**, 122, 4247.
134. Cornish, V. W.; Lin, H.; Abide, W. M.; Sauer, R. T., Dexamethasone-methotrexate: An efficient chemical inducer of protein dimerization in vivo. *Biochemistry* **2000**, 39, 124.
135. Abida, W. M.; Carter, B. T.; Althoff, E. A.; Lin, H. N.; Cornish, V. W., Receptor-dependence of the transcription read-out in a small-molecule three-hybrid system. *Chembiochem* **2002**, 3, 887.
136. Baker, K.; Sengupta, D.; Salazar-Jimenez, G.; Cornish, V. W., An optimized dexamethasone-methotrexate yeast 3-hybrid system for high-throughput screening of small molecule-protein interactions. *Anal. Biochem.* **2003**, 315, 134.

VITA

Jingqi Wang

Permanent Address:

Buding 8, Apt 1104
Jinding Street, District 3
Beijing, P. R. China, 100041

Educational Background:

B.M., Clinical Medicine, Tianjin Medical University, P. R. China, 1996.
Ph.D., Chemistry, Vanderbilt University, Nashville, TN, 2009.

Research Experience:

- Research Assistant: Department of Chemistry, Vanderbilt University (Nashville, TN), 08/2004 – 10/2009
Research Project: Synthetic Studies on Apoptolidin Congeners in Support of Target Identification of a Cell Selective Cytotoxic Agent
Research Advisor: Dr. Gary A. Sulikowski
- Research Assistant: Department of Chemistry and Biochemistry, Florida Atlantic University (Boca Raton, FL), 08/2002 - 07/2004
Research Project: Synthesis of quinazoline derivatives as new antibacterial drugs
Research Advisor: Dr. Cyril Párkányi
- Research Assistant: Department of Plastic Surgery, Anhua Hospital (Beijing, China), 09/1996 -07/2001
Research Project: Effect of EGF on the growth regulation of skin fibroblast
Research Advisor: Dr. Guangzhen Feng

Scholarship and Honors

Maria Kace Siegel Memorial Scholarship for Cancer Research, Florida Atlantic University, 03/2004

Publications:

1. Ghidu, V. P.; **Wang, J. Q.**; Wu, B.; Liu, Q. S.; Jacobs, A.; Marnett, L. J.; Sulikowski, G. A., Synthesis and evaluation of the cytotoxicity of

apoptolidinones A and D. *J. Org. Chem.* **2008**, 73, 4949

2. Ghidu, V. P.; Ntai, I.; **Wang, J. Q.**; Jacobs, A. T.; Marnett, L. J.; Bachmann, B. O.; Sulikowski, G. A., Combined Chemical and Biosynthetic Route to Access a New Apoptolidin Congener. *Org. Lett.* **2009**, 11, 3032.